

**THE ROLE OF RAC1 IN THE EPIDERMIS
AND IN THE HAIR FOLLICLE**

DISSERTATION ZUR ERLANGUNG
DES DOKTORGRADES DER NATURWISSENSCHAFTEN (DR. RER. NAT.)
DER FAKULTÄT FÜR BIOLOGIE
DER LUDWIGS-MAXIMILIANS-UNIVERSITÄT MÜNCHEN

VORGELEGT VON
ANNA MAGDALENA CHROSTEK-GRASHOFF

AUS
KATOWICE, POLEN

MÜNCHEN – 2007

To

MY FAMILY

&

IN MEMORY OF

PROF. ZYGMUNT WASYLEWSKI

Hiermit erkläre ich, dass ich die vorliegende Dissertation selbständig und ohne unerlaubte Hilfe angefertigt habe. Sämtliche Experimente sind von mir selbstdurchgeführt, ausser wenn explizit auf Dritte verwiesen wird. Ich habe weder anderweitig versucht, eine Dissertation einzureichen oder eine Doktorprüfung durchzuführen, noch habe ich diese Dissertation oder Teile derselben einer anderen Prüfungskommission vorgelegt.

Anna Magdalena Chrostek-Grashoff

München, den 07.03.2007

Die vorliegende Arbeit wurde zwischen September 2002 und September 2006 unter Anleitung von Dr. Cord Brakebusch am Max-Planck-Institut für Biochemie in Martinsried durchgeführt. Wesentliche Teile dieser Arbeit sind in folgenden Publikationen veröffentlicht:

Chrostek, A., X. Wu, F. Quondamatteo, R. Hu, A. Sanecka, C. Niemann, L. Langbein, I. Haase and C. Brakebusch (2006). "Rac1 Is Crucial for Hair Follicle Integrity but Is Not Essential for Maintenance of the Epidermis." *Mol. Cell. Biol.* 26: 6957-70.

Tscharntke, M., R. Pofahl, **A. Chrostek-Grashoff**, N. Smyth, C. Niessen, C. Niemann, B. Hartwig, V. Herzog, H. Klein, T. Krieg, C. Brakebusch and I. Haase (2007). "Impaired epidermal wound healing *in vivo* upon inhibition or deletion of Rac1." *J. Cell Sci.* 120: 1480-90.

Promotionsgesuch eingereicht am 07.03.2007

Tag der mündlichen Prüfung: 17.04.2007

Erster Gutachter: Prof. Dr. Charles N. David

Zweiter Gutachter: Prof. Dr. Michael Schleicher

Sondergutachter: Prof. Dr. Cord Brakebusch

TABLE OF CONTENTS

Abbreviations	9
1 Introduction	11
1.1 Rac1 – a small Rho GTPase	11
1.1.1 The Rho family of small GTPases.....	11
1.1.2 Regulation of Rho GTPases.....	13
1.1.2.1 <i>GEFs</i>	14
1.1.2.2 <i>GAPs</i>	15
1.1.2.3 <i>GDI</i> s.....	15
1.1.3 Signalling through Rho GTPases	16
1.1.4 Crosstalk between Rho GTPases.....	19
1.1.5 The Rac subfamily	20
1.2 Skin	21
1.2.1 Epidermis morphology and differentiation.....	22
1.2.2 Hair follicle morphogenesis and cycling.....	24
1.3 Epithelial cell-cell adhesion and polarization	28
1.3.1 Role of Rac1 in the epithelial cell-cell adhesion	29
1.4 Aims of the project	31
2 Materials and Methods	33
2.1 Animals	33
2.2 Common materials	33
2.2.1 Chemicals.....	33
2.2.2 Disposable plastic materials	33
2.3 Antibodies	34
2.3.1 Primary	34
2.3.2 Secondary.....	35
2.4 Molecular biology methods	35
2.4.1 Plasmids and oligonucleotides	35
2.4.2 Bacteria culture	36
2.4.2.1 <i>Strains, growth conditions, media, selection and storage</i>	36
2.4.2.2 <i>Preparation of competent bacteria</i>	37
2.4.2.3 <i>Transformation</i>	37
2.4.3 Plasmid DNA preparation	38
2.4.3.1 <i>Analytical amounts – miniprep</i>	38
2.4.3.2 <i>Preparative amounts – maxiprep</i>	39
2.4.4 DNA cloning	39
2.4.4.1 <i>Restriction enzymes digestion</i>	39
2.4.4.2 <i>Gel electrophoresis</i>	40
2.4.4.3 <i>DNA extraction from agarose gel</i>	41
2.4.4.4 <i>DNA precipitation</i>	41
2.4.4.5 <i>Phosphorylation and annealing of oligonucleotides</i>	42
2.4.4.6 <i>Dephosphorylation of 5`- ends</i>	42
2.4.4.7 <i>Ligation of DNA fragments</i>	42

2.4.4.8	<i>Sequencing</i>	43
2.4.5	Isolation of genomic DNA.....	43
2.4.5.1	<i>DNA isolation from tissues</i>	43
2.4.5.2	<i>DNA isolation from cells</i>	44
2.4.6	Polymerase chain reaction – PCR.....	44
2.4.6.1	<i>Mice genotyping</i>	44
2.4.6.2	<i>Preparative PCR</i>	45
2.4.7	Southern blot analysis.....	45
2.4.7.1	<i>DNA processing and transfer to the membrane</i>	46
2.4.7.2	<i>Generation and radioactive labelling of the probe</i>	47
2.4.7.3	<i>Hybridization, washing and signal detection</i>	48
2.5	Cell culture materials and techniques	49
2.5.1	Embryonic stem cells (ES cells).....	49
2.5.1.1	<i>Culture condition, medium</i>	49
2.5.1.2	<i>Passaging, freezing and thawing</i>	50
2.5.2	Preparation of feeder cells.....	50
2.5.3	Embryoid bodies (EBs).....	51
2.5.3.1	<i>Culture conditions</i>	51
2.5.3.2	<i>Analysis of EBs structure</i>	52
2.5.3.3	<i>Analysis of the ES cells differentiation potential</i>	53
2.5.4	Primary keratinocytes.....	53
2.5.4.1	<i>Culture conditions</i>	53
2.5.4.2	<i>Surface coating</i>	54
2.5.4.3	<i>Isolation of primary keratinocytes from adult mice</i>	54
2.5.4.4	<i>Immunofluorescence staining of cells</i>	55
2.5.4.5	<i>Adhesion assay</i>	55
2.5.4.6	<i>Time-lapse video microscopy and cell spreading analysis</i>	56
2.5.4.7	<i>Isolation of primary keratinocytes from 3d old mice</i>	56
2.6	Generation of a conditional knock-out mouse	57
2.6.1	Cre-loxP system.....	57
2.6.2	Targeting construct preparation.....	58
2.6.2.1	<i>Modification of the selection cassette</i>	58
2.6.2.2	<i>Cloning of the targeting construct</i>	59
2.6.2.3	<i>Preparation of DNA for the electroporation</i>	60
2.6.3	Homologous recombination of the targeting construct.....	60
2.6.3.1	<i>Electroporation of ES cells</i>	61
2.6.3.2	<i>Selection and picking of clones after the recombination</i>	61
2.6.3.3	<i>Screening of ES cell clones</i>	62
2.6.4	Removal of the selection cassette.....	62
2.6.5	Blastocyst injection.....	63
2.6.6	Breeding schemes.....	63
2.6.7	Generation of knock-out ES cells.....	64
2.7	Skin phenotype analysis	65
2.7.1	Histology.....	65
2.7.1.1	<i>Skin isolation and embedding</i>	65
2.7.1.2	<i>Cryo-embedded sections preparation</i>	65
2.7.1.3	<i>Paraffin sections preparation</i>	66
2.7.1.4	<i>Hematoxylin-eosin (HE) staining</i>	66
2.7.2	Immunohistochemistry.....	67
2.7.2.1	<i>Detection of marker proteins in skin using immunofluorescence</i>	67
2.7.2.2	<i>BrdU incorporation assay</i>	67

2.7.2.3	<i>Apoptosis analysis</i>	68
2.7.2.4	<i>FACS cytometry analysis</i>	69
2.7.3	Electron microscopy (EM)	70
2.7.4	Analysis of the tamoxifen influence on skin	70
2.7.5	Wound healing analysis	70
2.8	Biochemical methods	71
2.8.1	Protein isolation.....	71
2.8.1.1	<i>Preparation of protein lysates from ES cells</i>	71
2.8.1.2	<i>Preparation of epidermal lysates</i>	72
2.8.2	Protein concentration assay	72
2.8.3	Western blot analysis	73
2.8.3.1	<i>SDS-Polyacrylamide gel electrophoresis (SDS-PAGE)</i>	73
2.8.3.2	<i>Transfer of proteins to the membrane</i>	74
2.8.3.3	<i>Protein detection on the membrane</i>	75
2.8.4	GTPase activity assay.....	76
2.9	Analysis of mRNA expression	76
2.9.1	RNA isolation.....	76
2.9.1.1	<i>RNA gel electrophoresis</i>	77
2.9.2	Reverse transcription of total RNA	77
2.9.3	Real-time PCR	78
3	Results	79
3.1	Generation of mice with a keratinocyte-restricted deletion of the <i>rac1</i> gene.	79
3.1.1	The <i>rac1</i> gene structure and the conditional knock-out strategy	79
3.1.2	Modification of the <i>rac1</i> gene and generation of mutant mice.....	81
3.1.3	Gross phenotype after the K5-Cre induced loss of Rac1	82
3.2	Analysis of the hair follicle (HF) phenotype in the absence of Rac1	85
3.2.1	Defective HF morphogenesis	85
3.2.2	Loss of the HF specific differentiation	88
3.2.3	Removal of the lower part of mutant HFs by macrophages	96
3.3	Phenotype analysis of the Rac1-deficient epidermis	98
3.3.1	Normal differentiation of the epidermis	98
3.3.2	Normal expression of adhesion and ECM proteins	99
3.3.3	Normal formation of cell-cell and cell-ECM contacts	101
3.4	Biochemical analysis of signalling pathways in the absence of Rac1	102
3.4.1	No significant changes in the c-Myc expression	102
3.4.2	No apparent defects in activation of NF- κ B, JNK, p38 or Akt	102
3.4.3	No obvious compensation of Rac1 by related Rho GTPases.	103
3.5	Analysis of the wound healing process in the absence of Rac1	105
3.6	Analysis of the 4-hydroxy-tamoxifen influence on the Rac1-deficient epidermis	107
3.7	<i>In vitro</i> analysis of Rac1-deficient primary keratinocytes	108
3.7.1	Mutant keratinocytes do not survive <i>in vitro</i>	108
3.7.2	Slightly impaired adhesion of Rac1-deficient keratinocytes.	110
3.7.3	No increase in the apoptosis or terminal differentiation of keratinocytes in the absence of Rac1.	111
3.7.4	Severe spreading defect of Rac1-deficient keratinocytes	112
3.8	<i>In vitro</i> analysis of ES cell differentiation in the absence of Rac1	114

3.8.1	Generation of Rac1 (-/-) ES cells	115
3.8.2	Differentiation of Rac1-deficient ES cells into EBs.....	117
3.8.3	Analysis of the epiblast polarization in the absence of Rac1	118
3.8.4	Analysis of the cell-cell contacts formation in Rac1-deficient EBs	119
3.8.5	Analysis of the Rac1-deficient ES cells differentiation potential.....	121
4	Discussion.....	123
4.1	The absence of Rac1 leads to the HF degeneration	123
4.2	Epidermis maintenance does not depend on the presence of Rac1.....	126
4.3	Wound healing is impaired in the absence of Rac1	127
4.4	Severe spreading defect leads to death of Rac1-deficient primary keratinocytes <i>in vitro</i>	128
4.5	Discrepancies between epidermal phenotypes resulting from the lack of Rac1	128
4.6	The role of Rac1 in embryonic development	130
4.7	Future prospects.....	131
5	Summary.....	133
6	References.....	135
7	Appendix CD	145
	Acknowledgments	147
	Curriculum Vitae.....	149

ABBREVIATIONS

#	number	GAPDH	glyceraldehyde -3-phosphate dehydrogenase
–	null allele	GAPs	GTPase-activating proteins
×	multiplication symbol	GDI	guanine nucleotide dissociation inhibitors
APS	ammonium persulfate	GEFs	guanine nucleotide exchange factors
BM	basement membrane	GPSRs	G-protein-coupled receptors
bp/kbp	base pairs/1000 base pairs	GTP	guanosine triphosphate
BrdU	bromodeoxyuridine	HE	hematoxylin-eosin
BSA	bovine serum albumine	HF(s)	hair follicle(s)
CA	constitutively active	HRP	horseradish peroxidase
cDNA	complementary DNA	HS	hair shaft
Col	collagen	i.e.	that is (<i>lat. id est</i>)
ctrl	control samples/mice (in figures)	IF	immunofluorescence
DAPI	4',6-diamidino-2-phenylindole	IRS	inner root sheath
ddH ₂ O	double-distilled water	JNK	c-Jun N-terminal kinase
DEPC	diethylpyrocarbonate	K5, K14	keratin 5, keratin 14
DH	Dbl homology	K-Ac	potassium acetate
DMSO	dimethylsulfoxide	kDa	kilo dalton
DN	dominant-negative	KO	mutant samples/mice (in figures)
dNTP	deoxynucleotide triphosphates	LB	lysogeny broth
DP	dermal papilla	LIF	leukemia inhibitory factor
DTT	dithiothreitol	LN5	laminin 5
e.g.	for example (<i>lat. exempli gratia</i>)	MCS	multiple cloning site
EBs	embryoid bodies	MDCK cells	Madin-Darby Canine Kidney cells
ECM	extracellular matrix	MEFs	mouse embryonic fibroblasts
EDTA	ethylene-diamine-tetraacetic acid	MeOH	methanol
EM	electron microscopy	MTOC	Microtubule Organizing Center
ES cells	embryonic stem cells	Na-Ac	sodium acetate
EtOH	ethanol	Nd	nidogen
FACS	fluorescence activated cell sorter	neo	neomycin resistance gene
FCS	foetal calf serum	Ø	diameter
FIAU	1-2'-deoxy-2'-fluoro-b-D-arabinofuranosyl-5-iodouracil	O/N	overnight
FITC	fluorescein isothiocyanate	OD	optical density
fl	conditional allele	ORS	outer root sheath
FN	fibronectin		

Abbreviations

p-	phospho-	RT	room temperature
PAK	p21-activated kinase	RT-PCR	reverse transcription PCR
PBS	phosphate-buffered saline	SDS	sodium dodecyl sulphate
PCR	polymerase chain reaction	SDS-PAGE	SDS-polyacrylamide gel electrophoresis
PFA	paraformaldehyd	SGs	sebaceous glands
PH	pleckstrin homology	TBS	tris-buffered saline
POD	peroxidase	TK	thymidine kinase
PVDF	polyvinylidene fluoride	Tris	tris-hydroxymethyl-aminomethane
Rac1 (-/-)	Rac1-null ES cells	U	unit of enzyme activity
Rac1 (fl/-)	control ES cells	w/o	without
<i>rac1^{fl/+}cre</i>	control mice	wt (+)	wild type allele
<i>rac1^{fl/fl},cre</i>	mutant mice	X-gal	5-bromo-4-chloro-3-indolyl-β-D-galactopyranoside
RNase	ribonuclease		
rpm	rotations per minute		

1 INTRODUCTION

1.1 Rac1 – a small Rho GTPase

1.1.1 The Rho family of small GTPases

Rho GTPases belong to the Ras superfamily of small GTPases. They are 20-25 kDa signalling molecules, which regulate many cellular processes (1.1.3) acting as molecular switches (1.1.2). They are characterized by the presence of the ~20 kDa structurally conserved G-domain (six-stranded β -sheet surrounded by five α -helices), which conveys the ability to bind and to hydrolyze GTP (Vetter and Wittinghofer, 2001). Members of the Rho family are distinguished from other small GTPases by the Rho insert (conserved α -helical domain) located between the fifth β -strand and the fourth α -helix of the GTPase domain (Hirshberg *et al.*, 1997).

In mammals, the Rho family comprises 22 genes. They encode at least 25 proteins, which can be classified into sub-families on the basis of their amino acid sequence identity, structural motifs and biological functions (Fig. 1.1).

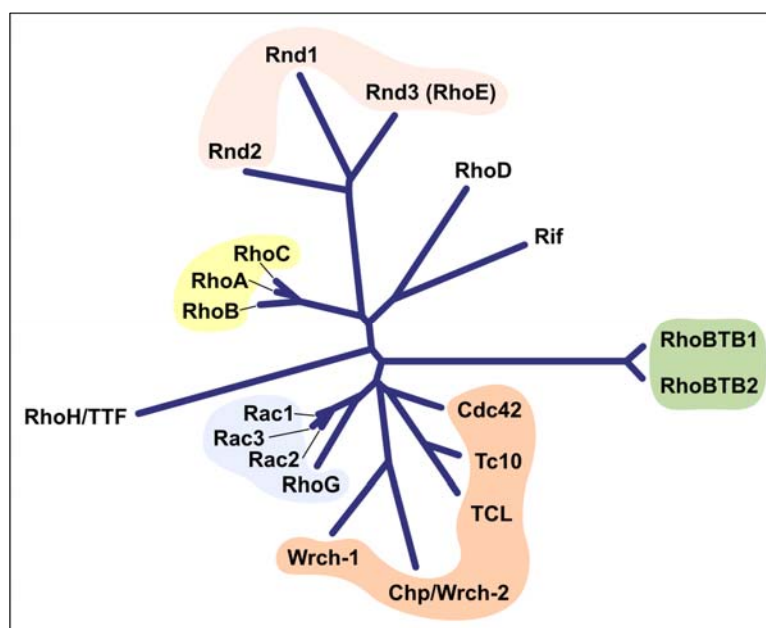


Fig. 1.1 Phylogenetic tree of the Rho family GTPase. On the basis of primary amino acid sequence identity, closely related proteins can be further grouped within the family (colour patches). Sequences were aligned using the ClustalW algorithm and sequence distances displayed as unrooted dendrograms in TreeView. The alignment considered only the Rho GTPase domain in BTB-containing Rho GTPases. Miro proteins were not included (modified from Wherlock and Mellor, 2002).

Classical Rho GTPases comprise four sub-families – Rho (RhoA, RhoB, RhoC), Rac (Rac1, Rac2, Rac3, RhoG), Cdc42 (Cdc42, TC10, TCL, Wrch-1, Chp/Wrch-2) and Rnd (Rnd1, Rnd2,

Rnd3/RhoE) – and three proteins that do not fall into any of the above groups – RhoD, Rif and RhoH/TTF. They consist only of a GTPase domain with short N- and C-terminal sequences and share 40-95% amino acid sequence identity. Most differences between members of subfamilies are found in the C-terminal sequence (Wennerberg and Der, 2004).

With exception of Chp/Wrch-2, all classical members of the Rho family undergo post-translational modifications at the C-terminal end, which are determined by the presence of the CAAX motif (C: cysteine, A: aliphatic and X: any amino acid). The cysteine residue becomes isoprenylated with either geranylgeranyl (C₂₀) or farnesyl (C₁₅). Subsequently, the AAX tripeptide is proteolytically removed and the cysteine becomes carboxymethylated (Clarke, 1992; Zhang and Casey, 1996). Some Rho GTPases are additionally modified with palmitoyl at another cysteine residue, which directly precedes the CAAX motif (Fig. 1.2).

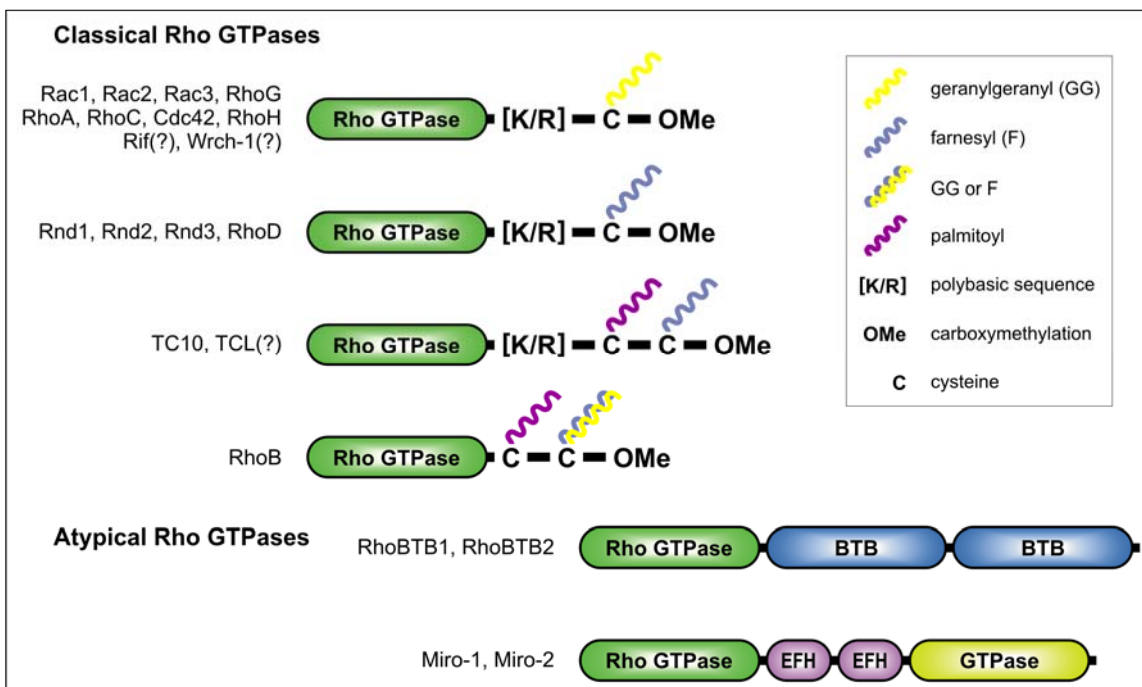


Fig. 1.2 Differences in the domain structure and the variety of post-translational modifications of Rho GTPases. Classical Rho GTPases terminate with the CAAX motif, which determines the isoprenylation and the subsequent carboxymethylation of the cysteine residue (after the removal of AAX residues). When a cysteine residue is present before the CAAX motif, it is modified with palmitoyl. The polybasic sequence is an additional membrane targeting signal. The atypical Rho GTPases are significantly bigger than other members of the family and contain additional domains after the Rho GTPase domain. Chp/Wrch-2 and the atypical Rho GTPases do not terminate with the CAAX sequence and do not undergo any known post-translational modifications. The proteins, which modifications are predicted but have not been experimentally verified, are marked with a question mark (?). EFH: EF-hand domain (based on a figure from Wennerberg and Der, 2004).

Lipid moieties and a highly variable polybasic sequence present within the majority of C-terminal sequences (Fig. 1.2) mediate the association of Rho GTPases with cellular membranes, which is essential for their function. The diversity of post-translational modifications is likely to influence the translocation to a specific site within the cell and

contribute to the diversity of functions seen in otherwise closely related members of subfamilies.

Members of RhoBTB (RhoBTB1 and RhoBTB2) and Miro (Miro-1 and Miro-2) subfamilies are much bigger (~70 kDa) and structurally different from other Rho GTPases (Rivero *et al.*, 2001; Fransson *et al.*, 2003). They have extensive C-terminal sequences that form additional domains (Fig. 1.2) and they do not undergo any post-translational modifications, as they lack the CAAX motif. In addition, Miro subfamily members do not contain the characteristic Rho insert within the GTPase domain, which sets them apart from all other members of the Rho family. Atypical Rho GTPases, unlike classical members of the Rho family (with the exception of RhoH), do not influence the actin cytoskeleton or cell morphology (Aspenstrom *et al.*, 2004).

1.1.2 Regulation of Rho GTPases.

The biological role of Rho proteins as molecular switches is based on their ability to shuttle between an inactive (GDP-bound) and an active (GTP-bound) state in a tightly regulated manner (Fig. 1.3).

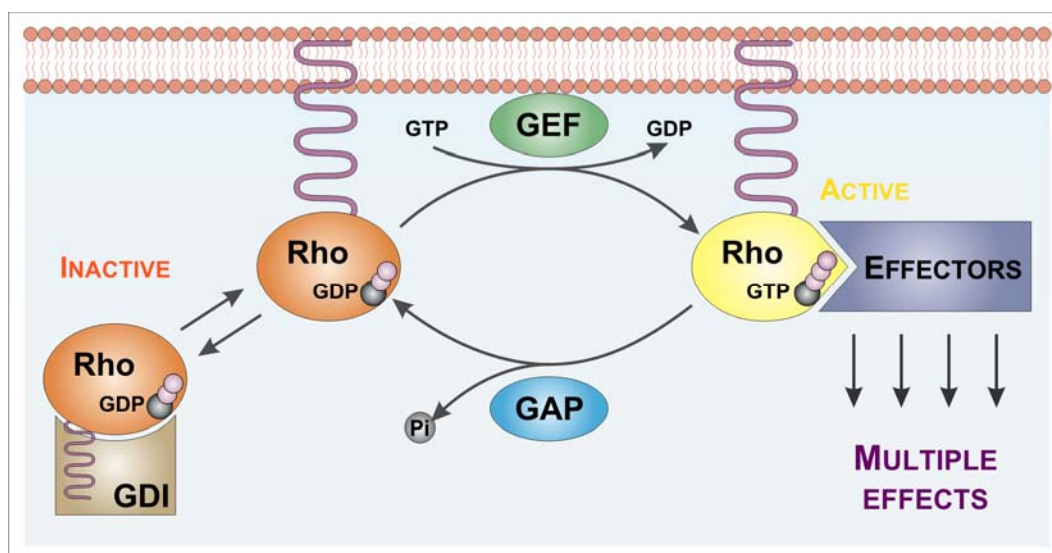


Fig. 1.3 Regulation of the GTPase cycle. The role of Rho proteins as ‘molecular switches’ is based on their ability to cycle between an inactive GDP-bound form and an active GTP-bound form, in which they can interact with different effector molecules. The exchange of nucleotides is regulated by GEFs, GAPs and GDIs. The latter are involved in controlling the distribution of Rho GTPases within the cell as well. Pi: inorganic phosphate; wavy line: lipid moiety (modified from Aktories and Barbieri, 2005).

GTPases bind nucleotides with high-affinity in the presence of Mg^{2+} as a cofactor. The interaction induces conformational changes of the protein structure, which are confined primarily to two highly conserved regions named switch I and II and depend on the type of the bound nucleotide. The configuration of switch regions in the GTP-bound state enables interactions with a multitude of effector proteins (Vetter and Wittinghofer, 2001). The hydrolysis of GTP to GDP, catalysed by an intrinsic GTPase activity, leads to the release of an inorganic phosphate (Pi) and

the inactivation of the protein due to remodelling of switch regions. Three types of regulating proteins control the exchange cycle: guanine nucleotide-exchange factors (GEFs), GTPase-activating proteins (GAPs) and guanine nucleotide dissociation inhibitors (GDIs).

In addition, the activity of Rho proteins is regulated through their association with membranes and subcellular localisation, which are influenced by post-translational modifications of the C-terminus (1.1.1) and interaction with GDIs (1.1.2.3).

Some Rho GTPases seem to be regulated at the expression level as well. They are expressed only in certain tissues (e.g. Rac2 in hematopoietic system) or only when they are needed, in response to a specific stimulus (e.g. growth-induced RhoG; (Vincent *et al.*, 1992). Transcriptional regulation might be especially important for members of the Rho family, which are GTPase-deficient (Rnd1-3, RhoH/TTF) and therefore can not be controlled through the classical switch mechanism (Wennerberg and Der, 2004).

1.1.2.1 *GEFs*

In response to diverse extracellular stimuli, GEFs activate Rho GTPases by facilitating the exchange of GTP to GDP. The majority of mammalian GEFs belong to the Dbl family, which comprises 69 known proteins. They are characterized by the presence of a Dbl homology (DH) domain that is essential for the GEF activity.

With the exception of three conserved regions (CR1, CR2, and CR3), DH domains share little sequence homology with each other. However, their three-dimensional structures are very similar. CR1 and CR3, together with conserved residues within the C-terminal helix of the DH domain, participate in the formation of the GTPase interface surface. It interacts with switch regions of GDP-bound Rho GTPases and induces their remodelling. This leads to an alteration of the nucleotide-binding pocket and the dissociation of both GDP and Mg^{2+} cofactor. Because of the high intracellular ratio of GTP to GDP, the exposed pocket is preferentially filled with $GTP \cdot Mg^{2+}$, which results in another conformational change of switch regions and the dissociation of the GEF-GTPase complex (Cherfils and Chardin, 1999; Rossman *et al.*, 2005).

Almost all members of the Dbl family contain a pleckstrin homology (PH) domain (adjacent and C-terminal to the DH domain), which is thought to mediate the translocation of GEFs to membranes and to regulate the activity of the DH domain through allosteric mechanisms. The PH domain can also function as a docking site for proteins that are associated with signalling cascades regulated by Rho GTPases (Rossman *et al.*, 2005). Apart from the DH–PH module, most GEFs contain additional functional domains (e.g. SH2, SH3, Ser/Thr kinase, Ras-GEF, Rho-GAP, PDZ or more PH domains). These are likely to be involved in coupling GEFs to

upstream receptors and signalling molecules (Schmidt and Hall, 2002). The diversity of protein domains and motifs that flank the DH–PH tandem signifies the multitude of different signalling pathways, into which Dbl-family members are integrated.

The DOCK180 family is a genetically distinct group of proteins that have the ability to act as GEFs for Rho GTPases. Currently, 11 mammalian Dock180-related proteins are identified and only Rac and Cdc42 have been shown to be regulated by them. Dock180 family members do not contain the characteristic Dbl homology (DH) domain. Instead, they have a conserved CZH2 domain, which mediates the nucleotide exchange (Cote and Vuori, 2002; Meller *et al.*, 2002). Some members of the Dock180 family need to bind an evolutionarily conserved cofactor ELMO in order to activate Rac (Lu and Ravichandran, 2006).

1.1.2.2 *GAPs*

In general, GAPs act as negative regulators of Rho GTPases by stimulating the weak intrinsic hydrolytic capacity and thereby promoting the transition into GDP-bound form, which results in termination of signalling. The GAP family comprises around 80 proteins, which contain a conserved RhoGAP domain. It consists of about 150 amino acids and shares at least 20% sequence identity between family members, but has no significant resemblance to GAP domains of other Ras superfamily GTPases. The RhoGAP domain is sufficient for interacting with GTP-bound Rho proteins and accelerating their GTPase activity. However, like GEFs, GAPs typically contain additional functional motifs (e.g. Rho-GEF, Arf-GAP, SH2, SH3, Ser/Thr kinase or PH domains), which indicate their integration in various signalling pathways. Some even seem to facilitate the signalling acting as effectors (Moon and Zheng, 2003).

The RhoGAP domain interacts with switch regions and acts by inserting a highly conserved arginine residue, referred to as “arginine finger”, into the GTPase active site. The direct interaction with a conserved glutamine residue in the catalytic center of a Rho protein stabilizes the water molecule in a correct position for the phosphoryl transfer and may reduce the energy barrier for GTP hydrolysis. The arginine residue also interacts with GTP and a water molecule of the hydrated Mg^{2+} ion to stabilize the configuration of the triphosphate group and the ion, as well as to neutralize the charges of the phosphate group (Hakoshima *et al.*, 2003).

1.1.2.3 *GDI*s

In contrast to the abundance of described GAPs and GEFs, only three mammalian RhoGDIs have been identified. They differ in the expression pattern, the localization within the cell and the specificity of interaction with different members of the Rho family. RhoGDI1 is the most abundant and ubiquitous representative, and it is able to form cytosolic complexes with most

members of the Rho family. Expression of RhoGDI2 (Ly/D4GDI) is restricted to hematopoietic cells and is specific for the Rac subfamily GTPases. RhoGDI3 (RhoGDI γ), which is expressed in lung, brain and testis, is associated with the Golgi apparatus and exhibits specificity for RhoB and RhoG (DerMardirossian and Bokoch, 2005)

GDI was first described as a negative regulator of the Rho proteins. They inhibit the spontaneous dissociation of GDP and prevent the interaction with GEFs, sequestering inactive GTPases in the cytoplasm. In addition, they were shown to be able to bind Rho proteins in the active state, blocking the intrinsic GTPase activity and GAP-induced inactivation, as well as preventing the interaction with effector proteins.

However, an equally important function of GDIs seems to be their ability to positively influence Rho signalling, by regulating the membrane-cytosol shuttling of GTPases. They are thought to be actively targeting Rho proteins to specific locations within the cell through interaction with protein complexes or receptors that still remain to be identified (Olofsson, 1999; Dransart *et al.*, 2005).

The GDI structure comprises two structurally distinct regions: the N-terminal flexible domain and the C-terminal immunoglobulin-like fold. Both domains contribute to the binding of Rho proteins and consequently to the regulatory actions of GDIs through protein–protein and protein–lipid interactions. The N-terminal domain interacts with the switch regions of the GTPases and affects the GDP–GTP cycling. The C-terminal domain accommodates the isoprenyl moiety of the GTPase in its hydrophobic pocket, regulating the cytosol-membrane shuttling (Dovas and Couchman, 2005). The exact mechanisms of the membrane targeting and the extraction of Rho GTPases from the complex with GDIs or from the membrane are still not fully understood.

1.1.3 Signalling through Rho GTPases

Extracellular stimuli, such as soluble molecules (growth factors, cytokines and hormones), adhesive interactions (extracellular matrix and cell-cell adhesion) or mechanical stress (tension, compression and fluid shear stress), activate various receptors on the surface of the cell, including G-protein-coupled receptors (GPCRs), tyrosine kinase receptors, cytokine receptors and adhesion receptors such as integrins or cadherins (Kjoller and Hall, 1999).

Relayed through GAPs, GEFs and GDIs, those signals influence the activation state of Rho GTPases. Once activated, Rho proteins interact with a wide spectrum of effectors to stimulate a multitude of downstream signalling pathways (Fig. 1.4).

Rho-family proteins are involved in regulation of the actin cytoskeleton dynamics, cell migration, cell-cell and cell-ECM adhesion, cell-cycle progression, gene transcription, phagocytosis, cytokinesis, neurite growth, cellular morphogenesis and polarization, growth and cell survival (Braga, 2002; Etienne-Manneville and Hall, 2002; Raftopoulou and Hall, 2004; Jaffe and Hall, 2005). In addition, abnormal changes in the activation of Rho GTPases promote malignant transformation of cells and their activity is needed to relay Ras transforming signals (Sahai and Marshall, 2002; Ridley, 2004).

RhoA, Rac1 and Cdc42 are the most extensively characterized members of the Rho family and the current knowledge about the function of Rho GTPases is based predominantly on data obtained during studies of those three members of the family. As other Rho proteins are further analysed, some of their functions seem to overlap with those already described, while others are clearly distinct, especially in case of the atypical Rho GTPases (Wennerberg and Der, 2004). The best described role of the three classic Rho GTPases, which seems to be shared by majority of the family members, is their involvement in the actin cytoskeleton regulation. However, their respective functions are quite distinct. RhoA regulates the formation of contractile actin/myosin stress fibres and the organization of focal contacts (Ridley and Hall, 1992), Rac1 is involved in the formation of lamellipodia and focal complexes (Ridley *et al.*, 1992) and Cdc42 triggers the formation of filopodia as well as focal contacts (Kozma *et al.*, 1995; Nobes and Hall, 1995).

Less-analysed members of the Rho family may prove to be involved in biological phenomena, which currently are thought to be controlled solely by RhoA, Rac1 or Cdc42, because they were the only Rho proteins considered and analysed at the time. In addition, dominant-negative (DN) and constitutively active (CA) forms of GTPases, commonly used for the analysis, might exert unspecific effects. DN GTPases have higher affinity to GEFs and lower affinity to nucleotides than wild-type forms. Therefore, they successfully compete with endogenous proteins for GEF-binding and sequester available GEFs by remaining longer in the complex (1.1.2.1). Moreover, even if bound with GTP, DN forms are not able to interact with effectors. Expression of DN mutants at high enough concentration to ensure complete saturation of GEFs is crucial for an effective inhibition of wild-type GTPases. Since many GEFs are not specific for a single Rho GTPase, DN mutants may inhibit more than one Rho GTPase, making the interpretation of results difficult (Feig, 1999). Therefore, studies using cells with genetically induced ablation of GTPases seem to be a good alternative tool to refine the knowledge obtained using DN forms. CA mutants lack the intrinsic GTPase activity and are thought to be permanently bound with GTP. As their activation can not be controlled endogenously, they may cause atypical effects, especially when overexpressed.

1.1.4 Crosstalk between Rho GTPases

In their role as regulators of intracellular processes, Rho GTPases influence downstream signalling pathways, not only by controlling their effector molecules, but also through modulating the activation of other GTPases. Many examples of crosstalk between members of Rho family (Fig. 1.5), as well as with other GTPases from the Ras superfamily have been described. There are examples where one family member suppresses the activity of another by stimulating a GAP, or elevates it by stimulating a GEF. In addition, there are proteins (e.g. Bcr and Abr) that contain both GAP and GEF domains for different Rho members. The interplay between family members is also mediated by interactions between their respective downstream signalling pathways (Burrige and Wennerberg, 2004).

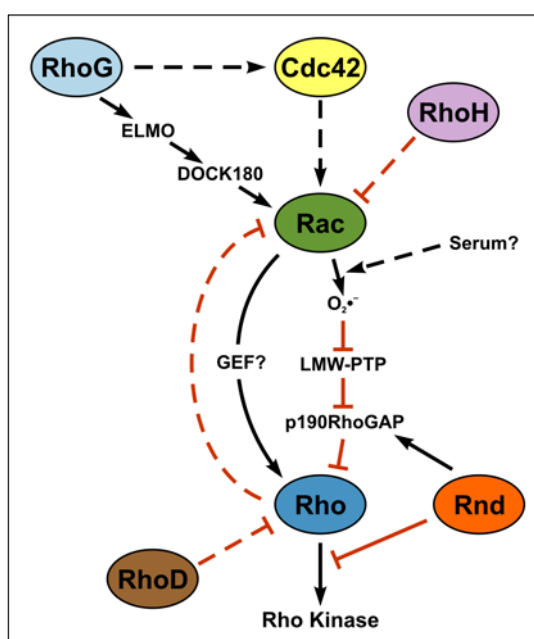


Fig. 1.5 Crosstalk between Rho GTPases. Activating signals are shown as black arrows, inactivating as red. Direct signals are drawn as solid lines, whereas signals with unknown signalling intermediates are drawn as dashed lines. O₂^{•-}: superoxide anion; LMW-PTP: low molecular weight protein tyrosine phosphatase (modified from Burrige and Wennerberg, 2004).

The first described example of crosstalk between Rho GTPases was a hierarchical cascade linking Rho, Rac and Cdc42. In serum-starved Swiss 3T3 fibroblasts, activation of Cdc42 induces activation of Rac, which in turn leads to activation of Rho (Ridley *et al.*, 1992; Kozma *et al.*, 1995; Nobes and Hall, 1995). In contrast, active Rac inhibits Rho function in growing NIH3T3 cells (Sander *et al.*, 1999). A possible mechanism of Rho inhibition was recently described (Fig. 1.5). The Rac-mediated production of oxygen radicals causes an inhibition of the low molecular weight protein tyrosine phosphatase (LMW-PTP), which in turn leads to the activation of p190RhoGAP that stops Rho signalling (Nimnual *et al.*, 2003).

RhoG was reported to activate Rac1 and Cdc42 (Gauthier-Rouviere *et al.*, 1998) and a

signalling pathway influencing Rac1 was recently described (Fig. 1.5). Activated RhoG interacts directly with ELMO and forms a ternary complex with Dock180 to induce activation of Rac1 (Kato and Negishi, 2003).

Rnd GTPases can inhibit RhoA signalling by activating p190RhoGAP (Wennerberg *et al.*, 2003). In addition, Rnd3/RhoE can bind and inactivate Rho Kinase (Riento *et al.*, 2003). RhoH was shown to inhibit Rac1, Cdc42 and RhoA induced signalling (Li *et al.*, 2002), while RhoD counteracts RhoA activity (Tsubakimoto *et al.*, 1999).

1.1.5 The Rac subfamily

The Rac1 subfamily comprises four proteins. Rac1, Rac2 and Rac3 share ~88% sequence identity and differ primarily within the last 15 amino acid residues. RhoG is the most divergent member of the subfamily and shares 72% of the overall amino acid sequence with Rac1. All Rac-related GTPases are able to stimulate the formation of lamellipodia and membrane ruffles, but they were shown to have distinct functions as well (Wennerberg and Der, 2004).

Rac1 is expressed ubiquitously and its constitutive ablation results in embryonic lethality around day 8.5 of development (Sugihara *et al.*, 1998). *In vitro* studies showed that, in addition to the involvement in the regulation of the actin cytoskeleton organization (Ridley *et al.*, 1992), Rac1 plays a role in the cell-cycle progression (Olson *et al.*, 1995), the activation of the JNK/SAPK and p38 MAP kinase cascades (Coso *et al.*, 1995; Minden *et al.*, 1995), the regulation of NADPH oxidase activity resulting in the production of superoxide radicals (Diekmann *et al.*, 1994) and the activation of NF- κ B (Perona *et al.*, 1997). In addition, Rac1-mediated signalling was found to be involved in the regulation of tight junction properties (Jou *et al.*, 1998; Mertens *et al.*, 2005), cadherin-mediated cell-cell adhesion (Braga *et al.*, 1997; Takaishi *et al.*, 1997; Braga *et al.*, 1999; Braga *et al.*, 2000), integrin-mediated cell-matrix adhesion (Hotchin and Hall, 1995; Nobes and Hall, 1995; Price *et al.*, 1998) and establishment of cell polarity (O'Brien *et al.*, 2001).

A splice variant of Rac1 was described to be expressed in humans, preferentially in breast and colon cancers (Jordan *et al.*, 1999; Schnelzer *et al.*, 2000). Rac1b is generated by an alternative exon usage and contains an additional 19-residue insert directly after the switch II region. It exhibits properties consistent with a constitutively activated protein as it shows an increased intrinsic guanine nucleotide exchange rate, decreased intrinsic GTPase activity and enhanced association with the plasma membrane, likely because of its inability to interact with GDIs (Matos *et al.*, 2003; Fiegen *et al.*, 2004). In addition, it has different from Rac1 signalling properties, as it is unable to stimulate formation of lamellipodia or activation of the protein

kinase PAK and the JNK pathway, but retains the ability to activate the NF- κ B transcription factor (Matos *et al.*, 2003).

Rac2 is expressed only in hematopoietic cells, where it seems to have specialized functions, setting it apart from Rac1. Rac2 deficiency allows for normal development but results in several neutrophilic, phagocytic and lymphocytic defects (Roberts *et al.*, 1999; Li *et al.*, 2000; Croker *et al.*, 2002; Gu and Williams, 2002). Many of these defects seem to be caused by the lack of Rac2-specific activation of NADPH oxidase. Comparison of defects in hematopoietic cell function, observed after single and combined ablations of Rac1 and Rac2, demonstrated both overlapping and distinct roles of these two related GTPases in hematopoietic cells (Gu *et al.*, 2003; Walmsley *et al.*, 2003; Benvenuti *et al.*, 2004).

Rac3 is most highly expressed in the developing nervous system and in adult brain. In addition it was described to be upregulated in fibroblasts upon serum stimulation (Haataja *et al.*, 1997) and to be hyperactive in breast cancers (Mira *et al.*, 2000). Rac3-deficient mice have no obvious anatomical or physiological defects. However, they show interesting behavioural abnormalities (Corbetta *et al.*, 2005). A study using mice lacking Rac3 showed its stimulatory influence on the development of lymphoblastic leukaemia (Cho *et al.*, 2005).

Transcriptionally regulated expression of RhoG is elevated during the G1 phase of the cell cycle, and it has been implicated in cell growth (Vincent *et al.*, 1992). RhoG interacts with some but not all of the same effectors as Rac1 (Wennerberg *et al.*, 2002; Prieto-Sanchez and Bustelo, 2003), and it has also been shown to activate Rac1 and Cdc42 (Gauthier-Rouviere *et al.*, 1998; Katoh *et al.*, 2006) (1.1.4). In addition RhoG was reported to play a specific role in the nerve growth factor (NGF)-mediated neurite outgrowth in PC12 cells (Katoh *et al.*, 2000).

1.2 Skin

The primary purpose of skin and its appendages (i.e. hairs and glands) is to provide the body with a barrier against the environment. It protects the body from dehydration, temperature changes, radiation, mechanical trauma and infections, as well as mediates the interaction with the environment (sensory function).

The skin can be roughly divided into the outward epidermis and the underlying dermis, which are separated by the basement membrane (BM). The mesoderm-derived dermis provides mechanical support and nourishment for the avascular epidermis. In addition, it is a source of signalling cues inducing the differentiation of the epidermis and the development of hair follicles. The dermis consists mostly of fibroblasts, surrounded by an extracellular matrix secreted by these cells. The matrix is composed of collagen and elastin fibres, which convey the

strength and elasticity of the skin, and of a proteoglycan gel that imparts the capacity to retain water. The aqueous portion of the matrix permits diffusion of nutrients, metabolites and signalling molecules and creates turgor pressure able to withstand considerable compression force (Byrne and Hardman, 2002). Below the dermis lays the subcutaneous layer consisting mainly of adipocytes. It provides thermal isolation, cushions the skin, and attaches it to the underlying muscle. In mouse skin, thickness of the subcutis changes periodically as it is adjusted to the length of the hair follicles.

The BM originates from components secreted by both keratinocytes (epidermal cells) and fibroblasts, which include laminins (5, 6 and 10), nidogen (Nd), collagen IV and heparin sulphate proteoglycan (HSPG). Anchoring fibrils, composed of collagen VII, attach the BM to the underlying dermis (McMillan *et al.*, 2003), while the epidermis is anchored to the BM mainly through integrin receptors. Integrins $\alpha_2\beta_1$ and $\alpha_3\beta_1$ bind collagen IV and laminin 5 (LN5), respectively, and connect the BM to the actin cytoskeleton in the cell. The $\alpha_4\beta_6$ integrins form hemidesmosomes, which anchor the intermediate filament network inside the keratinocytes to LN5 within the BM (Watt, 2002). Attachment to the BM plays a critical role in the establishment of epithelial polarity providing a spatial cue for reorganization of cell morphology.

1.2.1 Epidermis morphology and differentiation

The epidermis is a stratified squamous epithelium derived from the ectoderm, a single-cell sheet of undifferentiated epithelial cells constituting the outer layer of the post-gastrulation embryo. The distinct layers of the epidermis represent successive stages of the terminal differentiation process, which results in the formation of a cornified protective barrier of the body (Fig. 1.6). The ectoderm gives rise not only to the epidermis but to hair follicles (HFs), sebaceous glands (SGs) and apocrine glands as well (Byrne and Hardman, 2002).

Cells attached to the BM form the basal layer of the epidermis and comprise the only keratinocytes in the epidermis capable of proliferation. Stem cells, residing in the basal layer ensure the continuous self renewal of those transit amplifying cells and thus the whole epidermis (Blanpain and Fuchs, 2006). In addition, melanocytes (pigment producing cells) and Merkel cells (mechanoreceptors), which constitute 5-10% of all epidermal cells, are located in the basal layer. Other non-epithelial cells found in the epidermis are Langerhans cells, immature dendritic cells involved in the immunological response to a pathogen infection (antigen uptake, processing and presentation). They reside in the spinous layer and constitute around 5% of all epidermal cells.

Mitotically active keratinocytes express keratins 5 and 14 (K5/K14) (Fuchs and Green, 1980) and extracellular matrix components (mainly LN5). The latter are secreted at the basal side

and assembled into the BM by integrin receptors that mediate cell-ECM adhesion of epidermal cells (Watt, 2002). Cell-cell adhesion between basal keratinocytes is maintained by desmosomes and adherens junctions (cadherin-dependent cell–cell contacts), which are associated with the actin cytoskeleton and the intermediate filament network, respectively (1.3). After undergoing a limited number of divisions, transit amplifying cells withdraw from the cell cycle. They downregulate expression of integrins, matrix components and K5/K14, detach from the BM and move upwards starting the terminal differentiation process.

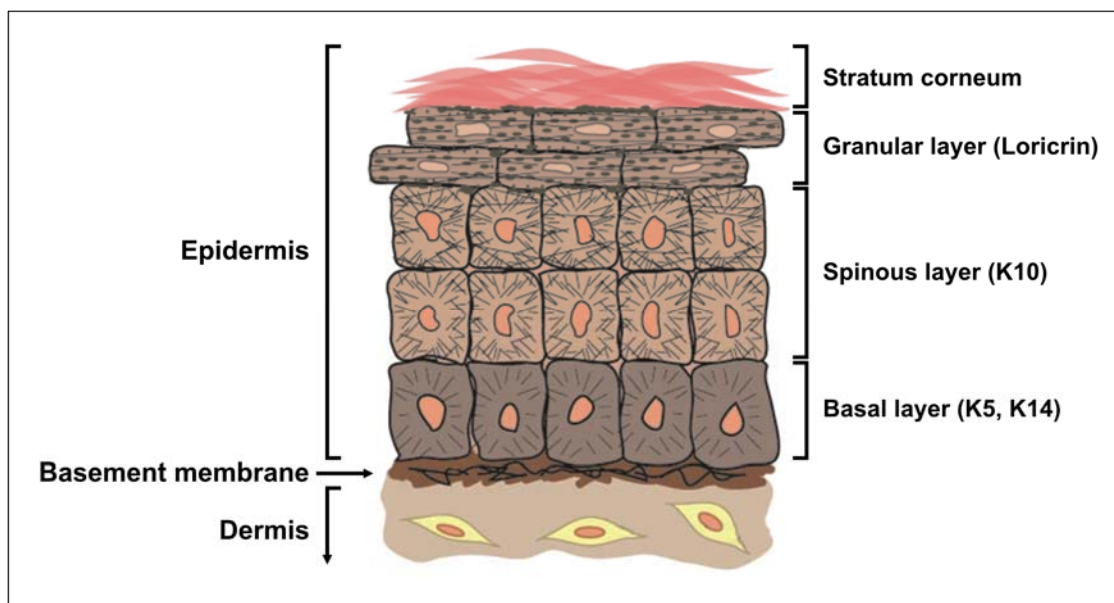


Fig. 1.6 Schematic representation of the epidermis. Skin, the outer layer of the body, consists of the epidermis and the dermis, which are separated by the basement membrane (BM). The epidermis is an example of a stratified epithelium and consists of distinct layers of keratinocytes, representing successive stages of a terminal differentiation process. Cells in each layer of the epidermis express specific keratins (brackets) (modified from Alonso and Fuchs, 2003).

Suprabasal keratinocytes in the spinous layer express high amounts of K1 and K10 (Fuchs and Green, 1980). These keratins are assembled into intermediate filaments, which aggregate into resilient bundles. The filament network facilitates an increase in the tensile strength of cells by anchoring to desmosomes, which are abundant in the suprabasal layer and enable dissipation of tension across the epithelial sheet (Fuchs and Cleveland, 1998). Transition into the granular layer is characterized by expression of filaggrin and loricrin (Rothnagel *et al.*, 1987; Mehrel *et al.*, 1990). Filaggrin aggregates the keratin filaments into tight bundles, which promote the collapse of cells into a flattened shape. Tight junctions are formed between cells in the granular layer, contributing to barrier properties of the epidermis (Furuse *et al.*, 2002). Keratinocytes complete the differentiation as they form the cornified envelope beneath the plasma membrane, which consists of proteins (involucrin, loricrin, trichohyalin) crosslinked by transglutaminases and specific lipids on the outside. Finally, terminally differentiated keratinocytes cease

transcriptional and metabolic activity, undergo an apoptosis-related cell death and become squames that constitute the stratum corneum (cornified layer) (Kalinin *et al.*, 2002; Candi *et al.*, 2005). Outer squames are shed from the surface of the skin and are constantly replaced by new layers of terminally differentiated keratinocytes. In mouse skin, the entire transition process from a basal layer keratinocyte to a squame cell takes 10–14 days (Potten, 1975).

The molecular mechanisms controlling epidermal morphogenesis are still being investigated, however the transcription factor p63, Ca^{2+} , Notch and IKK α signalling pathways have been shown to play an important role in the differentiation of the epidermis (Koster and Roop, 2004).

1.2.2 Hair follicle morphogenesis and cycling

Hair follicles (HFs) vary in size and shape, depending on their location, but they all have the same basic structure and follow the same developmental path. After the morphogenesis HFs enter a perpetual cycle of deterioration and regrowth (Fig. 1.7).

The formation of HFs starts during embryogenesis and the precise distribution, number and type of HFs are established at the time of the initiation. The morphogenesis of murine pelage hairs starts between day 14 and 17 of the embryonic development (depending on the hair type) and is completed by day 8 after birth (Schmidt-Ullrich and Paus, 2005).

The HF development is controlled by the signal exchange between the epidermis and the underlying dermal cells (Millar, 2002; Schmidt-Ullrich and Paus, 2005) and it can be divided into nine distinct morphological stages (Hardy, 1992; Paus *et al.*, 1999). The signal initiating the HF formation comes from the dermis and leads to the activation of basal layer keratinocytes (stage 0), which change shape, organize into morphologically distinct hair placodes and signal in turn to the underlying fibroblasts, causing them to gather below (stage 1) (Fig. 1.7). The signalling crosstalk between the mesenchymal condensate and the epithelial hair placode drives proliferation in both structures, causing the downgrowth of the hair germ and a cap-like aggregation of fibroblasts at its proximal end (stage 2). Proliferating epithelial cells form the hair peg, an elongated column consisting of multiple layers of undifferentiated keratinocytes concentrically arranged around the follicular axis. The fibroblast cap transforms into the ball-shaped dermal papilla (DP), located in a cavity developed at the proximal end of the column (stage 3) (Fig. 1.7). The elongating hair peg forms a bulb-like thickening at the proximal end, which starts to engulf the DP. Proliferating keratinocytes in the proximity of the DP, begin to terminally differentiate into the inner root sheath (IRS), forming a cone-shaped structure above the DP (stage 4). In the subsequent bulbous peg stage (stage 5) (Fig. 1.7) the HF reaches the subcutis and the DP is almost completely enclosed by the hair bulb. The melanin-containing hair

shaft (HS) begins to form from the matrix cells in the bulb and grows upwards within a rigid tube of the keratinized IRS, which extends already halfway up the HF. In addition, in the distal part of the HF, first sebocytes develop from epithelial cells and the bulge (follicular stem cells niche; Cotsarelis *et al.*, 1990) is formed within the outer layer of the HF, which will become the outer root sheath (ORS).

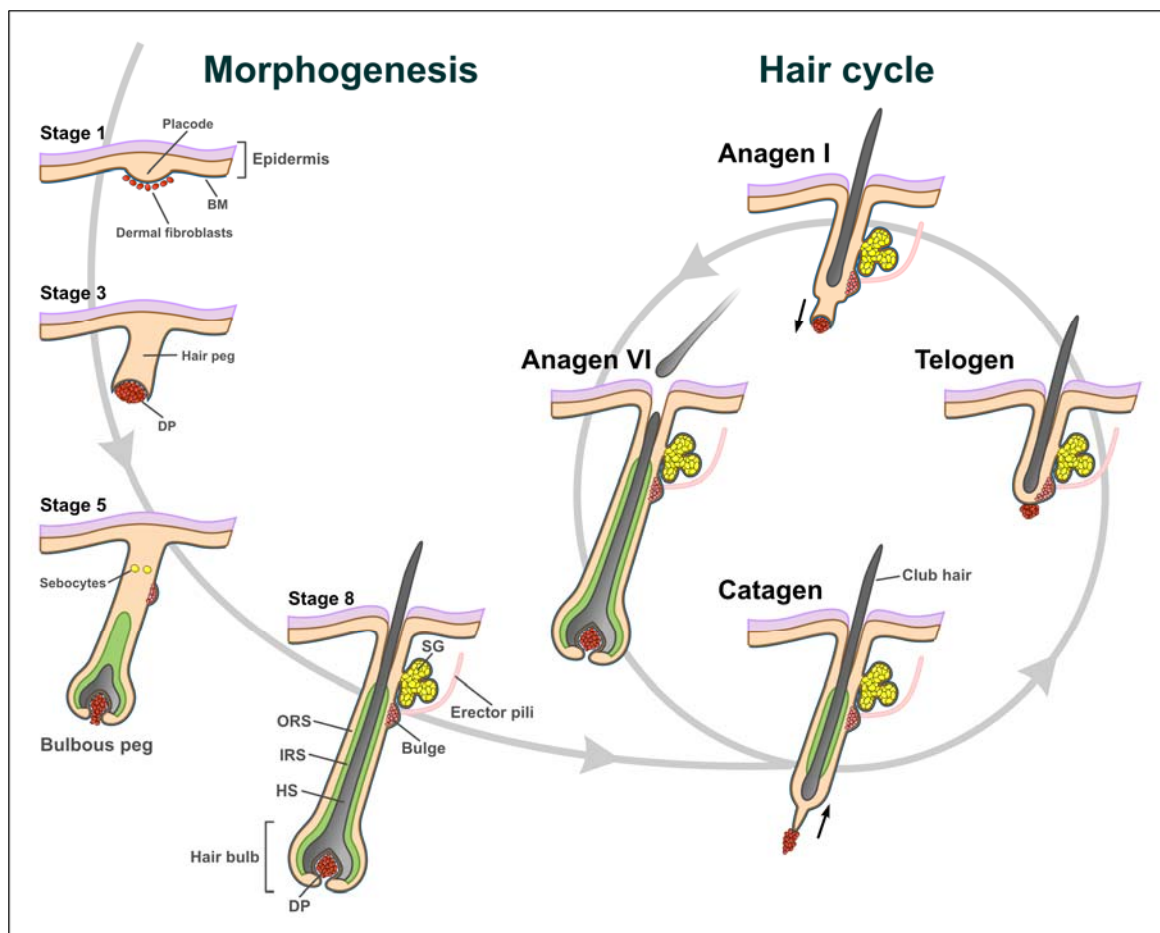


Fig. 1.7 Key stages of the HF morphogenesis and the hair cycle. Crosstalk between epidermis and dermis leads to the formation of the hair germ (placode) and the aggregation of dermal fibroblast beneath (stage 1). Downward growth of the placode, with attached at the bottom fibroblasts, results in the growth of the hair peg, which proximal end starts to engulf the dermal papilla (DP) formed from dermal fibroblasts (stage 3). Signalling from the DP induces the formation of the bulb and the differentiation of precursor cells within into the inner root sheath (IRS) and hair shaft (HS) lineages. The bulge and first sebocytes appear in the upper part of the bulbous peg (stage 5). Further development leads to the formation of a mature HF with the HS emerging through the epidermis (stage 8). After the completed morphogenesis, the HF enters a continuous growth-regression cycle, which consists of three stages: growth (anagen), involution (catagen) and rest (telogen). The upper part of the HF, containing the sebaceous gland (SG) and the bulge, remains intact. After telogen, crosstalk between the DP and stem cells residing in the bulge leads to the formation of the proliferating hair germ (anagen I) and regrowth of the HF (anagen VI). The entire follicle is surrounded by the BM, which is engulfed in turn by the dermal sheath (not shown) (based on Paus *et al.*, 1999; Muller-Rover *et al.*, 2001).

Further development of the HF (stage 6-7) includes: formation of the hair canal (infundibulum), organization of sebocytes into the sebaceous gland (SG), elongation of the IRS and the HS and final enclosure of the DP by the hair bulb. The morphogenesis ends when the

HF, with fully differentiated layers, reaches the subcutaneous muscle and the HS emerges from the epidermis. A fully grown HF is accompanied by the erector pilli muscle, attached at the level of the bulge (stage 8) (Fig. 1.7) (Paus *et al.*, 1999). The progenitor matrix cells at the base of the HF continue to proliferate and differentiate, yielding a period of active hair growth, lasting around a week in case of murine pelage hairs.

When the proliferative potential of bulb cells is exhausted, HFs enter a perpetual cycle of growth and regression which affects only the lower part of the HF (Fig. 1.7). It starts from catagen, the involution phase, during which the HF structure below the bulge region undergoes a controlled, apoptosis-driven degeneration, beginning in the hair bulb and continuing upwards. The HS detaches from the proliferative matrix and forms the club hair, which coincides with upwards regression of the IRS. Subsequently, the club hair, surrounded by the ORS, is moving up to the level of the bulge. An epithelial strand, stretching from the retracting ORS, pulls the DP behind, until the base of the permanent segment of the HF, where it rests in the proximity of the bulge (Muller-Rover *et al.*, 2001). During late catagen stem cells from the lowermost portion of the bulge form the secondary hair germ at the bottom of the permanent part of the HF (Ito *et al.*, 2004). After 3-4 days, catagen is completed and the HF enters a resting phase, telogen, during which it remains relatively dormant (Fig. 1.7). The first telogen in the murine hair cycle last only 1-2 days, but the following ones are more than two weeks long (Alonso and Fuchs, 2006).

The transition from telogen to anagen, the growth phase, is initiated by signalling crosstalk between the DP and the bulge (Stenn and Paus, 2001). The dormant progenitor cells in the secondary hair germ are activated and begin to proliferate forming a growing hair germ, which emerges from the bottom of the permanent part of the HF and starts to engulf the DP (anagen I) (Fig. 1.7). The further growth and differentiation of the HF resembles the development during the HF morphogenesis and results in the reconstitution of the lower part of the HF (anagen VI) (Muller-Rover *et al.*, 2001). The duration of anagen determines the length of the hair and is dependent upon continued proliferation and differentiation of matrix cells at the follicle base. In the mouse pelage it lasts around 3 weeks.

The mature HF consists of several distinct concentric layers of cells (Fig. 1.8). The most outer layer, the ORS, is continuous with the basal layer of the epidermis and surrounds the whole HF. It constitutes a single-layered epithelial sheath around the lowermost hair bulb and the DP, but is multilayered along the length of the HF. Although the ORS cells exhibit horizontal differentiation, they do not become keratinized, with exception of the uppermost section of the HF (Stenn and Paus, 2001). In the isthmus (between the insertion of the SG and the bulge) and the infundibulum, ORS layers show trichilemmal keratinisation (Pinkus *et al.*, 1981) and

epidermal-type terminal differentiation, respectively. The ORS is established during the early stages of anagen by the downward growth of the regenerating epithelium and then maintains itself, independent of the germinative matrix in the hair bulb, by basal cell growth (Stenn and Paus, 2001).

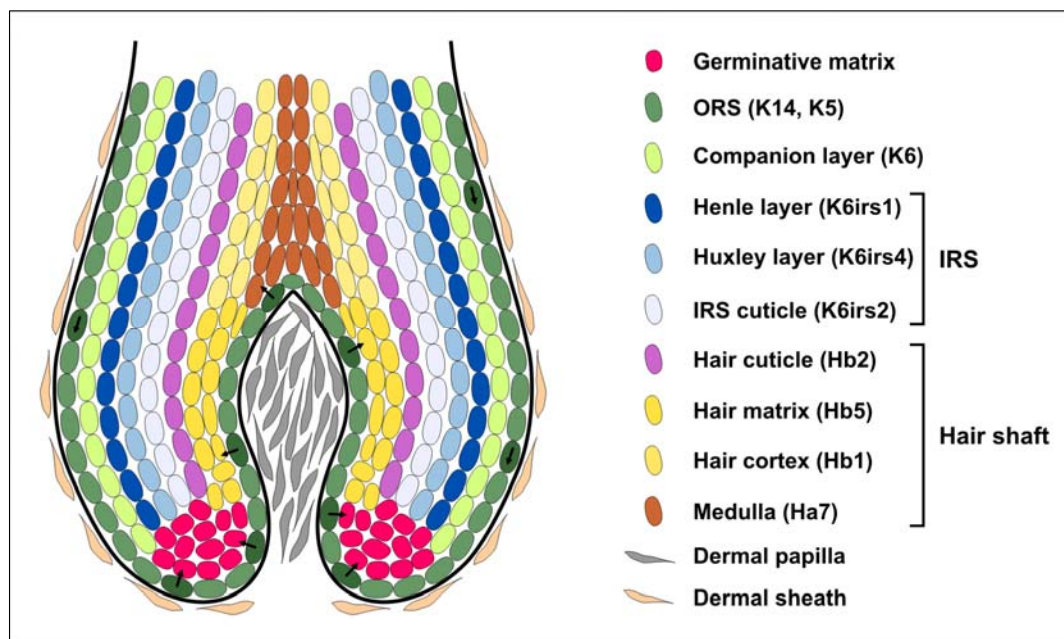


Fig. 1.8 Distinct hair follicle layers generated in the hair bulb. Several lineages of keratinocytes differentiate from the germinative matrix and form concentric layers of the HF and the HS. Stem cells migrating from the bulge down along the ORS (darker green) give rise to the germinative matrix as well as progenitor cells of the hair matrix and the medulla, directly (arrows). Examples of keratins specific for hair follicle compartments are given in brackets (based on Rogers, 2004; Langbein and Schweizer, 2005).

All the other layers differentiate from the germinative matrix, located at the bottom of the hair bulb around the dermal papilla. The germinative matrix contains undifferentiated transiently amplifying precursor cells derived from bulge stem cells during the formation of the HF. It was also shown to be resupplied during the anagen by the stem cells migrating down the ORS from the bulge region (Tumbar *et al.*, 2004). The companion layer (CL), whose role is not clear, is a single-cell layer separating the ORS and IRS (Rogers, 2004). The function of the IRS, a rigid tube-like structure, is to shape and support the HS. It consists of three distinct layers: the Henle layer, the Huxley layer and the IRS cuticle, which differ in the thickness and cell organization. The cells of the IRS undergo so called soft keratinisation by forming trichohyalin granules and are sloughed off after reaching the hair canal. The mature HS is a differentiation product of trichocytes, proliferating cells constituting the hair matrix and derived from the germinative matrix (Fig. 1.8). Hair matrix cells give rise to the hair cortex and the medulla (present in some types of hair). The cortex constitutes the bulk of the hair shaft and becomes fully keratinized in the terminal differentiation process. The surface of the HS is formed by the hair cuticle, which

comprises a single layer of scale-like keratinized cells, pointing upwards. They interlock with the IRS cuticle, composed of scale-like organized cells pointing downwards. As a result, both the HS and the IRS move up the HF as a single unit (Stenn and Paus, 2001; Rogers, 2004).

While many different epithelial (ORS, IRS) or hair (HS) keratins are expressed in the HF, keratinocytes of each layer express at least one unique keratin (Fig. 1.8). This feature enables detailed analysis of HF differentiation and morphology by using specific antibodies to visualize HF compartments. Interestingly, unlike follicular stem cells, transiently amplifying cells in the germinative matrix do not express any known epithelial or hair keratins (Langbein and Schweizer, 2005).

The molecular mechanisms controlling morphogenesis and cycling of the HF are not fully understood, but the genetic studies in mice showed the importance of Wnt/ β -catenin, bone morphogenetic protein (BMP), sonic hedgehog (SHH), fibroblast growth factor (FGF), epidermal growth factor receptor (EGF), NF- κ B, and Notch signalling pathways (Millar, 2002; Schmidt-Ullrich and Paus, 2005; Blanpain and Fuchs, 2006). Stem cells residing in the bulb not only sustain the HF cycling but are recruited during wound healing to help the repair of the epidermis (Ito *et al.*, 2005) and are thought to contribute to the SG lineage (Alonso and Fuchs, 2003).

1.3 Epithelial cell-cell adhesion and polarization

Cell–cell adhesion is essential for the integrity of epithelial sheets, as well as for the establishment and maintenance of the polarized epithelial phenotype (Yeaman *et al.*, 1999). In the stratified epithelium, adhesion between cells is mediated by three types of junctions: adherens junctions, desmosomes and tight junctions. Adherens junctions and desmosomes are present between keratinocytes throughout the whole epidermis, while tight junctions are formed only in the granulose layer of the epidermis (Perez-Moreno *et al.*, 2003) (1.2.1).

Both adherens junctions and desmosomes convey a strong cell-cell adhesion. Adherens junctions are the earliest contacts established between epithelial cells and are necessary for the formation of other adhesive structures. Through their interaction with the actin cytoskeleton, adherens junctions play a crucial role in the morphological changes leading to the polarization of the epithelium (Braga *et al.*, 2000). Desmosomes provide epithelial sheets with mechanical strength, which is required to maintain the integrity of the epidermis, by anchoring the intermediate filament network to the sites of cell-cell contacts (Green and Gaudry, 2000). Tight junctions control the permeability of the epithelial layers supporting the barrier function of the stratified epithelium (Furuse *et al.*, 2002).

Adherens junctions are formed by cadherins, transmembrane receptors mediating Ca^{2+} -dependent cell-cell adhesion. The extracellular domain of a cadherins is responsible for dimerization of receptors. The cytoplasmic tail binds p120-catenin that plays a role in the clustering of cadherins, and β -catenin. The interaction of β -catenin with α -catenin conveys the association of cell-cell contacts with the actin cytoskeleton after the initiation of adhesion. E-cadherin is the main cadherin found in adherens junctions between epidermal keratinocytes (Fukata and Kaibuchi, 2001).

Establishment of the cadherin-mediated cell-cell adhesion comprises several steps that lead to the development of the epithelial phenotype (Braga *et al.*, 2000). In the presence of Ca^{2+} , dimerized extracellular domains of cadherins change conformation and bind corresponding receptors of neighbouring cells. The homophilic interaction induces zipper-like clustering of cadherin receptors and engagement of actin filaments by cytoplasmic tail complexes. The accumulation of actin filaments at sites of cell-cell contacts stabilizes cadherin clusters and increases the strength of adhesion. The reorganization of the actin cytoskeleton (induced by anchoring to adherens junctions) and the subsequent rearrangement of the microtubule and intermediate filament networks lead to the morphological change characteristic for epithelial cells (cuboid shape). Signalling pathways triggered by the formation of cadherin contacts, contribute to the establishment of the epithelial phenotype by inducing different cellular processes (e.g. establishment of other adhesive structures and distinct membrane domains, changes in the vesicle transport, expression of epithelia-specific genes) (Braga, 2002).

In the epidermis, cell-cell adhesion is a highly dynamic process. As the epithelial sheets migrate upwards towards the skin surface during terminal differentiation, epidermal cells must constantly change their intercellular interactions. During wound healing, epidermal cells transiently downregulate intercellular adhesion concomitant with an increase in cell proliferation (Fuchs and Raghavan, 2002).

All three classical Rho GTPases (Rho, Rac and Cdc42) were shown to be involved in the formation and maintenance of adherens junctions and/or in the regulation of other cellular processes leading to the establishment of the epithelial phenotype *in vitro* (Braga *et al.*, 2000; Van Aelst and Symons, 2002).

1.3.1 Role of Rac1 in the epithelial cell-cell adhesion

The involvement of Rac1 in the regulation of the E-cadherin-dependent cell-cell adhesion of epithelial cells was demonstrated by several *in vitro* studies. However, the precise role of Rac1 in the assembly and maintenance of these structures is unclear, due to partially conflicting reports.

The presence of DN-Rac1 in both primary human keratinocytes and MDCK cells inhibited Ca^{2+} -induced formation of adherens junctions (Braga *et al.*, 1997; Takaishi *et al.*, 1997), suggesting that Rac1 activity is necessary for their establishment. In addition, microinjection of DN-Rac1 in primary human keratinocytes led to the disruption of adherens junctions (Braga *et al.*, 1997), indicating a critical role of Rac1 in the maintenance of those adhesion structures. However, the inhibitory effect of DN-Rac1 was dependent on the maturation state of the cell-cell contacts as newly formed junctions were more sensitive to the lack of the active Rac1 (Braga *et al.*, 1999). Those differences suggested a reduced requirement for Rac1 after the maturation of adherens junctions.

MDCK cells expressing CA-Rac1 or Tiam1 (a Rac1-specific GEF) displayed an increased E-cadherin accumulation and actin polymerization at cell-cell contacts (Hordijk *et al.*, 1997; Takaishi *et al.*, 1997) indicating that Rac1 promotes the formation of adherens junctions and mediates the reorganization of the actin cytoskeleton necessary for stabilization of cadherin-dependent adhesions. In contrast, CA-Rac1 microinjected into primary human keratinocytes had either no effect on the E-cadherin accumulation at the cell-cell contacts (Braga *et al.*, 1997) or caused a specific removal of E-cadherin from adherens junctions at higher concentrations (Braga *et al.*, 2000). While the initial formation of adherence junctions was not prevented by the presence of CA-Rac1, the stability of cadherin receptors was compromised. However, the susceptibility of cell-cell contacts to the CA-Rac1-induced disintegration was reduced after their maturation (Braga *et al.*, 2000). The discrepancy between the reported effects of CA-Rac1 on adherent junctions might have resulted from the differences in the cell type or the levels of CA-Rac1 used during the experiments.

Taken together those data suggested that Rac1 is essential for the formation of E-cadherin-dependent cell-cell contacts and plays a role in the maintenance of stable adherens junctions. The negative effects of both DN-Rac1 and elevated levels of activated Rac1 on the stability of E-cadherin-dependent cell-cell contacts seem to confirm the notion, that the amount of active Rac1 must be precisely regulated in the cell in order to fulfil the specific biological function.

Different studies showed that clustering of E-cadherin receptors activated Rac1 and recruited it to the sites of cell-cell contacts both in MDCK cells and primary keratinocytes (Nakagawa *et al.*, 2001; Noren *et al.*, 2001; Betson *et al.*, 2002). That suggested a feedback signalling model of Rac1 involvement in the formation of cell-cell contacts, in which initial adhesion activates Rac1, which in turn induces the reorganization of the actin cytoskeleton necessary for the stabilization of adherens junctions. Moreover, downstream signalling initiated by Rac1 was proposed to play

a role in the establishing of the polarized epithelial phenotype (Braga, 2002).

1.4 Aims of the project

Several *in vitro* studies showed an important function of Rac1 in the regulation of cadherin-dependent cell-cell contacts between epithelial cells. These contacts are essential for the establishment and maintenance of the polarized cell morphology characteristic for epidermal keratinocytes as well as for the integrity of epithelial sheets in the epidermis. However, no analysis of the potentially crucial role of Rac1 in the regulation of the cadherin-dependent cell-cell adhesion *in vivo* was performed, before this project was initiated.

Since constitutive deletion of the murine *rac1* gene leads to early embryonic lethality, preventing the analysis of the Rac1 function in differentiated tissues, the first goal of this project was to generate genetically modified mice, which would allow for a conditional deletion of the *rac1* gene.

The main aim of this work was to investigate the role of Rac1 in the epidermis and hair follicles, and thus to explain the function of Rac1 in the regulation of cell-cell contacts between epithelial cells *in vivo*. Therefore, mice with a keratinocyte-specific deletion of the *rac1* gene were generated and analysed.

A final aim was to study the function of Rac1 in the establishment of cell-cell contacts between differentiating cells and its role in the formation of polarized epithelium during early embryonic development. Thus, Rac1-deficient embryonic stem cells were generated and their ability to form embryoid bodies was analysed.

2 MATERIALS AND METHODS

2.1 Animals

Mice used in this study were housed under SPF (Specific Pathogen Free) conditions in an animal facility of the Max Planck Institute of Biochemistry in Martinsried. They had continuous access to drinking water and standard rodent food. Light regime was 12 h of light per day. In the course of breeding, offspring were normally weaned 3 weeks after birth. At that time animals were ear-marked and tail tips were cut for genotype analysis. When genotyping of younger animals was required, they were marked by toe-clipping within 5 days after birth. The genotyping was performed by PCR.

Animals used for experiments were sacrificed by cervical dislocation. Alternatively, very young mice (few days after birth) were decapitated or sacrificed using ether. All experiments were performed in accordance with German Animal Protection Law.

2.2 Common materials

2.2.1 Chemicals

Basic chemical compounds used in this study were purchased from the following companies: Merck, Sigma, Fluka/Riedel-de Haën or Roth.

Double-distilled water (ddH₂O), purified with the Milli-Q-System (Millipore) was preferably used to prepare the solutions and buffers. Buffers used in gross quantities (i.e. running buffers) were prepared or diluted from stock solutions with normal distilled water (dH₂O). In molecular biology procedures ddH₂O was autoclaved before the use.

10x PBS

<i>NaCl</i>	80.1 g	→ adjusted to pH 7.4
<i>KCl</i>	2.0 g	→ diluted to working solution (PBS) with ddH ₂ O
<i>Na₂HPO₄ × 2H₂O</i>	14.4 g	→ autoclaved for 30 min at 120°C (when used for cell culture)
<i>KH₂PO₄</i>	2.0 g	
<i>ddH₂O</i>	filled up to 1000 ml	

2.2.2 Disposable plastic materials

- bacteria: plates (10 cm Ø; #662102), tubes (14 cm; #191161) – Greiner Bio-One
- cell-culture: dishes (6/10 cm Ø), T-flasks with vent caps (25/75/175 cm³) – BD Falcon

- plates (6/24/96 well; #3516/26/96) – Corning
- pipettes (5/10/25 ml; #4487/8/9) – Corning (Costar)
- syringe filters (0.2 μm ; #06-001), syringes (10/20 ml, #300912/629) – Renner GmbH, BD
- tips (10/200/1000 μl), tubes (1.5/2 ml) – Josef Peske GmbH
- tubes (0.2 ml; #96.9852, 15/50 ml) – TreffLab, Corning, BD Falcon
- vacuum filter systems (volume 125 ml, 0.2 μm ; no.PV050/3) – Schleicher&Schuell
- vacuum filter systems (volume 500 ml, 0.22 μm ; no. 431097) – Corning

2.3 Antibodies

2.3.1 Primary

Antigen – Coupling	Species	Application	Dilution	Company/Source
BrdU - POD	mouse	ICH	1:40	Roche
K6, K10, K14	rabbit	IF	1:400	Covance
loricrin	rabbit	IF	1:400	Covance
K6irs2, K6irs4, Hb2	rabbit	IF	1:1000	Dr. L.Langbein; GCRC, Heidelberg, Germany
vimentin	guinea pig	IF	1:100	Dr. L.Langbein; GCRC, Heidelberg, Germany
E-cadherin	rat	IF	1:200	Zymed Laboratories
α -catenin	rabbit	IF	1:600	Sigma
β -catenin	rabbit	IF	1:500	Sigma
desmoplakin	rabbit	IF	1:200	Research Diagnostics
laminin-5 (γ 2 LE4-6)	rabbit	IF	1:200	Dr. T.Sasaki; MPI, Martinsried, Germany
laminin γ 1 (05-206)	rat	IF	1:40	Upstate
laminin α 1	rabbit	IF	1:200	Dr. P.Yurchenco; UMDNJ-RWJMS, Piscataway, NJ, USA
nidogen-1	rabbit	IF	1:800	Dr. T.Sasaki; MPI, Martinsried, Germany
p120-catenin – FITC	mouse	IF	1:50	Sigma
Mac1 (Ha2/5) – biotin	rat	IF	1:100	BD Pharmingen
paxillin	mouse	IF	1:300	Transduction Laboratories
vinculin	mouse	IF	1:500	Sigma
caspase-3 cleaved (Asp175)	rabbit	IF	1:100	Cell Signalling
ZO-1	rabbit	IF	1:1000	Zymed Laboratories
GM130 (clone 35)	mouse	IF	1:200	Transduction Laboratories
PECAM-1	rat	IF	1:80	BD Pharmingen
Neurofilamin-M	rabbit	IF	1:200	Chemicon
pericentrin	rabbit	IF	1:200	Covance
β 4-integrin (346-11A)	rat	IF/FACS	1:100/1:200	BD Pharmingen
α 6-integrin (GoH3) – FITC	rat	IF/FACS	1:100/1:200	BD Pharmingen
α 1-integrin (Ha31/8)	hamster	FACS	1:200	BD Pharmingen
α 2-integrin (Ha1/29) – FITC	hamster	FACS	1:200	BD Pharmingen
α 4-integrin (9C10) – PE	rat	FACS	1:200	BD Pharmingen
α 5-integrin (5H10-27) – biotin	rat	FACS	1:200	BD Pharmingen
α v-integrin (RMV-7) – biotin	rat	FACS	1:200	BD Pharmingen
β 1-integrin (Ha2/5) – FITC	hamster	FACS	1:200	BD Pharmingen
β 2-integrin (C71.16) – biotin	rat	FACS	1:200	BD Pharmingen
β 3-integrin (2C9.G2) – biotin	hamster	FACS	1:200	BD Pharmingen
β 7-integrin (2C3.G2) – biotin	rat	FACS	1:200	BD Pharmingen
Rac1 (clone 102)	mouse	WB	1:2000	Transduction Laboratories
Rac1 (clone 23A8)	mouse	WB	1:1000	Upstate
Rac2	rabbit	WB	1:1000	Santa Cruz
Rac3	rabbit	WB	1:1500	Dr. Ivan de Curtis; SRSI, Milano, Italy
Cdc42	mouse	WB	1:333	Transduction Laboratories
RhoA (119)	rabbit	WB	1:5000	Santa Cruz
c-Myc (N-262)	rabbit	WB	1:500	Santa Cruz
I κ B- α (C-21)	rabbit	WB	1:1000	Santa Cruz
p-Akt (Ser473), Akt	rabbit	WB	1:1000	Cell Signaling
p-p38, p38	rabbit	WB	1:1000	Cell Signaling
p-JNK, JNK	rabbit	WB	1:1000	Biosource, Cell Signaling; Biosource
tubulin (YL1/2)	rat	WB	1:10000	Dr. J. Wehland; GBF, Braunschweig, Germany
GAPDH	mouse	WB	1:20000	Chemicon

2.3.2 Secondary

Antigen – Coupling	Species	Application	Dilution	Company/Source
mouse IgG – Cy3	goat	IF	1:400	Jackson ImmunoResearch
rabbit IgG – Cy3	donkey	IF	1:1000	Jackson ImmunoResearch
rat IgG – Cy3	goat	IF	1:800	Jackson ImmunoResearch
rat IgG – FITC	goat	IF	1:200	Jackson ImmunoResearch
rat IgG2a (RG7/1.30) – FITC	mouse	FACS	1:250	BD Pharmingen
hamster IgG (G70-204/G94-56) – FITC	mouse	FACS	1:250	BD Pharmingen
mouse IgG – HRP	goat	WB	1:10000	Biorad
rabbit IgG – HRP	goat	WB	1:10000/1:3000	Biorad/Daco
rat IgG – HRP	donkey	WB	1:10000	Jackson ImmunoResearch
phalloidin – Alexa 488/568	–	IF	1:600	Molecular Probes
streptavidin – Cy3	–	IF	1:500	Jackson ImmunoResearch
streptavidin – Cy5	–	FACS	1:500	Jackson ImmunoResearch

2.4 Molecular biology methods

2.4.1 Plasmids and oligonucleotides

The pBluescript II KS⁺ plasmid (pBS; Stratagene), depicted in Fig. 2.1 (obtained from the plasmid manual), was used as a parent vector during all cloning steps, as it is a high copy number plasmid (300–500 per cell) enabling an efficient amplification of cloned DNA.

DNA fragments, which were going to be modified (e.g. a selection cassette or a piece of genomic DNA), were inserted within the multiple cloning site (MCS) of the plasmid.

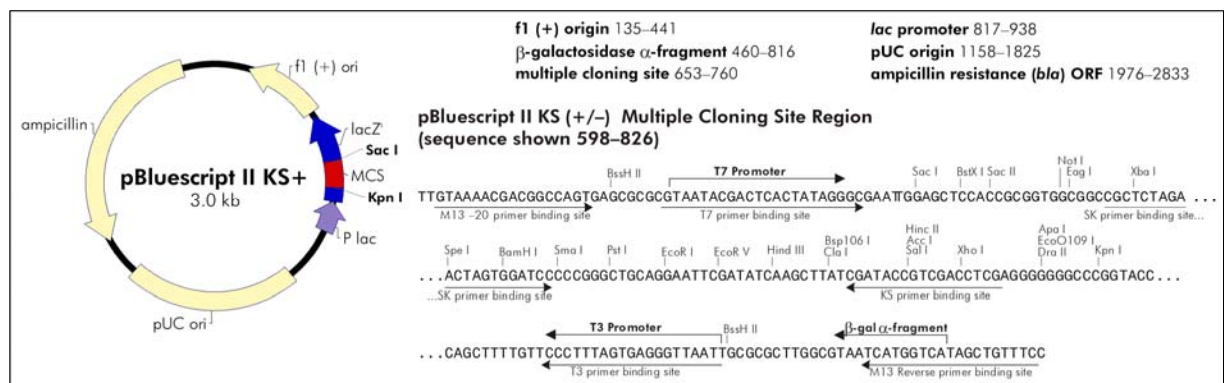


Fig. 2.1 Scheme of the pBS plasmid with a detailed sequence of the MCS (modified from the instruction manual provided by the manufacturer).

All oligonucleotides used in this study are summarized in the table below. Detailed description of each application can be found in respective chapters.

Name	Sequence (5' → 3')	T _m	Application
PAC1	GCG GGA TCC CTT TTC TGA GTT GCC TCT TAC	60°C	probe for PAC library screen
PAC2	GCG GAA TTC AAA TTC CAA ATT CTG GCT GGC	60°C	probe for PAC library screen
AC1	TAA TAA CTT CGT ATA GCA TAC ATT ATA CGA AGT TAT AAG CTT	–	linker (LloxP site)
AC2	TAA AGC TTA TTA CTT CGT ATA ATG TAT GCT ATA CGA AGT TAT	–	linker (LloxP site)
AC3	TCG AGA GTA CTC TGC AGA T	–	selection cassette modification
AC4	CGA TCT GCA GAG TAC TC	–	selection cassette modification
AC7	GCG GAA TTC GTA CCC TAA CTC CTG CCT C	60°C	internal probe
AC8	GCG GTC GAC TGC AGA CAG AGG ACA GCA C	60°C	internal probe
AC9	CTA GAT CGA TGA ATT CGC ATG CGC GGC CGC	–	linker (neo-tk cassette cloning. site)
AC10	CTA GGC GGC CGC GCA TGC GAA TTC ATC GTA	–	linker (neo-tk cassette cloning. site)
AC11	TAG CTC GAG CTC ATG GAG G	–	sequencing (LloxP site orientation)

Name	Sequence (5' → 3')	T _m	Application
AC12	TGA AGT CAA GTA GGT CCA GG	–	sequencing (linker AC9-10 orientation)
AC15	GCG GAA TTC CTG AGG TAT AGT TGG AAT GCC	62°C	external probe
AC16	GCG GTC GAC CAC TGG CTC TGC ACA TGC C	62°C	external probe
MG1	GTC TTG AGT TAC ATC TCT GG	58°C	mouse genotyping (Rac1 PCR)
MG2	CTG ACG CCA ACA ACT ATG C	58°C	mouse genotyping (Rac1 PCR)
MG5	TTG ATT TCC ATA AAG CTT ATA AC	58/60°C	mouse genotyping (KO PCR)
MG6	ACC AAG TGC CCA ATC GGC	58/60°C	mouse genotyping (KO PCR)
cre 3'	TTC GGA TCA TCA GCT ACA CC	58°C	mouse genotyping (cre PCR)
cre 5'	AAC ATG CTT CAT CGT CGG	58°C	mouse genotyping (cre PCR)
T3	AAT TAA CCC TCA CTA AAG GG	–	sequencing (short inserts in pBS)
T7	GTA ATA CGA CTC ACT ATA GGG C	–	sequencing (short inserts in pBS)
RhoG.F1	TTC CTA CCC TCA GAC CAA CG	60°C	real-time PCR
RhoG.R1	CAG GAG GAT AGG CAC GTC AG	60°C	real-time PCR
RhoG.F2	CTG AGA GCC CAG CCT GAT AC	60°C	real-time PCR
RhoG.R2	ATC GGT GTT GGG TTA AGC AC	60°C	real-time PCR
RhoG.F3	CTG TTT CTC CAT TGC CAG TC	60°C	real-time PCR
RhoG.R3	CTG GGC TCT CAG GTC CTT C	60°C	real-time PCR
GAPDH	CAC CAC CCT GTT GCT GTA GCC GTA T	60°C	real-time PCR
GAPDH	TCG TGG ATC TGA CGT GCC GCC TG	60°C	real-time PCR

2.4.2 Bacteria culture

2.4.2.1 Strains, growth conditions, media, selection and storage

The DH5 α strain of *E. coli* bacteria was used during all cloning steps, unless stated otherwise. Liquid cultures, for plasmid DNA preparation, were grown at 37°C in a standard Miller's LB medium (LB) and incubated at ~200 rpm in a bacteria shaker (Buchner Laboratories) for 8-16 h. For selection purposes bacteria were distributed on LB-Agar plates and incubated O/N at 37°C (Heraeus).

LB medium

NaCl 5.0 g
 Tryptone-peptone 5.0 g
 Yeast extract 2.5 g
 ddH₂O filled up to 500 ml

LB-Agar (plates)

Bacto-agar 7.5 g
 LB medium 500 ml
 → amount for 20-25 plates

Antibiotics

Ampicillin (100 mg/ml) 1:1000 (100 μ g/ml)

Additives

X-gal (20 mg/ml) 1:1000 (100 μ g/ml)

X-gal (5-bromo-4-chloro-3-indolyl-beta-D-galactopyranoside) is a colour-changing compound commonly used in a blue-white colony screening. The method is based on a presence of a fragment of the *lacZ* gene, encoding the first 146 amino acids of β -galactosidase within a cloning vector. The coding sequence contains a MCS. When an empty vector (e.g. pBS) is introduced into bacteria strain expressing the C-terminal fragment of β -galactosidase (e.g. DH5 α), an active enzyme, capable of processing X-gal, is synthesized (α -complementation) (Ullmann *et al.*, 1967). X-gal, cleaved by the enzyme, gives a water-insoluble, blue product that marks bacteria colonies. After the introduction of an insert within the MCS, *lacZ* becomes interrupted and transformed bacteria remain white.

LB medium was autoclaved for 30 min at 120°C and stored at 4°C. Before use, it was supplemented with ampicillin, unless stated otherwise. LB-Agar medium was autoclaved, cooled down to ~50°C, supplemented with ampicillin and X-gal, and poured into plastic Petri dishes (10 cm Ø). After the medium solidified, plates were stored at 4°C.

Small-volume liquid bacteria cultures for analytical plasmid isolation (2.4.3.1) and plates with colonies (sealed with Parafilm®; ANC Co.) were stored at 4°C up to one week. For long-time storage, glycerol stocks were prepared (600 µl of fresh bacteria culture mixed with 400 µl of autoclaved 87% glycerol) and kept at -20°C or -80°C (1.5 ml tubes).

2.4.2.2 Preparation of competent bacteria

Bacteria used for transformation were chemically pre-treated to enhance the uptake of a plasmid DNA. Modified LB medium (5 ml M-LB) was inoculated with 50 µl of *E. coli* (DH5α) glycerol stock and incubated O/N at 37°C/200 rpm. The following day, 1 ml of the starter culture was added to 150 ml of pre-warmed M-LB medium and incubated at 37°C/200 rpm until OD₆₀₀ reached 0.3-0.4 (~2 h). Subsequently, the culture was cooled down on ice for 10 min, transferred to 50 ml tubes (~37.5 ml/tube) and centrifuged for 10 min at 6000g (4°C). Bacteria were resuspended carefully in 37.5 ml of ice-cold TFB1, incubated on ice for 10 min and pelleted again (same conditions). Each pellet was resuspended in 3 ml of ice-cold TFB2, aliquoted into 1.5 ml tubes (50 µl) and shock-frozen in a dry-ice/isopropanol bath. Competent bacteria were stored at -80°C for several months.

TFB1

5 M K-Ac (potassium acetate) .. 1 ml (25 mM)
 1 M MnCl₂..... 10 ml (50 mM)
 1 M RbCl..... 20 ml (100 mM)
 1 M CaCl₂..... 2 ml (10 mM)
 ddH₂O 132 ml
 → adjusted to pH 5.8 (with 0.2 M CH₃COOH)
 → sterile filtered (MnCl₂ oxidizes if autoclaved)
 +
 87% glycerol (sterile) 34.5 ml (15%)

TFB2

1 M MOPS, pH 7.0..... 500 µl (10 mM)
 1 M CaCl₂..... 3.75 ml (75 mM)
 1 M RbCl..... 500 µl (10 mM)
 87% glycerol 8.75ml (15%)
 ddH₂O..... 36.5ml
 → autoclaved for 30 min at 120°C

M-LB medium

1 M Mg₂SO₄..... 4 ml (20 mM)
 1 M KCl..... 2 ml (1 mM)
 LB medium filled up to 200 ml

2.4.2.3 Transformation

Plasmid DNA was introduced into bacteria by a heat-shock transformation. Aliquots of competent bacteria (2.4.2.2) were thawed on ice and mixed with 10 µl of a post-ligation solution (2.4.4.7) or a suspension of purified plasmid containing an insert. Control transformations were

performed with 10 µl of ddH₂O (negative) or 2 ng of empty plasmid (positive).

After 30 min incubation on ice, tubes were transferred for 90 s to 42°C (dry heat block, Thermomixer compact; Eppendorf), cooled down on ice for 5 min and filled with 1 ml LB medium (w/o antibiotics) (2.4.2.1). Subsequently, bacteria were transferred to 14 ml polystyrene round-bottom tubes and incubated for 45-60 min at 37°C/200 rpm. After transferring back into 1.5 ml tubes, cells were spun down for 30 s at 20.000g (microcentrifuge; Microcentrifuge Eppendorf 5417C) and ~800 µl LB medium were removed. Bacteria were resuspended in remaining 200 µl of medium and distributed on LB-Agar plates (2.4.2.1) using a Drigalski spatula (sterilised with a Bunsen burner). Inverted plates were incubated at 37°C. Colonies usually appeared within 12-16 h.

2.4.3 Plasmid DNA preparation

2.4.3.1 Analytical amounts – miniprep

After transformation (2.4.2.3), single white colonies were picked with a pipette tip (200 µl) and inoculated in 2-3 ml LB medium (2.4.2.1), in 14 ml tubes. Cell suspension was transferred to a 1.5 ml tube and centrifuged for 30 s at 20,000g. Remaining bacteria were stored at 4°C until clones carrying the desired plasmid were identified.

The bacteria pellet was resuspended in 200 µl of P1 buffer and mixed with 200 µl of P2 buffer by vigorous shaking. After 5 min lysis at RT, 200 µl of ice-cold P3 buffer were added to neutralize the solution and precipitate everything but plasmid DNA. The suspension was thoroughly mixed, kept on ice for 5 min and subsequently spun down for 5 min at 20,000g. The supernatant was transferred to a new 1.5 ml tube, mixed with 500 µl of isopropanol in order to precipitate DNA and centrifuged again for 5 min at 20,000g. The supernatant was carefully removed (vacuum pump) and the pellet was washed with 1 ml of 70% EtOH. The subsequent centrifugation step was performed two times to remove all the residual alcohol. Plasmid DNA was resuspended in 50 µl of ddH₂O or TE buffer.

P1 buffer

Tris-HCl, pH 8.0.....50 mM

EDTA10 mM

RNase A100 µg/ml

P2 buffer

NaOH.....200 mM

SDS 1% (w/v)

P3 buffer

3 M *K-Ac, pH 5.5*

TE buffer

Tris-HCl, pH 8.010 mM

EDTA1 mM

Alternatively, QIAprep Spin Miniprep Kit (Qiagen) was used for plasmid DNA purification. The procedure was performed following the supplied protocol, starting from 2-3 ml of bacteria

culture obtained as described above. DNA was eluted with 50 µl of ddH₂O or TE buffer.

Miniprep plasmid DNA was stored at -20°C and used for restriction digest analysis (2.4.4.1) and sequencing (2.4.4.8). Average yield of a high copy plasmid isolated from 1.5 ml of bacteria culture was 5-10 µg.

2.4.3.2 Preparative amounts – maxiprep

Big scale preparation of a plasmid DNA was conducted with QIAGEN Plasmid Maxi Kit (Qiagen). Bacteria for the isolation were prepared by inoculation of 200 ml LB-medium with 200 µl of a glycerol stock or a miniprep culture. Subsequently, the purification protocol supplied with the kit was followed. Plasmid DNA was dissolved in 200-300 µl ddH₂O or TE buffer (depending on the size of a pellet) and stored at -20°C.

The concentration of purified DNA was determined by spectrophotometric measurement at 260 nm (GeneQuant II RNA/DNA Calculator; Amersham Pharmacia Biotech). Average yield of a high copy plasmid isolated from 200 ml of bacteria culture was 300 µg.

2.4.4 DNA cloning

2.4.4.1 Restriction enzymes digestion

Restriction enzymes were employed while generating the targeting construct and screening of bacteria or ES cell clones. Those enzymes recognize different palindromic sequences of nucleotides and cut DNA molecule at specific site within those sequences by hydrolyzing phosphodiester bounds. The cut ends after digestion can be “blunt” (no 5′ or 3′ overhang) or “sticky” (5′ and 3′ overhangs). The latter can be ligated (2.4.4.7) only with compatible ends, with a much higher efficiency than non-discriminative blunt ends. In this study only enzymes creating overhangs were used.

Restriction enzymes were purchased from New England Biolabs together with optimized reaction buffers. If double digestion was performed, a suitable buffer was chosen in which the highest possible activity of both enzymes was obtained. Different concentrations of enzymes (stock), depending on the application, were used; 5-10 U/µl during the cloning steps and 100 U/µl for genomic digest of ES cell DNA. Generally, around 5 U of an enzyme for 1 µg of cut DNA were utilized. The reaction mix was supplemented with 0.1 µg/µl BSA, in case of genomic digest or when enzymes requiring it for an optimal activity were used.

All digestion reactions were performed at 37°C (dry-heat block). A standard digestion (cloning and bacteria screening) was carried out for 1.5-2 h and the cutting of genomic DNA (Southern blot screening of PAC library, ES cell clones and mice) was conducted for 16-20 h.

Standard reaction mix:

Miniprep DNA	2 µl
Enzyme 1 (5-10 U).....	0.5 µl
Enzyme 2 (5-10 U).....	0.5 µl
BSA (2 µg/µl).....	1 µl
NEBuffer (10x).....	2 µl
ddH ₂ O	14 µl
	20 µl

Genomic digest reaction mix:

DNA	20 µl
NEBuffer (10x).....	3 µl
BSA (10 µg/µl).....	0.3 µl
Enzyme (100 U)	0.4 µl
ddH ₂ O.....	6.3 µl
	30 µl

2.4.4.2 Gel electrophoresis

DNA fragments after digestion (2.4.4.1) were routinely separated by an agarose gel electrophoresis in TAE buffer. Depending on the sizes of separated fragments, different concentrations of agarose, 0.7-2.0% (w/v), were used for the gel preparation. Agarose (Invitrogen) was dissolved in TAE buffer by heating in the microwave until the boiling point. Before pouring the solution into a casting tray, ethidium bromide (EtBr, Roth) was added. Samples were mixed with a 6x loading buffer, pipetted into the wells and the run in the gel with 3-6 V/cm (small; 23 cm chamber) or 1-3.5 V/cm (big; 35 cm chamber). The 1 Kb DNA Ladder (Invitrogen #15615-016) was standardly used as a size reference (Fig. 2.2). DNA was visualized under UV light and results archived with a LCD camera.

50x TAE

Tris-base	242 g (2 M)
Glacial acetic acid.....	57.1 ml
0.5 M EDTA.....	100 ml (50 mM)
ddH ₂ O.....	filled up to 1000 ml

DNA loading buffer (6x)

Glycerol	60% (v/v)
EDTA	60 mM
Bromophenol blue.....	0.1% (w/v)
Orange G	0.2% (w/v)
Xylene cyanol FF.....	0.1% (w/v)
Tris-HCl, pH 7.6*.....	10 mM
	→ (*) optional

→ choice of the dye depends on the size of separated fragments

The dyes differ in the colour and the migration rate. In 1% agarose gels bromophenol blue (navy blue) migrates with 300 bp, orange G (orange) – with 50 bp and xylene cyanol FF (light blue) – with 4000 bp DNA fragments.

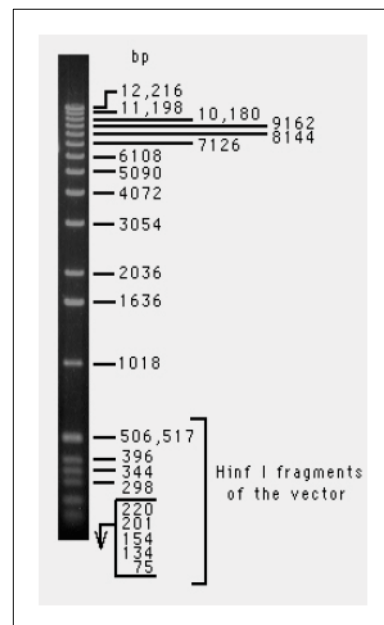


Fig. 2.2 The distribution pattern of the 1 Kb DNA Ladder. Fragments were separated in 0.9% agarose gel

Additives

EtBr (10 mg/ml)1:20,000 (5 µl/100 ml)

Ethidium bromide is DNA intercalating agent commonly used as a non-radioactive marker for visualizing nucleic acids. When exposed to ultraviolet light, it fluoresces with a red-orange light, intensifying almost 20-fold after binding to DNA. EtBr is a powerful **mutagen**.

2.4.4.3 DNA extraction from agarose gel

After an electrophoretic separation of preparative amounts of DNA, gel pieces containing fragments of the correct size were cut out and weighed. DNA was isolated from the gel and purified using preferably QIAquick Extraction Kit (QIAGEN) according to the supplied protocol. QIAquick columns contain a silica membrane which binds DNA in high-salt buffer. Washing steps remove primers, nucleotides, enzymes, salts, agarose, ethidium bromide and other impurities from DNA sample. Afterwards DNA is released from the column with low-salt buffer or water. Purified DNA was usually eluted with 30 µl ddH₂O and 2 µl of the solution were run in an agarose gel to confirm the size and to assess the concentration (a standard size marker was used as a reference).

Alternatively, GENE CLEAN® III Kit (Qbiogene, Inc.) or QIAEX II Gel Extraction Kit (Qiagen) was used, according to manufacturers' protocols. Those kits utilise DNA-adhesive silica-gel particles in suspension, which are added to a dissolved gel slice and then collected by a brief centrifugation step. After washing, pure DNA fragments are eluted with Tris buffer or water. In this study DNA was usually recovered with 20 µl ddH₂O and checked by running 2 µl of the suspension in an agarose gel.

Additionally, above methods were used to purify DNA fragments in suspension; e.g. miniprep DNA before sequencing.

2.4.4.4 DNA precipitation

When sample concentration was too low or dried DNA was required (e.g. for sequencing), DNA was precipitated. DNA solution was mixed with 3 M Na-Ac and EtOH as described below and incubated for 20 min at -80°C.

Precipitation recipe

DNA solution1 vol.

3 M Na-Ac, pH 5.20.1 vol.

100% EtOH2.5 vol.

Afterwards, the sample was centrifuged for 10 min at 20,000g and the supernatant was discarded. DNA pellet was washed with 500 µl of 70% EtOH, which was completely removed with two centrifugation steps. To obtain dried DNA, the pellet was additionally dried under

vacuum. Otherwise, DNA was resuspended in the appropriate amount of water or TE buffer.

2.4.4.5 *Phosphorylation and annealing of oligonucleotides*

Before introducing an oligonucleotide linker into a cloned construct, primers were phosphorylated on the 5'-end and annealed to each other. The reaction was conducted according to a protocol described below and 2-3 μ l of product solution were taken for one ligation reaction.

Reaction mix:

Primer 1 (100 pmol).....1 μ l
Primer 2 (100 pmol).....1 μ l
T4 PNK buffer (10x).....1 μ l
10 mM ATP1 μ l
ddH₂O5 μ l
T4 DNA kinase (PNK).....1 μ l
10 μ l

→ 60 min incubation at 37°C

Next added:

ddH₂O..... 17 μ l
0.5 M NaCl..... 2 μ l

30 μ l

→ 10 min incubation at 80°C (dry heat block)

→ slow cooling down (heat block switched off and samples taken out when 30°C is reached; 3-3.5 h)

2.4.4.6 *Dephosphorylation of 5'- ends*

If vector was digested with only one enzyme (linearized), phosphate groups from the 5' ends of the cut DNA were removed to prevent re-ligation. Calf intestinal phosphatase (CIP; Roche #713023) was added directly to the digestion reaction mix after a normal incubation time. The mixture was incubated with 5 U of the enzyme for 30 min at 37°C and subsequently for 30 min in 56°C. Both incubation steps were repeated after addition of fresh CIP. DNA was separated in an agarose gel (2.4.4.2) and purified before the ligation (2.4.4.3).

2.4.4.7 *Ligation of DNA fragments*

DNA fragments which had compatible ends, created e.g. with restriction enzymes (2.4.4.1), can be combined with T4 DNA ligase (Invitrogen #15224-041). This enzyme catalyzes the formation of a phosphodiester bond between 5'-phosphate and 3'-hydroxyl ends of double-stranded DNA molecules.

At least a 3:1 molar ratio of insert to vector was used in the reaction solution. Small inserts are incorporated easier; therefore in such case reaction was incubated for 1-2 h at RT. When large fragments were combined, ligation was performed O/N at 16°C (water-bath in 4°C). Usually, two control ligations were performed: negative and positive. In each case only vector was included in the mix, cut either with two enzymes (the same as for the insert ligation) or with only one, respectively. The resulting mixture was directly used for transformation (2.4.2.3).

<u>Reaction mix:</u>	<u>5x ligase buffer (supplied w/ligase):</u>
Vector DNA 10 - 100 ng	<i>Tris-HCl, pH 7.6</i> 250 mM
Insert DNA... 3-5x (vector amount)	<i>MgCl₂</i> 50 mM
Ligase buffer (5x) 4 µl	<i>ATP</i> 5 mM
T4-DNA-ligase (1 U/µl) 1 µl	<i>DTT</i> 5 mM
ddH ₂ O x µl	<i>PEG 8000</i> 25% (w/v)
20 µl	

2.4.4.8 Sequencing

After every cloning step, the modified DNA fragment was sequenced to confirm that correct changes, but no unwanted alterations, were introduced. Fragments of interest were amplified by one-primer PCR according to the Big-Dye Pre-Mix protocol. Reaction products were sent for the sequencing to a specialized facility. Sequences of good quality were usually 500-1000 bp long.

Standard T3 and T7 primers, which have binding sites on the opposite ends of multi-cloning site of pBS, were used for amplification if the manipulated insert was short or the changed site was close to the insert's end. Otherwise, custom primers were designed, homologous to a sequence located close to the modified site (2.4.1).

2.4.5 Isolation of genomic DNA

2.4.5.1 DNA isolation from tissues

Genomic DNA for mice genotyping was extracted from clipped tails or toes. Tissue fragments were placed in 1.5 ml tubes and incubated in 500 µl lysis buffer O/N at 55°C (at least 6 h). Lysates were stored at -20°C or directly processed.

DNA for genotyping PCR was isolated according to the short protocol. The suspension was centrifuged for 10 min at 20,000g (microcentrifuge) and the supernatant was transferred to a new 1.5 ml tube with 500 µl isopropanol. After short, vigorous shaking DNA became visible and was subsequently spun down for 5 min at 20,000g. The supernatant was discarded and the DNA pellet was washed with 1 ml of 70% EtOH. Two centrifugation steps, 5 min at 20,000g each, were performed to completely remove the alcohol and tubes were left open for 5 min to air-dry the pellet. DNA was resuspended in 300 µl ddH₂O and incubated O/N at 55°C (at least 5-6 h) and 2 µl of the suspension were taken for a PCR reaction (2.4.6.1).

DNA for southern blot analysis was isolated by phenol-chloroform extraction. Tissue was lysed as described above. After remnants were spun down, the supernatant was transferred to a new tube with 500 µl of phenol/chloroform/isoamylalcohol [25:24:1] solution (Roti; Roth #A156) and mixed by vigorous shaking. Phases were separated by 5 min centrifugation at

20,000g and the aqueous phase containing DNA (upper) was transferred to a new tube with 500 µl chloroform. The sample was mixed and centrifuged, and again the upper phase was transferred to a new tube. After thorough mixing with 500 µl isopropanol, DNA became visible and was further purified as in the short protocol. After diluting in 300 µl ddH₂O, 20 µl of DNA suspension were taken for a genomic digest (2.4.4.1).

Lysis buffer:

1 M Tris, pH 8.5.....	100 ml (100 mM)	→ stored at RT; shortly before use supplemented
5 M NaCl	40 ml (200 mM)	with:
0.5 M EDTA.....	10 ml (5 mM)	Proteinase K (10 mg/ml).....1:100
20% SDS.....	10 ml (0.2%)	→ stock solution stored at -20°C.
ddH ₂ O.....	filled up to 1000 ml	

2.4.5.2 DNA isolation from cells

Isolation of DNA from cultured cells was performed during the screening of ES cell clones (2.6.3.3). After cells were sufficiently expanded, 500 µl of the lysis buffer (2.4.5.1) were added to each well and incubated further at 37°C. As not all clones were ready at the same time, the lysis was initiated for 3 consecutive days, with the last group of clones lysed for at least 8 h. Afterwards, 500 µl isopropanol were added to each well and plates were shaken with 300 rpm for at least 8 h at RT (usually O/N), until DNA became visible (white web-like structure). DNA precipitates were fished with a small metal fork, transferred to 1.5 ml tubes containing 100 µl ddH₂O and incubated for 24 h at 55°C. Resuspended DNA was stored at -20°C.

2.4.6 Polymerase chain reaction – PCR

PCR is a quick and easy method to amplify fragments of DNA using two specific primers flanking the desired sequence. It may be used for analytical purposes or to obtain preparative amounts of a plasmid or a genomic DNA fragment.

2.4.6.1 Mice genotyping

Genotyping of mice was routinely performed by PCR analysis. Genomic DNA isolated from mouse tissues (2.4.5.1) was amplified with specific primers designed to recognize changes introduced into the *rac1* gene or the presence of the *cre* transgene (2.4.1). Reaction solutions were prepared in 0.2 ml tubes and run with the standard touch-down program after placing in a pre-heated thermocycler (hot start; T3 Thermocycler, Biometra). Annealing temperature depended on the used primer pair. Assuming that the calculated melting temperature was equal T_m , it started from $T_m + 5^\circ\text{C}$ and dropped to $T_m - 5^\circ\text{C}$ after 10 cycles. After the reaction was finished, the samples were analysed by agarose gel electrophoresis (2.4.4.2).

Genotyping PCR – reaction mix:

DNA template	2.0 μ l
Primer 1 (100 pmol).....	0.2 μ l
Primer 2 (100 pmol).....	0.2 μ l
PCR buffer (10x).....	2.0 μ l
50 mM Mg ²⁺	0.6 μ l
10 mM dNTP	0.4 μ l
Taq DNAPoly (5 U/ μ l)	0.1 μ l
ddH ₂ O	14.5 μ l
	20 μl

Touch-down PCR program (T_m = 60°C):

1. denaturation..... 94°C for 30 s
2. annealing..... 65°C for 30 s
3. elongation..... 72°C for 30 s
→ steps 1-3 – 10 cycles; annealing temperature reduced by 1°C every cycle;
4. denaturation..... 95°C for 30 s
5. annealing..... 55°C for 30 s
6. elongation..... 72°C for 30 s
→ steps 4-6 – 35 cycles;
7. pause.....4°C for ∞

2.4.6.2 Preparative PCR

Higher amounts of a PCR product were required if the amplified fragment was to be subcloned into a vector. To facilitate cloning, primer pairs with different restriction sites at 5'-ends were designed. After a two-enzyme digestion (2.4.4.1), the PCR product was combined with the plasmid in a correct orientation by a sticky-end ligation (2.4.4.7). Amplification was performed with a touch-down program (2.4.6.1), with each steps being 60 s long.

Genomic PCR – reaction mix:

DNA template	2.0 μ l
Primer 1 (100 pmol).....	1.0 μ l
Primer 2 (100 pmol).....	1.0 μ l
PCR buffer (10x).....	10.0 μ l
50 mM Mg ²⁺	4.0 μ l
10 mM dNTP	2.0 μ l
Taq DNAPoly (5 U/ μ l)	1.0 μ l
ddH ₂ O	14.5 μ l
	100 μl

Additionally, genomic PCR was used to obtain high amounts of Southern blot probes for labelling.

2.4.7 Southern blot analysis

The Southern blot technique is used for a precise identification of DNA fragments which contain a specific sequence. The method utilizes short single-stranded DNA fragments which are complementary to the sequence of interest. Electrophoretically separated fragments of analysed DNA samples are immobilised on a membrane and incubated with the labelled probe. The visualized pattern of hybridization shows, which DNA samples contain the particular sequence and what is the size of the DNA fragment containing it.

In this study Southern blot analysis was performed during screening of the PAC library (2.6.2.2) and ES cell clones (2.6.3.3), as well as for genotyping of mice (2.6.6).

2.4.7.1 DNA processing and transfer to the membrane

Genomic DNA was digested with an appropriate restriction enzyme (2.4.4.1) and separated by gel electrophoresis in 0.7% agarose gel (2.4.4.2) until the bromophenol blue dye travelled for ~15 cm (6-8 h at 3.5 V/cm). Due to the high amount of restriction fragments generated during the genomic digest, DNA after gel electrophoresis appeared as a smear rather than a set of discrete bands. The gel was photographed with a ruler placed next to the marker lane for a later band size reference. As only single-stranded DNA can hybridise with the probe, separated DNA was denatured in the denaturation solution. After 30 min incubation at RT, with a delicate agitation on a rocker, the gel was rinsed with dH₂O and incubated for 30 min in the neutralization solution.

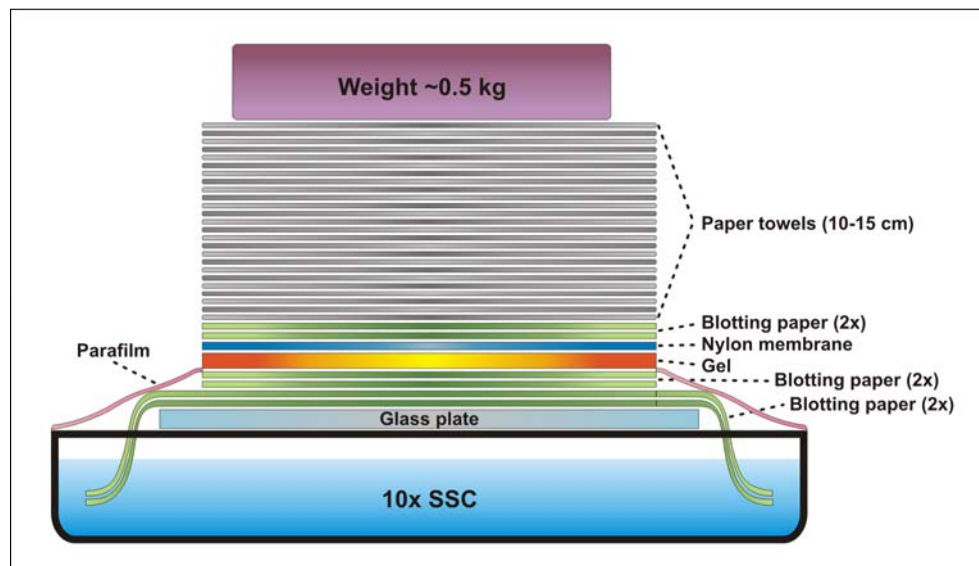


Fig. 2.3 Scheme of a Southern blot transfer stack.

DNA was subsequently transferred to a positively charged nylon membrane (Hybond-XL; Amersham Biosciences) by the capillary transfer method, using a setup shown in Fig. 2.3. The transfer buffer was drawn from a reservoir and forced through the gel by capillary action facilitated by a stack of dry paper towels placed on top. DNA fragments were carried along and became deposited on the membrane surface. As air bubbles trapped between blotting papers (3MM Chr; Whatman), gel and membrane would have interfered with the transfer, they were carefully removed during the assembly of the stack by rolling a plastic pipette over each layer. The outside of the gel was surrounded with Parafilm® (ANC Co) to prevent the buffer from migrating around it, which would also drastically decrease blotting efficiency.

The transfer was conducted in 10x SSC buffer at RT for 16-20 h. Positions of loading wells were marked on the membrane during the stack disassembly. The membrane was subsequently exposed to 254 nm UV-light (120 mJ/cm²; UV Stratalinker 1800; Stratagene) to induce the formation of covalent bonds between amino groups of the nylon and thymines of the DNA. Afterwards, the membrane was baked for at least 2 h at 80°C and stored at RT.

Denaturation solution

NaCl 438.8 g (1.5 M)
 NaOH..... 100.0 g (0.5 M)
 dH₂Ofilled up to 5000 ml

Neutralization solution

NaCl 438.8 g (1.5 M)
 Tris-base 302.9 g (0.5 M)
 dH₂Ofilled up to 5000 ml
 → adjusted to pH 8.0

20x SSC

NaCl 876.5 g (3.0 M)
 Na₃Citrate 441.0 g (0.3 M)
 dH₂Ofilled up to 5000 ml
 → adjusted to pH 7.0

2.4.7.2 Generation and radioactive labelling of the probe

After a region which should be recognized by a Southern blot probe had been selected, specific primers, which flanked that fragment, were designed. A chosen fragment was amplified by a genomic PCR (2.4.6.2) and subcloned into the pBS vector. The correct sequence of the probe was confirmed by sequencing (2.4.4.8). Prior to the labelling, the probe was released from the plasmid by a restriction digestion (2.4.4.1) or amplified by a preparative PCR (2.4.6.2) using the plasmid as a template.

For one labelling reaction, 2.5-25 ng of a probe DNA was diluted in 45 µl ddH₂O or TE buffer, denatured for 5 min at 95°C and snap-cooled for 5 min on ice. The solution was spun down and transferred to a Rediprime II reaction tube (Amersham Biosciences), containing a buffered mixture of nucleotides (dATP, dGTP, dTTP), exonuclease-free Klenow enzyme and random primers in a dried, stabilised form. Next, 5 µl of [³²P]dCTP (10 mCi/ml; Easytides; PerkinElmer) were added and mixed thoroughly by pipetting up and down. After ~30 min incubation at 37°C, the reaction solution was transferred on a Sepharose column (see below) and spun down for 2-3 min at 1000 rpm (Minifuge2; Heraeus). The labelled probe was collected in 1.5 ml tube placed under the column.

The column was made from Sepharose G-50 in a fine dosage syringe (1 ml; Braun or BD) without a piston. A piece of a glass microfibre filter (GF/C, 1.2 µm; Whatman #1822025) was placed at the bottom of a syringe to prevent the beads from leaking out, before it was placed in a 15 ml centrifugation tube and filled with Sepharose G-50/TE buffer suspension. After 2-3 min centrifugation at 1000 rpm (Allegra 6R; Beckman Coulter) most of the liquid was spun down leaving beads behind. If necessary, the procedure was repeated

until beads reached the 0.8 cm³ mark. The column was transferred to a new 15 ml tube with an open 1.5 ml screw-cup tube inside. It was directly used or sealed with Parafilm® and stored at 4°C (up to 1-2 weeks).

Around 100 µl of a probe solution was usually recovered after the centrifugation. To assess the labelling efficiency, 1 µl was transferred to a scintillation vial and the amount of counts per minute (cpm) was determined in a multi-purpose scintillation counter (LS 6500; Beckman). Around 100 µl of a labelled probe with a concentration of 300,000-500,000 cpm/µl were used for hybridization of 2-3 big membranes (30 DNA samples per filter).

2.4.7.3 Hybridization, washing and signal detection

A membrane with immobilized DNA was soaked in 2x SSC and placed, with the DNA-side facing inwards, in a glass hybridization bottle (3.5 x 30 cm) filled with 2x SSC. Subsequently, the membrane was pre-hybridized with 15 ml of Church buffer for 60 min at 65°C. The labelled probe was denatured for 5 min at 95°C, snap-cooled on ice for 3 min and mixed with Church buffer in the hybridization bottle.

Sodium Phosphate buffer (1 M) – NaPi

Na₂PO₄ × 2H₂O..... 89 g
85% H₃PO₄..... 4 ml
ddH₂Ofilled up to 1000 ml

Church buffer

NaPi 500 ml
BSA 10 g
20% SDS..... 350 ml
0.5 M EDTA..... 2 ml
salmon ssDNA (10 mg/ml).. 10 ml
ddH₂O.....filled up to 1000 ml

The membrane was incubated with the probe for 16-20 h at 65°C in a hybridization oven (Mini Hybridization Oven; Appligene). Afterwards, the buffer containing unbound probe was discarded and the membrane was washed twice for 30 min at 65°C, with the following buffer.

Washing buffer:

20x SSC..... 20 ml (0.4%)
20% SDS..... 50 ml (1%)
ddH₂Ofilled up to 1000 ml

The lower the content of SSC is, the more stringent the buffer. Washing with 1% SDS solution would strip a membrane.

The washed membrane was wrapped in a plastic foil and placed in a radiographic cassette with a sheet of a radiographic film. The film was exposed for around 24 h at -80°C and developed to assess the strength of the signal. If necessary, a new film was exposed for a shorter or a longer period of time to obtain optimal signal intensity.

2.5 Cell culture materials and techniques

2.5.1 Embryonic stem cells (ES cells)

ES cells are derived from the inner cell mass of the blastocyst and can undergo an unlimited number of symmetrical divisions without differentiating (long term self-renewal). They are pluripotent and can give rise to all differentiated cell types. Therefore, when introduced into a blastocyst, ES cells can integrate into all developing tissues, including the germ line. These features are utilized during generation of genetically modified mice. A chimeric mouse can pass on a modified gene to its offspring, starting a new strain. In this study R1 ES cells were used. They were derived from 3.5-day blastocyst obtained from F1 (129X1/SvJ x 129S1) mating (Nagy *et al.*, 1993).

Maintaining ES cells in an undifferentiated proliferative state and thus sustaining their potential to integrate into germ line is crucial for obtaining chimeric mice and the transmission of a modified gene to offspring. Therefore, great care must be taken while handling these cells in culture and special conditions are required. ES cells form colonies instead of a single-cell layer and changes in the shape and colour of the colonies are an indicator of differentiation.

2.5.1.1 Culture condition, medium

ES cells were grown on a subconfluent feeder layer of mitotically inactivated primary mouse embryonic fibroblasts (MEFs; 2.5.2) in ES medium at 37°C, in 5% CO₂ air with 95% humidity. Feeder cells provide a surface to attach, release nutrients to the medium and produce leukaemia inhibitory factor (LIF) that prevents differentiation of ES cells. The growth medium was additionally supplemented with LIF to guarantee its optimal concentration. No antibiotics were used as they might mask mycoplasma infections, which accompany bacterial infections but are resistant to antibiotics and can not be detected under a light microscope. Medium was replaced every day and pre-warmed to 37°C before the exchange.

ES medium:

<i>D-MEM (High Glucose)</i>	400 ml	[Gibco #31966-021]
<i>FCS</i>	100 ml	[Gibco #10270-106]
<i>Non-Essential Amino Acids</i>	5 ml	[Gibco #11140-035]
<i>LIF</i>	500 µl (1000 U/ml)	[ESGro, Gibco]
<i>β-mercaptoethanol</i>	3.5 µl (0.1 mM)	
→ <i>FCS was heat-inactivated by 30 min incubation at 56°C</i>		
→ <i>D-MEM contains: GlutaMAX™ I, 4500 mg/l D-glucose and sodium pyruvate.</i>		

2.5.1.2 *Passaging, freezing and thawing*

When the culture becomes too dense, ES cells start to differentiate. Therefore, they were passaged every 2-3 days (before colonies were starting to fuse and got brownish in the middle). The growth medium was changed 2 h before splitting. Cells were washed two times with PBS (volume of growth medium) and incubated with 1x trypsin/EDTA solution (diluted with PBS from 10x stock: 0.5% Trypsin, 0.2% EDTA·4Na [5,3 mM], 0.85% NaCl, pH 7.4; Gibco #15400-054) for 3-5 min at 37°C, until they could be easily detached from the surface. Colonies were dispersed by pipetting up and down with 5-7 ml ES medium and cells were spun down for 5 min at 500g. ES cells were resuspended in growth medium and usually split 1:3-1:5 into a new dish/flask. Splitting ratio was not exceeding 1:7 as ES cells should not be seeded too sparse. Depending on the area of the new flask, an appropriate amount of feeder cells was co-seeded.

The number of passages can have a negative effect on ES cells properties. Therefore, multiple aliquots of new clones were frozen as soon as possible. When ES cell colonies reached optimal density for splitting, cells were trypsinized as described above and resuspended in ice-cold ES medium supplemented with 10% DMSO (dimethylsulfoxide; Sigma #8779). The cell suspension was transferred to cryo-vials (Corning #430489) in 1 ml aliquots, frozen on dry-ice and stored in -80°C. For long-time storage, ES cells were transferred to liquid nitrogen. One frozen aliquot contained enough cells to repopulate a well in a 6 well plate or a small T-flask (see table below).

Container	Growth medium volume	1x TR/EDTA	Cryo-vials
6 well	3-4 ml	0.5 ml	1
Small – T/flask (25 cm ²)	5-6 ml	1.0 ml	3-4
Medium – T/flask (75 cm ²)	8-10 ml	1.5 ml	7-8
10 cm Ø dish	8-10 ml	1.5 ml	8-10
Big – T/flask (175 cm ²)	18-20 ml	2.5 ml	15-18

ES cells were thawed fast to reduce the exposure to toxic DMSO. A cryo-vial was removed from the freezer or liquid nitrogen and placed in a warm water bath (37°C). As soon as the medium thawed, the cell suspension was transferred to 5 ml of ES medium and spun down for 5 min at 500g to wash away DMSO. After discarding the supernatant, ES cells were resuspended in the growth medium and seeded together with an appropriate amount of feeder cells in a 6-well plate or a small T-flask.

2.5.2 **Preparation of feeder cells**

Feeder cells are prepared from MEFs isolated from transgenic mice carrying a neomycin resistance gene; therefore they can be used during ES cells selection steps. They are mitotically inactivated either by γ -irradiation or mitomycin C treatment. Feeder cells are seeded one day

before or together with ES cells (2.5.1) and can be used for around 10 days.

A pregnant female was sacrificed at day 13.5 or 14.5 *post coitum* (day 0.5 – the day when the plug is observed) and placed in a sterile hood (on several paper tissues). After washing the belly with 70% EtOH, the uterus was carefully dissected out and placed in a Petri dish (6 cm Ø) filled with 2 ml PBS. Embryos were released from the amnions and transferred to a new dish containing 2 ml PBS. Heads were cut off and all internal organs removed with a forceps. The remaining tissue was cut into small pieces and incubated in 1x trypsin/EDTA solution (1 ml/embryo) for 10 min at 37°C. The tissue was broken up by up-and-down pipetting, incubated for 10 min more at 37°C and fragmented again (with a smaller volume pipette). Afterwards, cells were resuspended in EF medium (D-MEM with 10% FCS; 2.5.1.1), seeded in 10 cm Ø dishes (1 embryo/dish) and incubated O/N at 37°C to check for potential contamination. The following day, the content of each dish was split into two big T-flasks. Afterwards, MEFs were grown without changing medium at 37°C, in 5% CO₂ air with 95% humidity and the density of cells was checked every day. After cells became confluent, they were cultured for 3 more days.

Next, MEFs were washed with PBS (15 ml/flask), trypsinized for 10 min at 37°C (1x trypsin/EDTA; 2.5 ml/flask) and thoroughly resuspended with 2.5 ml EF medium. Part of the cell suspension (0.5 ml) was reseeded in the flask and fresh EF medium was added (20 ml/flask). Remaining cells were collected in 50 ml tubes and centrifuged for 10 min at 500g. Medium was discarded (leaving just a thin layer of liquid to prevent cells from drying) and pellets were γ -irradiated with 40-60 Greys. Feeder cells were resuspended in ice-cold D-MEM medium supplemented with 10% DMSO and 20% FCS and frozen down on dry-ice. Three 1 ml aliquots were frozen from every T-flask (6 vials from an embryo). Reseeded cells were expanded and the procedure was repeated (omitting the reseeded step), 3 days after they reached confluency. Feeder cells were stored at -80°C. When used for ES cell culturing, one vial was usually seeded in a 10 cm Ø dish.

2.5.3 Embryoid bodies (EBs)

2.5.3.1 Culture conditions

Prior to the formation of EBs, ES cells were expanded in a standard growth medium (2.5.1) on a confluent feeder-cell layer (2.5.2). During passaging, colonies were carefully trypsinized in order to obtain small aggregates of ES cells instead of a single-cell suspension. When tightly packed colonies were covering about 70 % of a 10 cm Ø dish surface, they were best suited for the generation of EBs.

Cell aggregates optimal for differentiation into EBs (~5 cells/cluster) were obtained with a trypsin/EDTA treatment (0.25% Trypsin, 0.53 mM EDTA; 2 ml/dish). The process was monitored under the microscope and stopped when balls of ES cell colonies started to detach from the surface (~3-5 min). After neutralisation with 4 ml of EF medium, cells were transferred to a tube and let to sediment for 10 min. The supernatant, containing single ES and feeder cells, was discarded. After adding 2 ml of EB medium (ES medium w/o LIF, 2.5.1.1) colonies were dispersed into clusters of 2-5 cells, using a fine-tipped Pasteur pipette (outer Ø ~0.2 mm). ES cells were placed in tissue culture dishes and incubated for 1-3 h at 37°C to selectively remove feeder cells, which adhere much faster (panning). Next, the aggregates were transferred carefully into bacteriological Petri dishes (10 cm Ø) and cultured in EB medium for 7 to 14 days. The medium was changed the first time after 3 days and every other day thereafter.

The size of cell clusters is critical for an efficient development of EBs. Too large cell aggregates differentiate in a disorganized fashion. Single cells grow too slowly in suspension and usually fail to form EBs. An optimal density of EBs is very important and should not be higher than 1000 clusters/dish. Usually one dish of ES cells can be distributed into 6-8 bacterial dishes. After approximately 3 days of growing in a suspension culture, the endoderm and the BM are developed within EBs.

2.5.3.2 Analysis of EBs structure

IF staining and ultrastructural analysis of developing EBs was conducted by Dr. Shaohua Li in Dr. Peter Yurchenco's group (Department of Pathology and Laboratory Medicine, University of Medicine and Dentistry of New Jersey [UMDNJ], Robert Wood Johnson Medical School, Piscataway, NJ, USA), according to published protocols (Li and Yurchenco, 2006).

At selected time points EBs were collected in a 15 ml tube and allowed to sediment by gravity. Medium was removed and cells washed once with 0.5% BSA/PBS (resuspended and sedimented again).

For IF analysis, EBs were fixed in 3% PFA/PBS for 30 min at RT, incubated in 7.5% sucrose/PBS for 3 h at RT and subsequently in 15% sucrose/PBS, O/N at 4°C. Next, EBs were embedded in Tissue-Tek OCT (Miles, Inc.) and 4 µm section were cut with a cryotome. Primary antibodies were incubated for 1 h at RT, after 20 min blocking with 5% goat or donkey serum. Slides were mounted with 50 mM Tris-HCl buffer (pH 8.5) with 6% DABCO and 50% glycerol.

For EM analysis, EBs were fixed in 0.5% glutaraldehyde and 0.2% tannic acid in PBS for 1 h at RT, washed with 0.1 M Na-cacodylate buffer (3 × 5 min). Next, they were transferred to a

modified Karnovsky's fixative and subsequently post-fixed in 1% OsO₄ (osmium tetroxide) for 1 h, dehydrated and embedded in Epon. Sections were cut with a diamond knife on an ultramicrotome. Thick sections (1 μm) were stained with 1% methylene blue/1% borax/ddH₂O for the light microscopy analysis. Thin sections (90 nm) were stained for 20 min with saturated uranyl acetate followed by 2-5 min wash with 0.2% lead citrate and rinsing with ddH₂O. Images were photographed with an electron microscope (JEM-1200EX; JEOL USA, Inc.).

2.5.3.3 Analysis of the ES cells differentiation potential

After 6 days in a suspension culture, EBs were transferred into uncoated chamber slides (Nunc) and cultured in EB medium for 7 or 14 days to allow for further differentiation into different types of cells. Spontaneously developed tissues were identified by IF analysis of marker proteins, performed according to a standard staining protocol (2.5.4.4).

2.5.4 Primary keratinocytes

2.5.4.1 Culture conditions

After the isolation (2.5.4.3), primary keratinocytes were seeded on a plastic or glass surface, coated with collagen I and fibronectin (Col/FN) or a LN5-rich matrix (LN), and cultured in a special medium at 34°C in 5% CO₂ air with 95% humidity. The growth medium was changed one day after seeding and every 2-3 days afterwards. Keratinocytes were grown without splitting until control cells became fully confluent (7-10 days).

Keratinocyte Medium:

MEM.....	500 ml	[Sigma #M8167]
Chelated FCS.....	40 ml (8%)	
Insulin (5 mg/ml in 4 mM HCl).....	500 μl (5 μg/ml)	[Sigma #I5500]
EGF (200 μg/ml)*.....	5 μl (10 ng/ml)	[Sigma #E9644]
Transferrin (5 mg/ml)*.....	1000 μl (10 μg/ml)	[Sigma #T8158]
10 mM Phosphoethanolamine*.....	500 μl (10 μM)	[Sigma #P0503]
10 mM Ethanolamine*.....	500 μl (10 μM)	[Sigma #E0135]
Hydrocortisone (5 mg/ml in EtOH) ..	36 μl (0.36 μg/ml)	[Calbiochem #386698]
200 mM L-Glutamine (100x).....	5 ml	[Gibco # 25030-024]
Penicillin/streptomycin (100x).....	5 ml	[PAA Laboratories #P11-010]
→ medium was sterile filtered (0.22 μm) before adding antibiotics		
→ marked compounds (*) where diluted in PBS		

Before adding to the medium, FCS (Gibco #10270-106) was depleted of Ca²⁺ ions, which induce differentiation of keratinocytes. Chelex resin (Biorad #142-2832) was suspended in 5 l ddH₂O (40 g/l) and adjusted to pH 7.4 with HCl. Afterwards the suspension was filtered through

a paper filter (Schleicher&Schuell #314856) and the buffered resin was gently stirred with 500 ml of a heat inactivated FCS, O/N at 4°C. Chelex beads were removed by filtering and subsequent centrifugation (5 min, 8000 rpm). FCS was sterilized with a vacuum filter system (Corning #431097), aliquoted (40 ml) and stored at -20°C.

2.5.4.2 *Surface coating*

The Col/FN-coated surface was prepared by incubating dishes/plates/chamber slides with the coating medium for 2-4 h at 37°C. Afterwards, containers were directly used or sealed with Parafilm (ANC Co) and stored at 4°C. Before seeding cells, coating medium was removed and the dishes were washed with PBS.

Coating medium

MEM.....	(21.5 ml)	25 ml	[Sigma #M8167]
BSA, pH 7.0 (1 mg/ml)*.....	2.5 ml	(0.1 mg/ml)	[PAA Laboratories #K41-001-100]
1 M HEPES, pH 7.3.....	500 µl	(20 mM)	[Sigma #H0887]
Vitrogen-collagen I (3 mg/ml)	250 µl	(30 µg/ml)	[Cohesion #FXP-019/Nutacon #5409]
Fibronectin (1 mg/ml).....	250 µl	(10 µg/ml)	[Invitrogen #33016-015]
100 mM CaCl ₂ *.....	290 µl	(1 mM)	
→ fibronectin was diluted in sterile ddH ₂ O			
→ marked compounds (*) where diluted in PBS and sterilized by filtration (0.2 µl)			

The LN matrix was deposited by RAC-11P/SD squamous cell carcinoma cells (Sonnenberg *et al.*, 1993) and prepared according to a previously published protocol (Delwel *et al.*, 1993), with modifications. In short, cells were seeded in a dish/plate/chamber slide and grown until confluency in D-MEM containing 10% FCS. Afterwards, cells were washed three times with PBS and incubated O/N at 4°C with sterile 20 mM EDTA/PBS solution supplemented with protease inhibitor cocktail tablets (cOmplete, Mini, EDTA-free tablets; Roche #11836170001). The following day, cells were removed as a single sheet by short pipetting (along the walls of the dish). The matrix was washed once and stored in PBS at 4°C until use.

2.5.4.3 *Isolation of primary keratinocytes from adult mice*

Isolation of epidermis keratinocytes from older mice was carried out according to a modified protocol of Romero and colleagues (Romero *et al.*, 1999). Sacrificed mice were shaved and sequentially washed in an iodine solution, distilled water and 70% EtOH (~60 s in each). After limbs were cut off, the skin was peeled off from the trunk and placed in a sterile Petri dish (10 cm Ø). The subcutaneous layer was removed very thoroughly with a scalpel (scraped off), as any remaining fat would drastically reduce the activity of trypsin. Skin was cut into fragments (~3-5 cm²) and placed (epidermis down) in a dish filled with 25 ml of antibiotics-containing PBS

for 5-10 min. Afterwards, skin fragments were transferred (epidermis up) to a new dish filled with 25 ml of 0.8% trypsin/PBS (Trypsin 1:250; Invitrogen #27250-018) and incubated for 50 min at 37°C. Epidermis was separated with forceps, transferred to the DNase medium (MEM supplemented with 0.25 mg/ml DNase I [deoxyribonuclease; Sigma #DN25] and 8% chelated FCS; 2.5.4.1; sterile filtered – 0.2 µm) and incubated with shaking for 30 min at 37°C in a water bath. Afterwards, the suspension was filtered through a 70 µm cell strainer (BD Biosciences). Collected cells were spun down (5 min, 500g) and washed once with the DNase medium. Subsequently cells were resuspended in the growth medium (2.5.4.1), counted and seeded on a coated surface (2.5.4.2) at a density of $\sim 6 \times 10^6$ cells per dish (10 cm Ø), $1-1.5 \times 10^6$ cells per well (6 well plate) and $2-4 \times 10^5$ cells per chamber slide well.

Antibiotics-PBS

PBS 500 ml

Penicillin/streptomycin (100x)..... 10 ml [PAA Laboratories #P11-010]

Nystatin (10000 U/ml)..... 10 ml [Sigma #N1638]

Fungizone (250 µg/ml)..... 10 ml [Gibco # 15290-026]

2.5.4.4 Immunofluorescence staining of cells

Cells intended for IF analysis were grown on glass chamber slides (Nunc) coated with a suitable substrate. At chosen time points they were briefly rinsed in PBS and fixed for 10 min in freshly prepared cold 3.7% PFA/PBS. A permeabilization with 0.1% Triton X-100/PBS was performed for 15 min before 60 min blocking with 2% BSA/PBS. Alternatively Triton X-100 was added to the blocking solution. After rinsing with PBS, primary antibodies were applied and incubated for 60 min at RT. The rest of staining procedure was performed as described for skin IF (2.7.2.1). Slides were dried O/N at RT and stored at 4°C. Staining results were analysed using a fluorescence microscope (DM RA2; Leica) and archived with a digital camera (OrcaER; Hamamatsu).

2.5.4.5 Adhesion assay

Wells for the adhesion assay (96-well plate) were coated with substrates used for standard keratinocyte culture. The Col/FN coating was obtained by incubating a surface with PBS containing 30 µg/ml collagen I and 10 µg/ml fibronectin O/N at 4°C. The LN matrix was prepared as described in chapter 2.5.4.2. Before seeding cells, plates were washed with PBS, blocked with 1% BSA/PBS (PAA Laboratories) for 90 min at 37°C and washed again.

After isolation from adult mice, keratinocytes were resuspended in a standard growth medium (2.5.4.1) without FCS and seeded in 100 µl at a density of 10^5 cells/well. Three maximal value samples were transferred to a 1.5 ml tube (3×10^5 cells in 300 µl). Cells seeded on the plate

were incubated for 1-2 h at 37°C. Afterwards non-attached cells were removed by washing 3 times with PBS and 50 µl of substrate buffer were added to each well. Keratinocytes in the tube were spun down, resuspended in 150 µl of the substrate buffer and transferred to 3 empty wells (50 µl/well). The plate was incubated O/N at 37°C. The following day, 75 µl of the stop buffer were added to each well and the absorbance was measured at 405 nm with a plate reader (Dynatech MR5000).

Substrate buffer

A:
 NPAG (Sigma #N9376)..... 25.7 mg
 0.1 M Na-citrate, pH 5.0..... 10 ml

B:
 Triton X-100..... 0.5 %
 → both buffers prepared in ddH₂O
 → A + B mixed [1:1] and stored at -20°C

Stop buffer

Glycine, pH 10.4..... 50 mM
 EDTA..... 5 mM
 → prepared in ddH₂O

2.5.4.6 Time-lapse video microscopy and cell spreading analysis

Live cell recordings of freshly isolated keratinocytes (from 8-months-old mice) were performed using a Zeiss Axiovert 200 M microscope with a motor-controlled CCD camera (OrcaER, Hamamatsu). Images of cells were captured every 20 min for 42 h (at 37°C, 5% CO₂). The recording was started immediately after keratinocytes were seeded on Col/FN coated plastic (6-well plates). The cell size for spreading analysis was assessed by measuring the pixel area of 30-40 randomly picked cells in pictures taken at indicated time points. Evaluation and processing of images were performed with the Metamorph software (Universal Imaging Corporation).

2.5.4.7 Isolation of primary keratinocytes from 3d old mice

Epidermis of 3-day-old mice was isolated according to a modified protocol previously described by Caldelari and co-authors (Caldelari *et al.*, 2000). In short, mice were sacrificed using ether (10-15 min) and washed in an iodine solution and 70% EtOH (60 s in each). After limbs and the tail were cut off, the skin was peeled off and placed, dermis up, in a Petri dish (6 cm Ø) filled with 4-5 ml of 10 µg/ml gentamicin/PBS solution (stock: 5 mg/ml; Sigma #G1397). The washing step was performed for 5-10 min, twice. Subsequently, the skin was transferred, epidermis up, to a dish containing 4-5 ml of dispase-II solution and incubated O/N at 4°C.

The following day epidermis was separated from dermis and torn into pieces using forceps. Fragments were placed in 15 ml tube with 10 ml of 5x trypsin/EDTA solution (Gibco #15400-054; 2.5.1.2) and incubated for 10 min at 37°C. During the trypsinization, the suspension

was mixed a few times to keep the tissue pieces afloat. Afterwards, part of the cell suspension (~5 ml) was transferred to a new tube, avoiding the epidermis pieces. K-SFM medium containing 10% FCS (5 ml) was added to the remaining part, mixed and transferred again. Cells were spun down for 5 min at 1000g, resuspended in the medium for counting and washed with PBS before the lysis.

Dispase II solution:

<i>K-SFM (not supplemented)</i> 45 ml	[Gibco #10744-019]
<i>Dispase II</i> 0.25 g (5 mg/ml)	[Roche #165859]
<i>Penicillin/streptomycin (100x)</i> 5 ml	[PAA Laboratories #P11-010]

→ solution was sterile filtered (0.2 µm) before adding antibiotics;

2.6 Generation of a conditional knock-out mouse

Conditional knock out of the murine *rac1* gene in the epidermis was generated in this study using the Cre-loxP system and following the guidelines published by Talts and co-authors (Talts *et al.*, 1999).

2.6.1 Cre-loxP system

The Cre-loxP system is a widely used tool, which enables tissue-specific and/or time-specific ablation of the gene of interest. It is very useful for studying the function of a gene in differentiated tissues, when a conventional knock-out leads to an early embryonic death.

Cre recombinase is a 38 kDa protein from bacteriophage P1 which mediates an intramolecular (excisive or inversional) and an intermolecular (integrative) site specific recombination between *loxP* sites (Sauer, 1993).

The *loxP* site (Fig. 2.4) consists of two 13 bp inverted repeats (black) separated by an asymmetric spacer region (8bp; red). The recombination (cross-over) occurs in the asymmetric spacer region, which determines the directionality of the site. Two *loxP* sequences in an opposite orientation to each other invert the DNA fragment between them. Two sites in a direct orientation dictate excision of the intervening DNA between them, leaving one *loxP* site behind.



Fig. 2.4 LoxP site consensus sequence. Flanking parts (black) create a palindromic sequence separated by asymmetric region (red) determining the direction of the site.

Two mouse lines are required for a conditional gene deletion. First, a transgenic mouse line with a Cre recombinase expression restricted to a specific tissue or cell type and second, a mouse strain carrying a modified target gene (endogenous gene or transgene) with a fragment flanked

by *loxP* sites in a direct orientation ("floxed gene"). An excision leading to the gene inactivation occurs only in cells expressing Cre recombinase and the target gene remains intact in all the other cells and tissues.

2.6.2 Targeting construct preparation

2.6.2.1 Modification of the selection cassette

The selection cassette used in this study contained genes encoding neomycin resistance (*neo*) and Herpes Simplex Virus thymidine kinase (TK). The product of the *neo* gene expressed in eukaryotic cells inactivates G418 (a gentamicin-related antibiotic). Therefore, a positive selection for cells carrying the gene is possible using medium containing G418. Cells expressing TK can be eliminated by a negative selection using FIAU (1-2'-deoxy-2'-fluoro-b-D-arabinofuranosyl-5-iodouracil). This compound is transformed by TK into an analogue of thymidine, which gets incorporated into DNA, effectively killing cells expressing the enzyme.

The selection cassette (4.7 kbp) was subcloned into the MCS of the pBS vector (3 kbp; Fig. 2.1) between *EcoRI* and *HindIII* sites as shown in Fig. 2.5A. Before inserting the cassette into the targeting construct, *SalI* site located within the cassette had to be removed, as *SalI* was later used to linearize the plasmid before the electroporation (2.6.2.3). In the first step, DNA was cut with *ClaI/XhoI* and ligated with an oligonucleotide linker (primers AC3+AC4; 2.4.1), which resulted in the removing of *SalI* site from the MCS of the vector (Fig. 2.5B). The incorporation was confirmed by *PstI* and *ScaI* digestions. Next, the plasmid was cut with *SalI* and the resulting overhangs filled in. After a blunt re-ligation, the absence of *SalI* site was confirmed with *BamHI* and *SalI/BamHI* digestions. The modified selection cassette (Fig. 2.5C) was cut out with *NotI/ClaI* digestion and combined with the targeting construct.

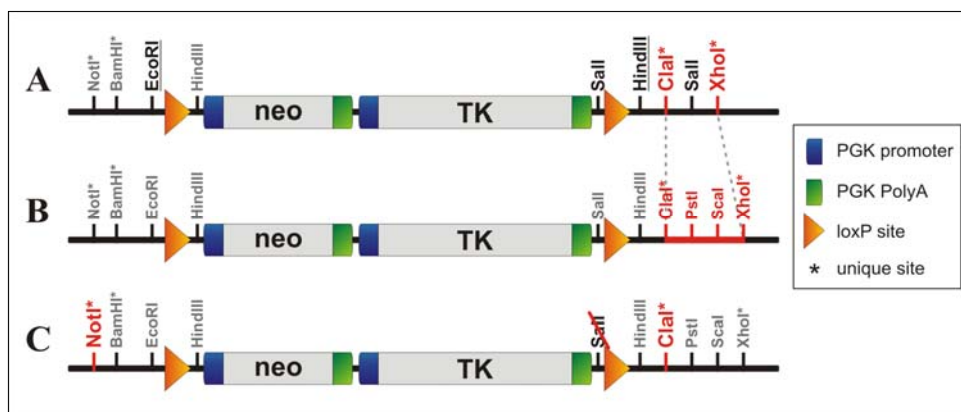


Fig. 2.5 Modification steps of the selection cassette. (A) The unmodified neo-TK selection cassette subcloned in the pBS between *EcoRI*/*HindIII* sites of the MCS (underlined). **(B)** Modification of the MCS sequence (red). **(C)** The final selection cassette. *NotI* and *ClaI* sites used for subcloning into the targeting vector are marked in red.

2.6.2.2 Cloning of the targeting construct

An EcoRI–Sall fragment of the *rac1* gene (11.7 kbp), containing exons 2 and 3 was isolated from a 129/Sv PAC library clone (Geneservice Ltd.; (Osoegawa *et al.*, 2000) and subcloned into the pBS vector (3 kbp; Fig. 2.6A). The correct PAC clone was identified in a Southern blot screening of the library. A piece of the Rac1 gene containing exon 3 sequence was used as a probe. It was generated with primers PAC1 and PAC2 (2.4.1) as described earlier (2.4.7.2).

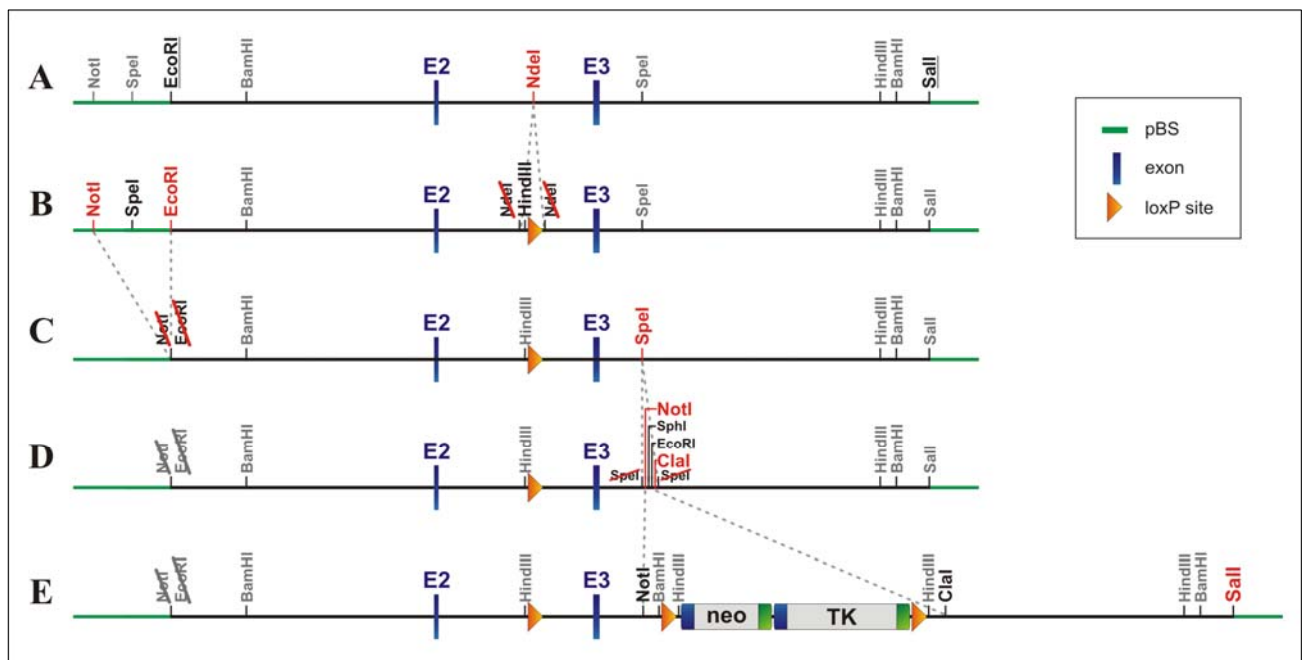


Fig. 2.6 Generation of the targeting construct. (A) A fragment of the *rac1* gene subcloned into the pBS vector between EcoRI and Sall sites (underlined). (B-D) Results of consecutive cloning steps described in the text. Changes marked in red. (E) The final targeting construct with Sall site used for linearization marked in red.

In the first step of the gene sequence modification, an oligonucleotide linker containing a HindIII site and the *loxP* sequence (primers AC1+AC2; 2.4.1) was introduced at NdeI site (Fig. 2.6B). The insertion was verified with HindIII digestion and the orientation of the *loxP* site was checked by sequencing with primer AC11 (2.4.1). Next, NotI and SpeI sites within the MCS were removed. After cutting with NotI/EcoRI, overhangs were filled in and the plasmid was religated (blunt). The resulting sequence, depicted in Fig. 2.6C, was confirmed by digestion with SpeI/EcoRI. Before the selection cassette introduction, NotI and ClaI sites had to be created downstream of exon 3. An oligonucleotide linker (primers AC9+AC10; 2.4.1) was introduced in SpeI site as shown in Fig. 2.6D. The correct orientation was verified by sequencing with primer AC12 (2.4.1).

ClaI is a methylation-sensitive restriction enzyme. Therefore, before the final cloning step, plasmids carrying both the unfinished targeting construct (Fig. 2.6D) and the selection cassette

(Fig. 2.5C) were transformed into JM110 strain of *E. coli*, which is deficient for methylases (Dam and Dcm). DNA purified from these bacteria was not methylated and could be cut by NotI/ClaI digestion. Both fragments were then combined to form the final targeting construct (19.4 kb; Fig. 2.6E).

2.6.2.3 Preparation of DNA for the electroporation

For an efficient uptake of a targeting construct and its successful integration in the genomic DNA, the plasmid must be completely linearized and purified.

The targeting construct was cut with SalI for 6-7 h at 37°C and the efficiency of digestion was checked with an agarose gel electrophoresis by the comparison with an uncut vector.

Targeting construct linearization:

DNA.....	~100 µg
SalI NEBuffer (10x).....	20 µl
BSA (10 µg/µl)	10 µl
SalI (160U).....	8 µl
ddH ₂ O	x µl
	200 µl

After digestion, the DNA suspension was mixed with 200 µl of phenol/chloroform solution [1:1] and centrifuged for 5 min at 20,000g. The upper phase (aqueous), containing DNA, was transferred to a new tube, mixed with 200 µl chloroform and centrifuged. Again, the upper phase was transferred to a new tube. To precipitate DNA, 20 µl of 3 M Na-Ac (pH 5.2) and 500 µl of 100% EtOH were added and thoroughly mixed. White, coiled DNA was transferred to a sterile 1.5 ml screw-cup tube filled with 1 ml of 70% EtOH. The tube was inverted several times to sterilize DNA and the inside of the tube. DNA was stored at -20°C until the electroporation day.

Shortly before the electroporation, EtOH was carefully removed (pipette with a 1000 µl tip) and DNA was air-dried in a sterile hood for 5-10 min (at RT). The pellet was resuspended in 700 µl PBS and incubated at 37°C until DNA dissolved completely.

2.6.3 Homologous recombination of the targeting construct

The modified part of gene can be inserted into ES cells (2.5.1) genome by utilizing a homologous recombination event, in which transfected DNA is exchanged with a complementary fragment within the chromosome sequence.

Electroporation is routinely used to introduce plasmid DNA into mammalian cells. In this procedure, a large electric pulse temporarily disturbs the cell membrane, allowing polar molecules, such as DNA, to pass into the cell.

2.6.3.1 Electroporation of ES cells

Usually, 4×10^7 ES cells were electroporated with $\sim 100 \mu\text{g}$ of a linearized targeting construct and 360 clones were picked to screen for homologous recombinants. If a lower number of clones was going to be screened, only 2×10^7 ES cells were used for the electroporation.

When 4×10^7 ES cells were going to be electroporated, 8 dishes (10 cm \varnothing) with subconfluent layers of feeder cells (2.5.2) were prepared. Feeders were thawed and seeded (1 vial/dish) several hours or a day before the electroporation. Alternatively, cells were thawed shortly before the electroporation, resuspended in ES medium and co-seeded with electroporated ES cells.

An aliquot of ES cells, from the passage previously checked for a germ-line transmission capability, was thawed and expanded to obtain sufficient amount of cells. Before the electroporation, ES cells were trypsinized and thoroughly resuspended in 10 ml ES medium to obtain a single-cell suspension. Cells were counted and washed twice with 10 ml PBS (5 min at 500g). After the last centrifugation, PBS was decanted and the pellet ($\sim 4 \times 10^7$ cells) was resuspended by flicking the tube with a finger. ES cells were mixed with 700 μl of the DNA suspension (2.6.2.3) and transferred with a Pasteur pipette to a sterile electrocuvette (0.4 cm; BioRad #165-2088). The electroporation was performed at RT with a Gene Pulser (model 1652077; BioRad) at 0.8 kV/3 μF , with the time constant (decay of the electric field) of 0.04 ms. Immediately afterwards, cells were carefully transferred to ES medium and seeded in 8 cell-culture dishes (10 cm \varnothing) with previously prepared feeder cells. ES cells were incubated in 8 ml/dish of the growth medium at standard conditions.

2.6.3.2 Selection and picking of clones after the recombination

The positive selection was started ~ 24 h after the electroporation. ES medium was supplemented with 500 $\mu\text{g/ml}$ G418 Sulphate (Geneticin; Gibco #01811), which selectively kills cells without neomycin resistance gene. Therefore, only successfully electroporated ES cells, which had the targeting vector incorporated into the genome, were able to survive. The selection medium was changed every day. After 6 days, when resistant ES cells had formed big enough colonies, 360 clones were picked.

Clones were grown in 24-well plates on a feeder layer prepared the previous day or few hours earlier. Feeder cells (2.5.2) were thawed (1 vial/plate), seeded in plates and incubated in EF medium at 37°C. Shortly before picking, EF medium was exchanged for G418 containing ES medium (1 ml/well). If feeder cells were thawed on the day of picking, they were seeded directly in ES medium with G418. Trypsin/EDTA solution (1x) was aliquoted into 96-well plates (150 μl /well) and pre-warmed to 37°C.

Picking of selected ES cells clones was conducted under the stereomicroscope (Stemi SV6; Zeiss) placed in a laminar flow hood. Single colonies were lifted from the feeder cell layer with a sterile tip (200 μ l) and transferred to the trypsin solution. After 24 clones were picked, the plate was incubated for 5-10 min at 37°C. Next, each colony was dispersed by pipetting with 150 μ l of G418 supplemented ES medium and transferred to a 24-well plate with prepared feeder cells. A full plate was placed in an incubator and the next 24 clones were picked. ES cells were grown at standard conditions. The medium was changed only once, on the following day.

When, after 3-5 days, the medium started to turn yellow, ES cell clones were frozen. Cells were washed twice with PBS and incubated with \sim 150 μ l of 1x trypsin/EDTA solution, for 5 min at 37°C. Ice-cold freezing medium was added to each well (1 ml/well) and cells were resuspended thoroughly. For each clone, 0.5-0.6 ml of the cell suspension were transferred to a cryo-vial and placed immediately on dry-ice (in a freezer-box). Full boxes were transferred to -80°C. ES medium (w/o G418) was added to remaining cells (1.5 ml/well) and exchanged the following day (1 ml/well) to remove residual DMSO. ES cells were grown until medium turned yellow in order to isolate sufficient amount of DNA for screening (2.6.3.3).

2.6.3.3 Screening of ES cell clones

When ES cell clones were expanded after freezing (2.6.3.2), DNA was extracted (2.4.5.2) and screened by a Southern blot analysis (2.4.7). Homologously recombined clones were identified after HindIII digestion with the external probe (0.33 kbp), which was created (2.4.7.2) using primers AC15 and AC16 (2.4.1). Positive clones were checked for random integration of the targeting construct with Southern blot analysis of HindIII digested DNA using the internal probe (1.2 kbp) obtained with primers AC6 and AC7 (2.4.1).

2.6.4 Removal of the selection cassette

Before injecting into the blastocysts, the selection cassette was removed from ES cell clones with a successfully recombined allele. Transient expression of the Cre recombinase led to an excision of DNA fragments between *loxP* sites. As the modified gene contained three *loxP* sites (3loxP), different fragments could have been removed: only exon 3, only the selection cassette (resulting in the conditional allele) or both (resulting in the null allele) (Fig. 3.2). The presence of HSV-tk gene in the selection cassette enabled a negative selection. ES cells not recombined after *cre* transfection or still carrying the cassette were eliminated with FIAU treatment.

Two different *rac1*^{3loxP/+} clones were thawed and expanded to obtain \sim 1 \times 10⁷ cells (full 25 cm² T-flask). After trypsinization, the fifth part of cells was electroporated with PBS alone as a control and plated with feeder cells in a dish (10 cm \emptyset). The remaining cells were

electroporated (2.6.3.1) with 20 µg of pIC-Cre plasmid in PBS (Gu *et al.*, 1993) (gift from Dr. Werner Müller, University of Cologne, Germany) and seeded with feeder cells in four 10 cm Ø dishes. After 2 days cells were trypsinized and the fifth part from each dish was reseeded. The selection was started 24 h later. ES medium containing 0.2 µM FIAU was applied and changed every day (twice a day during the death peak). After 5-6 days, ES cell colonies were picked, expanded and frozen as described earlier (2.6.3.2). To identify the ES cell clones with the conditional or the null allele, a Southern blot analysis of BamHI-digested genomic DNA was conducted with the internal probe (2.6.3.3).

2.6.5 Blastocyst injection

Clones selected for injection were thawed and grown in 6-well plate for 1-2 days. ES cells were trypsinized, resuspended in 3 ml of [1:1] mixture of ES medium and flush medium (10% FCS D-MEM buffered with 20 mM HEPES, pH 7.4), and kept on ice until the injection procedure. Blastocyst injections were performed by Dr. Michael Bösel (Transgenic Service, Max Planck Institute of Biochemistry, Martinsried).

As mentioned before (2.5.1), R1 ES cells used in this study are derived from blastocyst from 129/Sv mouse strain. They have a male genotype (XY) and carry the dominant coat-colour marker agouti. Blastocysts used for the injection, derived from C57BL/6 mouse strain, were carrying the recessive coat-colour marker black and had a random genotype. ES cells (10-15) were injected into the cavity of blastocysts, which were transferred afterwards into the uterus of a pseudo-pregnant mouse (foster mother). Both type of cells contributed to developing foetuses resulting in a birth of chimeric mice. The ratio of the ES cells contribution was roughly assessed by the percentage of the agouti-coloured coat.

2.6.6 Breeding schemes

Male chimeras with the highest contribution of ES cells were mated with C57BL/6 females. As agouti mice could only develop from ES-cell-derived sperm, the coat colour of the offspring was a first indicator of germ-line transmission. Offspring carrying the conditional allele were identified by PCR genotyping (2.4.6.1) with primers designed to distinguish between the wild type and the floxed allele (Fig. 3.2, blue arrows). The results were confirmed by a Southern blot analysis with the internal probe. Heterozygote mice were mated to obtain homozygote animals. After the lack of a phenotype in *rac1^{fl/fl}* mice was confirmed, they were intercrossed with mice carrying *cre* transgene to obtain tissue specific deletion of Rac1 protein.

Transgenic mice, which were used in this study, express Cre recombinase under the control

of the K5 promoter (K5-Cre) (Ramirez *et al.*, 2004), which is activated in HF_s (ORS, bulge and SG_s) and in the epidermis (basal keratinocytes), as well as in other stratified epithelia (i.e. tongue, esophagus, forestomach) (Byrne and Fuchs, 1993). An efficient recombination of a floxed gene in the back skin of mice carrying the *cre* transgene was shown from day 15.5 of the embryonic development onwards (Ramirez *et al.*, 2004). The presence of the *cre* transgene during breeding of mice was confirmed with Cre PCR.

The final breeding scheme used to obtain mutant and control animals for experiments is shown in Fig. 2.7. Females carrying K5-Cre were not used for breeding because the expression of Cre recombinase occurs in late-stage oocytes. The protein presence persists into a developing embryo leading to a constitutive recombination of the gene (Ramirez *et al.*, 2004).

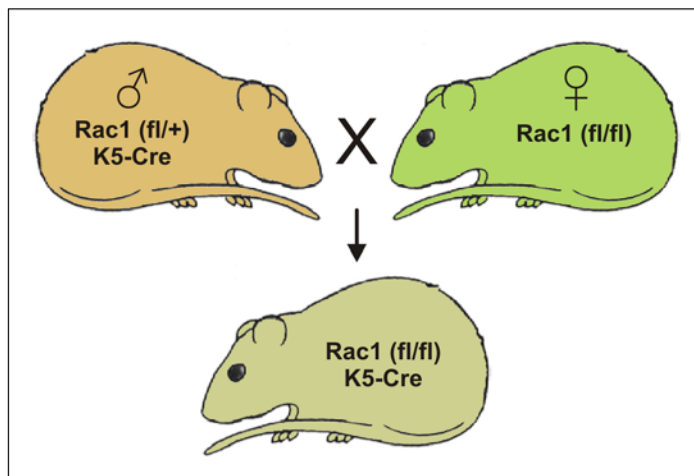


Fig. 2.7 Mating scheme used to obtain mice with a skin-specific *Rac1* deletion.

Presence of the null allele in mice carrying both the *rac1* conditional allele and the *cre* transgene was confirmed with KO PCR (Fig. 3.2, pink arrows). All primers used for mice genotyping are summarized in chapter 2.4.1.

2.6.7 Generation of knock-out ES cells.

Rac1-deficient ES cells – *Rac1* ($-/-$) – were obtained from *rac1*^{-/+} clones generated during Cre induced elimination of selection cassette (2.6.4). Cells with one null allele were expanded and electroporated again with the targeting construct (2.6.3). After identification of homologously recombined *rac1*^{3loxP/-} clones, second round of Cre transfection and FIAU selection was performed (2.6.4) and surviving clones were screened for *rac1*^{-/-} and *rac1*^{fl/-} genotypes. The latter were used as control clones – *Rac1* (fl/-).

2.7 Skin phenotype analysis

2.7.1 Histology

2.7.1.1 *Skin isolation and embedding*

At selected time points, skin was isolated for the analysis of the epidermis and HF morphology. Mutant and control mice were sacrificed and the fur on the back was shaved, if necessary (older control animals). A fragment of back skin (Fig. 2.8A) was separated at the subcutis level (below the subcutaneous muscle) and spread on a nylon membrane (Hybond-XL; Amersham Biosciences). The skin piece was cut along the midline (spine) and then divided into smaller fragments as shown on Fig. 2.8B. Pieces from one side were fixed before the subsequent embedding in paraffin (2.7.1.3). Remaining fragments were immediately cryo-embedded (2.7.1.2). During the final setting into a block (paraffin or cryomatrix), skin samples were positioned perpendicular to the cutting plane with the midline edge directed towards it (Fig. 2.8C). Samples were embedded with the membrane to prevent folding and wrinkling of skin fragments.

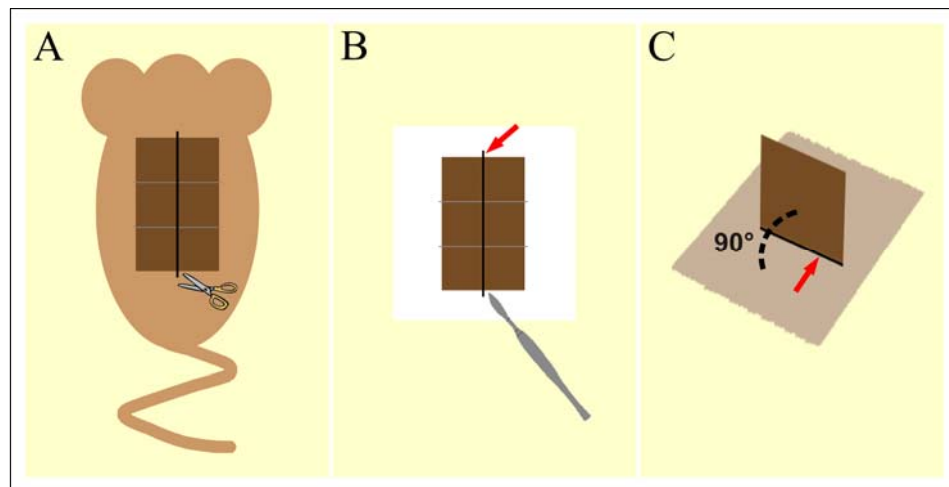


Fig. 2.8 Schematic presentation of the skin isolation procedure. Detailed description in the text. Red arrow points out the midline.

2.7.1.2 *Cryo-embedded sections preparation*

Skin fragments were isolated as described above (2.7.1.1). Plastics cryo-molds (Tissue-Tek; Sakura) were placed on a copper plate laying on dry-ice. Each sample was thoroughly covered in Shandon Cryomatrix compound (Thermo Electron Corporation) before placing in a pre-cooled plastic form. When the skin fragment (positioned as shown in Fig. 2.8C) was stabilized, the container was filled up with the cryomatrix. Frozen blocks were stored at -80°C . Before cutting, samples were warmed up to -20°C .

Frozen tissue was cut with a cryotome (Cryostat HM5000M; Microm) into $10\ \mu\text{m}$ thick

sections. They were collected on positively charged glass slides (SuperFrost Plus; Menzel-Gläser), air-dried for ~30 min at RT and stored at -80°C.

2.7.1.3 Paraffin sections preparation

Skin fragments were isolated as described above (2.7.1.1) and fixed in a fresh 4% PFA/PBS solution O/N at 4°C. The following day, samples were dehydrated in consecutive baths with a gradually increasing concentration of EtOH: 50%, 70% and 80% for 60 min, 90% – O/N and 100% – 3 × 60 min. The whole procedure was conducted at RT. Next, skin fragments were placed in xylol for 2 × 15 min and subsequently transferred to a container with liquefied paraffin (kept at 56°C in an oven). To remove all traces of xylol, paraffin solution was changed twice during the incubation time (60 + 60 + 90 min). In the end, skin fragments were set in paraffin blocks using an embedding station (Shandon Histocentre2; Thermo Electron Corporation). Samples were stored at 4°C. Before cutting, they were cooled down on ice or in a -20°C freezer.

Paraffin embedded tissue was cut using a microtome (HM355S, Microm) into 6 µm thick sections. They were collected on positively charged glass slides (SuperFrost Plus; Menzel-Gläser) and stored at RT or 4°C.

2.7.1.4 Hematoxylin-eosin (HE) staining

The skin morphology was visualized with a commonly used histological technique – HE staining, in which tissue components are stained on the basis of their charge. Hematoxylin has an affinity for negatively charged molecules and therefore reveals, with a blue/purple staining, acidic tissue components, such as nucleic acids or acidic proteins. Eosin stains, in pink/red, alkaline tissue components, e.g. collagens or keratins. The staining was performed manually at RT, as described below, or using an automated system (Shandon Linistain GLX; Thermo Electron Corporation).

Paraffin was removed from sections with xylol (2 × 5 min). Samples were rehydrated by consecutive incubations in a graded series of EtOH dilutions – 100%, 100%, 95%, 90%, 80% and 70% (2-3 min in each) – followed by 2-3 min wash in ddH₂O. Sections were stained for 60 s in [1:3] Mayer's hemalaum/ddH₂O solution (Merck) and differentiated by rinsing in tap water. Subsequently, slides were incubated for 60 s in 0.1% eosin solution (Eosin Y; Merck) and rinsed again in tap water. Sections were dehydrated in a reversed EtOH row, washed 2 × 5 min with xylol and mounted with Entellan (Entellan New; Merck). Pictures of tissue were taken using a phase contrast microscope (Axioskop; Zeiss) with Leica DC500 camera.

2.7.2 Immunohistochemistry

2.7.2.1 *Detection of marker proteins in skin using immunofluorescence*

Immunofluorescence (IF) staining was performed on cryo-sections. Control and mutant samples were warmed up to RT for 60 min and fixed for 20 min in fresh 4% PFA/PBS solution (in case of antibodies against HF-specific markers: 10 min in MeOH at -20°C). Subsequently, sections were washed 3 × 5 min in PBS and permeabilized with 0.1% Triton X-100/PBS for 5 min on ice. Tissue was blocked with 2-3% BSA/PBS solution, either for 60 min in RT or O/N at 4°C. After short rinsing with PBS, each section was circled with a hydrophobic barrier pen (ImmEdge™ Pen; Vector Laboratories) and a primary antibody solution was applied. All antibodies used in this study are summarized in chapter 2.3, along with a dilution, a source species and a provider. They were diluted in 1% BSA/PBS and ~80 µl were applied on each section. Incubations were carried out in a humidified atmosphere at RT, in the dark (metal box with wet paper-lining). Primary antibodies were incubated for 90 min. As a rule, one section on each slide was incubated with a dilution buffer only, as a negative control. After 3 × 5 min washing with PBS, secondary antibodies were applied on all sections and incubated for 60 min. In case of a double staining, when a cross-reaction was excluded, primary and subsequently secondary antibodies were applied at the same time. Otherwise, staining was done sequentially. Primary antibodies conjugated with a dye were applied together with secondary antibodies, to avoid unnecessary bleaching. Nuclear DNA was visualized with DAPI (4',6-Diamidino-2-phenylindole dihydrochloride; Sigma #D9542). The 0.1 µg/ml DAPI/PBS solution was applied on sections for 5 min after the last antibody incubation. Afterwards sections were washed 3 × 5 min in PBS, mounted with Elvanol and stored at -20°C. Stained tissue was analysed and pictures taken using a confocal microscope (Leica TSC SP2) with inverted stage (DM IRE2; Leica).

Elvanol

<i>Mowiol 4-88 (Roth #0713)..... 12 g</i>	→ mixed for 2-3 h at 65°C and spun down for 25 min at 2000g
<i>ddH₂O 30 ml</i>	→ the supernatant was transferred to a glass flask
→ mixed for 10 min (in glass)	supplemented with:
→ incubated for 2-3 h at RT	<i>DABCO (Sigma #D2522) 2 g (2.5%)</i>
<i>0.2 M Tris-HCl, pH 8.5 60 ml</i>	→ mixed for 10 min and kept O/N at 4°C to remove bubbles,
<i>87% glycerol 30 ml</i>	→ aliquoted and stored at -20°C

2.7.2.2 *BrdU incorporation assay*

Bromodeoxyuridine (BrdU) is a thymidine analogue, which is incorporated into DNA. This feature is utilized to analyse proliferation of cells *in vivo*. Upon introducing into the organism,

BrdU is used by cells during DNA synthesis, in the S-phase of the cell-cycle. Cells that have incorporated BrdU can be later visualized using an anti-BrdU antibody. In this study, the BrdU incorporation assay was used to analyse proliferation of keratinocytes in the epidermis.

Mice at selected age were sacrificed 2 h after an intraperitoneal injection of BrdU solution (50 µg/g [body weight]) and paraffin sections (2.7.1.3) were prepared from isolated back skin (2.7.1.1). Tissue was hydrated as described earlier (2.7.1.4; all steps 5 min) and fixed for 20 min in 4 N HCl solution (37% HCl/ddH₂O, mixed [1:2]). After 5 min washing with ddH₂O, slides were incubated in a pre-warmed 0.1% trypsin/0.1% CaCl₂/ddH₂O solution for 20 min at 37°C and washed again with ddH₂O (5 min). Endogenous peroxidases were inactivated with [75 ml MeOH + 2.5 ml of 30% H₂O₂] solution by 10 min incubation at RT. Subsequently, sections were washed with PBS (3 × 5 min), blocked with 0.5% BSA/0.1% Tween20/PBS solution (3 × 5 min) and each section was circled with a hydrophobic barrier pen (ImmEdge™ Pen, Vector Laboratories). Anti-BrdU antibody, conjugated with the horseradish peroxidase (POD), was diluted in the blocking buffer and incubated O/N at 4°C. After washing with PBS (3 × 5 min), sections were incubated for 5-10 min in DAB solution (in the dark at RT) until clearly visible colour developed. The intensity of the staining was controlled under the microscope and the reaction was stopped with ddH₂O (10 min wash). Tissue was counterstained with [1:5] Mayer's hemalaun/H₂O solution (Merck/tap water). Slides were dipped in the solution (5-8 × 10 s) and washed with tap water in between. The staining progress was controlled under the microscope. When the intensity of staining became optimal, sections were washed in tap water for 10 min. After dehydration with EtOH (95%, 2 × 100%, 5 min each) and xylol (2 × 5 min), slides were mounted with Entellan New (Merck # 1.07961) and stored at RT.

DAB solution:

ddH₂O..... 45 ml
1 M Tris-HCl, pH 7.4..... 50 ml
Stock I (DAB)..... 5 ml
Stock II..... 120 µl
 → both Stock solution are prepared just before use

Stock I

DAB (Sigma #D5637)..... 27 mg
ddH₂O..... 5 ml
 → keep in the dark

Stock II

30 % H₂O₂..... 20 µl
ddH₂O..... 100 µl

The horseradish peroxidase conjugated with the anti-BrdU antibody catalyzes an oxidation reaction of diaminobenzidine (DAB) in the presence of hydrogen peroxide. The reaction product is brown and insoluble in EtOH or H₂O. DAB solution is very toxic.

2.7.2.3 Apoptosis analysis

Cleavage of the genomic DNA during apoptosis results in a formation of small double-stranded fragments or single strand breaks (“nicks”) within the helix. Free 3’-OH ends can be

labelled with the TUNEL technique (terminal deoxynucleotidyl transferase -mediated dUTP nick end-labelling). In this study, apoptotic cells in skin were visualized using In Situ Cell Death Detection Kit (Roche #11684817910). Labelling was performed on cryo-sections according to a protocol provided by the manufacturer. Pictures were taken using a confocal microscope.

2.7.2.4 FACS cytometry analysis

Flow cytometry is a technique which enables a multi-parametric analysis of single cells flowing in a stream through a detection system. Cells can be described, counted and sorted based on the measurements of scattered and fluorescent light, which is collected when a suspension of cells is passing through the light beam. Scattered light gives information about size and physical complexity of cells. As several „colours” of fluorescent light can be measured at the same time, the simultaneous use of different dye-conjugated antibodies enables description of biochemical or physiological properties. Distinct subpopulation of cells can be distinguished and their lineage, maturation stage or activation state described, based on differences in surface molecules expression. In this study, expression of integrins on the surface of freshly isolated keratinocytes was investigated by FACS.

Staining was performed in 96-well round bottom plate and 1% BSA/PBS buffer was used during all steps. Samples were always kept on ice and centrifuged at 4°C to prevent the receptor internalization of integrins. For each combination of antibodies, 10⁶ cells were used. When primary antibodies were conjugated with biotin or not directly labelled, additional samples (10⁶ cells each) were stained with secondary compounds only as negative controls. All used antibodies are summarized in chapter 2.3.

After isolation (2.5.4.3), keratinocytes were counted, resuspended in an appropriate amount of the buffer, distributed into the wells (200 µl/well) and spun down for 5 min at 1500 rpm (Allegra 6R; Beckman Coulter). Supernatants were carefully removed and cells were resuspended in 50 µl of a primary antibody solution; negative control samples were resuspended in the buffer only. After 30 min incubation (in the dark), cells were washed with 200 µl of the buffer, spun down and 50 µl of a secondary antibody and/or streptavidin-Cy5 solution were added. The incubation was conducted for 15 min (in the dark). Afterwards cells were washed (200 µl), resuspended in 200 µl of the buffer and transferred into FACS tubes (Alpha Laboratories Ltd.). Dead cells were stained with propidium iodide (1:40; stock: 1 mg/ml) directly before FACS analysis. The measurements were conducted using FACSCalibur Flow Cytometry System (BD) and results analysed with the CellQuest software (BD).

2.7.3 Electron microscopy (EM)

Electron microscopy analysis of the epidermis was performed by Dr. Fabio Quondamatteo (Department of Histology, Georg-August University of Göttingen, Göttingen, Germany).

Small fragments of back skin were isolated and immediately immersed in a buffer. Skin was quickly cut into small fragments (~1 mm³) and placed in a fixation solution. Some samples were dissected in PBS and fixed in 0.2 M Sörensen's buffer (pH 7.4) containing 3% PFA and 3% glutaraldehyde. After at least 24 h incubation, pieces were washed for 20 min in 0.2 Sörensen's buffer and post-fixed in 1% OsO₄ (osmium tetroxide) in PBS. For more detailed analysis of desmosomes and adherent junctions, samples were dissected in 0.1 M Na-cacodylate buffer supplemented with 2 mM CaCl₂ and subsequently fixed for at least 24 h in a mixture of 2% glutaraldehyde and 4% PFA in (0.1 mM Na-cacodylate + 2 mM CaCl₂) buffer. After washing, skin was post-fixed in 1% OsO₄ in (0.1 mM Na-cacodylate + 2 mM CaCl₂) buffer.

Fixed samples were dehydrated in a graded EtOH series and embedded in Epon. For orientation purposes, semithin sections (1 µm) were cut and stained with Richardson's solution (1% azure II/ddH₂O + 1% methylene blue/1% borax/ddH₂O, mixed [1:1]; (Richardson *et al.*, 1960). Ultrathin sections (90 nm) were cut with a ultramicrotome (Reichert-Jung), collected on formvar-coated nickel grids, stained with uranyl acetate for 10 min and subsequently with lead citrate for 7 min. Samples were examined with an electron microscope (LEO 906E, Zeiss).

2.7.4 Analysis of the tamoxifen influence on skin

Effects of 4-hydroxy-tamoxifen (4OHT) on the epidermis were analysed in a 2-3 months-old control and mutant skin. Clipped area of back skin 1-2 cm² was treated every third day for 15 days with 250 µl acetone or 250 µl 4OHT/acetone solution (10 mg/ml; Sigma #H6278). Fragments of the treated skin were isolated 1 day or 2 weeks after the last application and HE staining of paraffin sections was performed.

2.7.5 Wound healing analysis

Wound healing studies were conducted in collaboration with Dr. Ingo Haase's group (Dept. of Dermatology and Center for Molecular Medicine, University of Cologne, Cologne, Germany). The experiments were performed by Michael Tschardt and carried out after obtaining an approval of local authorities.

Wounds were created in back skin of anaesthetised control and mutant mice using a 4 mm biopsy punch. Five days after the wounding, animals were sacrificed and wounded areas, with surrounding margins, were excised. Samples were fixed in 4% PFA O/N, bisected and embedded

in paraffin (the dissection edge placed at the beginning of a block). The first complete section (4 μm) from each half of the respective wound was HE stained and used for the analysis. Morphometric measurements were performed using Leica DM 4000 B microscope (Leica) equipped with KY-F75U digital camera (JVC) and Diskus software (Carl H. Hilgers, Technisches Büro, Germany).

For visualization of proliferating keratinocytes in the wound tissue, mice were injected intraperitoneally with 3.2 mg of BrdU solution (2 h before killing). Detection of the incorporated BrdU was performed on 4 μm paraffin sections (2.7.2.2). Results were expressed in the average number of BrdU⁺ cells per microscopic field.

2.8 Biochemical methods

2.8.1 Protein isolation

2.8.1.1 Preparation of protein lysates from ES cells

ES cells were grown in Petri dishes (10 cm \varnothing) in normal conditions until they reached high density. Prior to the lysis, feeder cells were removed using a panning technique. In short, cells were trypsinized, seeded in a new dish and incubated at 37°C. After 30 min, medium with still unattached cells was collected and transferred to a new dish. The procedure was repeated 3 times and resulted in separation of fibroblasts, which adhere much faster than ES cells. The suspension contained almost exclusively ES cells, which were counted, seeded in a new dish ($1-2 \times 10^7$ cells per dish) and incubated O/N at 37°C. The following day cells were washed once with ice-cold PBS and incubated for 30 min in 750 μl of the modified RIPA lysis buffer on ice. Next, lysed cells were collected using a rubber cell scraper (Costar) and the suspension was centrifuged at 20,000g for 15 min at 4°C. The cleared lysate was aliquoted, frozen on dry-ice and stored at -80°C. A small aliquot was used for a protein concentration assay.

Modified RIPA lysis buffer (10 ml)

10% TritonX-100	1000 μl (1%)	50 mM EGTA.....	200 μl (1 mM)
10% Na-deoxycholate*...	1000 μl (1%)	100 mM Na ₃ VO ₄	100 μl (1 mM)
20% SDS	50 μl (0.1%)	ddH ₂ O.....	3685 μl
1 M HEPES, pH 7.4	500 μl (50 mM)		→ supplemented with 1 tablet of protease
5 M NaCl.....	300 μl (150 mM)		inhibitors (cOmplete Mini EDTA-free; Roche)
87% glycerol.....	1150 μl (10%)		→marked compound (*) was prepared shortly
1 M NaF.....	1000 μl (100 mM)		before use
100 mM Na ₄ P ₂ O ₇	1000 μl (10 mM)		
1 M MgCl ₂	15 μl (1.5 mM)		

2.8.1.2 Preparation of epidermal lysates

Depending on the age of mice, epidermal lysates were prepared by following different isolation protocols. Epidermal keratinocytes from 3-day-old mice were isolated as described in chapter 2.5.4.7. Keratinocytes from adult mice were obtained as described earlier (2.5.4.3), with modified last steps. After separation from the dermis, cells were placed in 25 ml of DNase medium, mixed thoroughly by a vigorous shaking and incubated for 5 min at 37°C. The suspension was filtered through a 70 µm cell strainer (BD Biosciences) and collected keratinocytes were washed once with cold PBS.

Pelleted cells were resuspended in an ice-cold lysis buffer and incubated for 30 min on ice. Cell debris was spun down at 20,000g for 15 min at 4°C. Cleared lysate was aliquoted into 1.5 ml tubes, immediately frozen down on dry-ice and stored at -80°C. A small aliquot was used for a protein concentration assay.

Alternatively, the epidermis from 3-day-old mice was placed in the lysis buffer directly after separation (2.5.4.7) and homogenized with Ultra-Turrax® T 8 (IKA-Werke GmbH). The suspension was cleared by centrifugation and stored as described above.

Lysis buffer:

Tris-HCl (pH 7.6) 50 mM

NaCl 150 mM

NaF 1 mM

Na₃VO₄..... 1 mM

EDTA 1 mM

Triton X-100..... 1%

→ supplemented with protease inhibitors: 1 tablet/10ml (cOomplete Mini EDTA-free; Roche)

2.8.2 Protein concentration assay

Concentration of proteins in cell and epidermal lysates was assessed using a colorimetric assay based on the biuret reaction and presence of bicinchoninic acid (BCA™ Protein Assay Kit; Pierce). Under alkaline conditions, peptide bonds reduce Cu⁺² to Cu⁺¹ in a concentration-dependent manner. Bicinchoninic acid selectively chelates Cu⁺¹ ions [2:1] forming water-soluble, purple-coloured complex. Absorbance at 562 nm is directly proportional to the protein concentration and increases nearly linearly over a broad working range (20-2,000 µg/ml). The protein concentration in samples is determined using a reference curve obtained by measuring in the same test a set of standard protein dilutions with known concentrations.

BSA stock solution (20 µg/µl) was used to prepare a series of standard dilutions from 2.0 µg/µl to 0.031 µg/µl, in the sample lysis buffer. Next, 10 µl of each solution (analysed

samples, standard dilutions and the lysis buffer) were transferred into a 96-well plate. Reagents A and B were mixed shortly before use (50+1) and 190 μ l were added to each well. Samples were incubated for 15-20 min at 37°C and the absorbance was measured at 550 nm with a plate reader (Dynatech MR5000) using a well with the lysis buffer as a blank control.

2.8.3 Western blot analysis

2.8.3.1 SDS-Polyacrylamide gel electrophoresis (SDS-PAGE)

Proteins were separated electrophoretically according to their molecular weight in SDS-polyacrylamide gels using Mini PROTEAN 3 System (Bio-Rad). Gels consisted of stacking (5% acrylamide) and separating part (10% or 12% acrylamide). Acrylamide content in the latter depended on sizes of separated proteins. Standardly, 1.5 mm thick gels with 10 sample wells were prepared.

After the electrophoresis apparatus was assembled and filled with the running buffer, combs were removed and wells were washed using a pipette. Samples containing 15-20 mg protein were mixed with loading buffer, incubated at 99°C for 5-10 min and loaded into the wells. As a size reference, 10-20 μ l of the standard protein solution (SDS-PAGE Molecular Weight Standards, Broad Range; Biorad #161-0317) (Fig. 2.9) were run with analysed samples. Electrophoresis was carried out until bromophenol blue reached the bottom of the separating gel.

Separating gel (10%/12%) – for 2 gels

30% acrylamid mix* 6.7/8.0 ml
 1.5 M Tris, pH 8.8..... 5.0 ml
 ddH₂O 7.9/6.0 ml
 10% SDS 200 μ l
 10% APS 200 μ l
 TEMED (Sigma #T22500) 8 μ l

→ * Proto-Gel; National Diagnostics #EC-890

Loading buffer (4x)

Tris-HCl, pH 6.8 200 mM
 EDTA 4 mM
 Glycerol 40%
 SDS 8%
 β -mercaptoethanol* 4%
 Bromophenol blue 0.1 mg/ml

→ * added shortly before use

Stacking gel (4%) – for 2 gels

30% acrylamid mix* 1.3 ml
 1.0 M Tris, pH 6.8..... 1.0 ml
 ddH₂O 5.5 ml
 10% SDS 80 μ l
 10% APS 80 μ l
 TEMED 8 μ l

Running buffer (10x)

Tris-base 30.3 g
 Glycine 144.0 g
 SDS 10 g
 ddH₂O filled up to 1000 ml

Molecular Weight Standards, Broad Range

<i>Myosin</i>	200.0 kDa
<i>β-galactosidase</i>	116.2 kDa
<i>Phosphorylase b</i>	97.4 kDa
<i>Serum albumin</i>	66.2 kDa
<i>Ovalbumin</i>	45.0 kDa
<i>Carbonic anhydrase</i>	31.0 kDa
<i>Trypsin inhibitor</i>	21.5 kDa
<i>Lysozyme</i>	14.4 kDa
<i>Aprotinin</i>	6.5 kDa

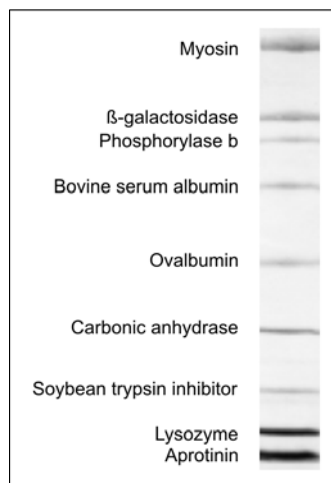


Fig. 2.9 Broad range molecular weight standards for SDS-PAGE. Proteins were separated in 4-20% gradient gel and stained with Coomassie R-250.

2.8.3.2 Transfer of proteins to the membrane

Separated proteins were transferred to a PVDF membrane (Immobilon-P, Milipore #IPVH00010) using Mini Trans-Blot electrophoretic transfer cell (Borad). The membrane was activated with MeOH (5-10 s), rinsed with water and equilibrated in the blotting buffer for 5-10 min. Afterwards, the transfer sandwich was assembled (Fig. 2.10) and air bubbles were carefully removed from between layers, especially from between the gel and the membrane. The cassette was placed in an electrode module (black side towards the cathode). The blotting was conducted for 90 min at 100 V or O/N at 25 V. Subsequently, the sandwich was disassembled and the membrane was stained with Ponceau-S red solution (Sigma #P7170) to visualize bound proteins. The membrane was cut if necessary and protein standard bands were marked. Afterwards, the membrane was washed several times with TBS-T to remove the dye.

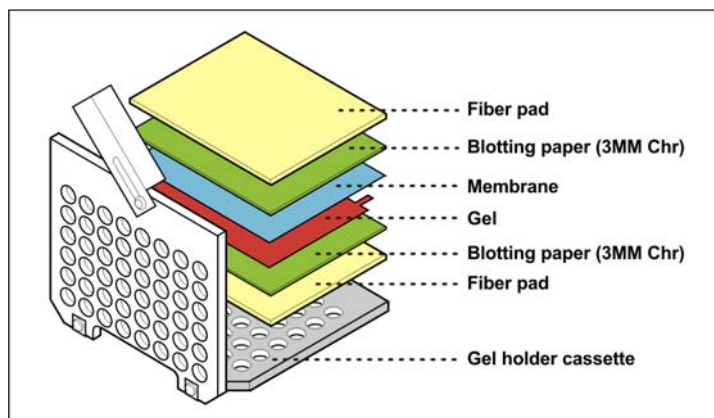


Fig. 2.10 Scheme of the western blot transfer sandwich.

Blotting buffer (10x)

Tris-base 30.2 g (0.25 M)
 Glycine 144 g (1.92 M)
 ddH₂O filled up to 1000 ml
 → working solution (1x) contained 20% MeOH

TBS (10x)

Tris-base 24.2 g (0.2 M)
 NaCl 88.0 g (1.5 M)
 ddH₂O filled up to 1000 ml
 → adjusted to pH 7.6

TBS-T

10x TBS 100 ml
 Tween 20 1 ml
 ddH₂O filled up to 1000 ml

2.8.3.3 Protein detection on the membrane

The membrane with bound proteins was blocked to prevent non-specific background binding of antibodies. The standard blocking buffer contained 5% non-fat milk (Skim Milk Powder, Fluka) and was incubated with the blot for 60 min at RT. If antibodies required blocking with BSA/TBS-T solution, the concentration suggested by manufacturer was used. Primary antibodies were generally diluted in a respective blocking buffer and incubated O/N at 4°C (unless suggested otherwise in a data sheet). If a different buffer was used for dilution, the membrane was washed after blocking with TBS-T (3 × 5 min). Afterwards, the membrane was washed again (3 × 5 min) and incubated for 90 min at RT with the appropriate HRP-conjugated secondary antibody (horse radish peroxidase) diluted in TBS-T containing 5% non-fat milk. All antibodies used in western blot analysis are summarized in chapter 2.3. After the final washing (3 × 5 min), bound antibodies were visualized with Western Lightning Chemiluminescence Reagent (Perkin Elmer) following the manufacturer's protocol. The signal was captured on Hyperfilm film (Amersham Biosciences).

If several different proteins were sequentially detected on one membrane, it had to be stripped in between. When primary antibodies were obtained from the same species (e.g. rabbit), complete removal of bound antibodies was necessary. In that case, the membrane was incubated for 30 min at 55°C in stripping buffer, washed with TBS-T (3 × 10 min) and blocked in an appropriate buffer before applying the next primary antibody.

Stripping buffer

1 M Tris-HCl, pH 6.7 31.2 ml (62.5 mM) → shortly before use added:
 20% SDS 50 ml (2%) β-mercaptoethanol 0.7 ml/100 ml
 ddH₂O filled up to 500 ml

Otherwise, the membrane was incubated for 30 min with 15% H₂O₂ at RT, rinsed with MeOH (5-10 s) and washed with TBS-T (5-10 min), before continuing with blocking. If MeOH

wash was not performed, the blocking step was skipped as well.

2.8.4 GTPase activity assay

GTPase activity assay (pull-down) was conducted with freshly isolated keratinocytes (2.8.1.2). Cells were lysed in 750 μ l of the NP-40 lysis buffer containing a biotinylated PAK-CRIB peptide – Cdc42/Rac interactive binding motif from PAK1B (gift from Dr. J. Collard; Division of Cell Biology, The Netherlands Cancer Institute, Amsterdam 1066 CX, The Netherlands) (Price *et al.*, 2003). Lysates were clarified by 10 min centrifugation at 20,000g (4°C) and then incubated with GST-Rhotekin (fusion protein of the Rho-binding domain of the Rho effector protein) coupled to glutathione conjugated sepharose beads (Glutathione Sepharose 4 Fast Flow; Amersham Biosciences #17-5132) for 45 min at 4°C (with gentle rotation). The lysate was subsequently incubated with streptavidin conjugated agarose beads (Sigma #S1638) for 30 min at 4°C to sequester Cdc42-PAK-CRIB. Beads with bound RhoA and Cdc42 were washed 3 times with the lysis buffer and resuspended in 2x SDS sample buffer (2.8.3.1). The protein content was analysed by Western blotting.

NP-40 lysis buffer

Tris-HCl, pH 7.4..... 50 mM

NaCl 100 mM

MgCl₂..... 2 mM

NaF 1 mM

Na₃VO₄..... 1 mM

Igepal CA-630 (Sigma #I8896)..... 1%

Glycerol 10%

→ supplemented with protease inhibitors: 1 tablet/10 ml (cOmplete Mini EDTA-free; Roche)

2.9 Analysis of mRNA expression

2.9.1 RNA isolation

Total RNA was extracted from $\sim 10^7$ freshly isolated keratinocytes (2.8.1.2) using the TRIzol Reagent (Invitrogen #15596-026) and following the provided protocol. In short, cells were resuspended in the reagent and homogenized by pipetting. After a chloroform extraction, RNA was precipitated with isopropanol and dissolved in 50 μ l of DEPC (diethylpyrocarbonate) treated ddH₂O. The concentration was measured spectrophotometrically at 260 nm (GeneQuant II RNA/DNA Calculator; Amersham Pharmacia Biotech) and the quality of obtained RNA was checked in a gel electrophoresis (2.9.1.1).

DEPC-ddH₂O

DEPC (Fluka #32490) 1 ml

→ mixed and incubated in the dark O/N at RT

ddH₂O 1000 ml

→ autoclaved

2.9.1.1 RNA gel electrophoresis

After isolation, RNA was checked for degradation by an electrophoresis in a special agarose gel. For a small gel (23 cm chamber, 12 lanes) 8 g of agarose was dissolved in exactly 81 ml ddH₂O (evaporation during heating was compensated). Before pouring in a cast, 2.5 ml of 40x MOPS and 16.5 ml of 37% formaldehyde were added. A small aliquot of isolated RNA (1 µl) was mixed with 6 µl of DEPC-ddH₂O and 12 µl of the denaturation buffer. After 15 min incubation at 55°C, 1 µl of 1 mg/ml EtBr solution and 2 µl of the RNA loading buffer were added and RNA was loaded on the gel and run for 2 h with 3.5 V/cm in 1x MOPS/ddH₂O.

Denaturation buffer

40x MOPS 2.5 ml

DEPC-ddH₂O 2.5 ml

37% formaldehyde 35 ml

Formamide (Invitrogen #15515).... 100 ml

RNA loading buffer (10x)

Glycerol (Fluka #49767) 50%

EDTA (ph 8.0) 10 mM

Bromophenol blue 0.25%

→ prepared in DEPC-ddH₂O**40x MOPS (pH 7.0)**

MOPS 167.4 g

Na-Ac 16.48 g

0.5 EDTA, pH 7.0-8.0 80 ml

DEPC-ddH₂O filled up to 1000 ml**2.9.2 Reverse transcription of total RNA**

First-strand synthesis of cDNA was performed with SuperScript III reverse transcriptase (Invitrogen #18080) according to the protocol provided with the enzyme.

RT-PCR

Random primers 1 µl

10 mM dNTP 1 µl

Total RNA 1 µg

ddH₂O filled up to 13 µl

→ 5 min incubation at 65°C

→ 1 min incubation on ice

Next added:

5x First strand buffer 4 µl

0.1 M DTT 1 µl

RNase OUT 1 µl

Super Script III RT 1 µl

→ 5 min incubation at 25°C

→ 60 min incubation at 55°C

→ 15 min incubation at 70°C

→ filled up with 20 µl of DEPC-ddH₂O

Obtained cDNA was used as a template in a standard PCR reaction and a real time PCR

analysis (2.9.3). Primers used for amplification are summarized in chapter 2.4.1.

PCR reaction

cDNA	2.0 µl
Primer 1 (100 pmol).....	0.2 µl
Primer 2 (100 pmol).....	0.2 µl
PCR buffer (10x).....	5.0 µl
50 mM Mg ²⁺	1.5 µl
10 mM dNTP	1.0 µl
Taq DNAPoly (5 U/µl)	0.2 µl
ddH ₂ O	37.9 µl
	20 µl

PCR program:

1. denaturation..... 94°C for 180 s
2. denaturation..... 94°C for 30 s
3. annealing T_m for 30 s
4. elongation..... 72°C for 90 s
→ steps 2-4 – **35 cycles**;
5. elongation..... 72°C for 300 s
6. pause..... 4°C for ∞

Products of a qualitative PCR reaction were analysed by agarose gel electrophoresis (2.4.4.2).

2.9.3 Real-time PCR

Real-time PCR was performed for quantitative analysis of mRNA expression, using iQ SYBR Green Supermix (Biorad). The cDNA obtained in a first-strand synthesis (2.9.2) was amplified with primers specific for analysed genes (2.4.1). At the same time a reaction with primers for the reference gene (GAPDH) was conducted for each sample.

Reaction mix:

cDNA	0.5 µl
iQ SYBR Green Supermix..	12,5 µl
Primer 1 (100 pmol).....	1 µl
Primer 2 (100 pmol).....	1 µl
ddH ₂ O	10 µl
	25 µl

Triplicate repeats were prepared for each primer set and samples were transferred to a special 96-well plate. The amplification progress was monitored in iCycler (Biorad) and results were evaluated using software provided with the thermocycler.

3 RESULTS

3.1 Generation of mice with a keratinocyte-restricted deletion of the *rac1* gene.

The constitutive deletion of the murine *rac1* gene leads to embryonic death around day 8.5 of the development (Sugihara *et al.*, 1998). Therefore, a conditional knock-out approach was employed in this study, which enabled the analysis of Rac1 function *in vivo* by circumventing the lethal phenotype. A tissue specific ablation of the *rac1* gene was obtained using the Cre-loxP system (2.6.1).

3.1.1 The *rac1* gene structure and the conditional knock-out strategy

The murine *rac1* gene is located on chromosome 5 and consists of 6 exons, with the translation start codon located in exon 1 (Fig. 3.1). No splice variants have been reported to date.

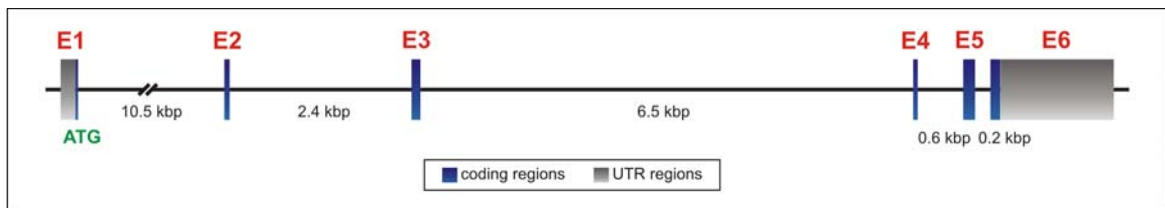


Fig. 3.1 Schematic presentation of the *rac1* gene exon structure.

A common approach used to obtain an efficient deletion of the targeted protein, including the absence of any truncated forms, is the removal of the ATG-containing exon that ensures the lack of mRNA translation. However, exon 1 was not selected for the deletion in this study in order to avoid the risk of interfering with gene regulation, resulting from the insertion of the *loxP* site within the gene promoter.

The absence of exon 2 could lead to an alternative splicing of exon 1 into exon 3, which would result in an in-frame transcript, due to a compatible codon phasing (Table 3.1). While the hypothetical protein would lack 24 amino acids, it might potentially retain some functionality.

Exon	Size [bp]	Start phase	End phase
1	196* + 35	–	2
2	72	2	2
3	118	2	0
4	63	0	0
5	160	0	1
6	131 + 1493*	1	–

Table 3.1 Summary of the size and phase of *rac1* gene exons. Marked numbers (*) correspond to UTR parts of the transcript.

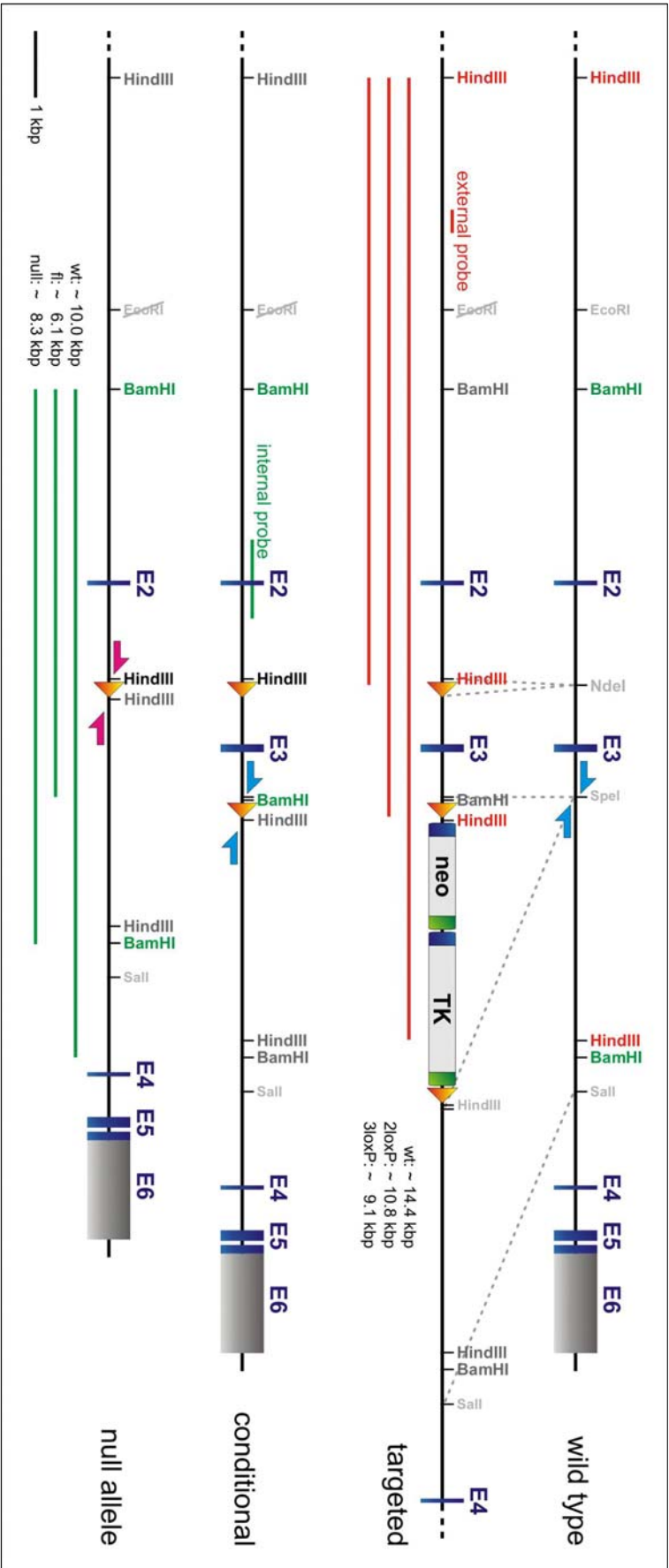


Fig 3.2 Strategy of the *rael* gene conditional knock-out. The wild type (wt) *rael* allele was modified by a homologous recombination with the targeting construct. The targeted allele (3loxP), identified by a Southern blot analysis with the external probe, contained the *loxP* site (triangle) upstream and the floxed neo-TK selection cassette (boxes) downstream of exon 3 (E3). The conditional allele (fl) was obtained *in vitro* by a transient *cre* transfection, which resulted in the floxed exon 3 after the removal of the selection cassette. The Cre-mediated *in vivo* recombination led to the excision of exon 3, resulting in the null allele. The internal probe was used to identify both the conditional and the null allele. Arrows represent PCR primers used for the genotyping of mice. First pair differentiated between the wild type and the conditional allele (blue arrows) and was used for *Rac1* PCR. The second set recognized the null allele (pink arrows) and was used for KO PCR.

Therefore, exon 3 was selected for the deletion and flanked by *loxP* sites. It encodes amino acids 37-75 which form a part of the core effector domain (primary site for interaction with effectors) and the complete switch II region (1.1.2). A theoretical splicing of exon 2 into exon 4, exon 5, or exon 6 would result in a frame-shifted transcript (Table 3.1) and only unrelated amino acids would be added after the first 36 correct residues during the translation. Such fusion proteins would be terminated prematurely, as stop codons would be present after amino acids 39, 68 and 102, respectively. The truncated forms could not exert Rac1 functions, as they would lack domains essential for interaction with effector molecules (i.e. core domain, switch II, Rho insert domain). Moreover, they could not have a dominant negative effect, as they would lack the domain essential for interaction with GEFs (switch II).

The approach used to obtain the conditional ablation of the *rac1* gene is schematically depicted in Fig. 3.2.

3.1.2 Modification of the *rac1* gene and generation of mutant mice

The wild type allele of *rac1* was altered in ES cells by a homologous recombination with the targeting vector containing a modified fragment of the gene (2.6.2). Electroporation of the plasmid into cells and the subsequent selection for neomycin resistant cells resulted in obtaining ES cell clones carrying a modified *rac1* allele (2.6.3). Homologously recombined alleles contained either both modifications, the *loxP* site upstream and the floxed selection cassette downstream of exon 3 (3loxP; Fig. 3.2, targeted allele), or only the floxed selection cassette, created after a partial recombination event (2loxP). They were identified by Southern blot analysis (2.4.7) with the external probe (Fig. 3.3A). The presence of additional copies of the targeting construct, randomly incorporated into the genome of *rac1*^{3loxP/+} ES cell clones, was checked by the hybridization with the internal probe (Fig. 3.3B).

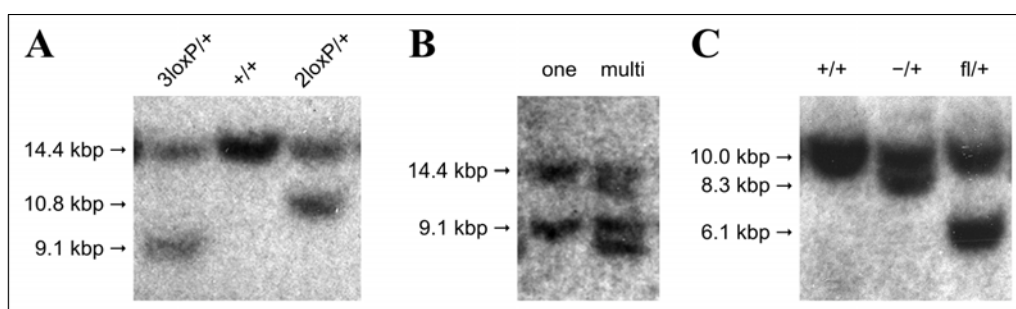


Fig. 3.3 Screening of ES cell clones. Results of Southern blot analysis of HindIII-digested DNA hybridized with (A) the external probe to check for the homologous recombination or (B) the internal probe to check for the possibility of a random integration of the targeting construct. Bands: wt (+) - 14.4 kbp, 2loxP - 10.8 kbp, 3loxP - 9.1 kbp. (C) After *cre* transfection, genomic DNA from ES cell clones was cut with BamHI and hybridized with the internal probe to check for the presence of the conditional or the null allele, generated by Cre-mediated recombination. Bands: wt (+) - 10.0 kbp, null (-) - 8.3 kbp, fl - 6.1 kbp.

The selection cassette was removed from *rac1*^{3loxP/+} clones *in vitro* by a transient transfection of a Cre-recombinase-expressing plasmid, followed by FIAU treatment (2.6.4). Clones carrying the conditional allele (*rac1*^{fl/+}) were identified by Southern blot analysis with the internal probe (Fig. 3.3C) and used for the generation of germ line chimeras by a blastocyst injection (2.6.5). Clones carrying the null allele (*rac1*^{-/-}) were used for generation of Rac1 (-/-) ES cells (2.6.7, 3.8).

Breeding of male chimeras with wild type C57BL/6 females resulted in *rac1*^{fl/+} offspring that were subsequently mated to obtain *rac1*^{fl/fl} animals. The presence of the conditional allele was confirmed with Southern blot analysis (Fig. 3.4A). Both heterozygous and homozygous animals were fertile and phenotypically indistinguishable from wild type littermates. Mice with keratinocyte specific ablation of Rac1 were obtained by intercrossing *rac1*^{fl/fl} animals with K5-Cre transgenic mice (2.6.6).

Mice were routinely genotyped by Rac1 PCR and Cre PCR (Fig. 3.4B) (2.4.6.1). KO PCR was performed to confirm *in vivo* recombination of the conditional allele into the null allele in the presence of K5-Cre recombinase.

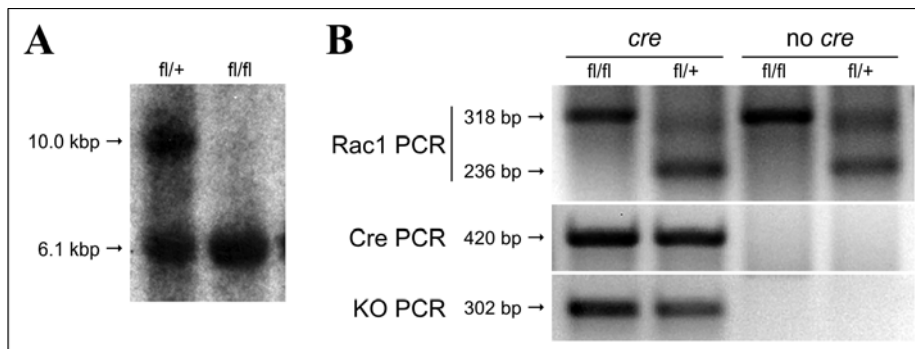


Fig. 3.4 Genotyping of mice. (A) **Southern blot analysis.** Tail DNA was digested with BamHI and hybridized with the internal probe recognizing the wild type (+: 10.0 kbp) and the conditional (fl: 6.1 kbp) allele of the *rac1* gene. (B) **PCR analysis.** Rac1 PCR gave rise to two products: 318 bp from the wild type (+) and 236 bp from the conditional allele (fl). Cre PCR resulted in 420 bp product, when the *cre* transgene was present, and KO PCR gave rise to 302 bp product, when the null allele was present.

3.1.3 Gross phenotype after the K5-Cre induced loss of Rac1

An almost complete loss of Rac1 protein in the epidermis of *rac1*^{fl/fl},*cre* (KO) mice was confirmed by Western blot analysis (2.8.3) of epidermal lysates (2.8.1.2) from 3-day-, 14-day- and 8-month-old mice (Fig. 3.5). Control littermates – *rac1*^{fl/+},*cre* (ctrl) – expressed normal amounts of Rac1 protein.

Rac1-deficient mice were born close to the Mendelian ratio (~18%) and were indistinguishable from control littermates at birth. Mutant mice showed no increased lethality, were fertile and had no evident health problems.

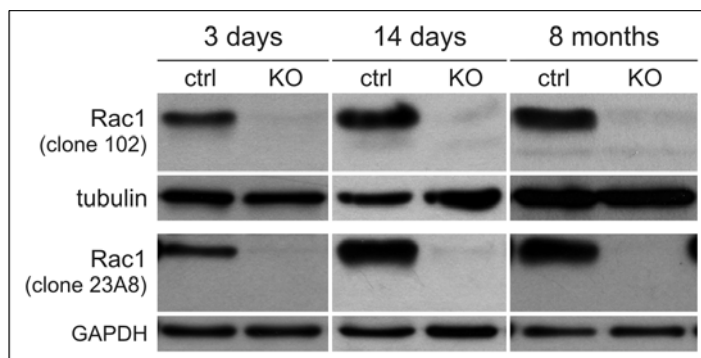


Fig. 3.5 Western blot analysis showed almost complete absence of Rac1 protein in the epidermis of $rac1^{fl/fl}, cre$ mice. Two different monoclonal antibodies were used to analyse Rac1 content in epidermal lysates obtained from control and mutant mice at 3 days, 14 days and 8 months of age. Tubulin and GAPDH levels were used as a loading control.

Within few days after birth, a difference in the pelage appearance between $rac1^{fl/fl}, cre$ and control mice became evident. Mutant mice displayed a reduced hair growth (Fig. 3.6A) combined with an early onset of a progressive hair loss, which led to a nearly complete lack of fur at 2 months of age (Fig. 3.6B). No additional defects, such as spontaneous wounds or blistering, were observed in the skin of $rac1^{fl/fl}, cre$ mice. The hair loss was permanent and no regrowth of fur was detected up to 24 months of age (Fig. 3.7). The vibrissae of $rac1^{fl/fl}, cre$ mice were lost along with the pelage hair.

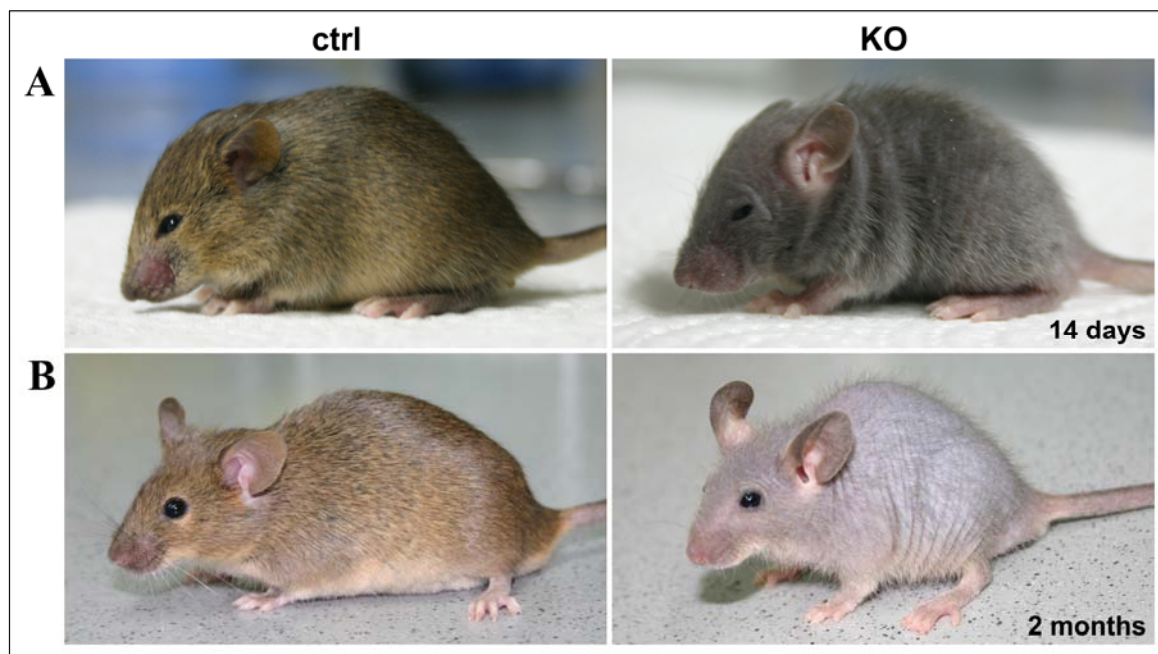


Fig. 3.6 Control and mutant mice at (A) 14 days and (B) 2 months of age. Rac1-deficient mice grew less hair and showed a progressive hair loss, but did not develop any other skin defects. The fur of mutant animals looked dull and faded.

Shortly after birth, $rac1^{fl/fl}, cre$ mice started to show about 20% reduction of body mass, when compared to control littermates, which persisted throughout the whole life span ($81.1 \pm$

8.5%; n=27/23). An almost complete lack of the fat tissue under the skin of adult mutant mice, which was always observed during dissection, most likely contributed to the weight difference. The lower amount of fat tissue was likely a secondary effect of the hair loss, resulting from increased energy requirements to maintain normal body temperature, as housing conditions were adjusted to accommodate mice with fur.



Fig. 3.7 Control and mutant mouse at 2 years of age. The apparent difference in size was mainly a result of a nearly complete lack of fur (KO). In addition, *rac1^{fl/n},cre* mice had almost no fat tissue, which normally accumulates under the skin of older mice (observed during dissection). The loss of vibrissae is clearly visible.

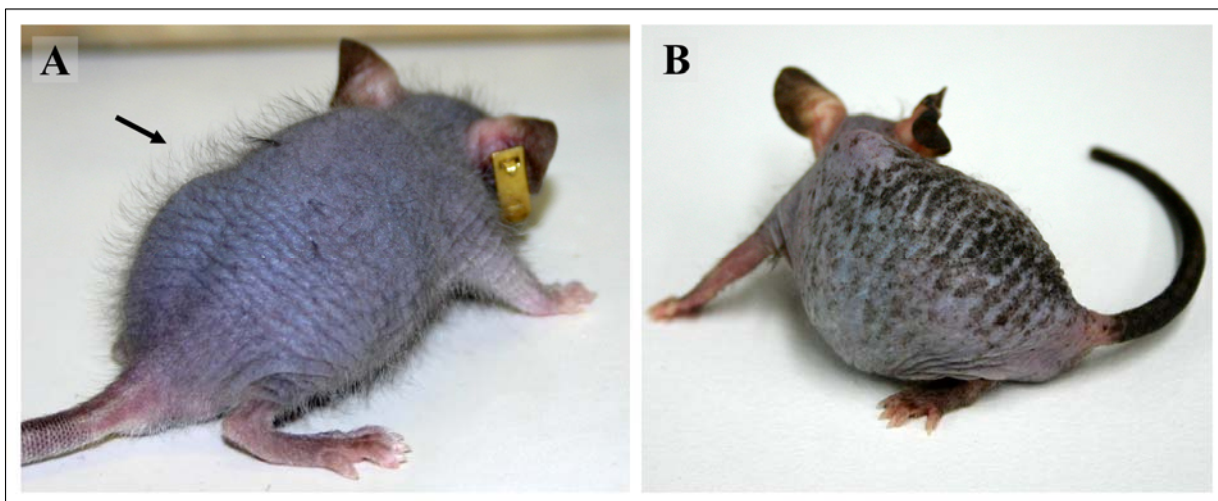


Fig. 3.8 (A) Evenly-spaced, frail hairs were often observed in adult mutant mice (arrow). They were usually present for several months after birth, while their amount was gradually reduced. However, in some mice they were sustained throughout the whole life span. Age: 2.5 months. **(B) Abnormal blackening of the lower back skin.** The change in the colour and texture of skin was sometimes observed in old mutant mice. Age: 2 years.

Interestingly, a small amount of evenly-spaced hairs was sustained in *Rac1*-deficient mice

after the general loss of pelage (Fig. 3.8A). The remaining hairs were frail, matt and greyish. Their amount was progressively reduced and the majority of old mice did not retain any fur at all. While the density of remaining hairs was varying from mouse to mouse, in general, females seemed to have more of them.

Sometimes, an unusual blackening and hardening of the lower back skin was observed in several-months-old *rac1^{fl/fl},cre* mice; mostly males (Fig. 3.8B). Similar changes of the tail skin were detected more frequently in both, male and female several-months-old mutant mice (Fig. 3.7).

3.2 Analysis of the hair follicle (HF) phenotype in the absence of Rac1

3.2.1 Defective HF morphogenesis

A histological analysis of skin was carried out to investigate the HF morphogenesis in the absence of Rac1. Fragments of back skin were isolated from control and mutant mice at different ages and HE staining of paraffin sections was performed (2.7.1).

The comparison of samples from 3-day-old control and mutant mice showed no apparent differences in shape, length and the amount of HFs at that stage (Fig. 3.9).

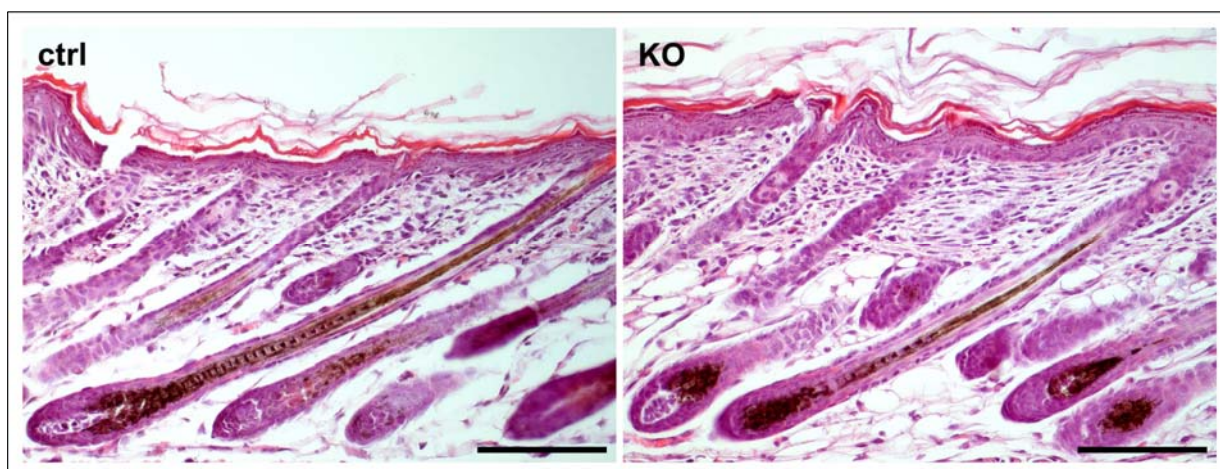


Fig. 3.9 HE staining of back skin sections from 3-day-old control and mutant mice. No obvious changes in the morphology of Rac1-deficient HFs were observed. Bar: 100 μ m.

Morphological aberrations of Rac1-deficient HFs became evident by day 9 after birth (Fig. 3.10). Many HFs displayed constrictions (arrowhead) or a kinked follicle shape (white arrow). Also, some hair shafts (HSs) showed abnormal structure. While the majority of hair bulbs looked rather normal, some had an unusual shape (black arrow). However, mutant HFs were only slightly shorter than control HFs and the skin thickness (from the epidermis to the subcutaneous muscle layer) was similar in control and mutant samples.

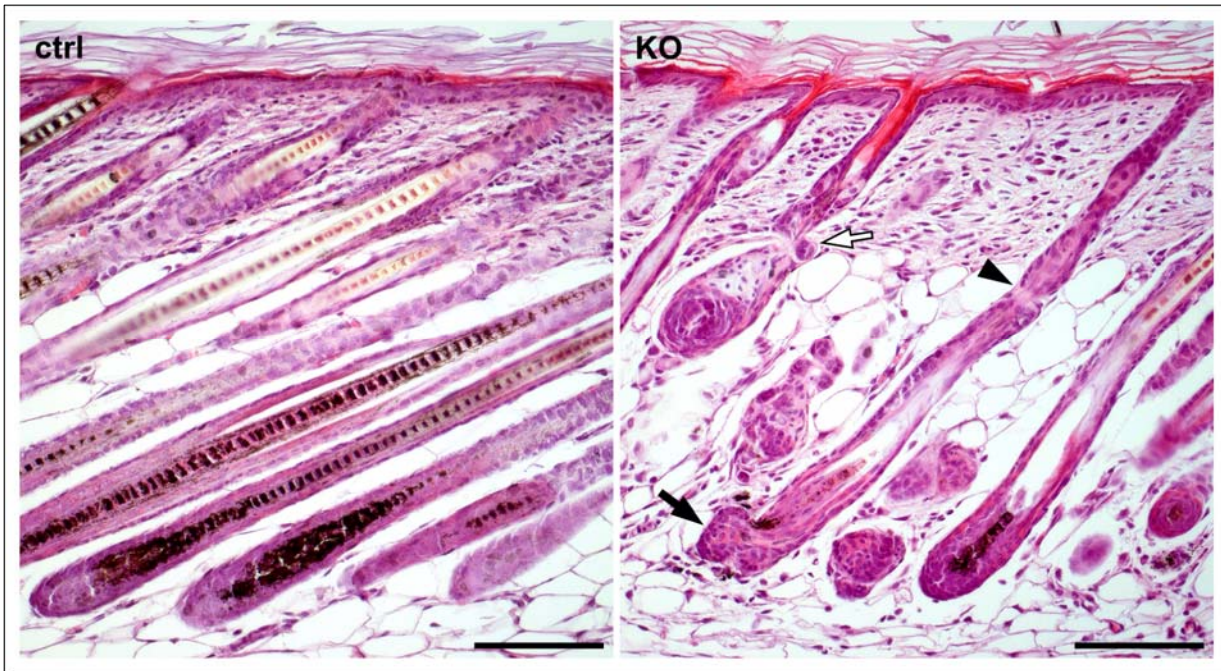


Fig. 3.10 HE staining of back skin sections from 9-day-old control and mutant mice. Arrows point out aberrations of the HF (white arrow, arrowhead) and the hair bulb (black arrow) morphology. Bar: 100 μ m.

The phenotype became drastically aggravated by day 14 after birth, when almost all *Rac1*-deficient HFs were defective and had lost the normal appearance (Fig. 3.11).

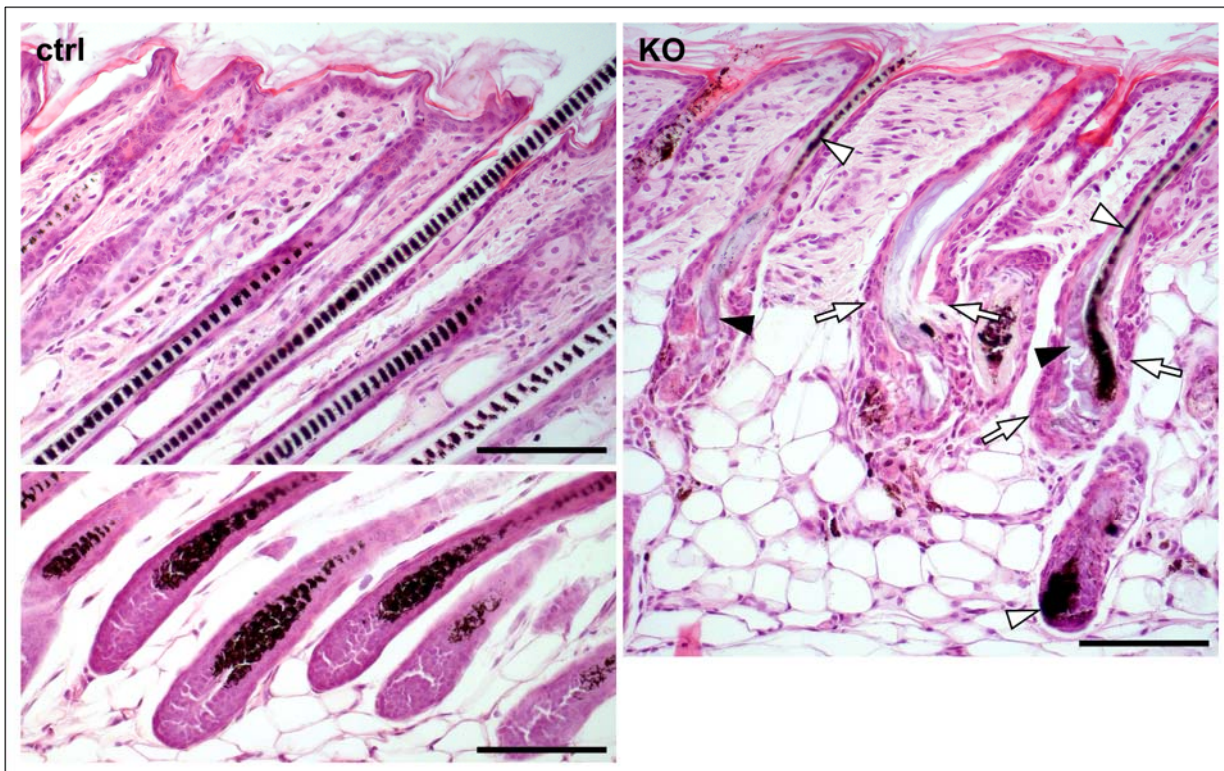


Fig. 3.11 HE staining of back skin section from 14-day-old control and mutant mice. *Rac1*-deficient HFs displayed severe changes in morphology: abnormal widening of the follicle, deformation of HSs (white arrowheads), abrupt ending of the outer layers (arrows) and a presence of unusual cells within some mutant HFs (black arrowheads). Bar: 100 μ m.

Mutant HF's became widened shortly below the sebaceous glands (SGs) and almost no hair bulbs were present. In many cases the follicles looked "open", as the outer layers ended abruptly (arrows). The cells in the lower regions of HF's were disorganized and seemed to be less compact. Unusual, large cells were observed within many HF's (black arrowheads). Hair shafts (HSs) had an irregular pigmentation pattern and majority of them were misshapen or entirely absent (white arrowheads). The skin thickness of *rac1^{fl/fl},cre* mice was significantly reduced, most likely due to the reduced length of HF's.

The degeneration of HF's progressed and resulted in almost complete loss of non-permanent regions of HF's in the skin of adult *rac1^{fl/fl},cre* mice. No regrowth of anagen HF's was observed in the absence of Rac1. Surprisingly, the upper parts of the HF's were maintained throughout the whole life span. However, while infundibula looked quite normal, SGs became abnormally enlarged in time (Fig. 3.12, arrowheads). This suggests that the bulge regions containing stem cells were also preserved, as they contribute to the SG renewal. Occasionally, a mild fibrosis could be observed locally in the skin of some adult mutant mice.

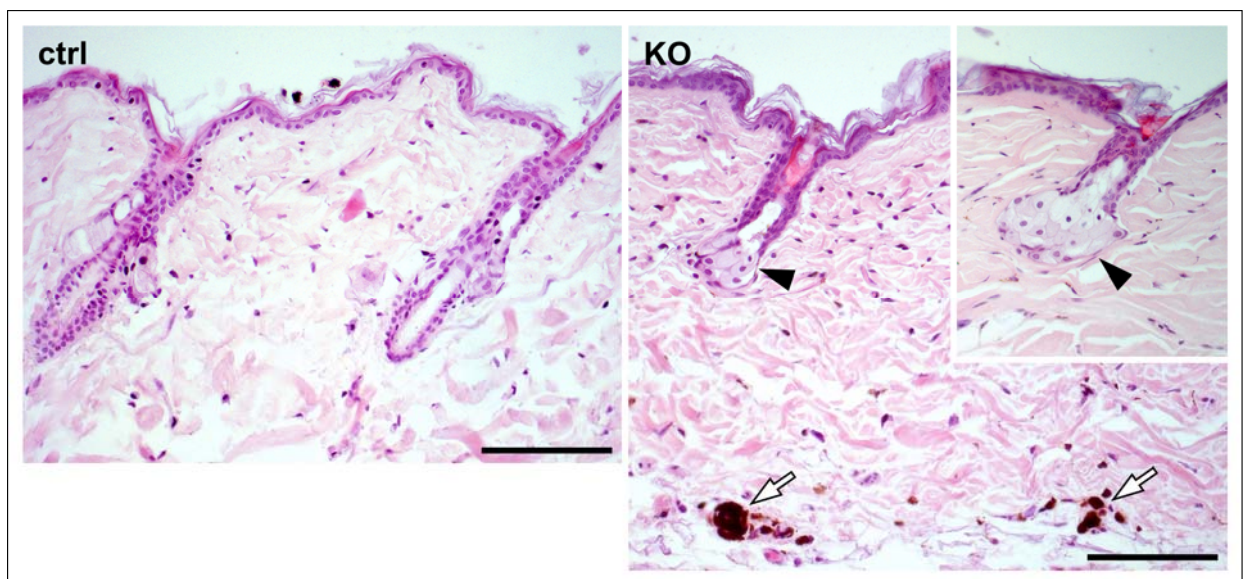


Fig. 3.12 HE staining of back skin sections from 13-month-old control and Rac1-deficient mice. Accumulations of melanin (arrows) and abnormally large SGs (arrowheads) were characteristic for older Rac1-deficient skin. The inset picture was taken with the same magnification as the rest of the figure. Bar: 100 μ m.

Accumulations of melanin, which were most likely remnants of disintegrated HF's, were frequently detected in the dermis and in the subcutis of adult *rac1^{fl/fl},cre* mice (Fig. 3.12, arrows). The presence of melanin clumps in the mutant skin was likely the cause of an abnormal colour of the dermis, which was consistently observed during the isolation of the epidermis and could explain the characteristic grey colour of the mutant skin (2.5.4.3).

Interestingly, all adult *rac1^{fl/fl},cre* mice had enlarged axillary and inguinal lymph nodes, which,

in addition, had an unusual black colour (Fig. 3.13). That phenotype was most likely the result of an accumulation of dendritic cells, which transported the remnants of disintegrated mutant HFs, including melanin particles, from the skin.



Fig. 3.13 Axial and inguinal lymph nodes of $rac1^{fl/fl}, cre$ mice were black and noticeably enlarged. A picture of axial lymph nodes isolated from adult control and mutant mice shows a difference in size and colour between both organs.

3.2.2 Loss of the HF specific differentiation

The HF consists of distinct cell layers, which can be identified by the expression pattern of specific epithelial and hair keratins (1.2.2). In order to investigate changes of the HF morphology in more detail, the expression of several marker proteins was analysed using IF staining and confocal microscopy techniques (2.7.2.1).

Basal keratinocytes of the outer root sheath (ORS), a HF layer adjacent to the basement membrane (BM), express a number of ECM proteins (e.g. laminins) and epithelium-specific ECM-binding receptors (e.g. integrins). One such a characteristic molecule is $\alpha 6$ integrin, normally localized to the basal side of ORS keratinocytes attached to the BM, throughout the whole length of the HF. This property makes it a good marker, which can be used to identify the surface of the ORS and to visualize the outline of HFs.

In the skin of 9-day-old $rac1^{fl/fl}, cre$ mice, the expression of $\alpha 6$ integrin was normal in a great majority of mutant HFs (Fig. 3.14-Fig. 3.17). At day 14 after birth, the layer consisting of $\alpha 6$ -positive keratinocytes ended abruptly shortly below SGs (white arrowheads) and the pattern of expression confirmed dramatic changes in the morphology of mutant HFs observed earlier during the histological analysis (3.2.1).

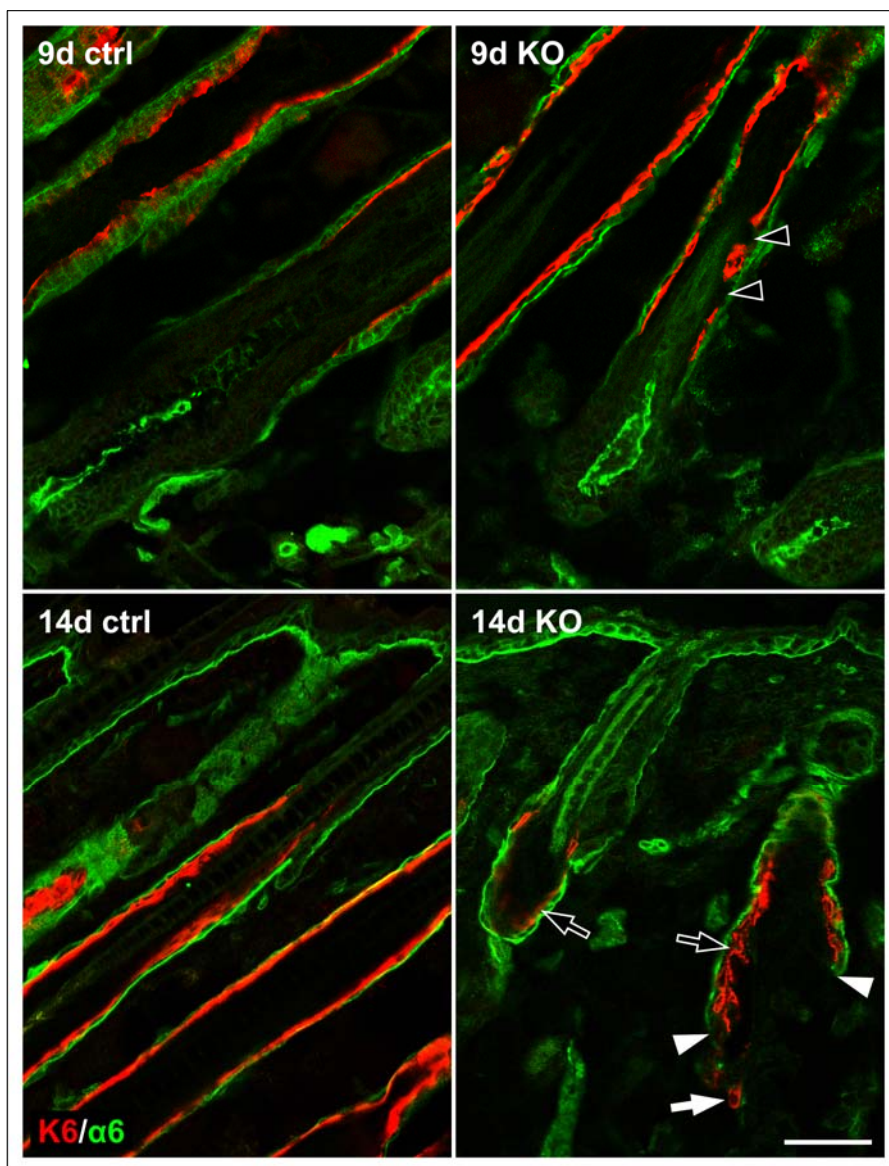


Fig. 3.14 K6 and $\alpha 6$ integrin IF staining of back skin sections from 9-day-old and 14-day-old control and mutant mice. Expression of both proteins was normal at day 9 after birth, with only local loss of K6 in some mutant HFs (black arrowheads). At day 14 after birth, K6 and $\alpha 6$ integrin were present only in upper regions of Rac1-deficient HFs (black arrows). Cell layers expressing those proteins were unexpectedly interrupted shortly below the SGs (white arrowheads). In some HFs, scattered K6-positive clusters were found below $\alpha 6$ -positive regions (white arrow). Bar: 50 μ m.

K6 is a keratin expressed in the companion layer (CL) directly underlying the ORS of the HF (Rothnagel and Roop, 1995) (1.2.2).

While K6 expression was mostly normal in the mutant skin at day 9 after birth, a local loss of K6 was already displayed in some HFs (Fig. 3.14, black arrowheads). At day 14 after birth, K6 was still expressed in cells neighbouring $\alpha 6$ -positive keratinocytes (black arrows), but it was absent or present only in scattered clumps below these regions (white arrow).

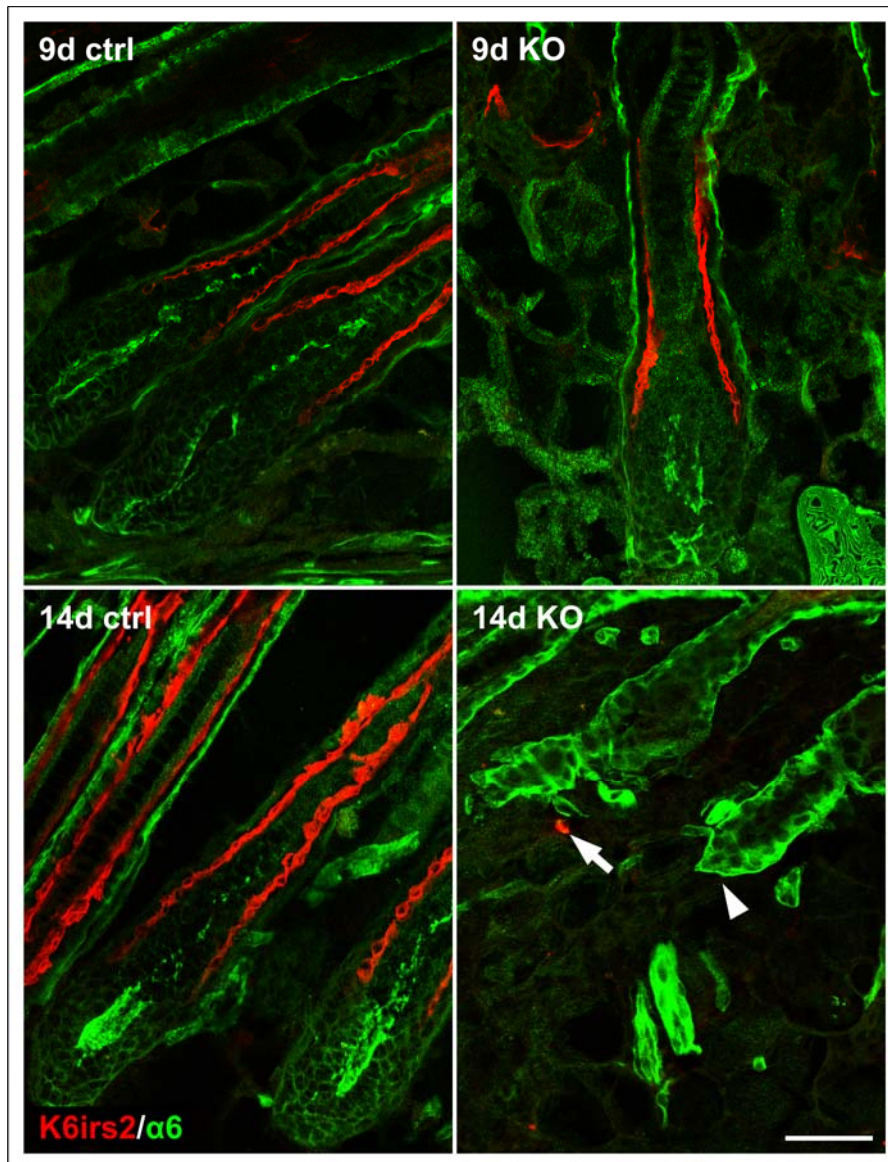


Fig. 3.15 K6irs2 and $\alpha 6$ integrin IF staining of back skin sections from 9-day-old and 14-day-old control and mutant mice. At day 9 after birth both proteins were expressed normally in the absence of Rac1. In 14-days-old mutant HFs, K6irs2 was almost completely absent; only few K6irs2-positive spots were observed (arrow). Expression of $\alpha 6$ integrin was discontinued shortly below SGs (arrowhead). Bar: 50 μ m.

K6irs2 and K6irs4 are expressed respectively in the cuticle and the Huxley layer of the inner root sheet (IRS), which is underlying the companion layer of the HF (Langbein *et al.*, 2003) (1.2.2).

At day 9 after birth their distribution in Rac1-deficient HFs was not obviously changed, when compared to control samples (Fig. 3.15 and Fig. 3.16). However, no normal expression of K6irs2 and K6irs4 was detected in 14-day-old mutant skin, indicating the complete absence of the IRS. Only scattered clumps of these keratins were present below $\alpha 6$ -positive regions in few of distorted HFs (arrows).

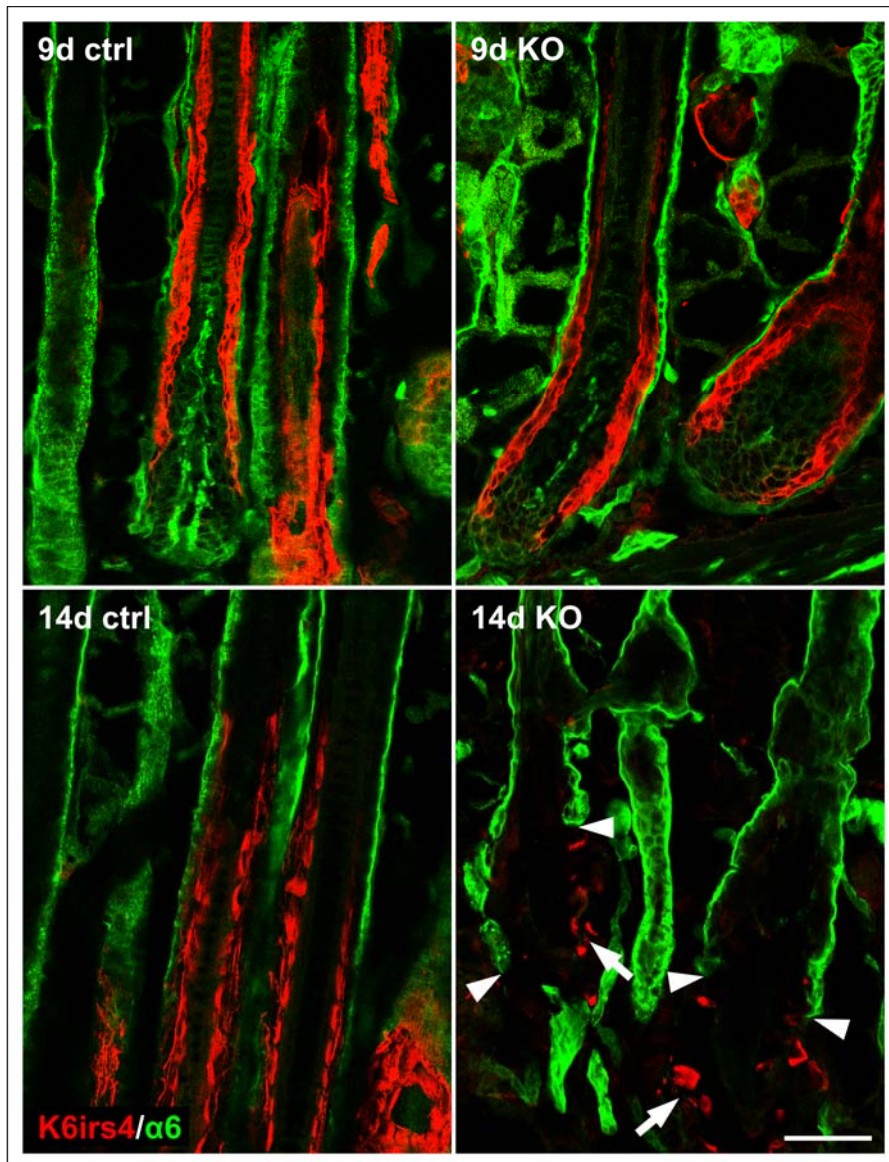


Fig. 3.16 K6irs4 and $\alpha 6$ integrin IF staining of back skin sections from 9-day-old and 14-day-old control and mutant mice. At day 9 after birth the expression of K6irs4 and $\alpha 6$ integrin was normal in the absence of Rac1. The layer expressing $\alpha 6$ integrin was abruptly terminated shortly below SGs (arrowheads) and only small clumps of K6irs4-positive cells were detected in the lower region (arrows) in the 14-day-old mutant skin. Bar: 50 μ m.

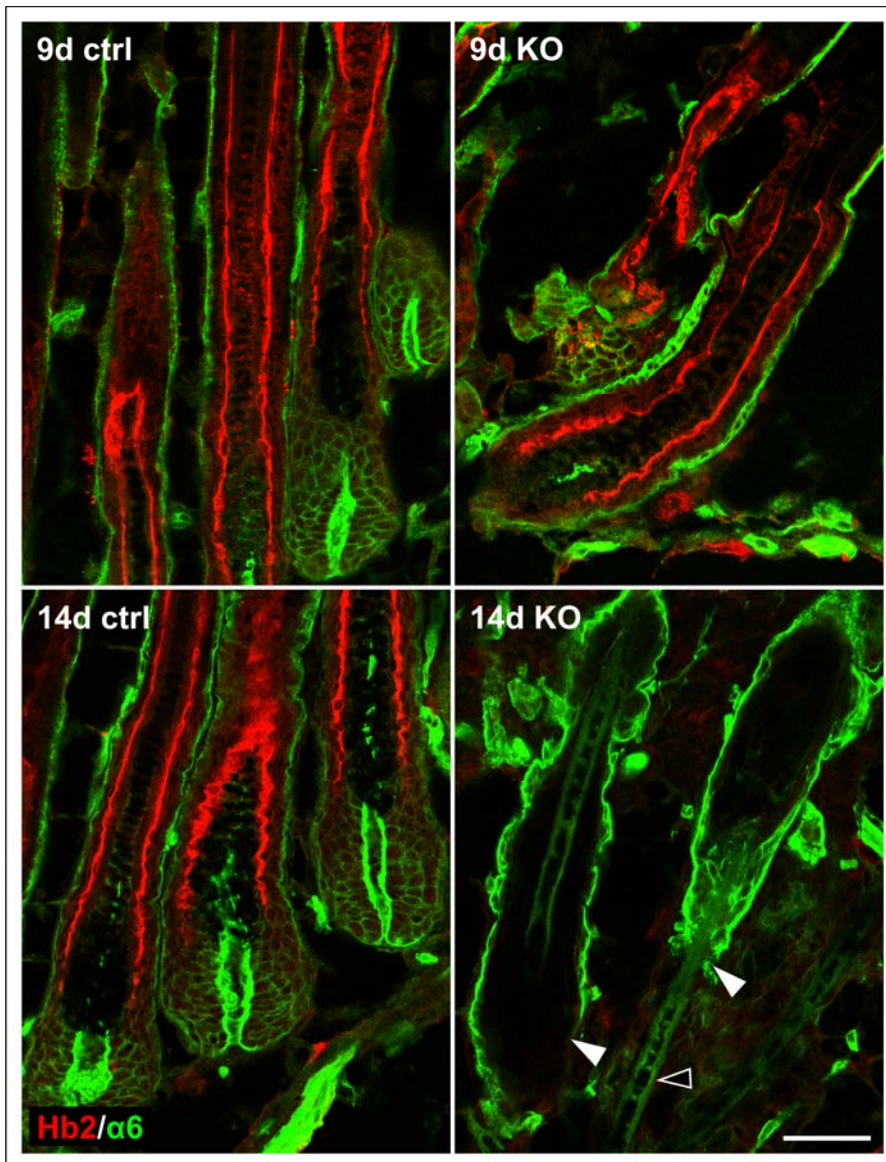


Fig. 3.17 Hb2 and $\alpha 6$ integrin IF staining of back skin sections from 9-day-old and 14-day-old control and mutant mice. Normal expression of Hb2 at day 9 after birth was replaced by its complete absence in 14-day-old mutant HF. Expression pattern of $\alpha 6$ integrin showed abnormal termination of the ORS layer (white arrowheads) at day 14 after birth. Unspecific staining of the HSs revealed occasionally a "naked" hair, not surrounded by any HF layers (black arrowhead). Bar: 50 μ m.

Hb2 is one of the hair keratins expressed by the cuticle, which constitutes the outer layer of the HS (Langbein *et al.*, 2001) (1.2.2).

In 9-day-old *Rac1*-deficient HF the distribution of Hb2 was not obviously altered. However, no expression of the keratin was detected in the mutant skin at day 14 after birth (Fig. 3.17).

Interestingly, in 14-day-old mutant HF, normal-looking HSs were occasionally observed below regions expressing $\alpha 6$ integrin and other layer specific markers (Fig. 3.17, black arrowhead). They were not surrounded by any follicle-like structures.

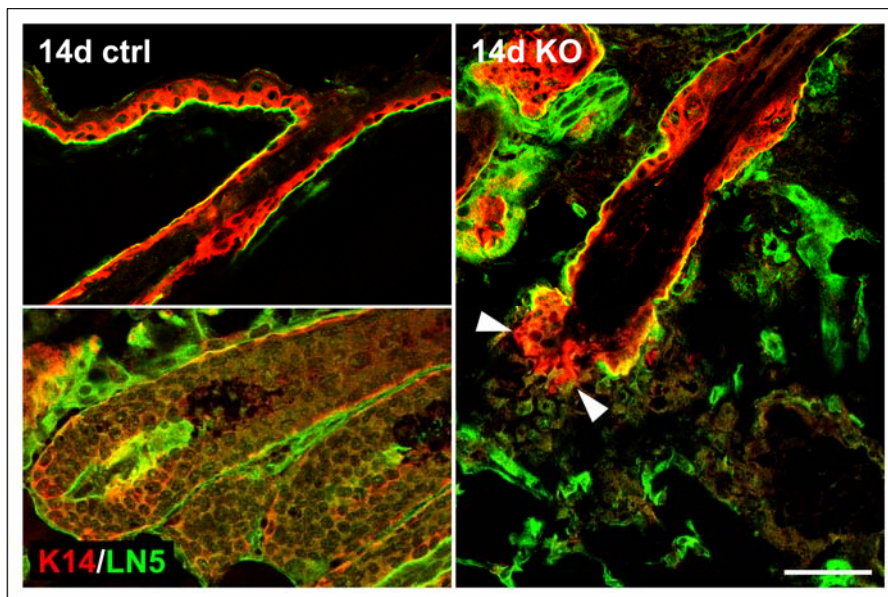


Fig. 3.18 K14 and LN5 IF staining of back skin section from 14-day-old control and mutant mice. Expression pattern of both proteins shows unexpected termination of ORS layer in Rac1-deficient HFs. Some of ORS keratinocytes lost polarization (lack of LN5 expression) but still expressed K14 (arrowheads). Bar: 50 μ m.

Laminin 5 (LN5) is one of the BM components deposited by basal ORS keratinocytes, which express K14 along the whole length of the HF (Fig. 3.18). As in case of $\alpha 6$ integrin, the expression pattern of K14 showed an abrupt termination of the ORS layer in 14-day-old mutant skin. The BM was discontinued in majority of HFs together with the ORS. However, cells expressing K14 but not LN5 were found in some HFs, suggesting that fully differentiated ORS keratinocytes have lost the ability to deposit BM and thus the polarization.

E-cadherin is an epithelial marker and an adhesion protein expressed in all ORS cells of the HF (Fig. 3.19). While it was still present in 9-day-old Rac1-deficient HFs, the expression pattern revealed changes in the normal shape of HFs (black arrowheads) and distortions of hair bulbs (arrows). At day 14 after birth, no E-cadherin-positive keratinocytes were detected below $\alpha 6$ integrin-positive regions of the mutant HFs (white arrowheads). Also, a normal expression pattern of β -catenin, another cell-cell adhesion molecule, was lost in the lower regions of Rac1-deficient HFs (Fig. 3.20).

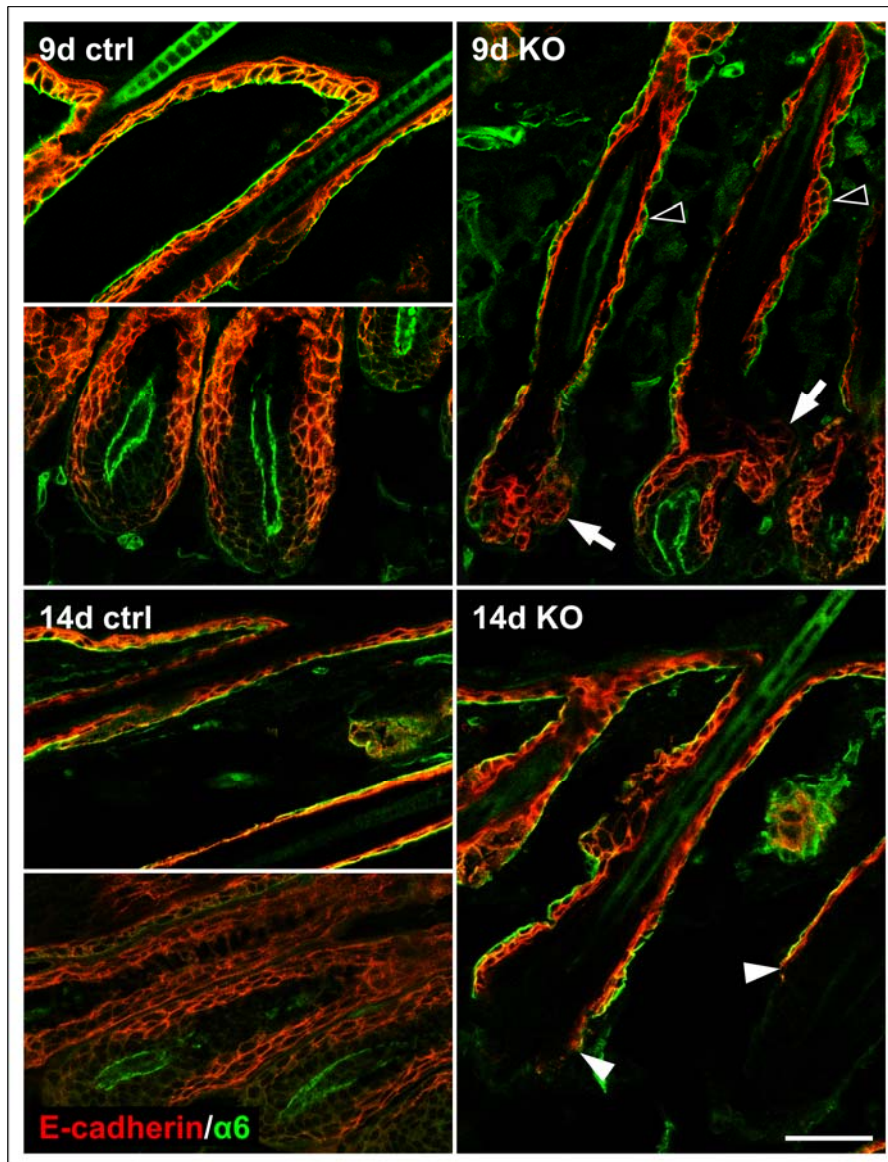


Fig. 3.19 E-cadherin and $\alpha 6$ integrin IF staining of back skin sections from 9-day-old and 14-day-old control and mutant mice. At day 9 after birth E-cadherin was present along the whole length of *Rac1*-deficient HFs, however the staining showed first changes of the HF shape (black arrowheads) and deformations of some hair bulbs (arrows). 14-day-old ORS keratinocytes lost E-cadherin expression together with $\alpha 6$ integrin expression (arrowheads). Bar: 50 μ m.

While there was almost no detectable expression of epithelial or HF markers, a presence of nucleated cells in the lower regions of mutant HFs was confirmed with DAPI staining (Fig. 3.20 and Fig. 3.21, arrows). The location of those cells and the apparent continuity with the upper parts of HFs suggested that they once belonged to the HF structure, even though they seemed to have lost HF-specific differentiation.

Expression pattern of vimentin, a mesenchymal intermediate filament, was analysed to determine the lineage of cells in the lower parts of mutant HFs. Interestingly, IF staining showed that vimentin-negative cells, which seemed to be derived from HF structures (Fig. 3.21, arrows), surrounded by a great number of mesenchymal cells. No accumulation of vimentin-positive cells

was observed around the lower parts of control HF.

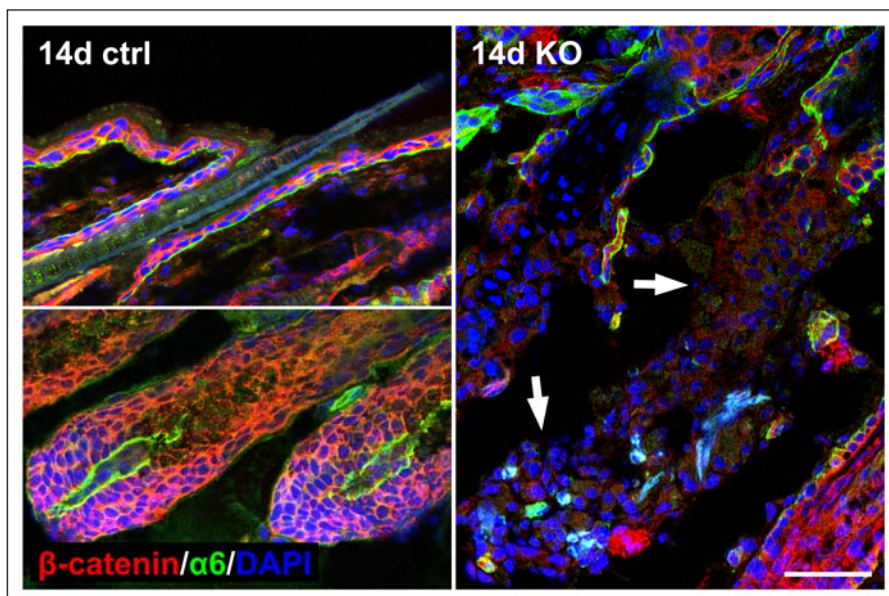


Fig. 3.20 β -catenin and $\alpha 6$ integrin IF staining of back skin sections from 14-day-old control and mutant mice. Nucleated cells were observed in the lower regions of mutant HF, although expression of both β -catenin and $\alpha 6$ integrin was lost. DAPI was used to visualize nuclei. Bar: 50 μ m.

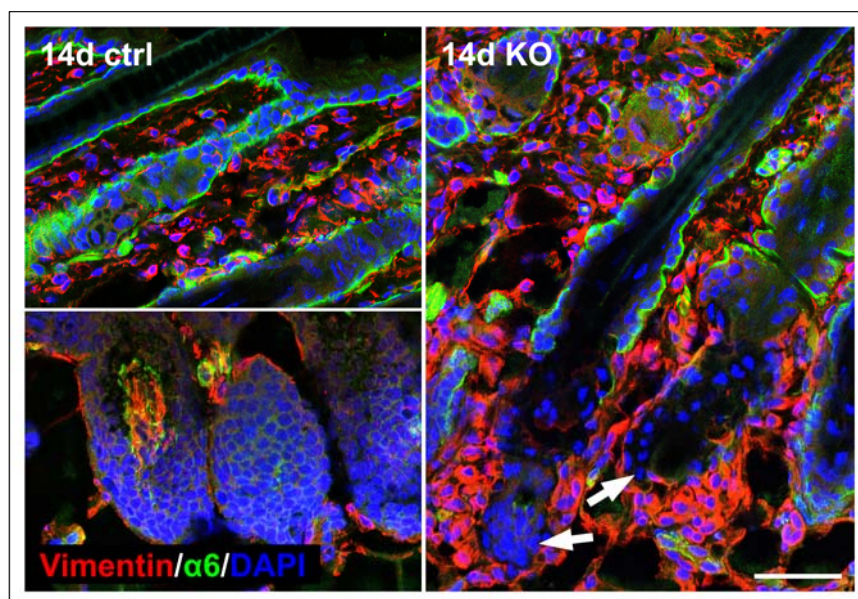


Fig. 3.21 Vimentin and $\alpha 6$ integrin IF staining of back skin sections from 14-day-old control and mutant mice. Cells in the lower parts of HF, which were not enclosed by $\alpha 6$ integrin-expressing ORS keratinocytes, did not contain vimentin (arrows). However, they seemed to be surrounded by mesenchymal cells. Nuclear DNA was visualized with DAPI. Bar: 50 μ m.

Taken together, the results of the IF analysis of the HF-specific protein expression indicated that keratinocytes within the HF are not able to sustain their differentiated state in the absence of Rac1.

3.2.3 Removal of the lower part of mutant HF's by macrophages.

Pathological changes in morphology of HF's can cause an increased infiltration of phagocytic cells as was previously shown for example in the $\beta 1$ -integrin-deficient skin (Brakebusch *et al.*, 2000). The absence of the lower parts of HF's in the adult skin of *rac1^{fl/fl}, cre* mice could have been a result of such an increased phagocytic activity. Therefore, the back skin of 9-day-old and 14-day-old control and mutant mice was analysed for the presence of macrophages and granulocytes.

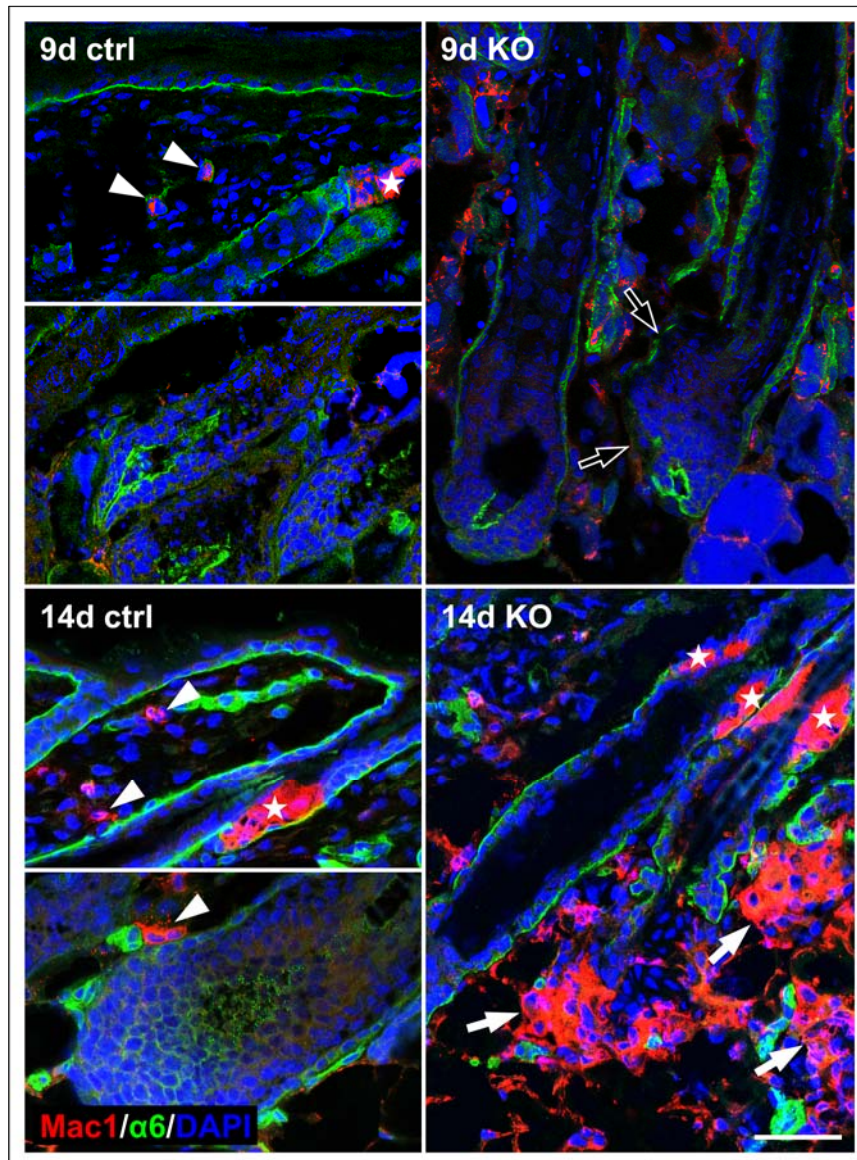


Fig. 3.22 Mac1 and $\alpha 6$ integrin staining of back skin sections from 9-day-old and 14-day-old control and mutant mice. Only a few macrophages were found in the skin of 9-day-old and 14-day-old control mice (arrowheads). In the 9-day-old mutant skin, no increased number of macrophages was detected, even around distorted hair bulbs (black arrows). At day 14 after birth, many Mac1^+ cells infiltrated the *Rac1*-deficient skin and accumulated around the lower parts of the HF's, below the regions where $\alpha 6$ integrin was still expressed in the outermost layer (white arrows). Fluorescently labeled streptavidin, used as a secondary reagent, non-specifically recognized SGs (stars) and subcutaneous fat cells. Nuclear DNA was visualized with DAPI. Bar: 50 μm ,

Only a few, evenly scattered, Mac1-positive cells were observed in the control skin (Fig. 3.22, arrowheads), which was consistent with the normal presence of macrophages in the skin. Also, no increase in the amount of macrophages was detected in samples from 9-day-old *rac1^{fl/fl},cre* mice, even though some HF's were already showing changes in the morphology (black arrows). However, there was a massive infiltration of macrophages in the skin of 14-day-old mutant mice (white arrows). The phagocytic cells were concentrated around the lower parts of mutant HF's, which suggested that macrophage-attracting signals were released by cells in that region.

Granulocytes (Gr^+), which are present in the skin only in pathological conditions, were not detected in either control or mutant skin of 14-day-old mice (data not shown). This result was consistent with the lack of apparent fibrosis in the absence of Rac1.

Phagocytes are attracted by apoptotic cells (Lauber *et al.*, 2004). Therefore, a TUNEL staining was performed (2.7.2.3) to determine if cells in the lower regions of Rac1-deficient HF's are dying, thereby causing the phagocytic removal. However, no increase in the amount of cells undergoing apoptosis was detected in the mutant HF's, when compared to the control samples (Fig. 3.23).

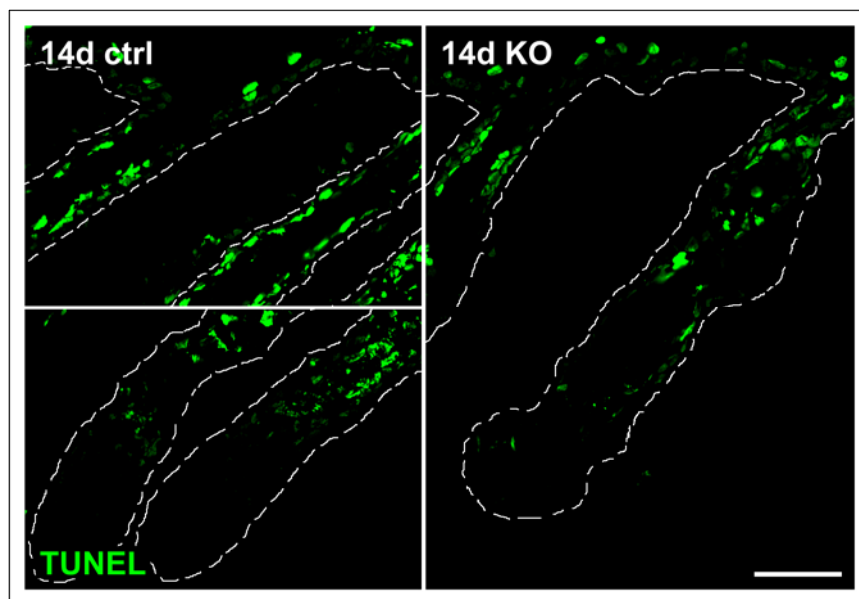


Fig. 3.23 TUNEL staining of back skin sections from 14-day-old control and mutant mice. No increase in the amount of TUNEL⁺ cells was detected in the lower regions of 14-day-old mutant HF's when compared to normal HF's. Bar: 50 μ m.

Those results showed that, while Rac1-deficient cells in the lower parts of HF's attracted macrophages, the programmed cell death was not the cause of the infiltration.

3.3 Phenotype analysis of the Rac1-deficient epidermis

In contrast to the severe HF phenotype, the epidermis of *rac1^{fl/fl},cre* mice seemed to be not affected by the loss of Rac1 (3.1.3 and Fig. 3.9-Fig. 3.12). The histological analysis (2.7.1) of the 14-day-old mutant skin did not reveal evident defects, such as an increased amount of layers or detachment of the Rac1-deficient epidermis from the dermis (Fig. 3.25, HE).

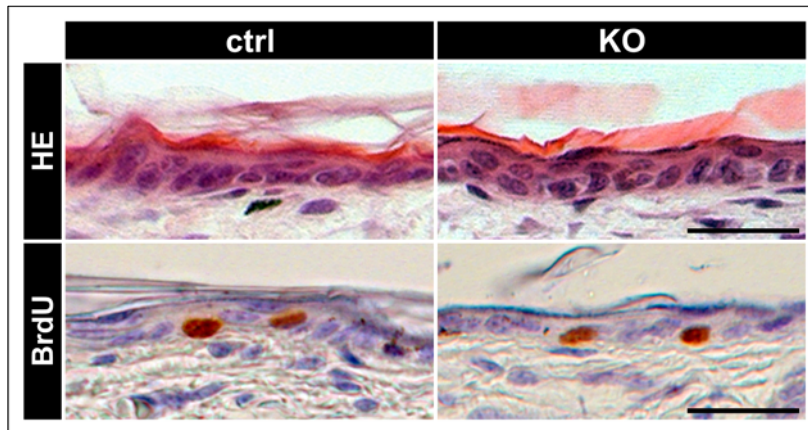


Fig. 3.24 Normal morphology and proliferation of the Rac1-deficient epidermis. HE staining of back skin sections from 14-day-old control and mutant mice showed no defects of the epidermis in the absence of Rac1. No changes in the proliferation of basal keratinocytes as well as no abnormal proliferation of suprabasal cells were detected with a BrdU-incorporation assay in the mutant epidermis. Bars: 25 μ m.

Mitotic activity of epidermal cells in the 14-day-old skin was analysed using a BrdU incorporation assay (2.7.2.2). The proliferation rate of basal keratinocytes in the mutant epidermis was similar to the control value (ctrl: 10.3% BrdU⁺ cells; KO: 11.4% BrdU⁺ cells). Also, no proliferation of Rac1-deficient suprabasal cells was detected (Fig. 3.24, BrdU). Those results were in agreement with the normal morphology of the Rac1-deficient epidermis.

In some older mice, regions with a slight thickening of the epidermis were observed, suggesting a local increase in the proliferation.

3.3.1 Normal differentiation of the epidermis

A normal layer composition of the epidermis in the absence of Rac1 was confirmed by the IF expression analysis of differentiation-specific keratins (2.7.2.1). Distribution patterns of K14 and K10, which are typical for basal and suprabasal keratinocytes, respectively (1.2.1), were comparable in the 14-day-old control and mutant epidermis (Fig. 3.25, K14 and K10). Also the presence of loricrin, which is normally expressed in terminally differentiated keratinocytes, was restricted to the cornified layer of the epidermis as in control samples (Fig. 3.25, loricrin).

The expression of K6 is induced in the epidermis only when the normal biology of keratinocytes is disturbed, e.g. under hyper- or hypoproliferative conditions (Dominey *et al.*,

1993; Sellheyer *et al.*, 1993). However, as in control samples, no K6 expression was detected in the mutant epidermis (Fig. 3.25, K6), further indicating that the absence of Rac1 does not lead to pathological changes.

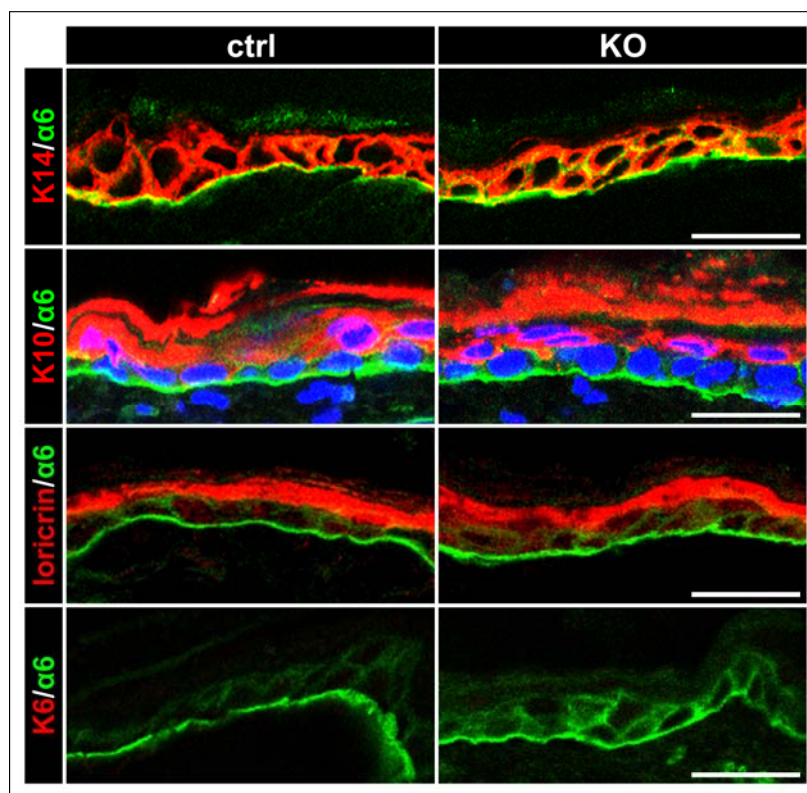


Fig. 3.25 Normal differentiation of the epidermis in the absence of Rac1. IF staining of back skin sections from 14-day-old control and mutant mice were carried out for K14, K10, loricrin and K6 to analyse differentiation of the epidermis. A counterstaining for $\alpha 6$ integrin was performed to visualize the dermal-epidermal junction. Nuclei were visualized with DAPI. Bars: 25 μ m.

3.3.2 Normal expression of adhesion and ECM proteins

In vitro studies with primary keratinocytes showed that Rac1 is required for the establishment and maintenance of the cadherin-mediated cell–cell adhesion (Braga *et al.*, 1997; Braga *et al.*, 1999). Surprisingly, IF staining of junctional proteins showed normal expression patterns and the intracellular distribution of E-cadherin, β -catenin, α -catenin and desmoplakin in the 14-day-old mutant epidermis (Fig. 3.26) giving no indication of a defect in the cell-cell adhesion between Rac1-deficient keratinocytes *in vivo*.

Furthermore, Rac1 was shown to be necessary for the assembly of laminin at the basal side and for the establishment of cell polarity in MDCK epithelial cysts grown in collagen (O'Brien *et al.*, 2001). However, the deposition of BM components such as LN5 and nidogen (Nd) was not altered in the 14-day-old mutant skin and remained restricted to the dermal-epidermal junction (Fig. 3.27, LN5 and Nd). Like in the control skin, the BM was linear and continuous.

In addition, integrins $\alpha 6$ and $\beta 4$ were present mainly at the basal side of keratinocytes

adherent to the BM, in both control and mutant epidermis, demonstrating that basal keratinocytes were polarized normally in the absence of Rac1 (Fig. 3.27, $\beta 4$).

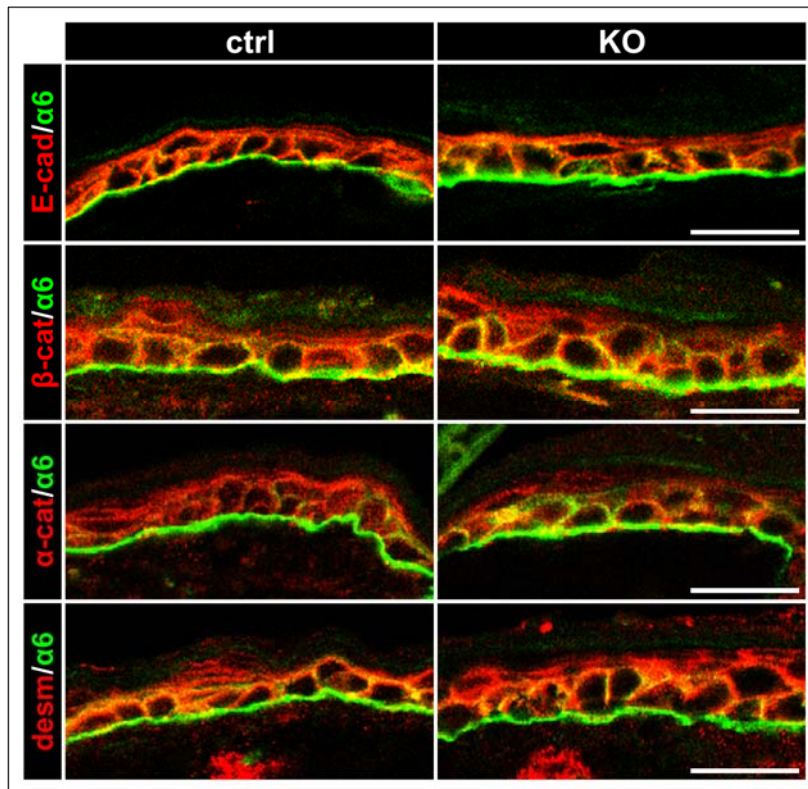


Fig. 3.26 Normal expression of cell-cell contact components in the Rac1-deficient epidermis. IF staining of back skin sections from 14-day-old control and mutant mice was carried out for E-cadherin (E-cad), β -catenin (β -cat), α -catenin (α -cat) and desmoplakin (desm) to analyse the expression of adhesion proteins in the epidermis. A counterstaining for $\alpha 6$ integrin was performed to visualize the dermal-epidermal junction. Bars: 25 μ m.

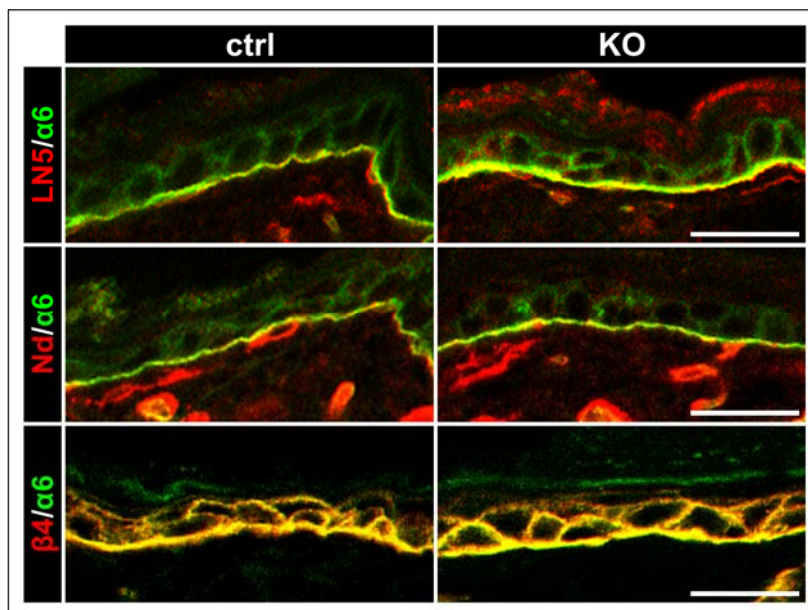


Fig. 3.27 Normal deposition of the BM and polarization of basal keratinocytes in the absence of Rac1. IF staining of back skin sections from 14-day-old control and mutant mice was carried out for LN5 and Nd to analyse the deposition of BM components. Polarization of basal keratinocytes was shown by visualizing the expression pattern of integrin $\alpha 6\beta 4$. Bars: 25 μ m.

3.3.3 Normal formation of cell-cell and cell-ECM contacts

An ultrastructural analysis of back skin (2.7.3) was performed to study in more detail the structure of cell-cell contacts and the attachment of basal keratinocytes to the BM.

EM pictures showed a normal presence of desmosomes (Fig. 3.28A and B, black arrows) between *Rac1*-deficient basal keratinocytes (K), which were accompanied by adherens junctions, as in the control epidermis (Fig. 3.28B, white arrowheads). Those results further indicated that the cell-cell adhesion between basal keratinocytes *in vivo* is not affected by the absence of *Rac1*.

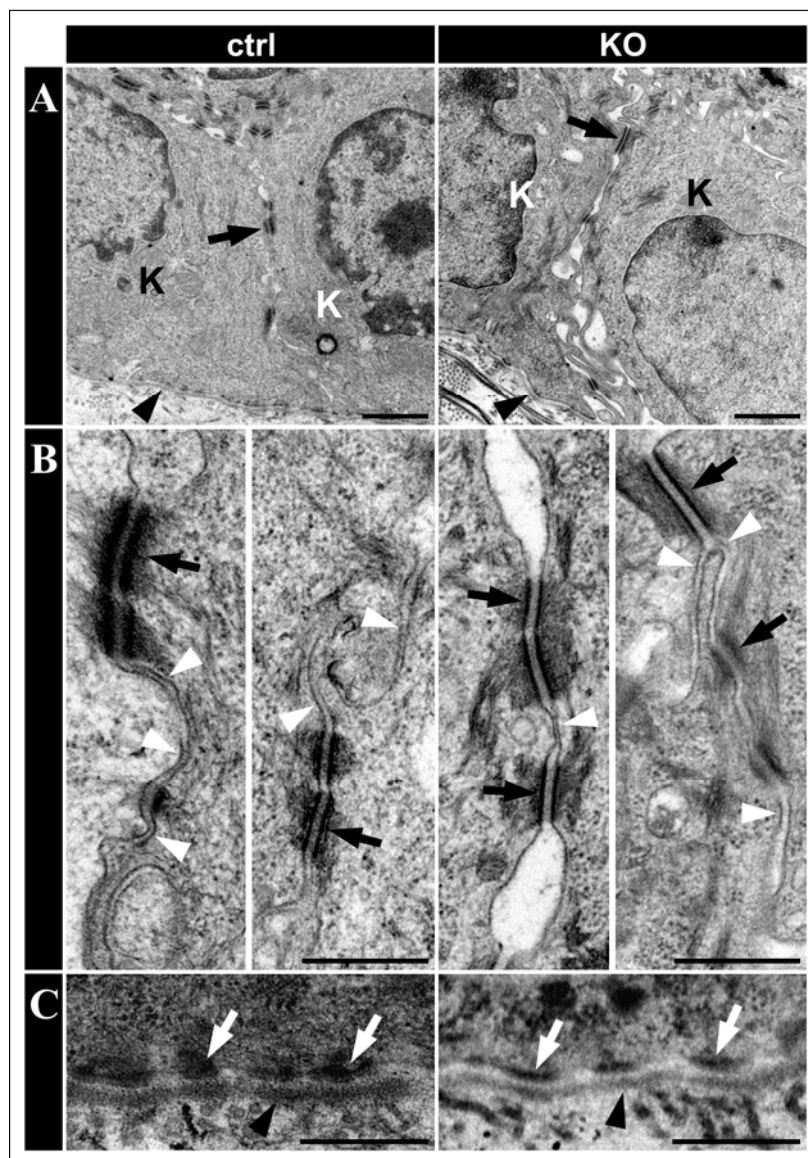


Fig. 3.28 No apparent defects of cell-cell and cell-ECM contacts in the *Rac1*-deficient epidermis. (A) EM pictures of back skin sections from 14-day-old control and mutant mice confirmed a normal presence of desmosomes (black arrows) between *Rac1*-deficient basal keratinocytes (K) attached to the BM (black arrowheads). Bar: 1 μ m. Higher magnification EM pictures showed: (B) normal adherens junctions (white arrowheads) formed next to desmosomes (black arrows) and (C) normal hemidesmosomes (white arrows) formed between basal keratinocytes and the BM (black arrowheads) in the absence of *Rac1*. Bars: 0.5 μ m.

The intercellular distance between some mutant basal keratinocytes was slightly increased,

when compared to control samples. However, that seemed to have no influence on the maintenance of adhesion structures.

The EM analysis confirmed a normal deposition of the BM in the absence of Rac1 (Fig. 3.28A and C, black arrowheads). In addition, higher magnification EM pictures showed a presence of hemidesmosomes in both control and mutant skin (Fig. 3.28C; white arrows). No detachment of the epidermis from the underlying BM was observed in the Rac1-deficient skin, as expected from the histological analysis.

Those data showed that adhesion capability of mutant keratinocytes *in vivo* was either not affected at all by the absence of Rac1 or, at the least, that it was not altered enough to cause a noticeable defect.

3.4 Biochemical analysis of signalling pathways in the absence of Rac1

3.4.1 No significant changes in the c-Myc expression

Recently it has been shown that an induced loss of Rac1 in keratinocytes *in vivo* leads to an increased expression of c-Myc resulting in the depletion of epidermal stem cells (Benitah *et al.*, 2005). In contrast to that report, Western blot analysis (2.8.3) of c-Myc protein levels in epidermal lysates (2.8.1.2) prepared from *rac1^{fl/fl},cre* mice showed no significant changes when compared to control samples (Fig. 3.29). That result, however, was in agreement with the lack of epidermal defects observed in the mutant mice generated in this study.

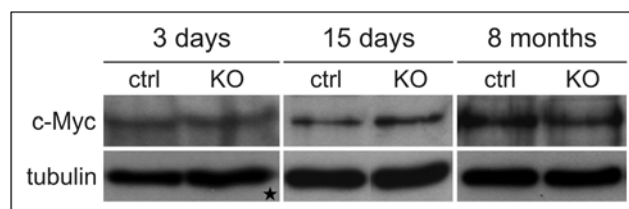


Fig. 3.29 No significant changes of c-Myc protein levels in the Rac1-deficient epidermis. Western blot analysis performed on epidermal lysates from 3-day-old, 15-day-old and 8-month-old control and mutant mice. Tubulin or GAPDH (star) content was used as a loading control.

3.4.2 No apparent defects in activation of NF- κ B, JNK, p38 or Akt

Several signalling pathways were shown to be Rac1 dependent (Van Aelst and D'Souza-Schorey, 1997; Bishop and Hall, 2000; Jaffe and Hall, 2005). Therefore, activation of JNK, p38, Akt and NF- κ B was analysed to investigate possible consequences of the Rac1 deletion in the epidermis.

Western blot analysis of epidermal lysates from control and mutant mice was performed to check the amount of phosphorylated forms of JNK, p38 and Akt. Activation of NF- κ B was tested

indirectly by assessing the amount of I κ B- α , which is degraded during the activation of NF- κ B.

No significant changes in the activation of any of the investigated proteins were detected in epidermal lysates from 3-day-old and 8-month-old mice (Fig. 3.30), indicating that the presence of Rac1 is not essential for normal signalling through those pathways in keratinocytes *in vivo*.

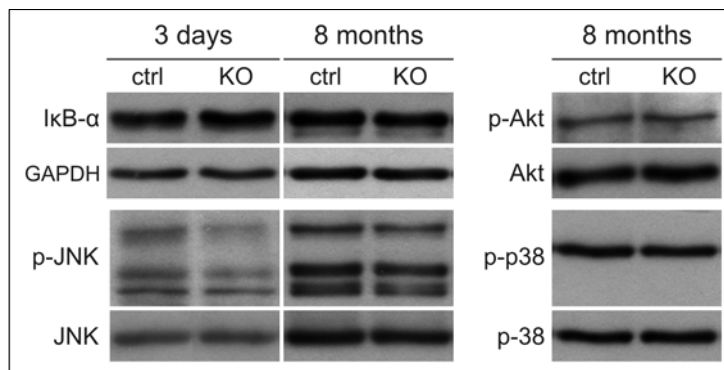


Fig. 3.30 No changes in the activation of NF- κ B, JNK, Akt and p38 in the Rac1-deficient epidermis. Western blot analysis performed on epidermal lysates from 3-day-old and 8-month-old control and mutant mice. Levels of I κ B- α were checked as an indirect test of NF- κ B activation. GAPDH content and total levels of JNK, Akt or p38 were used as a loading control (p: phosphorylated forms).

3.4.3 No obvious compensation of Rac1 by related Rho GTPases.

The lack of an obvious phenotype in the Rac1-deficient epidermis could be a result of compensatory mechanisms. An upregulation of the expression or activation of closely related Rho GTPase family members might have theoretically counterbalanced the lack of Rac1 in the epidermis.

Western blot analysis of Cdc42, RhoA, Rac2 and Rac3 protein levels (2.8.3) and a quantitative RT-PCR analysis of RhoG mRNA levels (2.9) in the epidermis of control and mutant mice were performed to investigate that possibility.

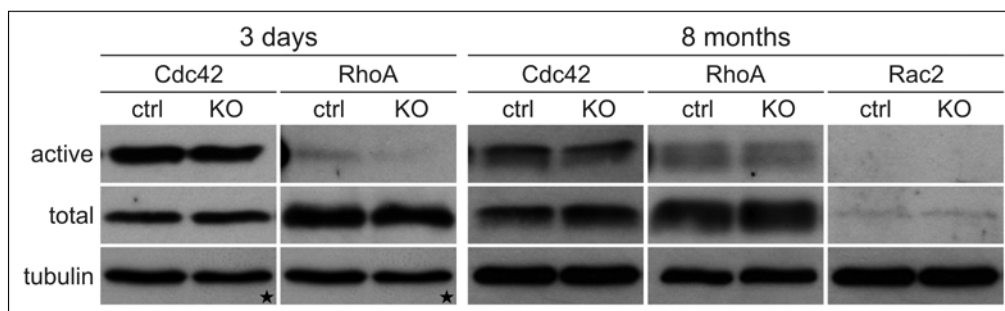


Fig. 3.31 No significant changes in the protein expression and the activation of Cdc42, RhoA and Rac2 in the absence of Rac1. Western blot analysis of GTPase-activity assays performed on epidermal lysates from 3-day-old and 8-month-old control and mutant mice. No presence of active Rac2 was detected in either lysate. Tubulin or GAPDH (star) content was used as a loading control.

The total protein content of Cdc42 and RhoA in the Rac1-deficient epidermis was comparable with control samples at 3 days and 8 months of age (Fig. 3.31). While Rac2 was not

detected in any of the epidermal lysates from 3-day-old mice (Fig. 3.32A), there were low amounts of the protein present in the epidermis of 8-month-old control and mutant mice, at similar levels in both samples (Fig. 3.31). Rac3 protein was not detected in epidermal lysates from neither 3-day-old nor 8-month-old control and mutant mice (data not shown and Fig. 3.32B, respectively).

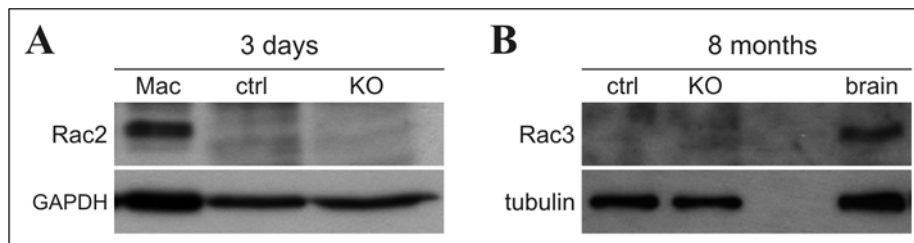


Fig. 3.32 No expression of Rac2 and Rac3 in the Rac1-deficient epidermis at 3 days and 8 months of age, respectively. Western blot analysis performed on epidermal lysates from control and mutant mice. Macrophage (Mac; A) or brain (B) lysate was used as a positive control. GAPDH (A) or tubulin (B) content was used as a loading control.

Activation of Cdc42, RhoA and Rac2 was analysed in GTPase-activity assays performed on epidermal lysates from 3-day-old and 8-month-old control and mutant mice (2.8.4).

In case of Cdc42 and RhoA, no significant changes in the amount of the GTP-bound form were observed after the loss of Rac1. No active form of Rac2 was detected in epidermal lysates from 8-month-old control or mutant mice (Fig. 3.31). The activity of Rac2 was analysed only in the epidermis of adult mice, as no protein was present in 3-day-old samples (Fig. 3.32A). For the same reason, lysates were not analysed for the presence of active Rac3.

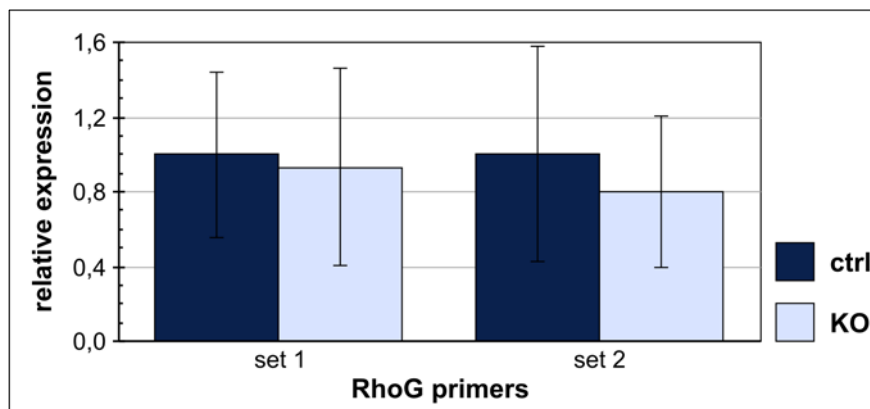


Fig. 3.33 No upregulation of the RhoG expression in the absence of Rac1. Real-time PCR analysis of RhoG mRNA levels in 6-month-old control and mutant epidermis was performed with two different sets of primers. No significant differences between control and Rac1-deficient samples were detected. GAPDH expression levels were used for standardization of samples.

RhoG expression levels were determined in the epidermis of 3-month-old and 6-month-old control and mutant mice by a quantitative RT-PCR (2.9.3) using two independent sets of primers. Neither of them showed a significant change in the expression of RhoG in the absence of Rac1 (Fig. 3.33).

Although those data did not exclude compensatory changes in the expression or the activation of other proteins in response to the absence of Rac1, they demonstrated that proteins most likely capable of the compensation are not involved.

3.5 Analysis of the wound healing process in the absence of Rac1

Data obtained in this study demonstrated that Rac1 is not essential for maintenance of the epidermis in physiological conditions. Still, a potential role of Rac1 in response to stress stimuli, i.e. skin injury, remained to be investigated. *In vitro* studies suggested the possibility of a Rac1 importance during the re-epithelialization process because of its involvement in the regulation of cell migration (Nobes and Hall, 1999; Fenteany *et al.*, 2000).

In order to study the consequences of the Rac1 absence for the regeneration of the epidermis, wound healing experiments were carried out in control and mutant mice (2.7.5). Two parameters were used for the analysis of the wound closure process. The first was a length of the epithelial tongue, used as readout of the migratory activity of keratinocytes. The distance was measured from the wound edge to the tip of the tongue (Fig. 3.34A; red line). The second analysed parameter was the total area covered by the neo-epidermis (yellow area), which was used as readout of the hyperplastic growth.

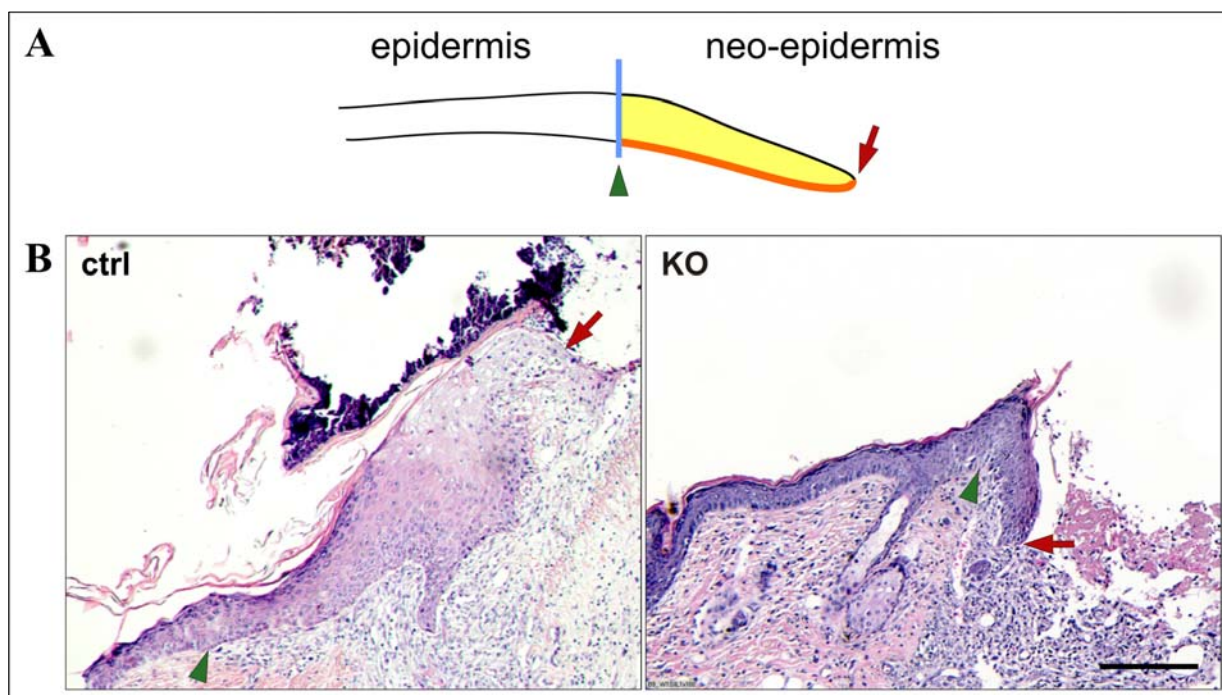


Fig. 3.34 Impaired wound re-epithelialization in Rac1-deficient epidermis. (A) Schematic representation of a wound. Neo-epidermis (yellow area) is expanding out of a wound margin (blue line) pointed out with the green arrowhead. The end of the epithelial tongue (red line) is marked with the red arrow. (B) HE staining of wound edge sections from control and mutant mice, isolated 5 days after the wounding. Arrows indicate the wound margin (green) and the front of the epithelial tongue (red), as in the scheme. Bar: 200 μ m.

Histological analysis of tissue samples, isolated from control and mutant mice 5 days after the wounding, showed a dramatic delay in the regeneration of the injured epithelium in the absence of Rac1 (Fig. 3.34B).

The differences were quantified by a histomorphometric analysis of wound cross-sections from 6 *rac1^{fl/+},cre* and 8 *rac1^{fl/fl},cre* mice. The results confirmed that Rac1-deficient epithelial tongues were significantly shorter than control ones, suggesting a defect in the migration of mutant keratinocytes into the wound. (Fig. 3.35A). While the hyperplastic neo-epidermis and wound edge epithelium were present in the mutant skin, the amount of new tissue formed in the absence of Rac1 was significantly lower in comparison to the control skin (Fig. 3.35B).

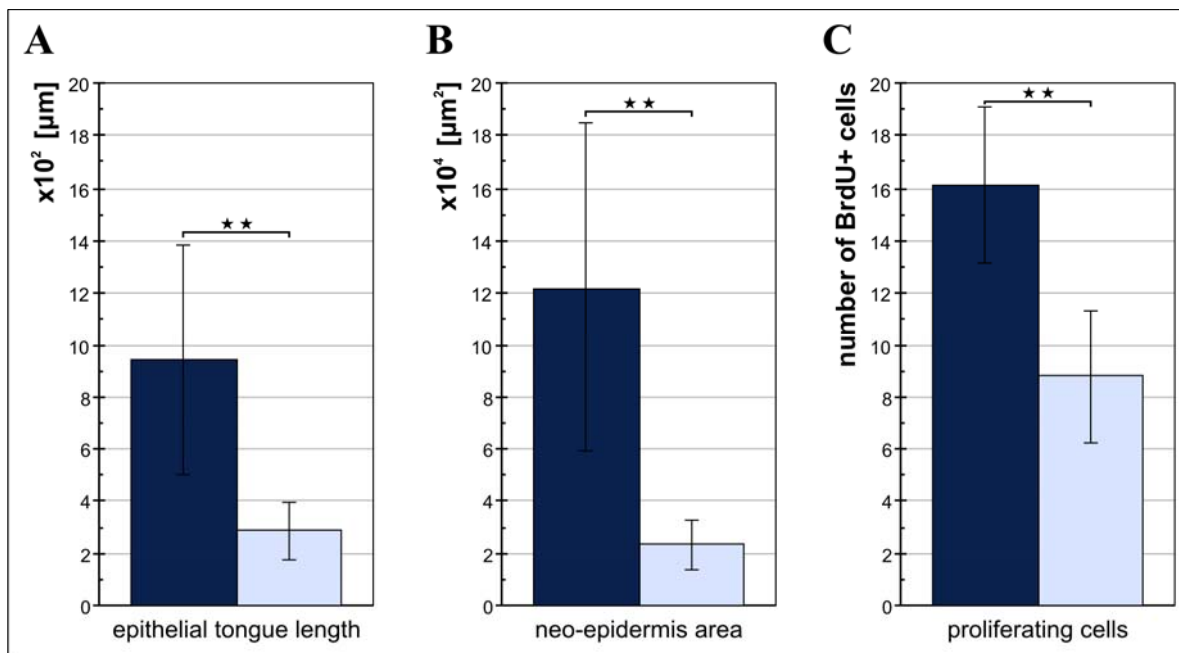


Fig. 3.35 Quantification of the re-epithelialization defect in the absence of Rac1. (A and B) Results of histomorphometric analysis of the epithelial tongue length (A) and the neo-epidermis area (B), conducted 5 days after the wounding, confirmed dramatic delay in the wound closure process. (C) Reduced number of BrdU-positive cells confirmed lower growth rate of mutant keratinocytes in the neo-epidermis. Error bars: \pm SD; stars: $p < 0.0001$.

Reduced hyperplasia of the neo-epidermis and the wound edge epidermis in *rac1^{fl/fl},cre* mice suggested that the proliferation rate of epidermal keratinocytes was decreased in the absence of Rac1. To check this assumption, the mitotic activity of keratinocytes in the wound tissue was quantified with a BrdU incorporation assay (2.7.5).

BrdU positive cells in the neo-epidermis and wound edge epidermis were counted in sections of 5-day-old wounds isolated from 8 control and 11 mutant mice. The analysis revealed a significantly decreased incorporation of BrdU within the wound epithelium of Rac1-deficient mice when compared to control animals (Fig. 3.35C). That result confirmed the dramatic decrease in the efficiency of the re-epithelialization in the absence of Rac1.

3.6 Analysis of the 4-hydroxy-tamoxifen influence on the Rac1-deficient epidermis

Maintenance of the epidermis in *rac1^{fl/fl},cre* mice generated for this study, in which the deletion of the protein was activated endogenously during the embryogenesis, is not affected by the lack of Rac1 (3.3). In contrast, recently reported keratinocyte-specific deletion of the *rac1* gene, induced locally in the skin of adult mice, resulted in a severe defect of the epidermis (Benitah *et al.*, 2005). The initial hyperthickening of the epidermis was followed by disorganization of the basal layer (a decrease in cellularity combined with an increased cell size) and resulted finally in a partial or complete loss of epidermal keratinocytes. The phenotype was attributed to an abnormal activation and terminal differentiation of epidermal stem cells, which led to the depletion of the stem cell pool.

One of the explanations for the striking discrepancy between both phenotypes could be the use of different methods leading to the removal of Rac1. Repetitive applications of 4-hydroxy-tamoxifen (4OHT) dissolved in acetone, which were used by Benitah and co-authors to induce the deletion, might theoretically lead to more severe effects in the epidermis lacking the Rac1 than in the normal skin. To test that possibility acetone or 4OHT/acetone solution was applied to a clipped area of back skin of *rac1^{fl/+},cre* and *rac1^{fl/fl},cre* mice, following the protocol described by Benitah and co-authors (2.7.4).

Acetone alone did not cause any obvious changes in either control or mutant epidermis (Fig. 3.36A). The application of the 4OHT/acetone solution, however, resulted in a significant hyperthickening of the Rac1-deficient epidermis (Fig. 3.36B). Surprisingly, mild alterations were detected also in the 4OHT-treated control skin, suggesting, that the compound might be not entirely neutral to the epidermis in general. Observed changes were transient though, as 2 weeks after stopping the treatment both the control and the Rac1-deficient epidermis looked normal. The recovery of the mutant epidermis demonstrated that the 4OHT-treatment did not cause irreversible changes in the epithelial stem cell pool (Fig. 3.36C).

Those data suggest that the treatment related effects might have contributed to the phenotype of the mice with a 4OHT-induced deletion of the Rac1 gene (Benitah *et al.*, 2005). However, consequences of the treatment alone were not sufficient to explain the dramatic difference between both phenotypes, indicating an involvement of other factors such as compensatory mechanisms or an influence of the genetic background.

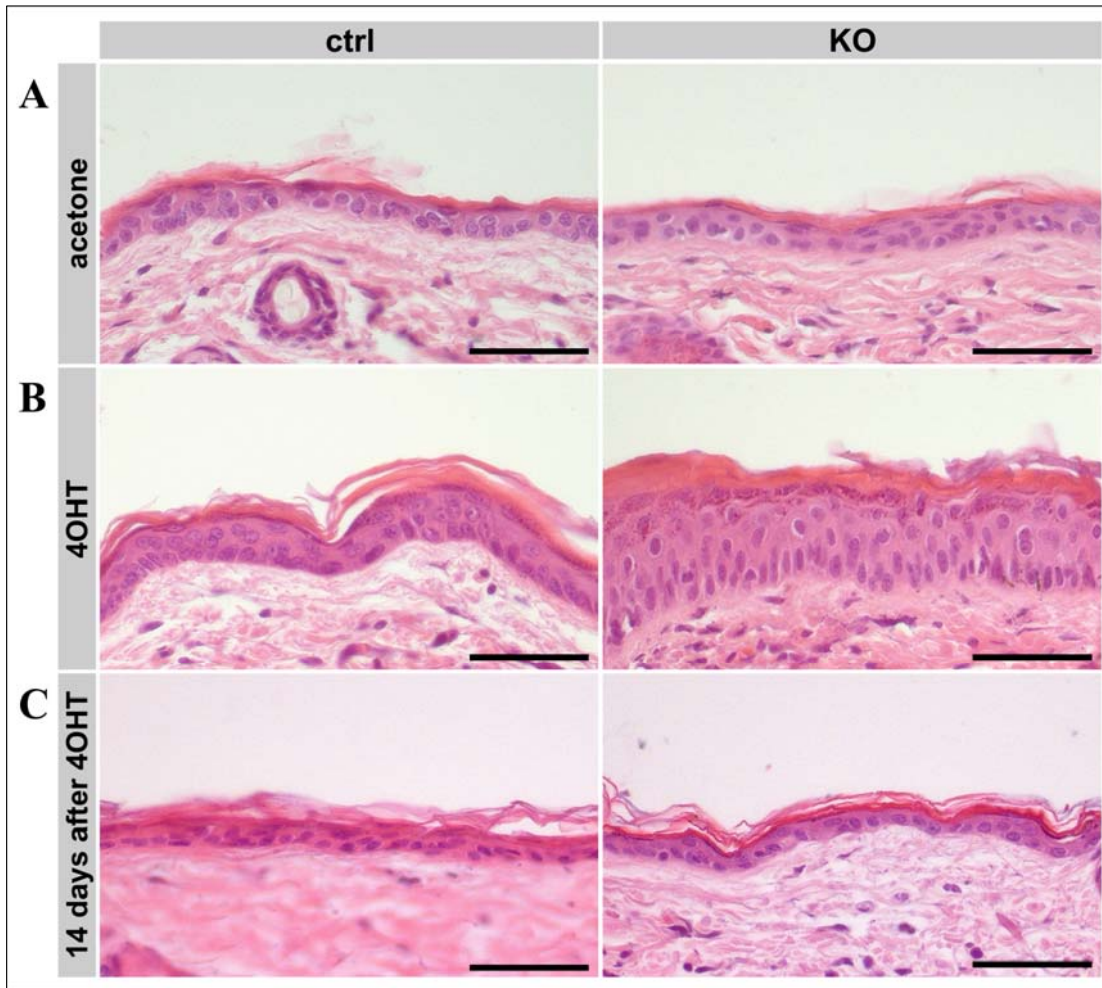


Fig. 3.36 Transient hyperthickening of *Rac1*-deficient epidermis caused by the application of 4-hydroxy-tamoxifen (4OHT). HE staining of back skin sections from control and mutant mice treated with acetone alone (A) or 4OHT/acetone (B and C) every 3 days for 15 days. The mice were sacrificed either 1 day (A and B) or 2 weeks (C) after the last application. Bars: 50 μ m.

3.7 *In vitro* analysis of *Rac1*-deficient primary keratinocytes

3.7.1 Mutant keratinocytes do not survive *in vitro*

Primary keratinocytes were isolated from *rac1^{fl/+},cre* and *rac1^{fl/fl},cre* adult mice (2.5.4.3) and cultured in a standard keratinocyte medium, containing low amount of Ca^{2+} to prevent the induction of terminal differentiation (2.5.4.1). Cells were seeded on the surface coated with collagen I and fibronectin (Col/FN) or the LN5-rich matrix (LN) (2.5.4.2). Control cells were growing normally and usually reached confluency within a week. However, it was not possible to sustain mutant keratinocytes *in vitro* on either of used substrates (Fig. 3.37).

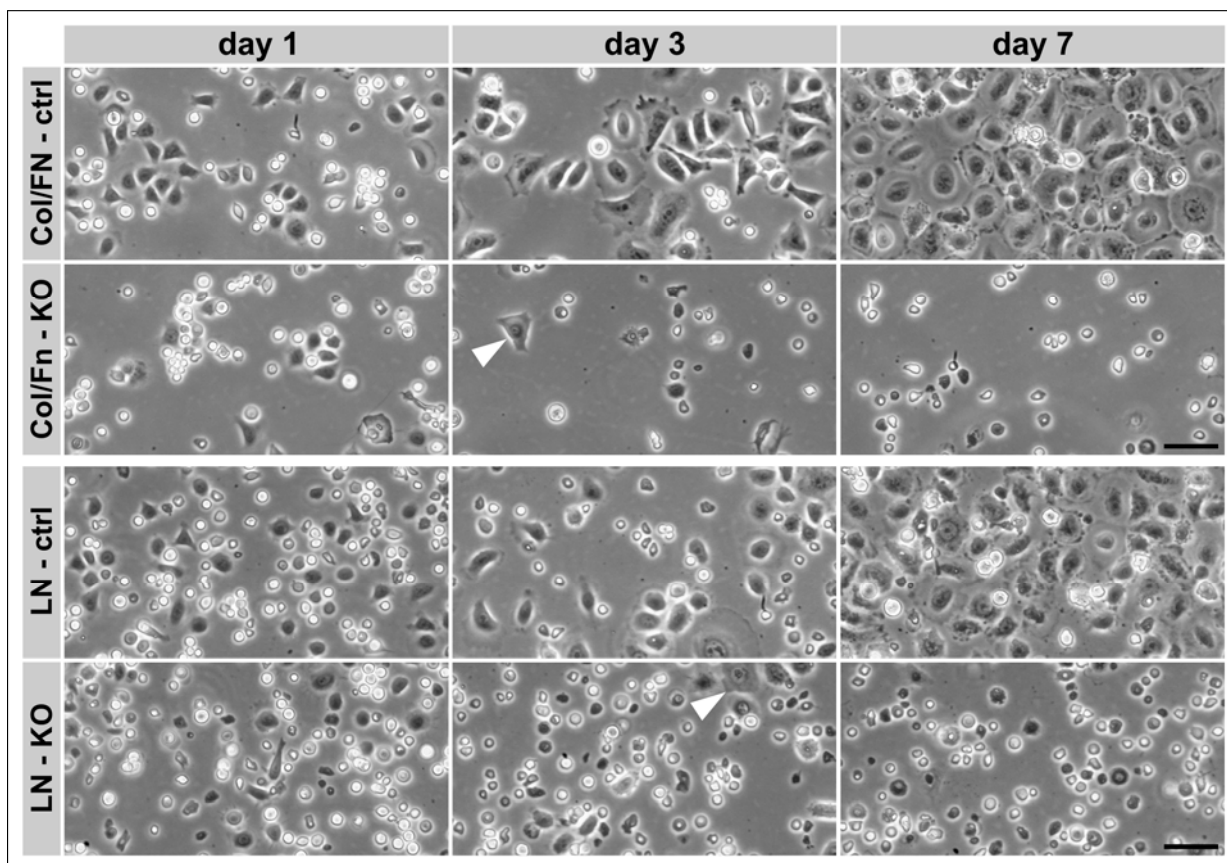


Fig. 3.37 Rac1-deficient primary keratinocytes could not be sustained *in vitro*. Keratinocytes isolated from adult control and mutant mice were seeded in culture dishes coated with collagen I and fibronectin (Col/FN) or the LN5-rich matrix (LN). On both substrates, a decreased number of attached Rac1-deficient cells was observed 1 day after seeding, when compared to control keratinocytes. Adherent mutant cells showed defective spreading and did not expand. Most of them died within a week. A few well-spread cells isolated from mutant mice (arrowheads) might have been cells that had escaped the deletion of the *rac1* gene. Bars: 50 μ m.

Already one day after the seeding, a difference in the amount of attached cells was visible. It was becoming more prominent with each day as control keratinocytes were expanding, while the number of Rac1-deficient cells was decreasing. Also a dramatic difference in the cell size became evident within a couple of days.

Nearly all Rac1-deficient cells died within a week. That, however, might have been a secondary effect, resulting from a too low number of initially (day 1) attached cells, as keratinocytes require quite a high cell density to survive and grow *in vitro*. Seeding mutant cells at a higher density did not rescue the culture, though, as the amount of attached cells after 24 h did not increase significantly.

Some cells isolated from the mutant epidermis could adhere and spread like control cells (Fig. 3.37, arrowheads). Most likely, these cells had escaped the deletion of the *rac1* gene.

3.7.2 Slightly impaired adhesion of Rac1-deficient keratinocytes.

The apparent attachment defect was further analysed with a standard adhesion assay. Experiments were performed with freshly isolated keratinocytes on both substrates (Col/FN and LN) in normal culture conditions (2.5.4.5). As defects in cell adhesion often result from changes in the cell surface expression of integrins, a FACS analysis of the integrin profile was performed as well (2.7.2.4) to investigate if that was the reason for the observed reduction in the amount of attached mutant keratinocytes.

Judging from the reduced number of adherent cells, observed 24 h after the seeding, a rather severe impairment of adhesion might have been expected. Surprisingly, the results revealed that within first 2 h the adhesion of Rac1-deficient keratinocytes to collagen I and fibronectin was only slightly reduced, while the attachment to LN5-rich matrix was not significantly impaired when compared to control cells (Fig. 3.38).

The data obtained from FACS analysis confirmed adhesion assay results, as no changes in the integrin presence on the cell surface were observed in Rac1-deficient keratinocytes. Integrins $\alpha 1$, $\alpha 6$, $\beta 2$ and $\beta 4$ were expressed in both types of cells at similar levels, and no abnormal upregulation of the expression of integrins $\alpha 1$, $\alpha 4$, $\alpha 5$, αv , $\beta 2$, $\beta 3$ and $\beta 7$ was detected in Rac1-deficient primary keratinocytes (Fig. 3.39).

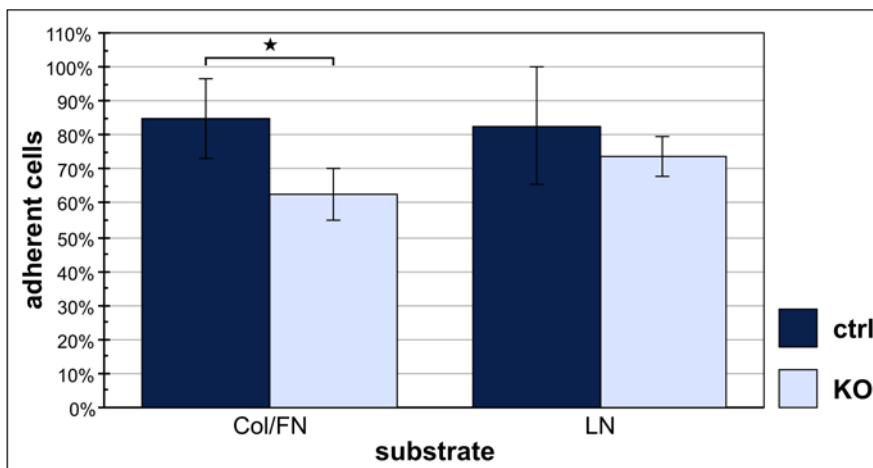


Fig. 3.38 Slightly impaired attachment to the Col/FN substrate and not significant reduction of adhesion to the LN matrix in the absence of Rac1. Adhesion assays were performed with freshly isolated keratinocytes from adult control and mutant mice. The amount of adherent cells is presented as a percentage of the seeded keratinocytes. Star: $p < 0.005$.

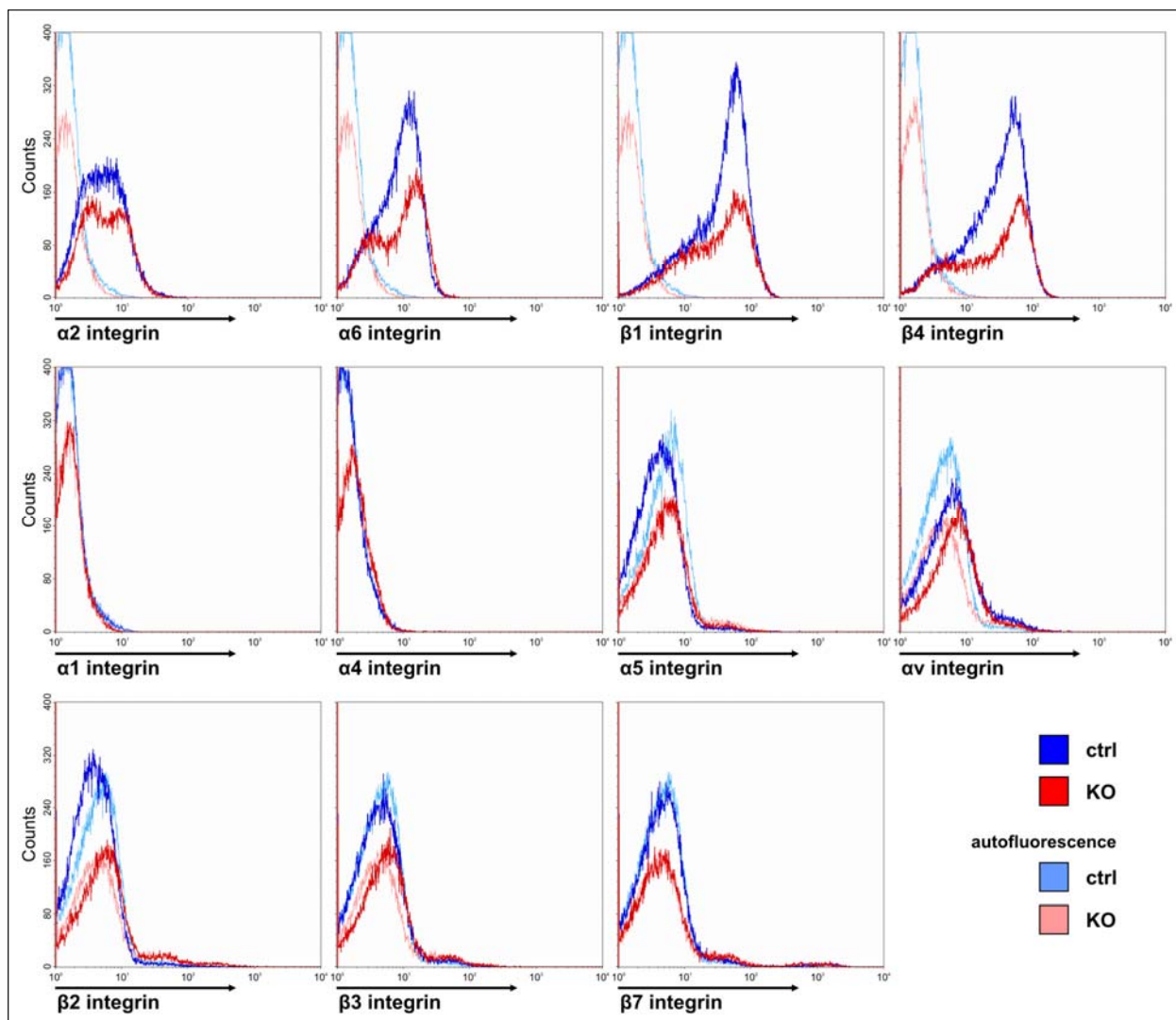


Fig. 3.39 Normal cell surface expression of integrins in the absence of Rac1. FACS analysis of freshly isolated keratinocytes from control (dark blue) and mutant (red) adult mice showed no differences in expression of integrins: $\alpha 1$, $\alpha 6$, $\beta 2$ and $\beta 4$. No expression of other integrins ($\alpha 1$, $\alpha 4$, $\alpha 5$, αv , $\beta 2$, $\beta 3$ and $\beta 7$) was detected in both control and mutant samples. The relative amount of suprabasal cells was slightly higher in mutant samples.

3.7.3 No increase in the apoptosis or terminal differentiation of keratinocytes in the absence of Rac1.

While the initial adhesion of Rac1-deficient keratinocytes was only slightly impaired, an increase in the cell death among attached mutant cells and/or their terminal differentiation might have been contributing factors in the observed reduction of the cell number. To investigate those possibilities control and mutant cells were IF stained 24 h after seeding for cleaved caspase-3, expression of which is characteristic for apoptotic cells, as well as for loricrin, a terminal differentiation marker.

Only 1.3% and 2.2% Rac1-deficient cells seeded on the Col/FN-coated surface and the LN matrix, respectively, expressed high amounts of cleaved caspase-3. These values were similar to

control: 0.4% (Col/FN) and 2.2% (LN). Furthermore, the amount of loricrin-positive cells was about the same in mutant and control keratinocytes: 0.6% on Col/FN coated surface and 0.9% on the LN matrix.

Those results were in agreement with *in vivo* data that showed no increase in the amount of apoptotic (Fig. 3.23) or terminally differentiated cells (Fig. 3.25) in the Rac1-deficient epidermis. However, they did not explain the difference between the amounts of attached control and mutant cells one day after the seeding.

3.7.4 Severe spreading defect of Rac1-deficient keratinocytes.

In order to explain the detachment of initially adherent keratinocytes, a time lapse video microscopy technique was employed to investigate the behaviour of control and mutant primary keratinocytes for 42 h after the seeding on the Col/FN-coated surface (2.5.4.6). This approach enabled to observe the attachment, spreading and movement of cells in a continuous manner, making it possible to analyse the phenotype of Rac1-deficient cells in more detail.

In standard conditions, only a fraction of primary murine keratinocytes is able to successfully attach. After initial adhesion, the spreading takes several hours, in contrast to, for example, fibroblasts, which spread within minutes.

Normal attachment and spreading were observed in case of control cells (Movie 1; see the appended CD) (7). Attached cells spread steadily and started to move around afterwards. At the end of the observation period, the majority of adherent cells were fully expanded.

In contrast, most of mutant keratinocytes, which attached initially, were not able to spread (Movie 2; see the appended CD) (7). Some cells, which started to expand, were not able to complete spreading (first three arrows). Others, while extending small protrusions, did not spread at all and remained round (fourth arrow). In the end, most of the Rac1-deficient adherent cells rounded up and detached, including some cells, which managed to fully spread (last two arrows). After 42 h, many fewer mutant keratinocytes were attached and the adherent Rac1-deficient cells were not spread to the same extend as control cells.

To better describe the observed spreading defect in the absence of Rac1, a quantitative analysis of the cell area was performed (2.5.4.6). Not surprisingly, dramatic differences in the cell size were confirmed (Fig. 3.40). Within the 36-hour-period of time, adherent control keratinocytes steadily increased their size. After the initial 12 h, the average size of attached Rac1-deficient cells was still comparable to the control value. However, mutant keratinocytes did not expand any further during the following 24 h.

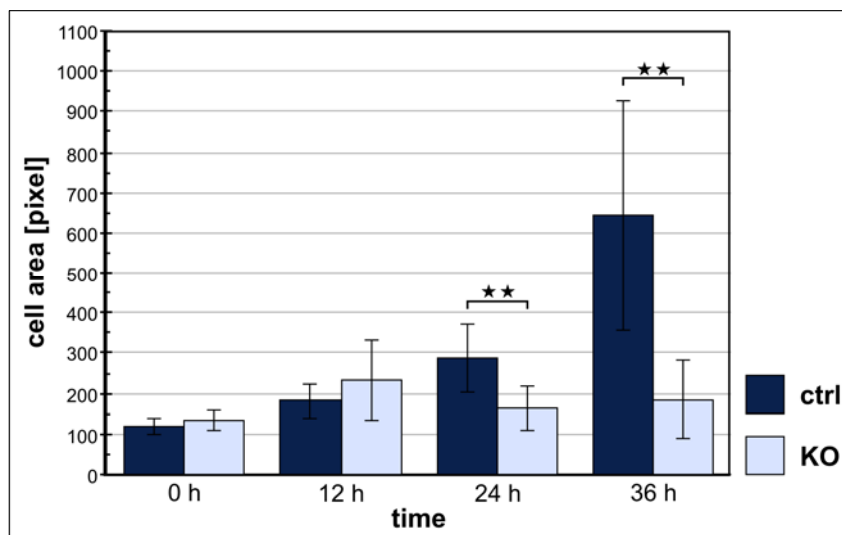


Fig. 3.40 Severe spreading defect of Rac1-deficient keratinocytes *in vitro*. Quantitative analysis of cell spreading performed on primary keratinocytes after seeding on Col/FN-coated plastic. Cell size was analysed at indicated time points by measuring the pixel area of 30-40 randomly chosen control and mutant cells. Initially, no significant differences were observed. After 12 hours Rac1-deficient cells stopped spreading while control cells continued to increase their size. Stars: $p < 0.0001$.

The severe spreading defect observed *in vitro* in mutant keratinocytes suggested strongly that an impairment of the F-actin assembly occurs in the absence of Rac1. To investigate that possibility, primary keratinocytes were isolated from adult mice and cultured for 1 and 3 days on the Col/FN-coated surface. Subsequently, the actin cytoskeleton and focal adhesions were immunofluorescently stained (2.5.4.4).

Results of the microscopic analysis showed that already 1 day after the seeding most control keratinocytes were spread and had fully developed focal adhesions (visualized with an antibody against paxillin) and a well organized actin cytoskeleton (visualized with a fluorescently labeled phalloidin) (Fig. 3.41). In contrast, the majority of Rac1-deficient cells remained much smaller than control keratinocytes, even 3 days after seeding. They formed paxillin containing focal adhesions, which was in agreement with the normal expression of the integrins. However they were not as developed as in control cells and the actin cytoskeleton was clearly disorganized.

Taken together, these results suggest that the impaired ability of Rac1-deficient keratinocytes to spread *in vitro*, which was most likely a consequence of a defect in the actin cytoskeleton organization, was the cause of the observed detachment of mutant cells.

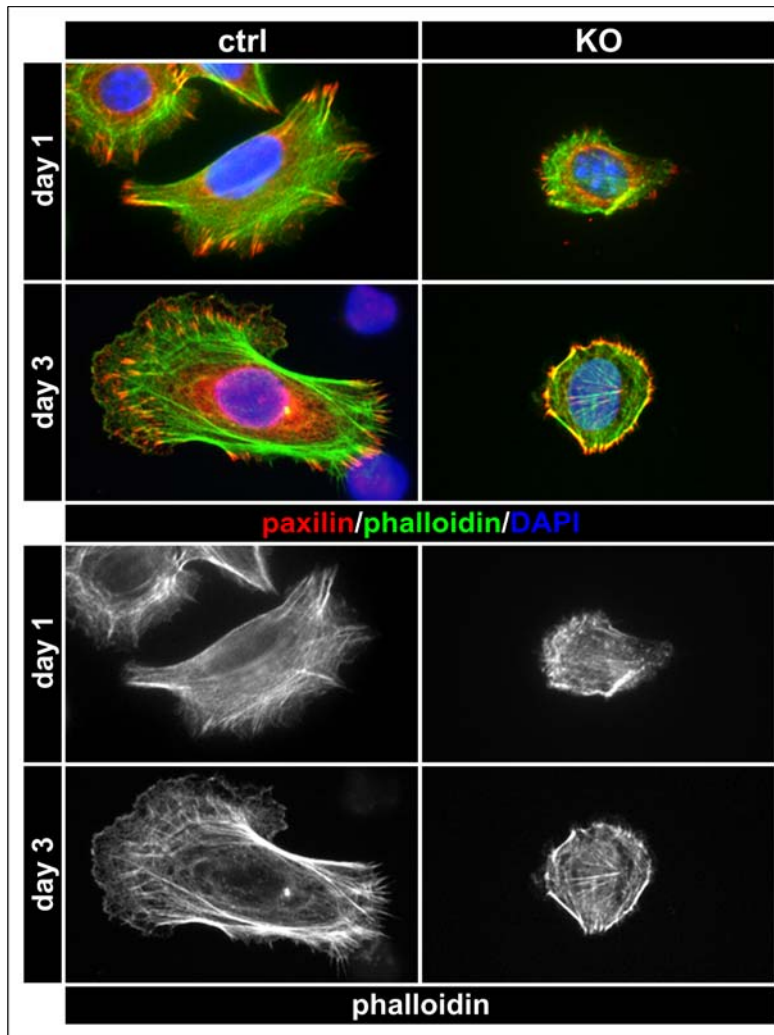


Fig. 3.41 Impaired organization of the actin cytoskeleton in Rac1-deficient keratinocytes *in vitro*. Mutant cells were much smaller and showed clear defect of the actin assembly, but were able to form focal adhesions. Control and mutant primary keratinocytes were seeded on a Col/FN-coated glass. IF staining for F-actin (with Alexa488-labeled phalloidin), paxillin and nuclear DNA (DAPI) was performed 1 and 3 days after the isolation.

3.8 *In vitro* analysis of ES cell differentiation in the absence of Rac1

The conditional deletion of the *rac1* gene, generated for this study, can not be used to study the role of Rac1 in the early stages of the epidermal development as the deletion is activated after the epithelial lineage commitment and first stages of epidermis differentiation.

The constitutive deletion of the *rac1* gene leads to a failure in the formation of three germ layers during gastrulation (Sugihara *et al.*, 1998). It would be difficult to explain the molecular mechanisms that underline the defect using the *in vivo* system, because of the low number of cells and inaccessibility of the embryos at the early stages of development.

In vitro differentiation of ES cells offers a unique approach to study events that occur during

early embryogenesis. Upon withdrawal of LIF and stromal contact, ES cells undergo spontaneous differentiation into three-dimensional structures called embryoid bodies (EBs), which consist of an outer layer of endodermal secretory cells, the BM, the polarized epiblast (primitive ectoderm layer, which later gives rise to all three germ layers) and the central cavity. This process recapitulates stages of the peri-implantation embryonic development and can be used as an *in vitro* tool to study cell differentiation, BM assembly, establishment of cell polarity and cell-cell contacts or mechanisms of apoptosis and cavitation (Li and Yurchenco, 2006). Obtained data would complement the analysis of *in vivo* gene deletion and enable a better understanding of the role of Rac1.

3.8.1 Generation of Rac1 (-/-) ES cells

Rac1-deficient ES cells were generated from one of *rac1*^{-/+} clones, which were obtained simultaneously with *rac1*^{fl/+} clones during generation of the conditional knock-out mice (3.1.2). The clone was re-electroporated with the targeting construct (2.6.3) in order to homologously recombine the remaining wild type allele. After the selection with G418, ES cell clones were picked and screened by a Southern blot analysis with the external probe for *rac1*^{-/3loxP} genotype (Fig. 3.42A). The subsequent *cre* transfection and FIAU selection (2.6.4) resulted in generation of clones carrying either the conditional allele (*rac1*^{-/fl}) or the additional null allele (*rac1*^{-/-}). Both types of clones were identified by a Southern blot analysis with the internal probe (Fig. 3.42B).

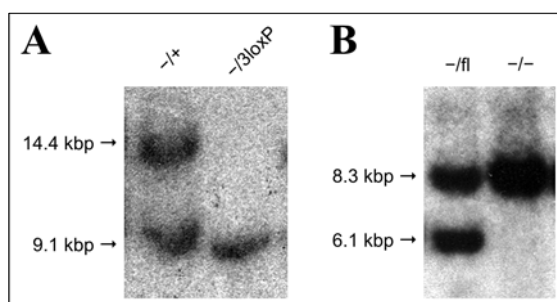


Fig. 3.42 Screening of ES cell clones. (A) Results of Southern blot analysis of HindIII-digested DNA, hybridized with the external probe to check for the homologous recombination of the targeting construct. Bands: wt (+) – 14.4 kbp, null (-) and 3loxP – 9.1 kbp. (B) Results of Southern blot analysis after the *cre* transfection. Genomic DNA from ES cell clones was cut with BamHI and hybridized with the internal probe to check for the presence of the conditional or the second null allele, generated through a Cre-mediated recombination. Bands: null (-) - 8.3 kbp, fl - 6.1 kbp.

The absence of Rac1 in ES cell clones carrying two null alleles of the *rac1* gene – Rac1 (-/-) – was confirmed with Western blot analysis. Rac1 (fl/-) clones were used as control cell lines during the analysis of Rac1-deficient ES cells.

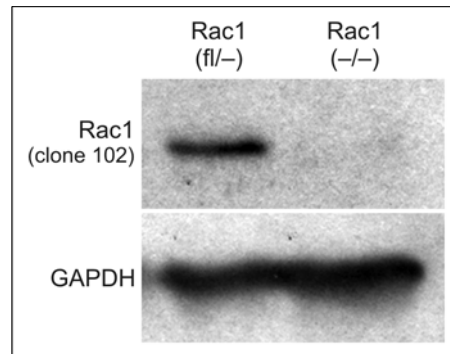


Fig. 3.43 *Rac1* (-/-) ES cells showed a complete loss of *Rac1* protein. Western blot analysis of protein lysates from control and mutant ES cells. GAPDH content was used as a loading control.

Normal ES cells form compact three-dimensional colonies when they are grown in standard culture conditions (2.5.1.1). In the undifferentiated state, the colonies have a smooth surface and borders between cells are not easily visible. As expected, no defects in the morphology of the *Rac1* (fl/-) ES cell colonies were observed (Fig. 3.44).

Rac1 (-/-) ES cell formed colonies; however, they were not as dense and smooth as the control ones. Mutant colonies resembled a raspberry and aggregates of cells were loosely attached to their surface (Fig. 3.44). Many cell clumps were detaching and floating in the medium.

The abnormal appearance of mutant ES cells suggested an adhesion defect in the absence of *Rac1*. However, it was not severe enough to prevent the expansion of *Rac1*-deficient ES cells in culture, as in case of mutant keratinocytes.

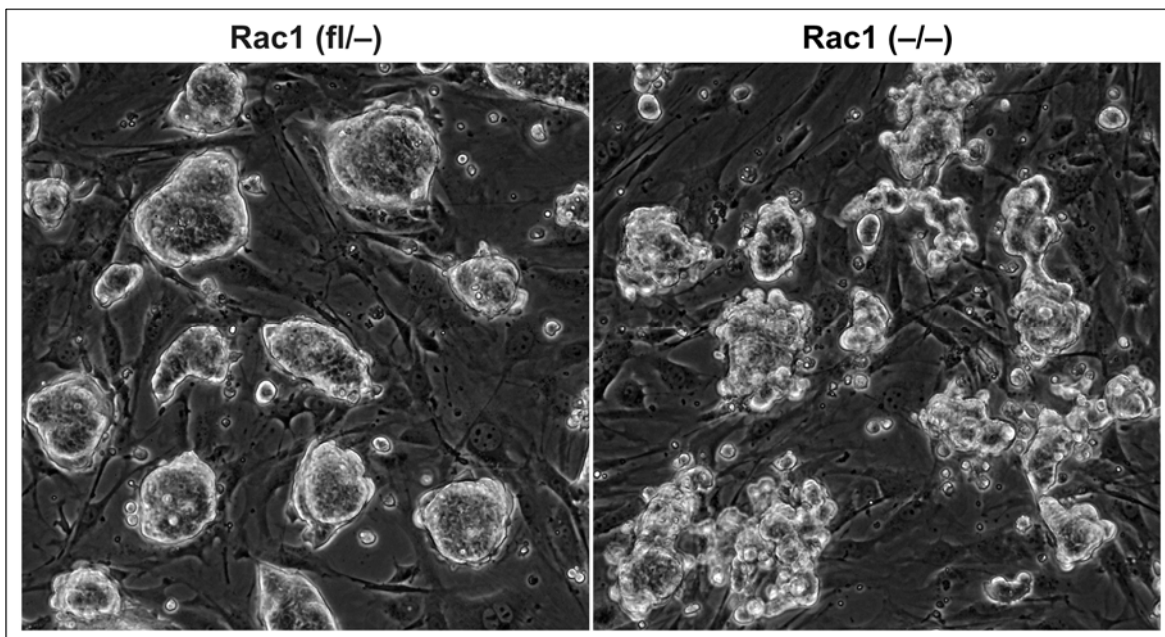


Fig. 3.44 Aberrant morphology of ES cell colonies in the absence of *Rac1*. Phase contrast pictures of control and mutant ES cells growing on a feeder cell layer. *Rac1* (-/-) colonies were less compact and, in contrast to a smooth-surfaced control colonies, showed a raspberry-like morphology.

3.8.2 Differentiation of Rac1-deficient ES cells into EBs

During normal development of EBs in suspension, small aggregates of ES cells become compacted balls of proliferating cells. Within 3 days, the outer layer of cells differentiates into the primitive endoderm. The subsequent transition into the secretory endoderm (mostly visceral) is followed by the deposition of ECM components on the inner (basal) side of the endoderm. Assembly of the BM induces transformation of underlying ES cells into the epiblast. The cells that are not in contact with the BM undergo apoptosis and the cavity is formed. The conversion of small clusters of ES cells into cystic EBs lasts normally 5-6 days in suspension culture (Li and Yurchenco, 2006).

Rac1 ($-/-$) and Rac1 (fl/−) ES cells were cultured in suspension for 7 days to promote differentiation into EBs (2.5.3.1). Control ES cells formed normal EBs with the well-developed endoderm, epiblast and cavity (Fig. 3.45).

Despite the observed adhesion defect, Rac1-deficient cells were able to aggregate and differentiate into EBs with all the normal components: the endoderm, the BM, the epiblast and the cavity. However, the epiblast was often abnormally thickened and some cells attached to the BM underwent cell death (Fig. 3.45, stars). That observation was analogous to the reported phenotype of Rac1-null murine embryos (Sugihara *et al.*, 1998), which showed the presence of apoptotic cells between the ectodermal and the endodermal layer. In addition, the initially normal endoderm often looked disorganized at the later stages of the mutant EBs' differentiation.

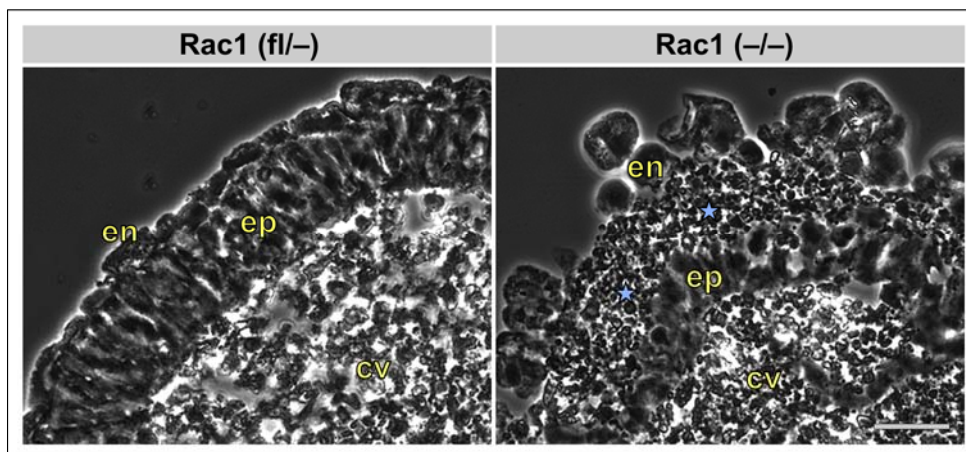


Fig. 3.45 Rac1-deficient EBs developed the endoderm (en) and the epiblast (ep), and formed the cavity (cv). Phase contrast pictures of control and mutant EBs taken after 7 days of differentiation in suspension. In the absence of Rac1, the epiblast (ep) was often thickened and the presence of dead cells, in proximity of the BM was observed (stars). Also the endoderm seemed to be affected by the lack of Rac1. Bar: 20 μ m.

3.8.3 Analysis of the epiblast polarization in the absence of Rac1

The BM is formed after 3-4 days of the EB's differentiation. Its presence induces profound changes in undifferentiated cells inside the EB. ES cells adjacent the BM differentiate into the primitive ectoderm. During this transition cells become polarized and change their polygonal shape into organized morphology of a pseudostratified columnar epithelium. The polarization is characterized by uniform translocation of specific proteins and organelles to the basal (e.g. integrins) or the apical side (e.g. Golgi complex) of the cell.

To analyse if Rac1-deficient ES cells can form the polarized epiblast, IF staining for actin (phalloidin), microtubule organizing centre (MTOC; pericentrin) and Golgi complex (GM130) was performed (2.5.3.2).

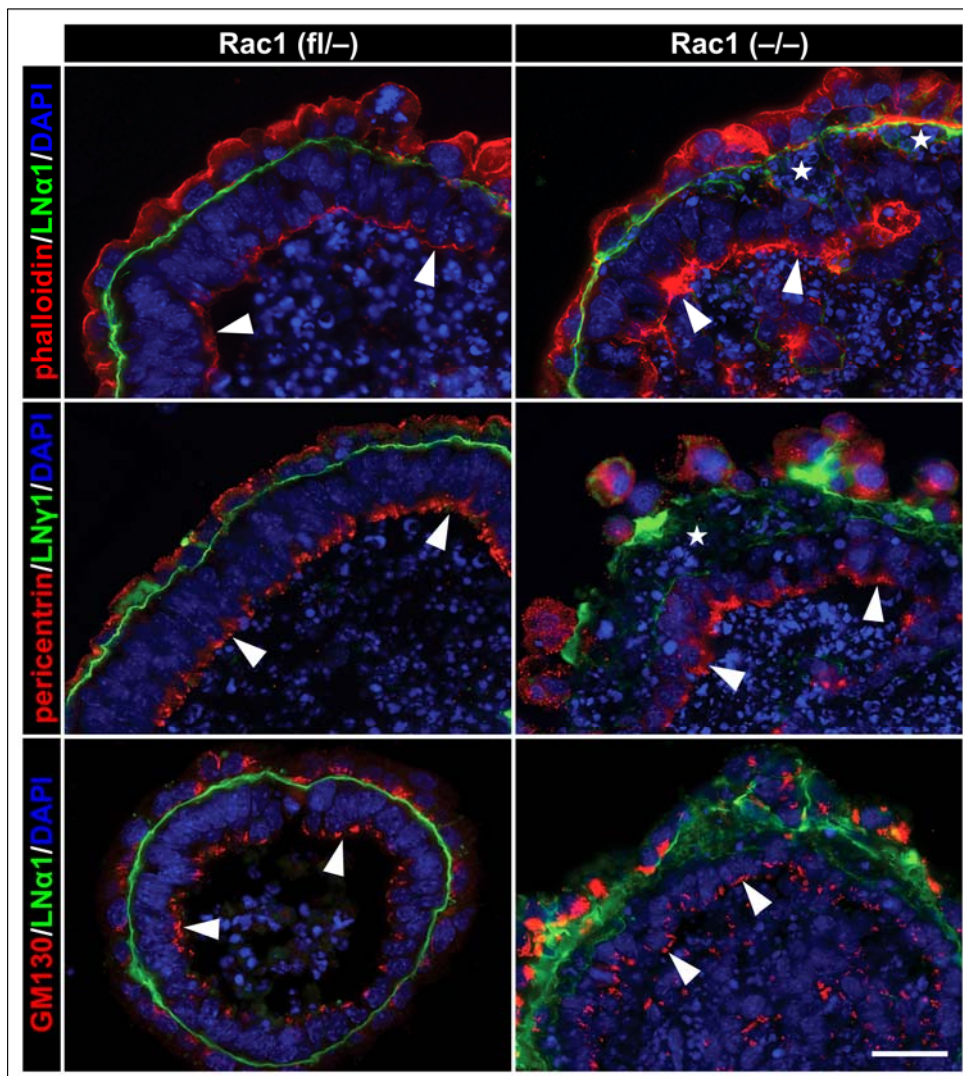


Fig. 3.46 Polarized distribution of F-actin, MTOC and Golgi apparatus in Rac1-deficient EBs. IF staining of control and mutant EBs was performed after 7 days of the differentiation. Antibodies against pericentrin and GM130 were used to visualize MTOC and Golgi complexes, respectively. F-actin was labeled with phalloidin (Alexa568). The BM was visualized with LN α 1 or LN γ 1, and nuclei with DAPI staining. Stars indicate dead epiblast cells observed at the BM in Rac1 (-/-) EBs. Bar: 20 μ m.

The distribution of tested marker proteins was comparable in control and mutant EBs (Fig. 3.47, arrowheads). That result was in agreement with *in vivo* data, which showed that Rac1-null embryos can develop an epiblast (Sugihara *et al.*, 1998). However, while the polarization of the primitive ectoderm seemed to be independent of the Rac1 presence, dying cells observed in the proximity of the BM (Fig. 3.47, stars) demonstrated a defect in the maintenance of Rac1-deficient epiblast cells. The defect might result from the inability of mutant cells to sustain the cell-ECM adhesion, but to explain the underlying mechanism further analysis is necessary.

After the epiblast is formed, remaining cells within the EB undergo a controlled apoptosis, which leads to the formation of the cystic EB with a large central lumen. Rac1-deficient EBs were able to form the cavity, however the process seemed to be not as efficient as in control EBs. After 7 days in suspension, when all inner cells of Rac1 (fl/−) EBs were clearly apoptotic and the formation of cavity was nearly completed (Fig. 3.47, DAPI), nucleated cells expressing analysed markers, were often detected inside the Rac1 (−/−) EBs. That observation suggested a defect in the regulation of apoptosis in the absence of Rac1, but more extensive studies are required to determine the exact role of Rac1 in the cavitation process.

3.8.4 Analysis of the cell-cell contacts formation in Rac1-deficient EBs

As shown earlier (3.3), cell-cell adhesion in the fully differentiated epidermis is not affected by the absence of Rac1. However, the *in vivo* system created in this study was not suitable for the analysis of the Rac1 role in the establishment of cell-cell contacts during the formation of the polarized epithelium. Therefore, the ability of Rac1-deficient cells to form adherens junctions during the differentiation of the epiblast was analysed in Rac1 (−/−) EBs. In addition, the establishment of tight junctions in the endoderm layer was investigated.

IF staining of control and mutant EBs (2.5.3.2) showed that E-cadherin was localized to the membrane and its concentration increased toward the apical side of the epiblast cells. The normal polarized distribution of the adherens junction-specific protein indicated that the formation of cell-cell contacts or their correct localization is not dependent on the presence of Rac1 (Fig. 3.47, E-cadherin).

In the developing endoderm of normal EBs, tight junctions between cells are formed close to the apical side. After 3 days of suspension culture, IF staining for ZO-1 (2.5.3.2), a component of tight junctions (Stevenson *et al.*, 1986), showed no differences in the presence or the localization of those cell-cell contacts between EBs differentiated from Rac1 (fl/−) and Rac1 (−/−) ES cells (Fig. 3.47, ZO-1).

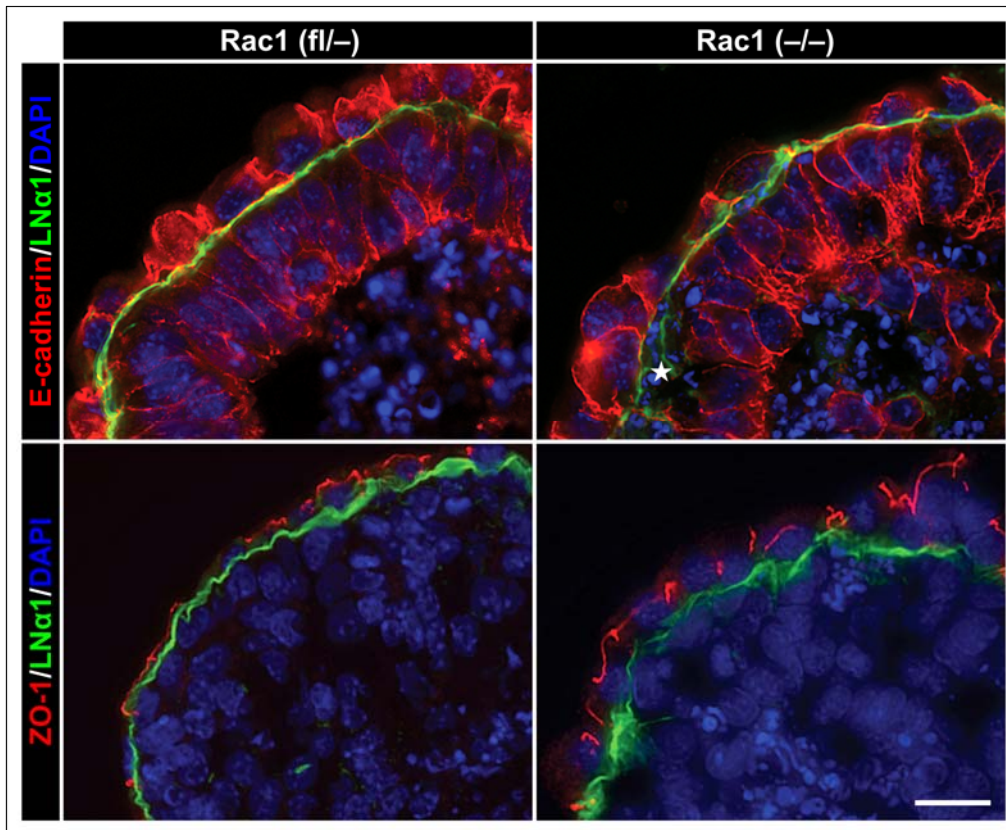


Fig. 3.47 Normal formation of polarized cell-cell junctions in *Rac1*-deficient EBs. IF staining of control and mutant EBs for E-cadherin and ZO-1 was performed after 7 and 3 days of differentiation, respectively. Normal cell membrane localization of E-cadherin was visualized in the absence of *Rac1* in both the endoderm and the epiblast, similar to control EBs. ZO-1 was present at the apical side of the endoderm in both control and mutant EBs. BM was visualized with LNA1 and nuclei with DAPI staining. Stars indicate dead epiblast cells observed at the BM in *Rac1* ($-/-$) EBs. Bar: 20 μ m.

In addition, the EM analysis of control and mutant EBs (2.5.3.2) showed a normal structure of tight junctions and their belt-like presence around the cell in the *Rac1*-deficient endoderm (Fig. 3.48), confirming that *Rac1* is not essential for the formation those cell-cell contacts.

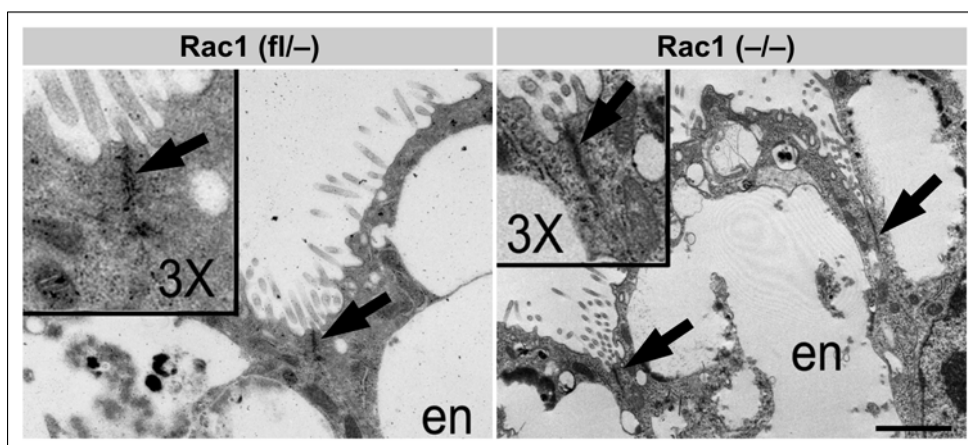


Fig. 3.48 Normal formation of tight junctions in the endoderm (en) of *Rac1*-deficient EBs. Ultrastructural analysis of control and mutant endoderm was performed after 3 days of EBs differentiation. The continuous (belt-like) presence of tight junctions was observed between endoderm cells in both *Rac1* ($fl/-$) and *Rac1* ($-/-$) EBs (arrows). Bar: 2 μ m.

However, while the endoderm developed from Rac1 ($-/-$) ES cells without obvious problems, the disorganized morphology of the outer cell layer, observed at later time points suggests, that the presence of Rac1 is not completely dispensable for its proper maintenance.

3.8.5 Analysis of the Rac1-deficient ES cells differentiation potential

Epiblast cells within long-term cultured EBs can differentiate into a variety of cell types representing derivatives of all three embryonic layers. The ability of Rac1 ($-/-$) ES cells to give rise to different cell lineages was analysed by allowing the progenitor cells developed within EBs to differentiate further.

After 6 days in suspension culture, EBs were transferred into standard cell-culture plates and cultured for 1-2 weeks more. After attaching, EBs continued to spontaneously differentiate and gave rise to various tissue-like structures. The presence of different cell types was confirmed with IF staining for selected tissue-specific markers (2.5.3.3).

After one week, some Rac1 (fl $-$) cells formed complex endothelial networks, visualized with PECAM staining. While Rac1 ($-/-$) ES cells were able to give rise to endothelial lineage, the formation of a vascular network seemed to be impaired (Fig. 3.49, PECAM).

Staining for E-cadherin showed well developed sheets of epithelial cells, which had differentiated from both control and Rac1-deficient ES cells. Again, cadherin dependent cell-cell contacts were seemingly not disturbed in the absence of Rac1. Interestingly, mutant cells were in general smaller than control ones (Fig. 3.49, E-cadherin).

Visualization of the actin cytoskeleton in single cells migrating out of the differentiating tissue-like structures, confirmed the difference in size between control and mutant cells. In addition, some of Rac1-deficient cells seemed to have an impaired actin cytoskeleton (Fig. 3.49, arrowheads). However, more experiments would be necessary to determine if that defect was random or cell type-specific.

Neurofilament-M-expressing cells developed from Rac1 (fl $-$) as well as from Rac1 ($-/-$) ES cells, showing that commitment to the neural cell type is not dependent on the presence of Rac1. However, the length of axon-like protrusions grown by Rac1-deficient cells seemed to be reduced (Fig. 3.49, Neurofilament-M).

In both cultures, rhythmically contracting cell formations were observed demonstrating an ability of Rac1-deficient ES cells to develop into functional cardiomyocytes (not shown).

These results are preliminary; however, they provide some insight into the differentiation capabilities of Rac1-deficient ES cells, pointing out directions for further studies, both *in vivo* and *in vitro*.

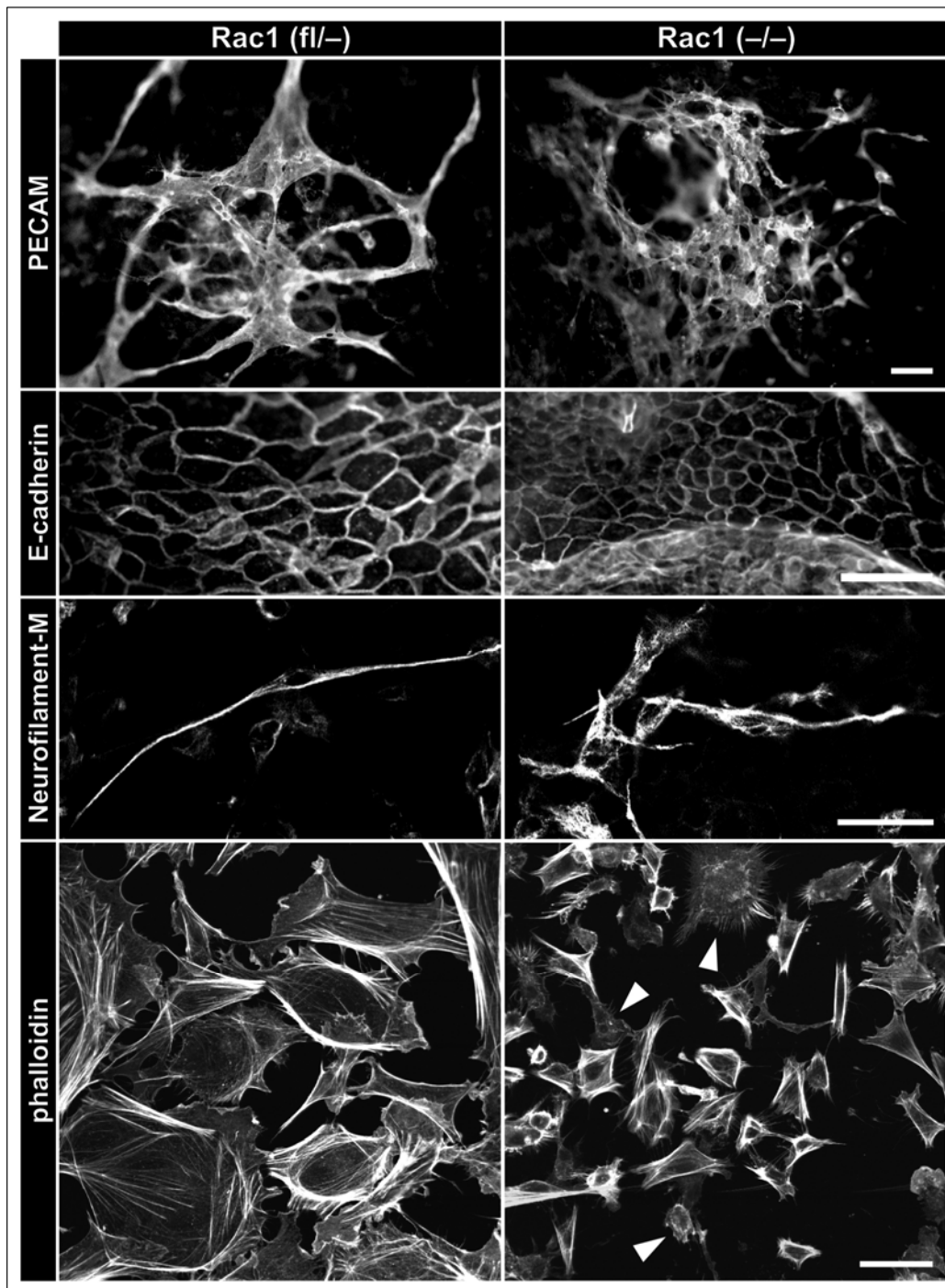


Fig. 3.49 Impaired formation of endothelial network and seemingly normal differentiation into epithelium and neural lineage in the absence of Rac1. After 6 days in suspension culture, Rac1 (fl/-) and Rac1 (-/-) EBs were plated on plastic and allowed to spontaneously differentiate for a week. To assess the differentiation potential of Rac1-deficient progenitor cells, IF staining was performed for proteins specific for endothelial, epithelial and neural cells: PECAM, E-cadherin and Neurofilament-M, respectively. Although PECAM-positive mutant cells were observed, formation of endothelial network seemed to be less efficient when compared to control cells. Rac1-deficient epithelial cells were forming normal E-cadherin-containing cell-cell contacts. Also, neural cells were developing in the absence of Rac1. However, the length of axon-like extensions seemed to be reduced. Mutant epithelial cells seemed smaller in comparison to control cells. Actin cytoskeleton staining, performed with fluorescently-labeled phalloidin, 2 weeks after the plating of EBs, showed a general reduction in cell size in the absence of Rac1 and an impaired actin cytoskeleton organization in some mutant cells (arrows). Bars: 50 μ m.

4 DISCUSSION

Rac1, a member of the Rho GTPase family, was first identified as one of the major regulators of the actin cytoskeleton (Ridley *et al.*, 1992). Over the last 15 years a multitude of studies described the involvement of Rac1 in a variety of cellular processes, including cell spreading, cell migration, cell-cell and cell-ECM adhesion, cell-cycle progression and gene expression (Jaffe and Hall, 2005). However, when this project was initiated, the knowledge of Rac1 function was based almost exclusively on *in vitro* studies using dominant-negative or constitutively active forms of the protein. Although mutant forms are very useful tools, they might influence the function of other members of the Rho family or cause unspecific effects due to overexpression and mislocalized activity within the cell. Also, cell culture conditions do not reflect the complexity of the *in vivo* situation.

At that time, only one study explored the function of Rac1 *in vivo* by generation and analysis of mice with a constitutive ablation of the *rac1* gene (Sugihara *et al.*, 1998), which resulted in the embryonic lethality at the onset of gastrulation (around day 8.5), thus demonstrating the essential role of Rac1 in the early murine development.

In order to circumvent the embryonic lethality effect, genetically modified mice allowing for the deletion of the *rac1* gene in a tissue- and time-specific manner, were generated in this study. Since *in vitro* studies suggested a crucial role of Rac1 in the formation and maintenance of cell-cell contacts between epithelial cells, mice with a keratinocyte-specific deletion of the *rac1* gene were generated and analysed.

4.1 The absence of Rac1 leads to the HF degeneration

The most obvious consequence of the *rac1* gene deletion in the murine epidermis was an almost complete loss of fur (3.1.3) caused by an impaired growth and progressive deterioration of the HFs. While the morphology of HFs shortly after birth was not obviously affected by the absence of Rac1, within 2 weeks the lower parts of HFs became increasingly distorted and lost their integrity (3.2.1), which was accompanied by the loss of expression of epithelial and HF-specific markers in those regions (3.2.2). Changes in the differentiation state of cells in the lower parts of HFs were followed by the infiltration of macrophages, which removed the non-permanent parts of HFs (3.2.3). No reconstitution of anagen HFs was observed afterwards. However, infundibula, SGs and most likely bulge regions were preserved throughout the whole

life span of mutant mice.

It is interesting to note, that, although Rac1 protein was clearly lost in the epidermis of *rac1^{fl/fl},cre* mice at least at day 3 after birth, no obvious changes in the HF morphology were visible until later stages of the morphogenesis, indicating that Rac1 is not crucial for the downward growth of the developing HF as well as for the initial differentiation of ORS, IRS and HS. However, the subsequent loss of HF layer-specific markers in the non-permanent part of the HF shows that Rac1 is required for the maintenance of HF keratinocytes in the differentiated state. The loss of HF-identity most likely reflects changes in gene expression, which could be either a direct result of the absence of Rac1 signalling or an indirect consequence of the loss of cell-cell and cell-ECM adhesion between the Rac1-deficient cells.

The direct involvement of Rac1 in the regulation of gene expression was demonstrated before in cell culture experiments. Rac1 was shown to act as a potent stimulator of MAPK signalling cascades by activating JNK and p38 (Coso *et al.*, 1995; Minden *et al.*, 1995). Activated JNK translocates to the nucleus, where it phosphorylates transcription factors such as c-Jun, while p38 is known to activate both transcription factors (e.g. ATF-2) and other kinases implicated in the regulation of gene expression (e.g. MAPKAP kinase 2) (Gupta *et al.*, 1995).

Rac1 was also implicated in the integrin-dependent activation of NF- κ B signalling pathway (Reyes-Reyes *et al.*, 2001), which was previously shown to play an important role in the HF morphogenesis (Schmidt-Ullrich *et al.*, 2001). In unstimulated cells, NF- κ B is sequestered in the cytoplasm by binding to members of the I κ B family. Upon activation, I κ B becomes degraded and NF- κ B translocates to the nucleus, where it can induce the transcription of many target genes.

Although no significant differences in the phosphorylation levels of JNK and p38 as well as no changes in the amount of I κ B- α were detected in epidermal lysates from *rac1^{fl/fl},cre* mice (3.4.2), it is possible that Rac1 plays a role in the activation of these signalling pathways specifically in HF keratinocytes. Such differences would most likely escape detection in whole epidermal lysates, where contribution of HF cells is rather low. The activation of p38 or JNK signalling pathways in mutant HFs could be analysed in more detail by IF staining of skin sections with antibodies specifically recognizing phosphorylated forms of these proteins. The activation of NF- κ B signalling in the absence of Rac1 could be further studied by crossing *rac1^{fl/fl},cre* mice with NF- κ B reporter mice (Schmidt-Ullrich *et al.*, 1996).

The lack of Rac1 could also indirectly influence the HF-specific gene expression by affecting the cell-cell and cell-ECM adhesion. This notion is supported by the observation that the loss of epithelial-specific markers in the absence of Rac1 seemed to be preceded by

morphological defects (Fig. 3.10, Fig. 3.19) and the loss of cell polarity (Fig. 3.18).

Although no obvious defects in the formation of cell-cell or cell-ECM contacts were observed in the epidermis of *rac1^{fl/fl},cre* mice (3.3), it is possible that Rac1 is more critical for their maintenance in the HF. A more detailed ultrastructural analysis of cell-cell contacts in the lower parts of HFs would be certainly helpful to further address this point.

During formation of the IRS, “Flügelzellen” from the Huxley layer of the IRS penetrate through the lower, less differentiated part of the Henle layer and come in contact with CL keratinocytes in a process apparently dependent on the formation of lamellipodia (Langbein *et al.*, 2003). Loss of Rac1 might impair this migration, thus contributing to the malformation of HFs during morphogenesis.

The exact molecular mechanism causing the infiltration of macrophages is not clear. Since no increase in apoptosis was observed in the lower parts of mutant HFs (Fig. 3.23), it is possible that the alterations of gene expression in Rac1-deficient HF keratinocytes lead to the secretion of macrophage attracting substances. This possibility could be investigated using an anti-inflammatory/immunosuppressive drug, such as dexamethasone, which would allow to determine if production of inflammatory cytokines and chemokines is involved in the skin inflammation of *rac1^{fl/fl},cre* mice. If successful, blocking of macrophage infiltration would also allow for a more detailed analysis of changes in the HF morphology.

Macrophage mediated removal of HFs is sometimes observed under normal conditions (Eichmuller *et al.*, 1998). It is possible that Rac1 is involved in the regulation of this process and its absence leads to an abnormal induction of such a programmed organ deletion.

The lack of the HF re-growth observed after the removal of the non-permanent parts of HFs can have different reasons. It is possible that the Rac1-mediated signalling plays an important role in the activation of bulge stem cells, which is necessary for the initiation of anagen (Stenn and Paus, 2001; Blanpain and Fuchs, 2006). Alternatively, the severe deterioration of the HFs and the lack of a proper involution phase (catagen), which normally leads to the retraction of the DP within the close proximity of the bulge, might have resulted in a separation of the DP fibroblasts from the HFs. Since anagen is induced by the crosstalk between DP cells and HF stem cells that would result in the inability of Rac1-deficient HFs to cycle.

4.2 Epidermis maintenance does not depend on the presence of Rac1

In contrast to the severe defect observed in the HFs, *rac1^{fl/fl},cre* mice showed no obvious aberrations of the epidermal morphology (3.3). Polarization, proliferation and terminal differentiation of epidermal keratinocytes were normal, as well as the formation of adherens junctions, desmosomes and hemidesmosomes. Also, the deposition of the BM was not affected in the absence of Rac1. A slight increase in the intercellular distance, detected by ultrastructural analysis between some basal keratinocytes, had no noticeable consequences for the integrity of the Rac1-deficient epidermis, which was maintained throughout the whole life span of *rac1^{fl/fl},cre* mice.

Those observations are surprising, as they stand in contrast to previous reports, which showed an essential role of Rac1 in the formation and maintenance of cadherin-dependent cell-cell contacts between epithelial cells *in vitro* (Braga *et al.*, 1997; Braga *et al.*, 1999) (1.3.1). Interestingly, it was also reported that the presence of DN-Rac1 disrupted cell-cell adhesion only in keratinocytes but not in endothelial cells or fibroblasts further indicating that Rac1 activity is especially important in epithelial cells (Braga *et al.*, 2000).

One possible explanation for the lack of defects after inactivation of the *rac1* gene could be that the absence of Rac1 was compensated by other members of the Rac family. However, Rac2 as well as Rac3 were hardly or not at all detectable in epidermal lysates from both control and *rac1^{fl/fl},cre* mice (Fig. 3.32). In addition, the expression levels of RhoG mRNA were not increased in the mutant epidermis (Fig. 3.33). Although, due to the unavailability of a RhoG antibody, it could not be excluded, that the activation of RhoG was increased, it seems unlikely that this rather distinct family member could fully compensate for the loss of Rac1.

The possibility of compensation by other closely related members of the Rho GTPase family was also analysed, as at least some of them have been shown to be involved in the maintenance of the epidermis (Wu *et al.*, 2006). However, both expression and activation levels of Cdc42 and RhoA were not significantly altered in epidermal lysates of *rac1^{fl/fl},cre* mice (Fig. 3.31).

While the compensation by other proteins can not be excluded at this point, these results show that most likely candidates are not involved.

Although these data do not rule out the involvement of Rac1 in the regulation of cell-cell contact formation and maintenance between keratinocytes *in vitro*, they clearly show that Rac1 is not essential for these processes *in vivo* and is dispensable for maintenance of epidermal homeostasis in physiological conditions. Thus, these results underline the importance of using *in*

in vivo models for identifying biologically relevant functions of proteins.

4.3 Wound healing is impaired in the absence of Rac1

Although the loss of Rac1 in keratinocytes had surprisingly little effect on epidermal homeostasis under physiological conditions, it resulted in a severe impairment of the epidermal response to the pathological situation caused by a skin injury (3.5). Wound closure was significantly less efficient in the absence of Rac1. Mutant keratinocytes showed an impaired migration into the wounded area as well as a reduced proliferation resulting in a slower growth of the neo-epidermis. Those defects were analogous to the *in vitro* phenotype of Rac1-deficient fibroblasts, which show decreased proliferation, impaired directed migration and wound closure (Vidali *et al.*, 2006).

While the reduced proliferation seemed to be caused by an impaired activation of the MAPK/ERK signalling cascade (Tschardt *et al.*, 2007), which is known to induce G1/S cell cycle progression (Roux and Blenis, 2004), the loss of Rac1 could affect cell migration in several ways. Because Rac1 was shown to regulate the formation of focal complexes (Rottner *et al.*, 1999), it is possible that the absence of Rac1 in migrating keratinocytes impairs the establishment of new cell-ECM contacts in the leading edge. The loss of Rac1 could also inhibit the formation of membrane protrusions as it was demonstrated in Rac1-deficient fibroblasts *in vitro* (Vidali *et al.*, 2006). In addition, the RhoA-dependent actin/myosin contractility, which is important for cell migration, could be reduced in the absence of Rac1.

Furthermore, Rac1 could be important for the recruitment of bulge stem cells during re-epithelialization. It was shown that, while bulge stem cells are not involved in epidermal homeostasis, they are mobilized during epidermal wound healing (Ito *et al.*, 2005). In addition to influencing the migration of progenitor cells from the bulge into the wounded area, Rac1 might play a role in the activation of bulge stem cells. In order to investigate the ability of Rac1-deficient bulge stem cells to contribute to the wound closure, *rac1^{fl/fl},cre* mice could be intercrossed with reporter mice allowing for the visualization of bulge stem cell-derived keratinocytes, which were described previously (Morris *et al.*, 2004).

Taken together, the data presented in this thesis show that Rac1 plays an important role during the epithelial wound closure *in vivo* by regulating proliferation and migration of epidermal keratinocytes.

4.4 Severe spreading defect leads to death of Rac1-deficient primary keratinocytes *in vitro*

An interesting finding of this study is that, in contrast to the rather mild phenotype observed *in vivo*, deletion of the *rac1* gene in keratinocytes has severe consequences *in vitro*. Although Rac1-deficient primary keratinocytes displayed only a mild adhesion defect, they were not able to spread and failed to form lamellipodia. Finally, almost all Rac1-deficient cells rounded up and detached. Mutant cells, which remained attached, could form focal contacts but failed to develop larger focal adhesions, most likely because of the strongly impaired actin cytoskeleton. The fact that neither apoptosis was increased nor the differentiation state of isolated keratinocytes was altered indicates that the cell detachment was caused primarily by the inability of Rac1-deficient cells to spread.

While not reflecting the *in vivo* situation, those defects resembled *in vitro* phenotypes observed in other cell types after inactivation of the *rac1* gene. The absence of Rac1 in murine embryonic fibroblasts causes impaired spreading as well as defective focal adhesion and stress fibre formation (Guo *et al.*, 2006; Vidali *et al.*, 2006). Rac1-deficient macrophages display dramatic cell shape changes and impaired podosome assembly (Wells *et al.*, 2004; Wheeler *et al.*, 2006). Also, epiblast cells isolated from Rac1-deficient embryos show spreading and adhesion defect (Sugihara *et al.*, 1998). Therefore, there seems to be no doubt that Rac1 is indeed crucial for the regulation of the actin cytoskeleton, cell spreading and the formation of integrin-based cell-ECM adhesions in different cell types *in vitro*.

However, the dramatic difference between the consequences of the *rac1* gene deletion in keratinocytes *in vivo* and *in vitro* demonstrates that the results obtained from studies of *in vitro* model systems have to be considered carefully and can not be simply used to predict the function of a given protein *in vivo*.

4.5 Discrepancies between epidermal phenotypes resulting from the lack of Rac1

While the study described in this thesis was ongoing, another group reported the analysis of mice with a keratinocyte-restricted deletion of the *rac1* gene (Benitah *et al.*, 2005). The loss of Rac1 was induced locally in the skin of adult mice and resulted in severe epidermal defects. Those mice displayed transient hyperproliferation of epidermal cells, which was followed by a progressive disorganization of the basal layer and, finally, a complete loss of epidermal keratinocytes. All mutant mice died shortly afterwards. The severe defects were attributed to the

increased expression of c-Myc, which caused an enhanced terminal differentiation of basal keratinocytes leading to the depletion of the epidermal stem cell compartment (Benitah *et al.*, 2005). That phenotype is dramatically different from the data obtained in this study, which show that the Rac1-deficient epidermis was maintained even in 2-year-old mice and that the expression of c-Myc was not altered in the absence of Rac1. The lack of epidermal keratinocytes deterioration in *rac1^{fl/fl},cre* mice, shows that the stem cell renewal was not compromised.

The simplest explanation for the contradictory results would be that Benitah and co-authors created a complete knockout, while some functional Rac1 protein was left in the mutant mice described here. The other group used mice, where the *rac1* gene was inactivated by deletion of exon 1 (Glogauer *et al.*, 2003), while in this study exon 3 was targeted. The latter strategy might theoretically result in a synthesis of a partial Rac1 protein, consisting of amino acids encoded by exon 1 and exon 2 (3.1). However, no evidence for the presence of such a polypeptide was provided by Western blot analysis performed with two different monoclonal antibodies (Fig. 3.5). In addition, it is extremely unlikely that such a short protein, which can not bind nucleotides or interact with effector proteins, could functionally replace full-length Rac1. It should be also noted, that the phenotype of Rac1-deficient EBs generated in this study closely reflects the defects of Rac1-null embryos, demonstrating that deletion of exon 3 leads to a complete absence of functional Rac1 protein.

Another explanation for the contrasting results could be the different time point of Rac1 deletion. While in the *rac1^{fl/fl},cre* mice the deletion of the *rac1* gene was endogenously activated during embryogenesis by Cre recombinase expressed under the control of K5 promoter, Benitah and co-authors induced the gene deletion in adult mice by application of 4-hydroxy-tamoxifen (4OHT), which activated the Cre-estrogen receptor fusion protein expressed under the control of K14 promoter (Vasioukhin *et al.*, 1999). It is possible, that the deletion of Rac1 during embryogenesis allows for a compensatory response, such as upregulation of other Rho GTPases, which can not be initiated in the adult tissue. While, the most likely candidates such as Rac2 and Rac3 or Cdc42 and RhoA seem to be not involved, as discussed above (4.2), compensatory upregulation of other signalling molecules can not be excluded.

Different genetic backgrounds of the mouse strains used for the analysis in these studies could also contribute to the observed differences. In epidermal growth factor receptor-deficient mice, for example, the phenotype varies from placental defects to postnatal defects in different tissues depending on the strain of analysed mice (Sibilia *et al.*, 1998).

Finally, it is possible that differences between epidermal phenotypes resulted from unspecific effects related to the 4OHT-treatment, which were more severe in the Rac1-deficient

epidermis. This notion is supported by the observation that the application of 4OHT/acetone to the skin of *rac1^{fl/fl},cre* mice caused a transient hyperthickening of the Rac1-deficient epidermis (Fig. 3.36), which was similar to the initial phenotype reported by Benitah and co-authors (Benitah *et al.*, 2005), while having only minor effect on the control epidermis. While the later defects described in that study were not observed, indicating that other factors also play a role, these data show that the 4OHT-treatment is not neutral and could have contributed to observed differences.

Altogether, the data of this study clearly demonstrate that the presence of Rac1 is not essential for stem cell maintenance in the epidermis. This conclusion is supported by a recent publication, which showed that transgenic mice expressing DN-Rac1 in basal keratinocytes do not display any epidermal defects under the physiological conditions as well (Tschardt *et al.*, 2007).

4.6 The role of Rac1 in embryonic development

Constitutive deletion of the *rac1* gene leads to early embryonic lethality at the onset of gastrulation. It was concluded that mutant embryos failed to develop the mesoderm due to migration and ECM-adhesion defects of epiblast cells (Sugihara *et al.*, 1998). In order to investigate the role of Rac1 during embryogenesis in more detail and to analyse its importance for the formation of cell-cell contacts during epithelial differentiation and polarization, EBs were generated from Rac1-deficient ES cells.

Similar to the *in vivo* situation, Rac1-deficient EBs were able to form the endoderm as well as the embryonic ectoderm (epiblast) (3.8.2). The differentiation and polarization of these cell layers as well as the deposition of the BM were rather normal in the absence of Rac1 (3.8.3). However, as *in vivo*, some mutant epiblast cells were apparently dying, despite their proximity to the BM, showing that the presence of Rac1 is important for sustained cell-ECM adhesion or adhesion-dependent cell survival. The role of Rac1 in the regulation of apoptosis and thus cavitation was also suggested by the observation that this process seemed to be less efficient in the absence of Rac1. As this *in vitro* model seems to closely replicate the *in vivo* phenotype resulting from the constitutive lack of Rac1, further studies of these defects should result in clarifying the exact functions of Rac1 in the early embryonic development.

It is also interesting to note that the absence of Rac1 had no apparent effect on the establishment of tight junctions as well as cadherin-based cell-cell contacts between differentiating cells (3.8.4), further indicating that the function of Rac1 in establishment of cell-cell adhesion is not as essential as suggested by previous *in vitro* studies.

Since the *in vivo* model generated in this study did not allow for the analysis of the role of Rac1 during the development of the epithelial cell lineage, Rac1-deficient EBs were further differentiated to investigate that process (3.8.5). The obtained results showed that epithelial sheets could form normally in the absence of Rac1. They demonstrated also that Rac1 is not required for the differentiation of ES cells into endothelial and neuronal cells as well as cardiomyocytes. As the formation of a vascular network seemed to be impaired, it could be interesting to analyse in the future the role of Rac1 during vasculogenesis *in vivo*.

4.7 Future prospects

The results of this study indicate that, while Rac1 is not essential for the epidermal homeostasis in physiological conditions, it seems to play an important role in pathological situations such as wound healing.

It is interesting to note, that Rac1 is frequently overexpressed in human breast cancers and oral squamous cell carcinomas (Fritz *et al.*, 1999; Liu *et al.*, 2004). In addition, it was shown that DN-Rac1 prevents Ras-induced transformation of fibroblasts (Qiu *et al.*, 1995) and decreases tumour formation and malignancy of a squamous cell carcinoma line (Kwei *et al.*, 2006). Moreover, mice lacking the Rac1-specific GEF Tiam1 are rather resistant to Ras-induced skin tumours (Malliri *et al.*, 2002). All these data suggest an involvement of Rac1 in tumorigenesis and tumour progression.

The mice lacking Rac1 in the epidermis, generated in this study, provide an excellent tool to study the role of Rac1 during chemically induced tumour formation and malignant conversion.

In addition, *rac1^{fl/fl}* mice, which were generated in this study, can be used to inactivate the *rac1* gene in other tissues by intercrossing them with different transgenic mice expressing the Cre recombinase in the cell type of interest.

They were already used to analyse the role of Rac1 in oligodendrocytes *in vivo*. Those experiments revealed that Rac1 regulates axon myelination in the central nervous system (Thurnherr *et al.*, 2006). In another study, the deletion of Rac1 in the peripheral nervous system demonstrated its role in radial sorting of axons in sciatic nerves (Benninger *et al.*, submitted manuscript).

Ongoing studies are investigating the role of Rac1 in other cell types, e.g. platelets or chondrocytes. They will no doubt contribute to the better understanding of the *in vivo* function of Rac1.

5 SUMMARY

Rac1 is a ubiquitously expressed member of the Rho family of small GTPases, which acts as a molecular switch by shuttling in a highly regulated manner between an active (GTP-bound) and an inactive (GDP-bound) state. Different signalling pathways, which involve integrins, growth factor receptors, cadherins as well as other Rho GTPases, can induce Rac1 activation. Only in the GTP-bound form, Rac1 can associate with different effector molecules to initiate cellular responses.

Initially described as an important regulator of the actin cytoskeleton, Rac1 was later found to be also involved in the modulation of other processes such as cell adhesion, proliferation, survival, differentiation and migration. In epithelial cells, Rac1 was shown to regulate the formation and maintenance of cadherin-dependent cell-cell contacts, which are essential for the establishment of the polarized cell morphology.

Before this project was initiated, almost all knowledge about the function of Rac1 was based on *in vitro* studies. As constitutive deletion of the murine *rac1* gene leads to early embryonic lethality, mice allowing for a conditional inactivation of the *rac1* gene were generated in this study to enable the analysis of the function of Rac1 in selected tissues. To investigate the role of Rac1 in the epidermis and hair follicles and to determine its function in the establishment and maintenance of cell-cell contacts between epithelial cells *in vivo*, mice with a keratinocyte-restricted ablation of the *rac1* gene were generated and analyzed.

The results obtained in this study showed that the absence of Rac1 in the murine epidermis leads to a progressive hair loss but surprisingly has no effect on the maintenance of the epidermis. The hair loss is caused by the inability of hair follicle keratinocytes to maintain their differentiation state, which leads to the phagocytic removal of the non-permanent parts of the hair follicles by infiltrating macrophages. In contrast, differentiation and proliferation of epidermal keratinocytes as well as the formation and maintenance of cell-cell and cell-matrix contacts, and the deposition of the basement membrane in the epidermis are not affected by the loss of Rac1. Biochemical analysis of epidermal lysates demonstrated that the absence of epidermal defects *in vivo* is not a result of compensatory upregulation of closely related members of the Rho family of GTPases, further indicating that the function of Rac1 in epithelial cells *in vivo* is limited. Also, the analysis of the formation of the embryoid bodies from Rac1-deficient embryonic stem cells showed that the presence of Rac1 is not required for the establishment of

cell-cell contacts during differentiation of the polarized primitive ectoderm and for the formation of epithelial sheets, supporting the conclusion that the function of Rac1 in the regulation of cell-cell adhesion between epithelial cells is dispensable.

However, the re-epithelialization after wounding was impaired in the mutant epidermis, demonstrating that Rac1 plays an important role in pathological conditions. The delayed wound closure in the absence of Rac1 is caused by impaired cell migration and proliferation of neo-epidermal keratinocytes.

Another interesting finding of this study was the observation that, in contrast to the steady state *in vivo* situation, isolated Rac1-deficient primary keratinocytes display severe defects in cell culture, which lead to their detachment from the matrix. While the initial adhesion is only mildly affected by the lack of Rac1, mutant keratinocytes are unable to spread, show an impaired organization of the actin cytoskeleton and fail to form mature focal adhesions.

The differences between *in vivo* and *in vitro* effects resulting from the inactivation of the *rac1* gene indicate that the function of Rac1 in epithelial cells depends on the complexity of the cellular system and emphasize the importance of performing *in vivo* studies to fully understand its role.

Taken together, the data presented in this study show that Rac1 plays an important role in the maintenance of hair follicles and during epidermal wound healing, but that it is not essential for the homeostasis of the epidermis in physiological conditions and for the formation and maintenance of cell-cell contacts between epithelial cells *in vivo*.

6 REFERENCES

- Aktories, K. and J.T. Barbieri** (2005). "Bacterial cytotoxins: targeting eukaryotic switches." *Nat. Rev. Microbiol.* 3: 397-410.
- Alonso, L. and E. Fuchs** (2003). "Stem cells of the skin epithelium." *Proc. Natl. Acad. Sci. U. S. A.* 100 Suppl 1: 11830-5.
- Alonso, L. and E. Fuchs** (2006). "The hair cycle." *J. Cell Sci.* 119: 391-93.
- Aspenstrom, P., A. Fransson and J. Saras** (2004). "Rho GTPases have diverse effects on the organization of the actin filament system." *Biochem. J.* 377: 327-37.
- Benitah, S.A., M. Frye, M. Glogauer and F.M. Watt** (2005). "Stem Cell Depletion Through Epidermal Deletion of Rac1." *Science* 309: 933-35.
- Benninger, Y., T. Thurnherr, S. Krause, X. Wu, A. Chrostek-Grashoff, K.-A. Nave, R.J.M. Franklin, D. Meijer, C. Brakebusch, U. Suter and J.B. Relvas** "Essential but different roles for cdc42 and rac1 in the regulation of Schwann cell biology and PNS myelination." submitted manuscript.
- Benvenuti, F., S. Hugues, M. Walmsley, S. Ruf, L. Fetler, M. Popoff, V.L. Tybulewicz and S. Amigorena** (2004). "Requirement of Rac1 and Rac2 expression by mature dendritic cells for T cell priming." *Science* 305: 1150-3.
- Betson, M., E. Lozano, J. Zhang and V.M. Braga** (2002). "Rac activation upon cell-cell contact formation is dependent on signaling from the epidermal growth factor receptor." *J. Biol. Chem.* 277: 36962-9.
- Bishop, A.L. and A. Hall** (2000). "Rho GTPases and their effector proteins." *Biochem. J.* 348: 241-55.
- Blanpain, C. and E. Fuchs** (2006). "Epidermal Stem Cells of the Skin." *Annu. Rev. Cell Dev. Biol.* 22: 339-73.
- Braga, V.M.** (2002). "Cell-cell adhesion and signalling." *Curr. Opin. Cell Biol.* 14: 546-56.
- Braga, V.M.M., L.M. Machesky, A. Hall and N.A. Hotchin** (1997). "The Small GTPases Rho and Rac Are Required for the Establishment of Cadherin-dependent Cell-Cell Contacts." *J. Cell Biol.* 137: 1421-31.
- Braga, V.M.M., A. Del Maschio, L. Machesky and E. Dejana** (1999). "Regulation of Cadherin Function by Rho and Rac: Modulation by Junction Maturation and Cellular Context." *Mol. Biol. Cell* 10: 9-22.
- Braga, V.M.M., M. Betson, X. Li and N. Lamarche-Vane** (2000). "Activation of the Small GTPase Rac Is Sufficient to Disrupt Cadherin-dependent Cell-Cell Adhesion in Normal Human Keratinocytes." *Mol. Biol. Cell* 11: 3703-21.
- Brakebusch, C., R. Grose, F. Quondamatteo, A. Ramirez, J.L. Jorcano, A. Pirro, M. Svensson, R. Herken, T. Sasaki, R. Timpl, S. Werner and R. Fassler** (2000). "Skin and hair follicle integrity is crucially dependent on beta 1 integrin expression on keratinocytes." *EMBO J.* 19: 3990-4003.
- Burridge, K. and K. Wennerberg** (2004). "Rho and Rac take center stage." *Cell* 116: 167-79.

- Byrne, C. and E. Fuchs** (1993). "Probing keratinocyte and differentiation specificity of the human K5 promoter in vitro and in transgenic mice." *Mol. Cell. Biol.* 13: 3176-90.
- Byrne, C. and M.J. Hardman** (2002). "Integumentary Structures". In *Mouse Development; Patterning, Morphogenesis and Organogenesis*, J. Rossant and P. Tam (eds). Academic Press. pp. 567-89.
- Caldelari, R., M.M. Suter, D. Baumann, A. de Bruin and E. Muller** (2000). "Long-Term Culture of Murine Epidermal Keratinocytes." *J. Invest. Dermatol.* 114: 1064-65.
- Candi, E., R. Schmidt and G. Melino** (2005). "The cornified envelope: a model of cell death in the skin." *Nat. Rev. Mol. Cell Biol.* 6: 328-40.
- Cherfils, J. and P. Chardin** (1999). "GEFs: structural basis for their activation of small GTP-binding proteins." *Trends Biochem. Sci.* 24: 306-11.
- Cho, Y.J., B. Zhang, V. Kaartinen, L. Haataja, I. de Curtis, J. Groffen and N. Heisterkamp** (2005). "Generation of rac3 null mutant mice: role of Rac3 in Bcr/Abl-caused lymphoblastic leukemia." *Mol. Cell. Biol.* 25: 5777-85.
- Clarke, S.** (1992). "Protein Isoprenylation and Methylation at Carboxyl-Terminal Cysteine Residues." *Annu. Rev. Biochem.* 61: 355-86.
- Corbetta, S., S. Gualdoni, C. Albertinazzi, S. Paris, L. Croci, G.G. Consalez and I. de Curtis** (2005). "Generation and characterization of Rac3 knockout mice." *Mol. Cell. Biol.* 25: 5763-76.
- Coso, O.A., M. Chiariello, J.C. Yu, H. Teramoto, P. Crespo, N. Xu, T. Miki and J.S. Gutkind** (1995). "The small GTP-binding proteins Rac1 and Cdc42 regulate the activity of the JNK/SAPK signaling pathway." *Cell* 81: 1137-46.
- Cote, J.F. and K. Vuori** (2002). "Identification of an evolutionarily conserved superfamily of DOCK180-related proteins with guanine nucleotide exchange activity." *J. Cell Sci.* 115: 4901-13.
- Cotsarelis, G., T.T. Sun and R.M. Lavker** (1990). "Label-retaining cells reside in the bulge area of pilosebaceous unit: implications for follicular stem cells, hair cycle, and skin carcinogenesis." *Cell* 61: 1329-37.
- Crocker, B.A., E. Handman, J.D. Hayball, T.M. Baldwin, V. Voigt, L.A. Cluse, F.C. Yang, D.A. Williams and A.W. Roberts** (2002). "Rac2-deficient mice display perturbed T-cell distribution and chemotaxis, but only minor abnormalities in T(H)1 responses." *Immunol. Cell Biol.* 80: 231-40.
- Delwel, G.O., F. Hogervorst, I. Kuikman, M. Paulsson, R. Timpl and A. Sonnenberg** (1993). "Expression and function of the cytoplasmic variants of the integrin alpha 6 subunit in transfected K562 cells. Activation-dependent adhesion and interaction with isoforms of laminin." *J. Biol. Chem.* 268: 25865-75.
- DerMardirossian, C. and G.M. Bokoch** (2005). "GDIs: central regulatory molecules in Rho GTPase activation." *Trends Cell Biol.* 15: 356-63.
- Diekmann, D., A. Abo, C. Johnston, A.W. Segal and A. Hall** (1994). "Interaction of Rac with p67phox and regulation of phagocytic NADPH oxidase activity." *Science* 265: 531-3.
- Dominey, A.M., X.J. Wang, L.E. King, Jr., L.B. Nanney, T.A. Gagne, K. Sellheyer, D.S. Bundman, M.A. Longley, J.A. Rothnagel, D.A. Greenhalgh and et al.** (1993). "Targeted overexpression of transforming growth factor alpha in the epidermis of transgenic mice elicits hyperplasia, hyperkeratosis, and spontaneous, squamous papillomas." *Cell Growth Differ.* 4: 1071-82.
- Dovas, A. and J.R. Couchman** (2005). "RhoGDI: multiple functions in the regulation of Rho family GTPase activities." *Biochem. J.* 390: 1-9.
- Dransart, E., B. Olofsson and J. Cherfils** (2005). "RhoGDIs revisited: novel roles in Rho regulation." *Traffic* 6: 957-66.

- Eichmuller, S., C. van der Veen, I. Moll, B. Hermes, U. Hofmann, S. Muller-Rover and R. Paus** (1998). "Clusters of Perifollicular Macrophages in Normal Murine Skin: Physiological Degeneration of Selected Hair Follicles by Programmed Organ Deletion." *J. Histochem. Cytochem.* 46: 361-70.
- Etienne-Manneville, S. and A. Hall** (2002). "Rho GTPases in cell biology." *Nature* 420: 629-35.
- Feig, L.A.** (1999). "Tools of the trade: use of dominant-inhibitory mutants of Ras-family GTPases." *Nat. Cell Biol.* 1: E25-7.
- Fenteany, G., P.A. Janmey and T.P. Stossel** (2000). "Signaling pathways and cell mechanics involved in wound closure by epithelial cell sheets." *Curr. Biol.* 10: 831-38.
- Fiegen, D., L.C. Haeusler, L. Blumenstein, U. Herbrand, R. Dvorsky, I.R. Vetter and M.R. Ahmadian** (2004). "Alternative splicing of Rac1 generates Rac1b, a self-activating GTPase." *J. Biol. Chem.* 279: 4743-49.
- Fransson, A., A. Ruusala and P. Aspenstrom** (2003). "Atypical Rho GTPases have roles in mitochondrial homeostasis and apoptosis." *J. Biol. Chem.* 278: 6495-502.
- Fritz, G., I. Just and B. Kaina** (1999). "Rho GTPases are over-expressed in human tumors." *Int. J. Cancer* 81: 682-7.
- Fuchs, E. and H. Green** (1980). "Changes in keratin gene expression during terminal differentiation of the keratinocyte." *Cell* 19: 1033-42.
- Fuchs, E. and D.W. Cleveland** (1998). "A structural scaffolding of intermediate filaments in health and disease." *Science* 279: 514-9.
- Fuchs, E. and S. Raghavan** (2002). "Getting under the skin of epidermal morphogenesis." *Nat. Rev. Genet.* 3: 199-209.
- Fukata, M. and K. Kaibuchi** (2001). "Rho-family GTPases in cadherin-mediated cell-cell adhesion." *Nat. Rev. Mol. Cell Biol.* 2: 887-97.
- Furuse, M., M. Hata, K. Furuse, Y. Yoshida, A. Haratake, Y. Sugitani, T. Noda, A. Kubo and S. Tsukita** (2002). "Claudin-based tight junctions are crucial for the mammalian epidermal barrier: a lesson from claudin-1-deficient mice." *J. Cell Biol.* 156: 1099-111.
- Gauthier-Rouviere, C., E. Vignal, M. Meriane, P. Roux, P. Montcourier and P. Fort** (1998). "RhoG GTPase controls a pathway that independently activates Rac1 and Cdc42Hs." *Mol. Biol. Cell* 9: 1379-94.
- Glogauer, M., C.C. Marchal, F. Zhu, A. Worku, B.E. Clausen, I. Foerster, P. Marks, G.P. Downey, M. Dinauer and D.J. Kwiatkowski** (2003). "Rac1 deletion in mouse neutrophils has selective effects on neutrophil functions." *J. Immunol.* 170: 5652-7.
- Green, K.J. and C.A. Gaudry** (2000). "Are desmosomes more than tethers for intermediate filaments?" *Nat. Rev. Mol. Cell Biol.* 1: 208-16.
- Gu, H., Y.-R. Zou and K. Rajewsky** (1993). "Independent control of immunoglobulin switch recombination at individual switch regions evidenced through Cre-loxP-mediated gene targeting." *Cell* 73: 1155-64.
- Gu, Y. and D.A. Williams** (2002). "RAC2 GTPase deficiency and myeloid cell dysfunction in human and mouse." *J. Pediatr. Hematol. Oncol.* 24: 791-4.
- Gu, Y., M.D. Filippi, J.A. Cancelas, J.E. Siefring, E.P. Williams, A.C. Jasti, C.E. Harris, A.W. Lee, R. Prabhakar, S.J. Atkinson, D.J. Kwiatkowski and D.A. Williams** (2003). "Hematopoietic cell regulation by Rac1 and Rac2 guanosine triphosphatases." *Science* 302: 445-9.
- Guo, F., M. Debidda, L. Yang, D.A. Williams and Y. Zheng** (2006). "Genetic Deletion of Rac1

- GTPase Reveals Its Critical Role in Actin Stress Fiber Formation and Focal Adhesion Complex Assembly." *J. Biol. Chem.* 281: 18652-59.
- Gupta, S., D. Campbell, B. Derijard and R.J. Davis** (1995). "Transcription factor ATF2 regulation by the JNK signal transduction pathway." *Science* 267: 389-93.
- Haataja, L., J. Groffen and N. Heisterkamp** (1997). "Characterization of RAC3, a novel member of the Rho family." *J. Biol. Chem.* 272: 20384-8.
- Hakoshima, T., T. Shimizu and R. Maesaki** (2003). "Structural basis of the Rho GTPase signaling." *J. Biochem. (Tokyo)*. 134: 327-31.
- Hardy, M.H.** (1992). "The secret life of the hair follicle." *Trends Genet.* 8: 55-61.
- Hirshberg, M., R.W. Stockley, G. Dodson and M.R. Webb** (1997). "The crystal structure of human rac1, a member of the rho-family complexed with a GTP analogue." *Nat. Struct. Biol.* 4: 147-52.
- Hordijk, P.L., J.P. ten Klooster, R.A. van der Kammen, F. Michiels, L.C. Oomen and J.G. Collard** (1997). "Inhibition of invasion of epithelial cells by Tiam1-Rac signaling." *Science* 278: 1464-6.
- Hotchin, N.A. and A. Hall** (1995). "The assembly of integrin adhesion complexes requires both extracellular matrix and intracellular rho/rac GTPases." *J. Cell Biol.* 131: 1857-65.
- Ito, M., K. Kizawa, K. Hamada and G. Cotsarelis** (2004). "Hair follicle stem cells in the lower bulge form the secondary germ, a biochemically distinct but functionally equivalent progenitor cell population, at the termination of catagen." *Differentiation* 72: 548-57.
- Ito, M., Y. Liu, Z. Yang, J. Nguyen, F. Liang, R.J. Morris and G. Cotsarelis** (2005). "Stem cells in the hair follicle bulge contribute to wound repair but not to homeostasis of the epidermis." *Nat. Med.* 11: 1351-54.
- Jaffe, A.B. and A. Hall** (2005). "Rho GTPases: Biochemistry and Biology." *Annu. Rev. Cell Dev. Biol.* 21: 247-69.
- Jordan, P., R. Brazao, M.G. Boavida, C. Gespach and E. Chastre** (1999). "Cloning of a novel human Rac1b splice variant with increased expression in colorectal tumors." *Oncogene* 18: 6835-9.
- Jou, T.-S., E.E. Schneeberger and W. James Nelson** (1998). "Structural and Functional Regulation of Tight Junctions by RhoA and Rac1 Small GTPases." *J. Cell Biol.* 142: 101-15.
- Kalinin, A.E., A.V. Kajava and P.M. Steinert** (2002). "Epithelial barrier function: assembly and structural features of the cornified cell envelope." *Bioessays* 24: 789-800.
- Katoh, H., H. Yasui, Y. Yamaguchi, J. Aoki, H. Fujita, K. Mori and M. Negishi** (2000). "Small GTPase RhoG is a key regulator for neurite outgrowth in PC12 cells." *Mol. Cell. Biol.* 20: 7378-87.
- Katoh, H. and M. Negishi** (2003). "RhoG activates Rac1 by direct interaction with the Dock180-binding protein Elmo." *Nature* 424: 461-4.
- Katoh, H., K. Hiramoto and M. Negishi** (2006). "Activation of Rac1 by RhoG regulates cell migration." *J. Cell Sci.* 119: 56-65.
- Kjoller, L. and A. Hall** (1999). "Signaling to Rho GTPases." *Exp. Cell Res.* 253: 166-79.
- Koster, M.I. and D.R. Roop** (2004). "Genetic pathways required for epidermal morphogenesis." *Eur. J. Cell Biol.* 83: 625-9.
- Kozma, R., S. Ahmed, A. Best and L. Lim** (1995). "The Ras-related protein Cdc42Hs and bradykinin promote formation of peripheral actin microspikes and filopodia in Swiss 3T3 fibroblasts." *Mol. Cell. Biol.* 15: 1942-52.
- Kwei, K.A., J.S. Finch, J. Ranger-Moore and G.T. Bowden** (2006). "The role of Rac1 in maintaining

- malignant phenotype of mouse skin tumor cells." *Cancer Lett.* 231: 326-38.
- Langbein, L., M.A. Rogers, H. Winter, S. Praetzel and J. Schweizer** (2001). "The Catalog of Human Hair Keratins. II. Expression of the six type II members in the hair follicle and the combined catalog of human type I and II keratins." *J. Biol. Chem.* 276: 35123-32.
- Langbein, L., M.A. Rogers, S. Praetzel, H. Winter and J. Schweizer** (2003). "K6irs1, K6irs2, K6irs3, and K6irs4 Represent the Inner-Root-Sheath-Specific Type II Epithelial Keratins of the Human Hair Follicle." *J. Invest. Dermatol.* 120: 512-22.
- Langbein, L. and J. Schweizer** (2005). "Keratins of the Human Hair Follicle." *Int. Rev. Cytol.* Volume 243: 1-78.
- Lauber, K., S.G. Blumenthal, M. Waibel and S. Wesselborg** (2004). "Clearance of Apoptotic Cells: Getting Rid of the Corpses." *Mol. Cell* 14: 277-87.
- Li, B., H. Yu, W.-p. Zheng, R. Voll, S. Na, A.W. Roberts, D.A. Williams, R.J. Davis, S. Ghosh and R.A. Flavell** (2000). "Role of the Guanosine Triphosphatase Rac2 in T Helper 1 Cell Differentiation." *Science* 288: 2219-22.
- Li, S. and P.D. Yurchenco** (2006). "Matrix assembly, cell polarization, and cell survival: analysis of peri-implantation development with cultured embryonic stem cells." *Methods Mol. Biol.* 329: 113-25.
- Li, X., X. Bu, B. Lu, H. Avraham, R.A. Flavell and B. Lim** (2002). "The hematopoiesis-specific GTP-binding protein RhoH is GTPase deficient and modulates activities of other Rho GTPases by an inhibitory function." *Mol. Cell. Biol.* 22: 1158-71.
- Liu, S.Y., C.Y. Yen, S.C. Yang, W.F. Chiang and K.W. Chang** (2004). "Overexpression of Rac-1 small GTPase binding protein in oral squamous cell carcinoma." *J. Oral Maxillofac. Surg.* 62: 702-7.
- Lu, M. and K.S. Ravichandran** (2006). "Dock180-ELMO cooperation in Rac activation." *Methods Enzymol.* 406: 388-402.
- Malliri, A., R.A. van der Kammen, K. Clark, M. van der Valk, F. Michiels and J.G. Collard** (2002). "Mice deficient in the Rac activator Tiam1 are resistant to Ras-induced skin tumours." *Nature* 417: 867-71.
- Matos, P., J.G. Collard and P. Jordan** (2003). "Tumor-related alternatively spliced Rac1b is not regulated by Rho-GDP dissociation inhibitors and exhibits selective downstream signaling." *J. Biol. Chem.* 278: 50442-8.
- McMillan, J.R., M. Akiyama and H. Shimizu** (2003). "Epidermal basement membrane zone components: ultrastructural distribution and molecular interactions." *J. Dermatol. Sci.* 31: 169-77.
- Mehrel, T., D. Hohl, J.A. Rothnagel, M.A. Longley, D. Bundman, C. Cheng, U. Lichti, M.E. Bisher, A.C. Steven, P.M. Steinert and et al.** (1990). "Identification of a major keratinocyte cell envelope protein, loricrin." *Cell* 61: 1103-12.
- Meller, N., M. Irani-Tehrani, W.B. Kiosses, M.A. Del Pozo and M.A. Schwartz** (2002). "Zizimin1, a novel Cdc42 activator, reveals a new GEF domain for Rho proteins." *Nat. Cell Biol.* 4: 639-47.
- Mertens, A.E.E., T.P. Rygiel, C. Olivo, R. van der Kammen and J.G. Collard** (2005). "The Rac activator Tiam1 controls tight junction biogenesis in keratinocytes through binding to and activation of the Par polarity complex." *J. Cell Biol.* 170: 1029-37.
- Millar, S.E.** (2002). "Molecular mechanisms regulating hair follicle development." *J. Invest. Dermatol.* 118: 216-25.
- Minden, A., A. Lin, F.X. Claret, A. Abo and M. Karin** (1995). "Selective activation of the JNK signaling cascade and c-Jun transcriptional activity by the small GTPases Rac and Cdc42Hs." *Cell* 81: 1147-57.

- Mira, J.P., V. Benard, J. Groffen, L.C. Sanders and U.G. Knaus** (2000). "Endogenous, hyperactive Rac3 controls proliferation of breast cancer cells by a p21-activated kinase-dependent pathway." *Proc. Natl. Acad. Sci. U. S. A.* 97: 185-9.
- Moon, S.Y. and Y. Zheng** (2003). "Rho GTPase-activating proteins in cell regulation." *Trends Cell Biol.* 13: 13-22.
- Morris, R.J., Y. Liu, L. Marles, Z. Yang, C. Trempus, S. Li, J.S. Lin, J.A. Sawicki and G. Cotsarelis** (2004). "Capturing and profiling adult hair follicle stem cells." *Nat. Biotechnol.* 22: 411-7.
- Muller-Rover, S., B. Handjiski, C. van der Veen, S. Eichmuller, K. Foitzik, I.A. McKay, K.S. Stenn and R. Paus** (2001). "A comprehensive guide for the accurate classification of murine hair follicles in distinct hair cycle stages." *J. Invest. Dermatol.* 117: 3-15.
- Nagy, A., J. Rossant, R. Nagy, W. Abramow-Newerly and J.C. Roder** (1993). "Derivation of Completely Cell Culture-Derived Mice from Early-Passage Embryonic Stem Cells." *Proc. Natl. Acad. Sci. U. S. A.* 90: 8424-28.
- Nakagawa, M., M. Fukata, M. Yamaga, N. Itoh and K. Kaibuchi** (2001). "Recruitment and activation of Rac1 by the formation of E-cadherin-mediated cell-cell adhesion sites." *J. Cell Sci.* 114: 1829-38.
- Nimmual, A.S., L.J. Taylor and D. Bar-Sagi** (2003). "Redox-dependent downregulation of Rho by Rac." *Nat. Cell Biol.* 5: 236-41.
- Nobes, C.D. and A. Hall** (1995). "Rho, rac, and cdc42 GTPases regulate the assembly of multimolecular focal complexes associated with actin stress fibers, lamellipodia, and filopodia." *Cell* 81: 53-62.
- Nobes, C.D. and A. Hall** (1999). "Rho GTPases control polarity, protrusion, and adhesion during cell movement." *J. Cell Biol.* 144: 1235-44.
- Noren, N.K., C.M. Niessen, B.M. Gumbiner and K. Burridge** (2001). "Cadherin engagement regulates Rho family GTPases." *J. Biol. Chem.* 276: 33305-8.
- O'Brien, L.E., T.-S. Jou, A.L. Pollack, Q. Zhang, S.H. Hansen, P. Yurchenco and K.E. Mostov** (2001). "Rac1 orientates epithelial apical polarity through effects on basolateral laminin assembly." *Nat. Cell Biol.* 3: 831-38.
- Olofsson, B.** (1999). "Rho guanine dissociation inhibitors: pivotal molecules in cellular signalling." *Cell. Signal.* 11: 545-54.
- Olson, M.F., A. Ashworth and A. Hall** (1995). "An essential role for Rho, Rac, and Cdc42 GTPases in cell cycle progression through G1." *Science* 269: 1270-2.
- Osoegawa, K., M. Tateno, P.Y. Woon, E. Frengen, A.G. Mammoser, J.J. Catanese, Y. Hayashizaki and P.J. de Jong** (2000). "Bacterial Artificial Chromosome Libraries for Mouse Sequencing and Functional Analysis." *Genome Res.* 10: 116-28.
- Paus, R., S. Muller-Rover, C. Van Der Veen, M. Maurer, S. Eichmuller, G. Ling, U. Hofmann, K. Foitzik, L. Mecklenburg and B. Handjiski** (1999). "A comprehensive guide for the recognition and classification of distinct stages of hair follicle morphogenesis." *J. Invest. Dermatol.* 113: 523-32.
- Perez-Moreno, M., C. Jamora and E. Fuchs** (2003). "Sticky business: orchestrating cellular signals at adherens junctions." *Cell* 112: 535-48.
- Perona, R., S. Montaner, L. Saniger, I. Sanchez-Perez, R. Bravo and J.C. Lacal** (1997). "Activation of the nuclear factor-kappaB by Rho, CDC42, and Rac-1 proteins." *Genes Dev.* 11: 463-75.
- Pinkus, H., T. Iwasaki and Y. Mishima** (1981). "Outer root sheath keratinization in anagen and catagen of the mammalian hair follicle. A seventh distinct type of keratinization in the hair follicle: trichilemmal keratinization." *J. Anat.* 133: 19-35.

-
- Potten, C.S.** (1975). "Epidermal transit times." *Br. J. Dermatol.* 93: 649-58.
- Price, L.S., J. Leng, M.A. Schwartz and G.M. Bokoch** (1998). "Activation of Rac and Cdc42 by Integrins Mediates Cell Spreading." *Mol. Biol. Cell* 9: 1863-71.
- Price, L.S., M. Langeslag, J.P.t. Klooster, P.L. Hordijk, K. Jalink and J.G. Collard** (2003). "Calcium Signaling Regulates Translocation and Activation of Rac." *J. Biol. Chem.* 278: 39413-21.
- Prieto-Sanchez, R.M. and X.R. Bustelo** (2003). "Structural basis for the signaling specificity of RhoG and Rac1 GTPases." *J. Biol. Chem.* 278: 37916-25.
- Qiu, R.G., J. Chen, D. Kirn, F. McCormick and M. Symons** (1995). "An essential role for Rac in Ras transformation." *Nature* 374: 457-9.
- Raftopoulou, M. and A. Hall** (2004). "Cell migration: Rho GTPases lead the way." *Dev. Biol.* 265: 23-32.
- Ramirez, A., A. Page, A. Gandarillas, J. Zanet, S. Pibre, M. Vidal, L. Tusell, A. Genesca, D.A. Whitaker, D.W. Melton and J.L. Jorcano** (2004). "A keratin K5Cre transgenic line appropriate for tissue-specific or generalized cre-mediated recombination." *Genesis* 39: 52-57.
- Reyes-Reyes, M., N. Mora, A. Zentella and C. Rosales** (2001). "Phosphatidylinositol 3-kinase mediates integrin-dependent NF-kappaB and MAPK activation through separate signaling pathways." *J. Cell Sci.* 114: 1579-89.
- Richardson, K.C., L. Jarett and E.H. Finke** (1960). "Embedding in epoxy resins for ultrathin sectioning in electron microscopy." *Stain Technol.* 35: 313-25.
- Ridley, A.J. and A. Hall** (1992). "The small GTP-binding protein rho regulates the assembly of focal adhesions and actin stress fibers in response to growth factors." *Cell* 70: 389-99.
- Ridley, A.J., H.F. Paterson, C.L. Johnston, D. Diekmann and A. Hall** (1992). "The small GTP-binding protein rac regulates growth factor-induced membrane ruffling." *Cell* 70: 401-10.
- Ridley, A.J.** (2004). "Rho proteins and cancer." *Breast Cancer Res. Treat.* 84: 13-9.
- Riento, K., R.M. Guasch, R. Garg, B. Jin and A.J. Ridley** (2003). "RhoE binds to ROCK I and inhibits downstream signaling." *Mol. Cell. Biol.* 23: 4219-29.
- Rivero, F., H. Dislich, G. Glockner and A.A. Noegel** (2001). "The Dictyostelium discoideum family of Rho-related proteins." *Nucleic Acids Res.* 29: 1068-79.
- Roberts, A.W., C. Kim, L. Zhen, J.B. Lowe, R. Kapur, B. Petryniak, A. Spaetti, J.D. Pollock, J.B. Borneo, G.B. Bradford, S.J. Atkinson, M.C. Dinauer and D.A. Williams** (1999). "Deficiency of the hematopoietic cell-specific Rho family GTPase Rac2 is characterized by abnormalities in neutrophil function and host defense." *Immunity* 10: 183-96.
- Rogers, G.E.** (2004). "Hair follicle differentiation and regulation." *Int. J. Dev. Biol.* 48: 163-70.
- Romero, M.R., J.M. Carroll and F.M. Watt** (1999). "Analysis of cultured keratinocytes from a transgenic mouse model of psoriasis: effects of suprabasal integrin expression on keratinocyte adhesion, proliferation and terminal differentiation." *Exp. Dermatol.* 8: 53-67.
- Rossmann, K.L., C.J. Der and J. Sodek** (2005). "GEF means go: turning on RHO GTPases with guanine nucleotide-exchange factors." *Nat. Rev. Mol. Cell Biol.* 6: 167-80.
- Rothnagel, J.A., T. Mehrel, W.W. Idler, D.R. Roop and P.M. Steinert** (1987). "The gene for mouse epidermal filaggrin precursor. Its partial characterization, expression, and sequence of a repeating filaggrin unit." *J. Biol. Chem.* 262: 15643-8.
- Rothnagel, J.A. and D.R. Roop** (1995). "Hair follicle companion layer: reacquainting an old friend." *J. Invest. Dermatol.* 104: 42S-43S.
-

- Rottner, K., A. Hall and J.V. Small** (1999). "Interplay between Rac and Rho in the control of substrate contact dynamics." *Curr. Biol.* 9: 640-8.
- Roux, P.P. and J. Blenis** (2004). "ERK and p38 MAPK-activated protein kinases: a family of protein kinases with diverse biological functions." *Microbiol. Mol. Biol. Rev.* 68: 320-44.
- Sahai, E. and C.J. Marshall** (2002). "RHO-GTPases and cancer." *Nat. Rev. Cancer* 2: 133-42.
- Sander, E.E., J.P. ten Klooster, S. van Delft, R.A. van der Kammen and J.G. Collard** (1999). "Rac downregulates Rho activity: reciprocal balance between both GTPases determines cellular morphology and migratory behavior." *J. Cell Biol.* 147: 1009-22.
- Sauer, B.** (1993). "Manipulation of transgenes by site-specific recombination: Use of cre recombinase." *Methods Enzymol.* 225: 890-900.
- Schmidt-Ullrich, R., S. Memet, A. Lilienbaum, J. Feuillard, M. Raphael and A. Israel** (1996). "NF-kappaB activity in transgenic mice: developmental regulation and tissue specificity." *Development* 122: 2117-28.
- Schmidt-Ullrich, R., T. Aebischer, J. Hulsken, W. Birchmeier, U. Klemm and C. Scheidereit** (2001). "Requirement of NF-kappaB/Rel for the development of hair follicles and other epidermal appendices." *Development* 128: 3843-53.
- Schmidt-Ullrich, R. and R. Paus** (2005). "Molecular principles of hair follicle induction and morphogenesis." *Bioessays* 27: 247-61.
- Schmidt, A. and A. Hall** (2002). "Guanine nucleotide exchange factors for Rho GTPases: turning on the switch." *Genes Dev.* 16: 1587-609.
- Schnelzer, A., D. Prechtel, U. Knaus, K. Dehne, M. Gerhard, H. Graeff, N. Harbeck, M. Schmitt and E. Lengyel** (2000). "Rac1 in human breast cancer: overexpression, mutation analysis, and characterization of a new isoform, Rac1b." *Oncogene* 19: 3013-20.
- Schwartz, M.** (2004). "Rho signalling at a glance." *J. Cell Sci.* 117: 5457-8.
- Sellheyer, K., J.R. Bickenbach, J.A. Rothnagel, D. Bundman, M.A. Longley, T. Krieg, N.S. Roche, A.B. Roberts and D.R. Roop** (1993). "Inhibition of Skin Development by Overexpression of Transforming Growth Factor {beta}1 in the Epidermis of Transgenic Mice." *Proc. Natl. Acad. Sci. U. S. A.* 90: 5237-41.
- Sibilia, M., J.P. Steinbach, L. Stingl, A. Aguzzi and E.F. Wagner** (1998). "A strain-independent postnatal neurodegeneration in mice lacking the EGF receptor." *EMBO J.* 17: 719-31.
- Sonnenberg, A., A.A. de Melker, A.M. Martinez de Velasco, H. Janssen, J. Calafat and C.M. Niessen** (1993). "Formation of hemidesmosomes in cells of a transformed murine mammary tumor cell line and mechanisms involved in adherence of these cells to laminin and kalinin." *J. Cell Sci.* 106: 1083-102.
- Stenn, K.S. and R. Paus** (2001). "Controls of hair follicle cycling." *Physiol. Rev.* 81: 449-94.
- Stevenson, B.R., J.D. Siliciano, M.S. Mooseker and D.A. Goodenough** (1986). "Identification of ZO-1: a high molecular weight polypeptide associated with the tight junction (zonula occludens) in a variety of epithelia." *J. Cell Biol.* 103: 755-66.
- Sugihara, K., N. Nakatsuji, K. Nakamura, K. Nakao, R. Hashimoto, H. Otani, H. Sakagami, H. Kondo, S. Nozawa, A. Aiba and M. Katsuki** (1998). "Rac1 is required for the formation of three germ layers during gastrulation." *Oncogene* 17: 3427-33.
- Takaishi, K., T. Sasaki, H. Kotani, H. Nishioka and Y. Takai** (1997). "Regulation of cell-cell adhesion by rac and rho small G proteins in MDCK cells." *J. Cell Biol.* 139: 1047-59.

-
- Talts, J.F., C. Brakebusch and F. Reinhard** (1999). "Integrin gene targeting." *Methods Mol. Biol.* 129: 153-87.
- Thurnherr, T., Y. Benninger, X. Wu, A. Chrostek, S.M. Krause, K.A. Nave, R.J. Franklin, C. Brakebusch, U. Suter and J.B. Relvas** (2006). "Cdc42 and Rac1 signaling are both required for and act synergistically in the correct formation of myelin sheaths in the CNS." *J. Neurosci.* 26: 10110-9.
- Tscharntke, M., R. Pofahl, A. Chrostek-Grashoff, N. Smyth, C. Niessen, C. Niemann, B. Hartwig, V. Herzog, H. Klein, T. Krieg, C. Brakebusch and I. Haase** (2007). "Impaired epidermal wound healing in vivo upon inhibition or deletion of Rac1." *J. Cell Sci.* in press.
- Tsubakimoto, K., K. Matsumoto, H. Abe, J. Ishii, M. Amano, K. Kaibuchi and T. Endo** (1999). "Small GTPase RhoD suppresses cell migration and cytokinesis." *Oncogene* 18: 2431-40.
- Tumbar, T., G. Guasch, V. Greco, C. Blanpain, W.E. Lowry, M. Rendl and E. Fuchs** (2004). "Defining the epithelial stem cell niche in skin." *Science* 303: 359-63.
- Ullmann, A., F. Jacob and J. Monod** (1967). "Characterization by in vitro complementation of a peptide corresponding to an operator-proximal segment of the beta-galactosidase structural gene of Escherichia coli." *J. Mol. Biol.* 24: 339-43.
- Van Aelst, L. and C. D'Souza-Schorey** (1997). "Rho GTPases and signaling networks." *Genes Dev.* 11: 2295-322.
- Van Aelst, L. and M. Symons** (2002). "Role of Rho family GTPases in epithelial morphogenesis." *Genes Dev.* 16: 1032-54.
- Vasioukhin, V., L. Degenstein, B. Wise and E. Fuchs** (1999). "The magical touch: Genome targeting in epidermal stem cells induced by tamoxifen application to mouse skin." *Proc. Natl. Acad. Sci. U. S. A.* 96: 8551-56.
- Vetter, I.R. and A. Wittinghofer** (2001). "The guanine nucleotide-binding switch in three dimensions." *Science* 294: 1299-304.
- Vidali, L., F. Chen, G. Cicchetti, Y. Ohta and D.J. Kwiatkowski** (2006). "Rac1-null Mouse Embryonic Fibroblasts Are Motile and Respond to Platelet-derived Growth Factor." *Mol. Biol. Cell* 17: 2377-90.
- Vincent, S., P. Jeanteur and P. Fort** (1992). "Growth-regulated expression of rhoG, a new member of the ras homolog gene family." *Mol. Cell. Biol.* 12: 3138-48.
- Walmsley, M.J., S.K. Ooi, L.F. Reynolds, S.H. Smith, S. Ruf, A. Mathiot, L. Vanes, D.A. Williams, M.P. Cancro and V.L. Tybulewicz** (2003). "Critical roles for Rac1 and Rac2 GTPases in B cell development and signaling." *Science* 302: 459-62.
- Watt, F.M.** (2002). "Role of integrins in regulating epidermal adhesion, growth and differentiation." *EMBO J.* 21: 3919-26.
- Wells, C.M., M. Walmsley, S. Ooi, V. Tybulewicz and A.J. Ridley** (2004). "Rac1-deficient macrophages exhibit defects in cell spreading and membrane ruffling but not migration." *J. Cell Sci.* 117: 1259-68.
- Wennerberg, K., S.M. Ellerbroek, R.Y. Liu, A.E. Karnoub, K. Burridge and C.J. Der** (2002). "RhoG signals in parallel with Rac1 and Cdc42." *J. Biol. Chem.* 277: 47810-7.
- Wennerberg, K., M.A. Forget, S.M. Ellerbroek, W.T. Arthur, K. Burridge, J. Settleman, C.J. Der and S.H. Hansen** (2003). "Rnd proteins function as RhoA antagonists by activating p190 RhoGAP." *Curr. Biol.* 13: 1106-15.
- Wennerberg, K. and C.J. Der** (2004). "Rho-family GTPases: it's not only Rac and Rho (and I like it)." *J. Cell Sci.* 117: 1301-12.
-

- Wheeler, A.P., C.M. Wells, S.D. Smith, F.M. Vega, R.B. Henderson, V.L. Tybulewicz and A.J. Ridley** (2006). "Rac1 and Rac2 regulate macrophage morphology but are not essential for migration." *J. Cell Sci.* 119: 2749-57.
- Wherlock, M. and H. Mellor** (2002). "The Rho GTPase family: a Racs to Wrchs story." *J. Cell Sci.* 115: 239-40.
- Wu, X., F. Quondamatteo, T. Lefever, A. Czuchra, H. Meyer, A. Chrostek, R. Paus, L. Langbein and C. Brakebusch** (2006). "Cdc42 controls progenitor cell differentiation and beta-catenin turnover in skin." *Genes Dev.* 20: 571-85.
- Yeaman, C., K.K. Grindstaff and W.J. Nelson** (1999). "New perspectives on mechanisms involved in generating epithelial cell polarity." *Physiol. Rev.* 79: 73-98.
- Zhang, F.L. and P.J. Casey** (1996). "Protein prenylation: molecular mechanisms and functional consequences." *Annu. Rev. Biochem.* 65: 241-69.

7 APPENDIX CD

Supplementary CD contains two time-lapse video microscopy movies (2.5.4.6) which are referred to in chapter: *Severe spreading defect of Rac1 deficient keratinocytes* (3.7.4). It can be found in the envelope glued to the inside back cover.

Movies are provided in two different formats and can be viewed using standard media players, e.g. Windows Media Player (*.avi) or QuickTime (*.mov).

Movie 1. Time lapse microscopy of primary control keratinocytes.

Cells isolated from an adult control mouse were seeded on collagen I/fibronectin (Col/FN) coated plastic and recorded for 42 h. Adherent keratinocytes spread and remained attached.

Pictures were taken every 20 min. Display rate: 5 frames/s. Time format: day/hour/minute. Bar: 100 μm .

Movie 2. Time lapse microscopy of primary Rac1-deficient keratinocytes.

Cells isolated from an adult mutant mouse were seeded on collagen I/fibronectin (Col/FN) coated plastic and recorded for 42 h. The majority of adherent Rac-1 null keratinocytes were not able to spread to the full extent (first three arrows) or not at all (fourth arrow). Finally, most of the mutant adherent cells rounded up and detached, including some cells that were almost fully spread (last two arrows). Many fewer cells were attached and spread after 42 h, compared to control keratinocytes (see Movie 1).

Pictures were taken every 20 min. Display rate: 5 frames/s. Time format: day/hour/minute. Bar: 100 μm .

ACKNOWLEDGMENTS

It would not be possible to carry out this work without help and support of many people to all of whom I am very grateful. I would like to express my sincere gratitude to:

Prof. Dr. Cord Brakebusch, my supervisor, for giving me the opportunity to work on this project, for teaching me how to be a scientist, and for being an exceptionally supportive and understanding boss during all those years.

Prof. Dr. Reinhard Fässler, the head of the department, for his generous support, especially during the final year of the project, and for the possibility to perform my study in such excellent conditions.

Prof. Dr. Charles N. David, my official “Doktorvater”, for assuming this troublesome responsibility, for his patience, and for reviewing my thesis in such a short time.

Prof. Dr. Michael Schleicher, the 2nd referee of my thesis, as well as Dr. Angelika Böttger, Prof. Dr. Hans-Ulrich Koop, Prof. Dr. Heinrich Leonhardt and Prof. Dr. George-Stephen Boyan, the members of my thesis committee, for agreeing to evaluate my work.

Dr. Fabio Quondamatteo, for a fruitful collaboration and for doing such a great job during the preparation of the revised manuscript of the paper.

Dr. Ingo Haase, Michael Tschardt, Dr. Shaohua Li and Dr. Peter Yurchenco, for their contribution to this project and for their willingness to share the data.

Dr. Walter Göhring, for solving all my equipment-related problems.

All members of the “Cord’s group”, for creating a friendly work environment and for all the fun we had together. I am especially grateful to Xunwei, Ola and Gerd, who were there from the beginning, for sharing the good and the bad of every day life in the lab.

Present and former members of the department, for all the help I received along the way.

Mola, Mario and Katie, for being wonderful friends.

My very special thanks go to my parents, my grandma and my sister Asia, for their love and for the continuous support during all the years of my studies and before.

Finally, I would like to thank Carsten, the most important person in my life, for his love, encouragement and unwavering optimism.

CURRICULUM VITAE

Personal information: **Anna Magdalena Chrostek-Grashoff**

Maiden name: Chrostek
Date of birth: 19.05.1978
Place of birth: Katowice, Poland
Nationality: Polish

Education:

- 09/2002 – present** **Max-Planck-Institute of Biochemistry** **Martinsried, Germany**
Ph.D. student under the supervision of Dr. Cord Brakebusch in the Department of Molecular Medicine headed by Prof. Dr. Reinhard Fässler
- 06/2002** **Jagiellonian University** **Kraków, Poland**
M.Sc. in Biotechnology - Specialisation: Molecular Biology
Master thesis: *“The influence of a point mutation within activating region AR1 on the structure of CRP and its interaction with α -subunit of RNA polymerase.”*
Supervisor: Prof. Dr. Zygmunt Wasylewski
Department of Physical Biochemistry, Institute of Molecular Biology
- 02/2002 - 06/2002** **Max-Planck-Institute of Biochemistry** **Martinsried, Germany**
SOCRATES-Erasmus Scholarship Program
Research training under the supervision of Dr. Cord Brakebusch in the Department of Molecular Medicine headed by Prof. Dr. Reinhard Fässler
- 10/1997 - 06/2002** **Jagiellonian University** **Kraków, Poland**
Biotechnology Studies at the Faculty of Biology and Earth Sciences
- 09/1993 - 06/1997** **Stefan Żeromski Secondary School** **Jelenia Góra, Poland**
Mathematics and Computer Science-oriented class
- 09/1985 - 06/1993** **Primary School** **Szklarska Poręba, Poland**